交 通 部 中 央 氣 象 局

三維海流預報作業模式建置及校驗分析研究（1/4）

期末報告

國 立 中 山 大 學

民國九十七年十二月

97 年度政府部門科技計畫期末摘要報告

計畫名稱：三維海流預報作業模式建置及校驗分析研究(1/4)

審議編號：	x	部會署原計畫編號：	MOTC-CWB-97- O-01
主管機關：	交通部中央氣象局	執行單位：	國立中山大學
計畫主持人：	于嘉順	聯絡人：	江朕榮
電話號碼：	07-5252000#5165	傳真號碼：	07-5255173
期程：	97 年 2 月 18 日至 97 年 12 月 31 日		
經費：(全程)	16,900 仟元	經費(年度)	3,600 仟元

執行情形：

1.執行進度：

	預定(%)	實際(%)	比較(%)
當年	100	100	0
全程	25	25	0

2.經費支用：

	預定	實際	支用率(%)
當年	3,600,000	3,600,000	100
全程	16,900,000	16,900,000	100

3.主要執行成果：

1、評估台灣海域作業化海洋環流模式系統

2、於中央氣象局之高速計算電腦系統進行公開海流模式的測試

3、提出未來年度海流模式發展策略及執行方向

4、舉辦國際研討會

5、建立國際與國內資料交流管道

4.計畫變更說明：

無

5.落後原因：

無

6.主管機關之因應對策(檢討與建議)：

「三維海流預報作業模式建置及校驗分析研究(1/4)」

期末報告

目錄

圖目錄

表目錄

摘　　要

海流預報作業一直是海象(洋)預報作業中最為艱鉅的一項工作，亦是近年歐美先進國家中一項積極發展及改進的項目。一方面提供即時預報海流作為航運、遊憩、漁業等公私部門做為規劃管理及作業之參考，另一方面並可隨時提供救難與緊急應變之需。應用現代高速電腦之計算與儲存技術之提高，運用在預報作業的時效與精度，提供有效的即時預警。研發多尺度台灣海域的海洋預報作業模式是急需完成的重點工作。

本計畫四年工作內容為：(第一年) 台灣海域即時海流預報作業模式建置可行性評估，訂定未來分年必須達成之工作目標與成果，並收集分析相關文獻與資料，(第二年)建立大範圍(太平洋或北太平洋尺度)模式與校驗，(第三年)建立區域（西北太平洋尺度，需涵蓋大部分颱風路徑）模式及建立台灣沿海及台灣海峽細格點模式(1/60 度解析度或非正交網格) 與校驗，(第四年)建立模式接合介面，將各種不同尺度與解析度的模式進行單向巢式接合，提升預報的精度與效率，巢式接合模式平行化作業，中央氣象歷年潮位、水溫、氣溫、颱風等紀錄之分析，長期模擬分析，作業化模式上線參與每日預報作業。

本年度為第一年，細部的工作如下：

(1) 蒐集分析目前世界各國作業海洋環流預報模式的發展現況，含數值方法、模式發展、作業策略、資料需求、預報能力及軟硬體相關技術指標等項目。
(2) 評估及建議中央氣象局台灣海域作業化海洋環流預報模式系統。
(3) 舉辦與本計畫相關之國際研討會一次，邀請實際負責作業化海流預報之國際專家學者與會，至少需涵蓋歐洲、美國及亞洲太平洋地區等地專家學者各一位，各主持一場演講及討論，所有經費均由本計畫支付。
(4) 建立國際與國內合作技術與資料交流管道。
(5) 於中央氣象局高速計算電腦系統測試網路上可公開使用之海流

模式，並附完整測試報告。

(6) 訂定模式發展策略，含各模式範圍、解析度及模式系統的嵌合數量、方式等，提供後續年度目標的詳細資訊。例如：模式動力過程、模式所需資料（氣象及海象）、模式組合或嵌合之解析度及預報的範圍。

本團隊今年蒐集國際間主要的海流模式作業化系統相關文獻，包括歐洲的 MERSAE 及 NEMO 系統，美國的 NOAA/NRL 系統，以及日本氣象廳 JMA 系統，透過分析整理相關文獻，訂出未來的模式發展策略。經評估數套模式，建議氣象局未來使用 ROMS 及 FVCOM 模式建置三維海流作業化預報系統，並針對影響海流計算的相關因子進行測試，並於氣象局高速電腦測試計算效率。另外亦於 9 月 10 日與氣象局共同舉辦海洋環流模式作業化預報研討會，要請四位國際專家與兩位國內學者與會演講並討論本計畫未來發展策略，並建立相關技術交流及資料交換的聯繫管道。

第一章 計畫背景

1.1 計畫目的

台灣海域為東亞航運必經之地，近年來的經濟快速開發，台灣對外的航運更趨頻繁，尤其是石化工業的興起，油品及化學品的進出口更增加了海域遭受船難與污染的危機，阿瑪斯號的油污染以及韓籍化學輪三湖兄弟號在新竹外海沈沒所造成的長期影響更是深遠。由於台灣附近海流經過所形成的生態系統豐富，亦是漁產豐盛的海域，近年興起的海面箱網養殖漁業與政府為保護漁業資源在台灣海域投擲大量的人工魚礁，更是易遭受污染的傷害。即時的海流預報作業，不但可以提供航運業者與航管單位即時的海流預報資訊，更可以提供做為早期預警與管理的工具，一旦船難發生時，亦可有立即的海流預報資訊，提供緊急應變單位預測油污染或化學品污染的漂移方向及擴散區域。此外，緊急的海難救助之搜尋工作，亦亟需詳盡的全域三維海流資訊，以提供救難單位即時預測評估搜救對象的可能地點，減低搜尋資源投入的成本，確保搜尋作業時效，因此即時海流預報作業確為緊急應變不可或缺的重要資訊。

近年來世界各地的氣象及海洋學者積極研究全球氣候變遷的問題，尤其是海流及海水溫度對海象及氣象的影響，海流的預報與長期模擬分析更是廣泛的被討論著。台灣附近海域的海流極為複雜，北太平洋環流-「黑潮」流經台灣東部海域，除了強盛的海流亦帶來高溫與高鹽度的海水環境，進入琉球海溝時亦有部分進入台灣北部海域，與來自台灣海峽的海流結合進入東海，每年東北季風期又會阻擾部分的表層洋流而促成黑潮的支流經過台灣南部海域進入南海北部及台灣海峽的南部。除了黑潮洋流的影響，秋冬的東北季風及夏季的西南季風均對台灣附近的海流有相當的影響。在台灣海峽及東海等大陸棚海域，潮汐又是一個主導海流的動力，季節變動所造成的溫度與河水排放的淡水亦會影響海流的分布，颱風所造成的擾動期間雖然不長，但是可以造成非常劇烈的局部影響，因此，為能夠及時提供台灣海域的海流資訊，一套涵蓋大範圍、多尺度、能夠達成預報時效的海流即

時預報模式是海象預報作業極為重要的工作。

海流預報作業一直是海象(洋)預報作業中最為艱鉅的一項工作，亦是近年歐美先進國家中一項積極發展及改進的項目。一方面提供即時預報海流作為航運、遊憩、漁業等公私部門做為規劃管理及作業之參考，另一方面並可隨時提供救難與緊急應變之需。應用現代高速電腦之計算與儲存技術之提高，運用在預報作業的時效與精度，提供有效的即時預警。研發多尺度台灣海域的海洋預報作業模式是急需完成的重點工作。

中央氣象局海象測報中心近年來致力於作業化模式的發展，目前已開發使用多尺度作業化潮汐及暴潮水位模式預報範圍，將颱風自形成開始的影響完整的包含在內的大尺度（115E-125E， 20N-30N）水動力數值模式，模式解析度改進為二十分之一度之精度及六十分之一度的台灣沿海模式，並包含深海平均潮、天文潮、大氣壓力及風場之影響。因此氣象局希望結合國內外三維海流預報模式專家之經驗，建立一套多尺度的臺灣海域海流即時預報作業化模式，模式範圍至少須涵蓋東經 105 度到 150 度，北緯 15 度到 42 度，大部分侵台的颱風影響即可在形成初期納入預報，一方面增加提前預報的時效，另一方面亦可將滯留颱風對台灣海域海流的影響納入預報，為求較為精確的區域模式計算邊界，建立更大範圍的模式將無可避免。同時在模式發展建置完成後，必須利用氣象局之相關衛星資料、台灣沿岸及浮標等實際量測資料進行校驗。預報模式系統亦必須配合氣象局新進建制之高速計算電腦系統(IBM P5)達成使用至少 256 組 CPU 的平行計算能力，以便達成每日預報時效。

本計畫擬分四年進行：(第一年) 台灣海域即時海流預報作業模式建置可行性評估，訂定未來分年必須達成之工作目標與成果，並收集分析相關文獻與資料，(第二年)建立大範圍(太平洋或北太平洋尺度)模式與校驗，(第三年)建立區域（西北太平洋尺度，需涵蓋大部分颱風路徑）模式及建立台灣沿海及台灣海峽細格點模式(1/60 度解析度或非正交網格) 與校驗，(第四年)建立模式接合介面，將各種不同尺度與解析度的模式進行單向巢式接合，提升預報的精度與效率，

巢式接合模式平行化作業，中央氣象歷年潮位、水溫、氣溫、颱風等紀錄之分析，長期模擬分析，作業化模式上線參與每日預報作業。

1.2 工作項目

本計畫擬分四年進行：

第一年 97 年(2008)：台灣海域海洋環流及潮流作業預報系統建置可行性評估，模式架構的評估，訂定未來分年必須達成的工作目標及成果。並收集分析相關文獻與資料。

(1) 蒐集分析目前世界各國作業海洋環流預報模式的發展現況，含數值方法、模式發展、作業策略、資料需求、預報能力及軟硬體相關技術指標等項目。

(2) 評估及建議中央氣象局台灣海域作業化海洋環流預報模式系統。

(3) 舉辦與本計畫相關之國際研討會一次，邀請實際負責作業化海流預報之國際專家學者與會，至少需涵蓋歐洲、美國及亞洲太平洋地區等地專家學者各一位，各主持一場演講及討論，所有經費均由本計畫支付。

(4) 建立國際與國內合作技術與資料交流管道。

(5) 於中央氣象局高速計算電腦系統測試網路上可公開使用之海流模式，並附完整測試報告。

(6) 訂定模式發展策略，含各模式範圍、解析度及模式系統的嵌合數量、方式等，提供後續年度目標的詳細資訊。例如：模式動力過程、模式所需資料（氣象及海象）、模式組合或嵌合之解析度及預報的範圍。

第二年 98 年(2009)：參考第一年計畫之評估建議，建立太平洋海域環流模式及北太平洋模式與校驗。

(1) 建立及校驗太平洋模式，模式範圍需涵蓋整個太平洋，水平網格不可大於 1/3 度，模式垂直分層以變化地形相對座標或是等密度分層至少 20 層。

(2) 建立及校驗北太平洋模式，模式的範圍需涵蓋 10˚N 到 70˚N，西起亞洲大陸東至美洲大陸，水平的解析度為 1/6 度，模式垂直分層以變化地形相對座標 20 層。

(3) 蒐集建置水深地形資料，以提供模式使用。

(4) 氣象資料輸入以中央氣象局每日氣象預報資料為主，並取得國際氣象單位提供之氣象資料以資比對。

(5) 訂定校正年份與驗證年份，並收集相關資料以資校驗。

(6) 預報時效測試與高速計算平行處理測試。

(7) 提供初步模式系統的預報案例。

(8) 製作模式操作手冊。

第三年 99 年(2010)：建立西北太平洋區域模式及台灣海域細格點模式與校驗

(1) 建立及校驗西北太平洋區域模式，模式的範圍需涵蓋 10˚N 到 50˚N，100˚E 到 150˚E。其水平網格不得大於 1/12 度，模式垂直分層以變化地形相對座標 25 層。

(2) 建立及校驗台灣海域細格點模式，模式的範圍需涵蓋 21˚N 到 27˚N，117˚E 到 123˚E，其水平網格必須解析台灣沿海複雜之海岸地形，定網格系統不得大於 1/60 度或以非正交網格系統（FEM 或 FDM），模式垂直分層以變化地形相對座標 15 層。

(3) 蒐集建置水深地形資料，以提供模式使用。

(4) 氣象資料輸入以中央氣象局每日氣象預報資料為主，並取得國際氣象單位提供之氣象資料以資比對。

(5) 訂定校正年份與驗證年份，並收集相關資料以資校驗。

(6) 預報時效測試與高速計算平行處理測試。

(7) 提供初步模式系統的預報案例。

(8) 製作模式操作手冊。

第四年 100 年(2011)：建立各層次模式作業化接合介面、模式系統測試與評估、長期模擬測試及分析、作業化模式上線測試，參與每日預報作業與觀測結果比較。

(1) 測試及校驗各級模式並建立各模式接合介面。

(2) 測試與評估模式耦合之敏感度至少一年。

(3) 因應中央氣象局電腦設備之軟硬體，完成模式程式最佳化的設定。

(4) 模式系統的測試結果與實測或文獻資料比對分析。

(5) 完成中央氣象局海洋環流作業系統建置及評估報告。

第二章 國際主要海流模式作業系統及海流模式

本章節主要介紹目前收集到的國際主要海流模式作業平台，以作為未來台灣三維海流預報作業模式架構的規劃參考及使用模式的評估。

近年來，西歐各國海流作業化模式的發展趨勢，由於模式技術已趨穩定，由於大範圍模式（全球海洋模式或大西洋海流模式等）之範圍、邊界、驅動力等條件多類似甚至相同，所以模式之發展已由各國或研究機構獨自發展建置而趨向於共同研發的模式系統，目前以NEMO 及 MERSEA 為較大型的跨國海洋環流作業化模式的平台，美國則以海軍研究所(NRL)發展的 HYCOM/MICOM 系統，以及 ROMS 及 POM 模式系統為主流，大型環流系統逐漸以 HYCOM 為系統整合方向，區域作業化預報則以 ROMS/TOMS 為主要整合方向，POM 大多以陸棚或沿海為主要應用方向，另有較屬於沿岸河口應用的模式如比利時結合歐盟數國研究機構所發展的 COHERENS 及以有限體積法發展的 FVCOM 等，亞洲各國亦多以這幾種系統為主要發展及應用為主，以下僅就其組織與模式系統略述於後：

NEMO (Nucleus for European Modelling of the Ocean)

NEMO 模式系統平台結合了歐洲幾個主要的海洋環流作業化模式的發展與執行單位，主要成員為法國國家氣象研究中心（CNRS）及 國家海洋作業化模式發展計畫（Mercator-Ocean）與英國氣象局（UKMO）及英國國家環境研究委員會（NERC）轄屬的相關研究機構（POL, SOTTON 等），以共同研究發展先進海洋作業化模式為主要目標，目前的大型作業化計算單位除英法主要研究與預報單位外，亦有德國、西班牙、義大利、日本等國之研究單位，區域型的應用亦極為廣泛。模式系統目前的發展進度為：

- 最新版 OPA9.0 海洋模式系統，以 OASIS 地球資源耦合系統結合相關之環境影響系統(如邊緣海、陸源、大氣、冰層等)，並完全以 FORTRAN90 程式語言改寫為適用於高速計算(平行計算）的編譯平台，以便提升計算效率。

- 使用比利時魯汶大學發展的南北極冰層動力模式（LIM2），以便準確計算海洋環流與南北極冰層的溫度動力，尤其近年來受全球氣候暖化的影響，冰層與洋流的關係，愈趨重要。
- 以 OPA9.0 內部的對流及擴散傳輸模式（TOP-1）驅動二個主要的海洋生地化模式（LOBSTER, PISCES）提供海洋生地化相關學者探討海洋生態平衡及全球碳循環等先驅研究。

MEARSEA

MERSEA ('Marine Environment and Security for the European Area') project，是歐洲聯盟贊助之大型跨國研究計畫，是屬於 GMES (Global Monitoring for Environment and Security)全球海洋監測架構計畫下相關的計畫，目的在整合歐洲各國所發展應用中的海洋模式及作業化相關技術（衛星資料分析整合、資料同化技術發展、提升計算效率及作業化技術發展等），自 2001 年起目前已進入第二階段，經比較評估後，目前以五個模式系統進行大西洋海域的模式分析比對：FOAM (Met. Office, United Kingdom), MERCATOR (MERCATOR-OCEAN, France), MFS (INGV, Italy) and TOPAZ (NERSC, Norway)等歐洲系統並與美國 HYCOM/MICOM (US)系統，如圖 2.1-1，目前 MEARSEA 計畫進行到 2008 年後，即會併入 NEMO 系統中。僅就這五個模式系統略述如後：

- FOAM（UK）

  Hadley Centre 所發展的模式，Z coordinate / Rigid Lid，涵蓋北大西洋、北極海、地中海及相關陸棚海域 (10° to 70°N, coast to coast), 水平解析度為 1/9° (12 km), 垂直分為 20 層。
- Mercator (France)

  OPA 模式，Z coordinate / Rigid Lid，涵蓋北大西洋、北極海、地中海及相關陸棚海域 (10° to 70°N, coast to coast), 水平解析度為 1/15° (5-7 km), 垂直分為 43 層。
- Topaz (Norway)

HYCOM 模式(HYbrid Coordinate Ocean Model),hybrid coordinates / free surface, 涵蓋北大西洋、北極海、波羅底海(北極至 60°S.),水平解析度為 20 to 30 km, 垂直分為 22 hybrid layers。

- MFS (ITALY)
  Modular Ocean Model (MOM-1), Z coord./Rigid Lid, 僅涵蓋地中海水平解析度為 1/8°, 垂直分為 31 層。
- HYCOM/MICOM (US)
  HYCOM 模式 (HYbrid Coordinate Ocean Model), hybrid coordinates / free surface, 涵蓋北大西洋(28°S-70°N, 98°W-36°W),水平解析度為 1/12° (平均 6,5km), 垂直分為 26 複合等密度層(hybrid isopycnal levels)。

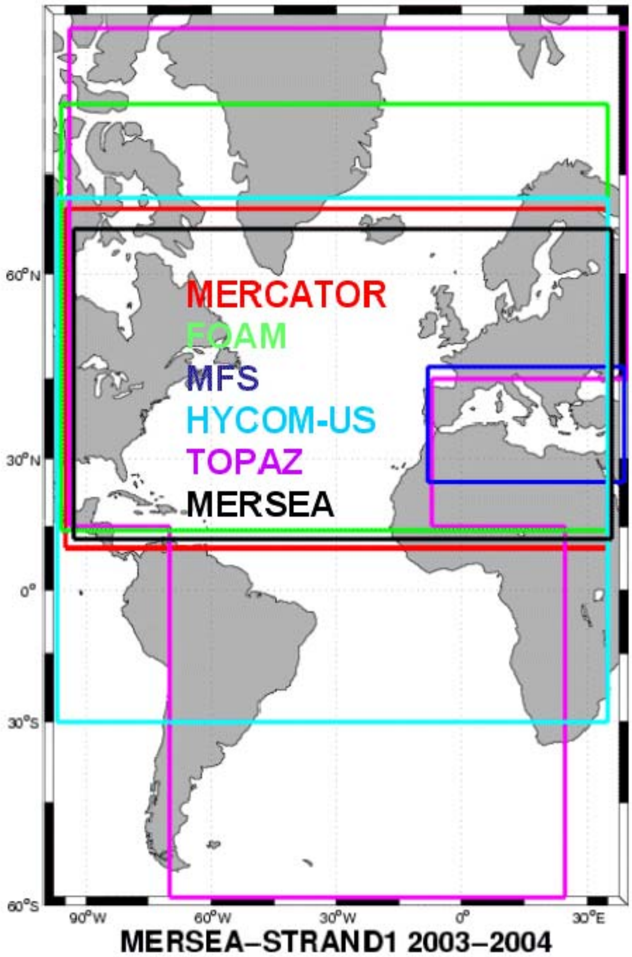

圖 2.1-1 MERSEA project model domains.
(http://strand1.mersea.eu.org/html/strand1/model.html)

NOAA/NRL

利用 HYCOM(Hybrid Coordinate Ocean Model)進行即時預報，HYCOM 模式主要由 HYCOM 協會發展，此協會是由 National Ocean Partnership Program(NOPP)等多個組織贊助，成員包含 Office of Naval Research、National Science Foundation、Department of Energy 以及 NOAA。目前運行的系統共有三組，第一組為全球即時現報系統，第二組為大西洋半即時現報/預報系統，此兩組系統皆運行於 NRL Stennis Space center，第三組為大西洋即時預報系統(Real-Time Ocean Forecast System, RTOFS)，此組系統運行於 NOAA/NCEP，以下就此三組系統進行介紹。

即時全球現報系統：

- 網隔水平解析度於赤道為 1/12 度，隨著緯度增加，最細解析度為 7 公里。垂直分層為 32 層。
- 輸出資料包含水位(SSH)、表層溫度(SST)、表層流場以及中層溫度及鹽度。
- 使用 Navy Coupled Ocean Data Assimilation(NCODA)系統進行資料同化。

大西洋半即時現報/預報系統

- 模式範圍為南緯 28 度至北緯 70 度
- 網隔為直角網格，水平解析度於赤道為 9 公里，隨著緯度增加，最細解析度為北緯 60 度的 4.5 公里，北緯 45 度則為 6.5 公里。垂直分層為 26 層。
- 輸出資料包含水位(SSH)、表層溫度(SST)、表層流場以及中層溫度及鹽度。
- 使用每日的 Modular Ocean Data Assimilation System(MODAS)進行資料同化。
- 每週執行一次。

大西洋即時預報系統(RTOFS)

- 模式範圍為南緯 25 度至北緯 70 度。
- 網格為正交曲面網格，水平解析度於美國海岸為 5 公里，東

部大西洋海岸為 9~17 公里。

- 輸出資料包含水位(SSH)、表層溫度(SST)、表層流場以及中層溫度及鹽度。
- 使用 GOES AVHRR、JASON GFO、ARGOS、XBT、CTD 及現場資料進行資料同化。
- 每日 GMT 0 時計算，GMT 14 時計算完成，含 1 日資料同化現報，120 小時預報。

日本氣象廳(JMA)

日本氣象廳下，目前進行海流運算的共有三個系統，一為 MOVE/MRI.COM-G(the Ocean Data Assimilation of JMA)，一為 JMA/MRI-CGCM(Coupled ocean-atmosphere General Circulation Model of JMA)，最後一個為 MOVE/MRI.COM-NP 及 WNP (Multivariate Ocean Variation Estimation/Meteorological Research Institute Community Ocean Model-Northern Pacific 及 Western North Pacific)，以下就此三組系統進行介紹。

MOVE/MRI.COM-G

- 使用 MRI.COM(MRI Community Ocean Model)進行全球範圍運算，南緯 75 度至北緯 75 度，不包括北極海。
- 模式水平網格解析度在南緯 15 度至北緯 15 度以外為 1 度，內縮至南緯 6 度至北緯 6 度為 0.3 度。
- 垂直網格為 sigma 及 z-coordinate 混合(Hybrid)網格，共分為 50 層，200 公尺以上為 24 層。
- 使用 JMA Climate Data Assimilation System(JCDAS)資料進行驅動。
- 使用 MOVE scheme 進行資料同化。

JMA/MRI-CGCM

- 此為海洋大氣耦合模式，海洋部份使用的模式為 MRI.COM，大氣部份使用較低解析度的 global spectral model(JMA 作業氣象預報模式系統)進行耦合。

- 模式設定與 MRI.COM-G 相同。
- 模式每小時進行耦合運算，海洋模式提供表層溫度與大氣模式，大氣模式則提供熱通量、風場及降雨等資訊給海洋模式。
- 資料同化部份，大氣模式及海洋模式利用每日的實測風場及表層溫度進行修正。
- 大氣模式初始場由 JCDAS 提供，海洋模式初始場則由 MOVE/MRI.COM-G 提供。
- 每五天執行一次。

MOVE/MRI.COM-NP 及 WNP

- 使用 MRI.COM 模式。
- NP 模式範圍為南緯 15 度至北緯 65 度，東經 100 度至西經 75 度。模式水平格點解析度為 1/2 度，垂直分層為 54 層
- WNP 模式範圍為北緯 15 度至北緯 65 度，東經 117 度至西經 160 度。模式水平格點解析度為 1/10 度，垂直分層為 54 層。
- WNP 模式邊界由 NP 提供。
- 提供日本周圍海域、西北太平洋及北太平洋每日及每月的溫度及流速平均資料。

上述為國際頂尖的海流模式系統，可瞭解系統皆是由多組解析度模式及觀測系統組成，可作為台灣海流模式預報系統規劃之參考。

第三章 模式發展策略

本章節介紹今年規劃的海流作業化預報模式系統架構，並且提出使用模式所需評估的項目，所需要的觀測資料及預報資料。

3.1 海流模式系統架構

本團隊參考了主要的海流模式預報平台，規劃了海洋環流預報作業化模式系統架構如圖 3.1-1 所示，主要分為兩個部份，一為模式系統，包括太平洋環流模式、北太平洋模式、西北太平洋模式及台灣海域模式，另一部份則為觀測資料系統，包括衛星資料、測站資料、浮標資料及船測資料，用以讓模式進行資料比對，並且可與模式進行資料同化，得到更精確的模式結果。

影響海流的因素相當多，而且各因素的尺度也不同，有全球尺度的大氣因子、洋流及潮流，中尺度的渦流系統，也有受到海岸線及區域地形影響的小尺度因子。為了要將大尺度的影響因素包含進來，模式的模擬範圍需要擴大，而為了解析區域因素，模式網格的精度需要增加，如此條件下，計算的網格數會以數十倍甚至數百倍增加，以目前現有的電腦計算架構，並無法達成此一目標，利用單一網格來模擬海流的狀況是不可能的，因此最好的方式就是利用巢式網格系統，所以在模式系統的部份，本團隊設定了四個階層的網格系統。

第一層太平洋環流模式，利用全球大氣模式作為驅動條件，進行太平洋洋流(北太平洋環流及南太平洋環流系統) 系統的模擬，結果可作為下一層模式的邊界條件。北太平洋模式則進行更細部的北太平洋環流模擬，由於使用太平洋環流模式的結果當成邊界條件，因此可將影響包含進北太平洋模式內。西北太平洋模式則在將範圍縮小，精度提高，並使用北太平洋模式的模擬結果作為邊界條件輸入，模擬此區的流場狀況，如此可將洋流的影響帶入，並且可以模擬中尺度的渦流系統。最後一層則是解析度及範圍最小的台灣海域模式，利用西北太平洋模式的結果當成邊界輸入，將洋流及渦流的影響帶進此系統，而解析度小可以解析更細部的海岸線及海底地形，透過此巢狀網格的機制，可以得到更精確的台灣海域海流狀況。

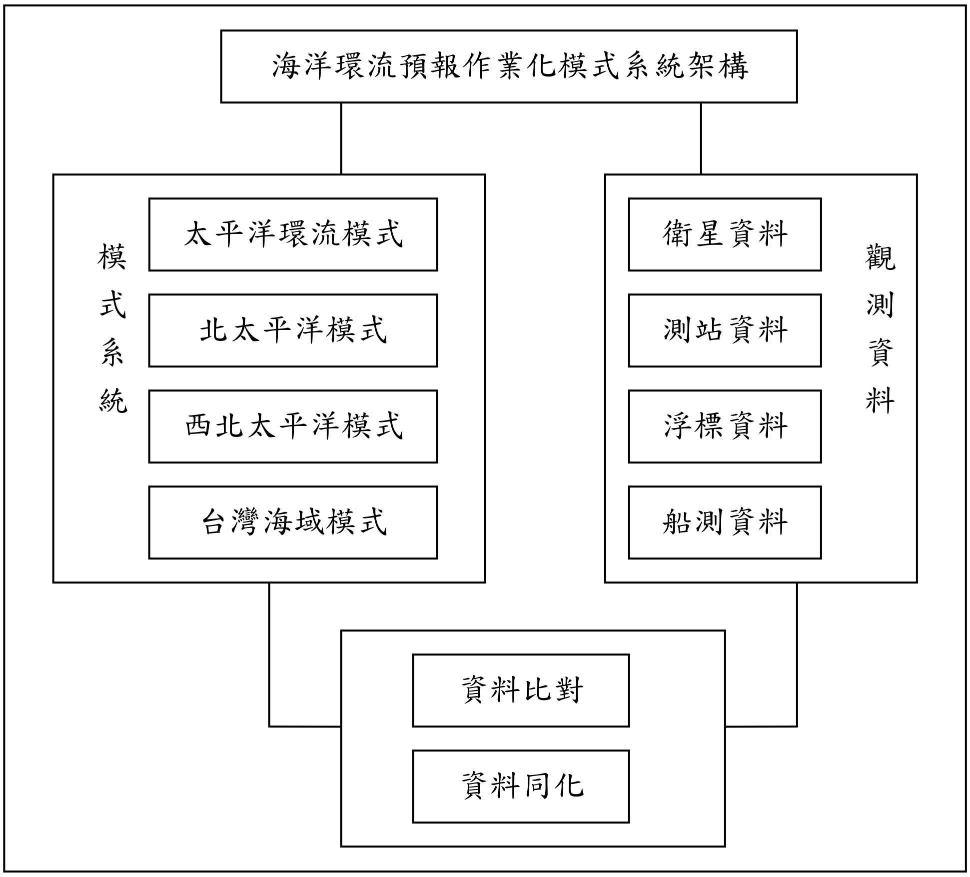

圖 3.1-1 台灣海流模式預報系統架構圖

圖 3.1-2 為海洋環流預報作業化模式系統的地形及範圍示意圖，目前將海洋環流海流模式設定為四個階層，用以解析完整的流場。黑色實線框為太平洋環流模式範圍，包含整個太平洋海域，主要用以解析完整的太平洋環流系統，並將影響帶入下一層模式，模式水平網格為 1/3 度以下，垂直分層分層至少 20 層。紅色虛線為北太平洋範圍模式，模式範圍為赤道以北的太平洋，接收太平洋環流模式的影響，並解析北太平洋更詳細的流場狀況，模式的範圍需涵蓋 20˚S 到 70˚N，西起亞洲大陸東至美洲大陸，模式水平的解析度為 1/6 度，垂直分層 20 層，預計此兩層將使用 ROMS 海洋環流模式進行模擬。第三層則是橘色點虛線框的西北太平洋模式，邊界輸入利用北太平洋模式的模擬結果，推算更細部的西北太平洋流場，模式的範圍涵蓋 10˚N 到 50˚N，100˚E 到 150˚E，其水平網格為 1/12 度以下，垂直分層 25 層，此層預計使用 ROMS 進行模擬。最後一層則為台灣海域模式，模式邊界輸入則利用西北太平洋模式的模擬結果，模式的範圍涵蓋

21°N 到 27°N，117°E 到 123°E，其水平網格必須解析台灣沿海複雜之海岸地形，定網格系統 1/60 度以下或以非正交網格系統（FEM 或 FDM）分割，垂直分層 15 層，此層將使用 FVCOM 或 COHERENS 河口海洋模式進行模擬。透過此四層模式的推算，台灣海域模式便可將洋流、潮流及風驅流的影響完整納入。

而未來規劃的各模式作業化時程如下：

- 太平洋模式：每月執行一次，含過去十年資料同化處理，組合預報未來三個月。
- 北太平洋模式：每二週執行一次，配合太平洋模式預報未來二個月
- 西北太平洋模式：每週執行一次，配合北太平洋模式預報未來一個月
- 台灣海域模式：每天執行一次，現報 24 小時及預報 48 小時

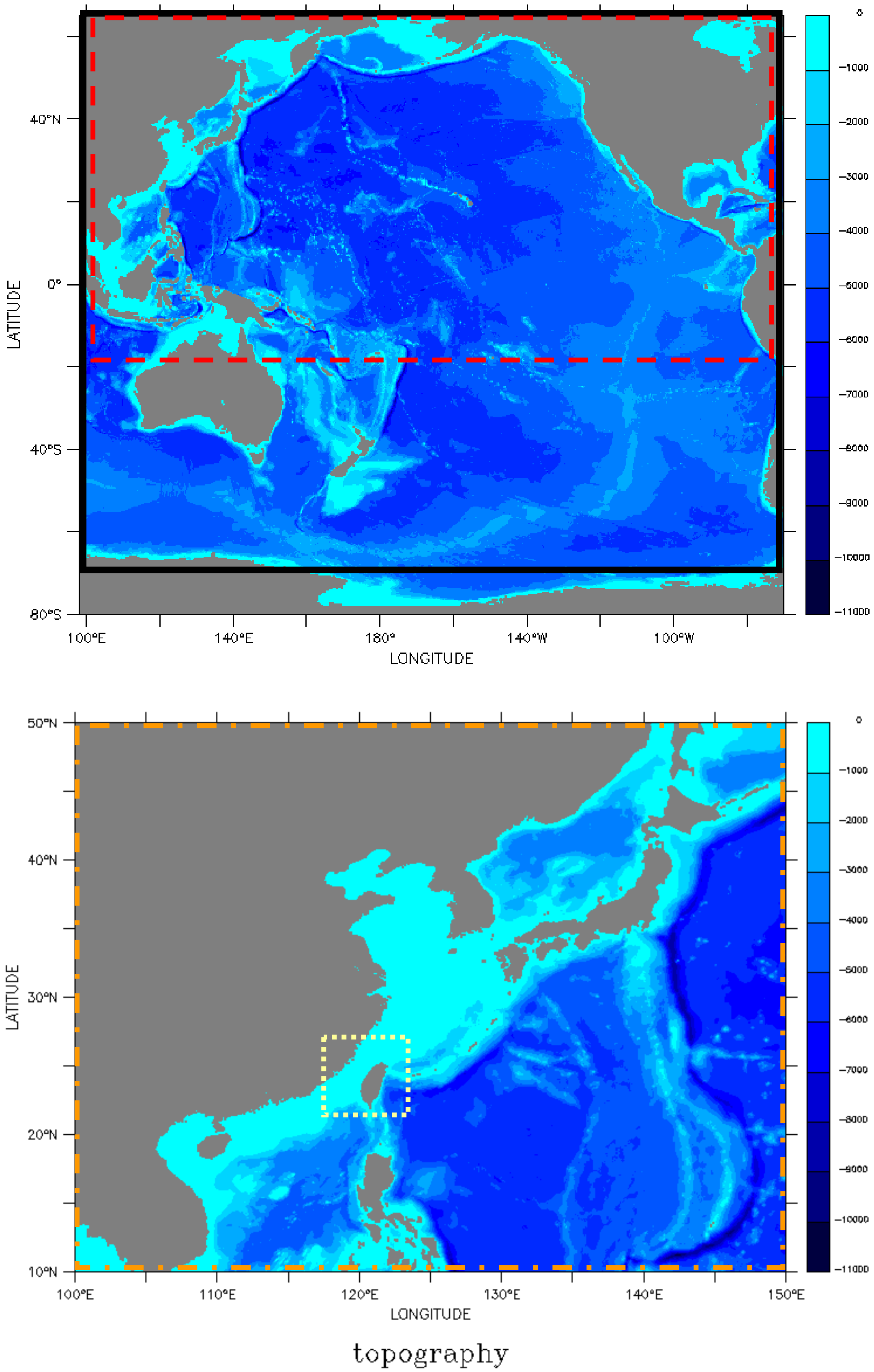

圖 3.1-2 海流模式系統模擬範圍示意圖(實線：太平洋環流模式、虛線：北太平洋模式、點虛線：西北太平洋模式、點線：台灣海域模式)

3.2 模式資料需求

模式發展過程需要利用實測資料進行比對及校驗，由於本系統包含四層模式，模擬範圍由太平洋至台灣海域，因此需要的資料相當多，以下列出所需資料及未來資料同化的方式，增進模式預報的精確度。

資料需求

- 地形資料：海科中心資料庫、ETOPO5, DBDB2, 其他近岸量測資料。
- 模式外部驅動力（External forcings）
  - 氣象資料（即時氣象預報資料）：輻射熱能及雲遮量、表面風場（10 米風速及風向）、氣壓場、氣溫、濕度、降雨量、蒸發量
  - 河川流量資料：河口淡水流量、水位變化、水溫、鹽度
- 起使條件：Levitus data 或是其他全球模式資料 (OPA, HYCOM, OCCAM)
- 校驗資料：
  - 水位：氣象局海象中心、港研中心、PMSL、T/P altimeter
  - 水溫：氣象局海象中心、港研中心、海科中心、MODIS, ARGO, HOT, GDP, …
  - 鹽度：海科中心、ARGO, HOT, …
  - 海流：港研中心、海科中心、WOCE, ARGO, GDP, …

表 3.2-1 為氣象局資訊中心可提供的氣象模式資料。

表 3.2-1 氣象局提供模式之可用資料(氣象局資訊中心)

模式名稱	解析度	區域	可用資料
ECMWF (EC01)	2.5x2.5	全球	1. 海平面氣壓 2. 850hPa 之溫度、風速及相對濕度
JMA GPV_GSM (JG06)	0.5x0.5	全球	1. 海平面氣壓及氣溫 2. 表面降雨及雲遮量 3. 2 米高之氣溫及相對濕度 4. 10 米高之風速
NCEP(NA01)	5x5	全球	1. 海平面氣壓及氣溫 2. 1000 及 850hPa 之溫度、風速及相對濕度
NCEP(NA03)	1.25x1.25	全球	1. 海平面氣壓 2. 1000 及 850hPa 之溫度、風速及相對濕度
NCEP AVN (NA05&NA09)	0.5x0.5	全球	1. 海平面氣壓及氣溫 2. 1000 及 850hPa 之溫度、風速及相對濕度 3. 2 米高之相對濕度 4. 10 米高之風速 5. 總降雨量 6. 反射率 7. Latent 及 Sensible 熱通量
NCEP(NA07)	1x1	全球	海平面氣溫
NOGAPS	1x1	全球	1. 海平面氣壓 2. 總降雨量,Latent 及 Sensible 熱通量 3. 2 米高之相對濕度 4. 10 米高之風速
UK(UK01)	1.25x1.25	全球	1. 海平面氣壓 2. 地表氣溫、風速及總降雨量 3. 1000hPa 之相對濕度
JMA GPV_RSM (JRNA)	0.25x0.2	20N~50N 120E~150E	1. 海平面氣壓 2. 表面降雨及雲遮量 3. 2 米高之氣溫及相對濕度 4. 10 米高之風速
JMA 海溫模式	0.25x0.25	0.125N~59.875N 100.125E~179.875E	海表面溫度
JMA MSM (二)	0.0625x 0.05	22.4~47.6 120E~150E	1. 海平面氣壓 2. 表面降雨及雲遮量 3. 1.5 米高之氣溫及相對濕度 4. 10 米高之風速

3.3 資料同化

3.3.1 資料同化概述

儘管目前數值模式具有高度的模擬能力，卻仍會有偶發誤差的現象，造成模式推算的不準確。這些模擬失誤大致上可歸因於：一為對於各現象運行的物理機制認識有限，二為數值處理不完善，造成數值誤差。由於模式中有許多參數，需要經過校正參數以具適用性，最簡單的方法為試誤法，此法雖簡易，但缺乏系統性，而資料同化(data assimilation)是一種將觀測值和數值預報值結合，決定出系統變數最佳估計值的方法，即只要有預報模式和觀測值，便可使用此法決定出最佳的系統變數值。

1957 年第一顆人造衛星的發射，啟發人類科學思維的創造力，也引領後來大氣科學及相關海洋研究之種種突破，在氣象衛星發射後，解決了測站分布不均及缺乏高準度觀測方式的問題。到了 1960 年代，資料同化出現於氣象預報研究中(Gandin, 1963)，為了改進氣象預報值之準確性，結合觀測值至數值模式內。

近幾年來海洋資訊的預報顯得益加重要，為了提供更精準的預報資訊，因此整合模式及觀測資料以得到最佳起始值的資料同化技術，更成了海象資訊預報模式必須採用的方法。

3.3.2 資料同化循環

進行海象分析及預報時，第一步工作就是蒐集資料，並做初步處理，以剔除錯誤及補遺，將資料的品質提高。接著把分布不規則測站上的資料內插到規則的格點(grid point)上，以便預報模式之執行，將資料內插到格點上的過程稱為客觀分析(objective analysis)。但實際上客觀分析場並不能直接當做數值預報模式的初始場，其原因在數值模式中存在著數值慣性重力波，若初始值未滿足動量及質量場間的平衡，則慣性重力波之振幅將在模擬過程中逐漸加大，進而影響預報場之準確度，故必須進行修正才能提升預測值之準確性，這就是所謂的初始化(initialization)，又稱平衡。在進行客觀分析時，因需要用到數

值預報值，所以資料初步處理、客觀分析、初始化及數值預報即構成了資料同化循環(data assimilation cycle)。

由觀測系統得到的資料一定有誤差，一般分為兩大類；一為自然誤差，如儀器誤差(instrument error)，和代表性誤差(error of representativeness)，其中代表性誤差和存在於大氣中卻不能被觀測網偵測到的小尺度氣象擾動有關，另一為重大誤差(gross error)，是由於人為因素、不當的儀器校準(calibration)所造成的。進行資料同化時，自然誤差可以妥善處理，如儀器誤差可自行調整，但重大誤差則需要檢驗並加以訂正或捨棄。一般來說，資料的品質控制主要有兩個方法，重大誤差檢驗(gross error check)和連續性檢驗(continuity check)。由於海象變數的值有一定範圍，如果不在此範圍內，就可認定此資料有誤而捨棄不用或做修正，這種檢驗稱重大誤差檢驗、物理合理性檢驗(physical limit check)或統計檢驗；連續性檢驗則是指將某一測站資料和周圍測站互相比較，若兩者相差太大，則此測站資料可能有誤。在進行資料初步處理之步驟時，應盡量把重大誤差找出，加以訂正並補足漏失的資料，否則會影響往後的分析和預報準確度。

資料同化的第二個部分為客觀分析，簡單來說就是將分布不規則測站上所觀測到的海象資料內插到規則的格點上，以便進行海象分析和預報，由於以下種種原因，客觀分析不只是單純的內插。

- 海象資料在空間和時間上分布相當零亂，有些地方甚至完全沒有資料，若直接使用一般的內插法會產生不真實的分析值。
- 海象觀測系統歧異大，例如船測資料和衛星資料在空間與時間分佈完全不同。
- 海洋中有各種不同尺度的運動，因此進行大尺度海象分析和預報時，須將海象資料裡面的中小尺度擾動除去，也就是做平滑和濾波(smoothing and filtering)的工作。

最常見的客觀分析法，並非直接將觀測站上之觀測值內插到格點上，而是將觀測值對初始猜測值之偏差(deviation)做內插。由於海象預報準確性的提昇，因此初始猜測值可採用預報模式之預報值作為背景場(background field)。圖 3.3.2-1 為 200mb 風場客觀分析的步驟，首

先將 6 小時預報場格點上的預報值(圖 3.3.2-1-a)內插到觀測站(圖 3.3.2-1-b)上，獲得觀測站之背景場，然後計算觀測值與背景場之偏差值，此偏差值即為觀測增量(observation increment)(圖 3.3.2-1-c)，之後將觀測增量利用特殊方法內插至計算格點上，得到所謂的分析增量(analysis increment)(圖 3.3.2-1-d)，最後再將此分析增量加到背景場裡，便可得到分析場(圖 3.3.2-1-e)。由前文可知背景場為分析場一定程度上準確的猜測值，觀測增量和分析增量再對背景場做微小的修正，因此在完全沒有觀測資料的地區，分析場可由短時間之預報場替代。

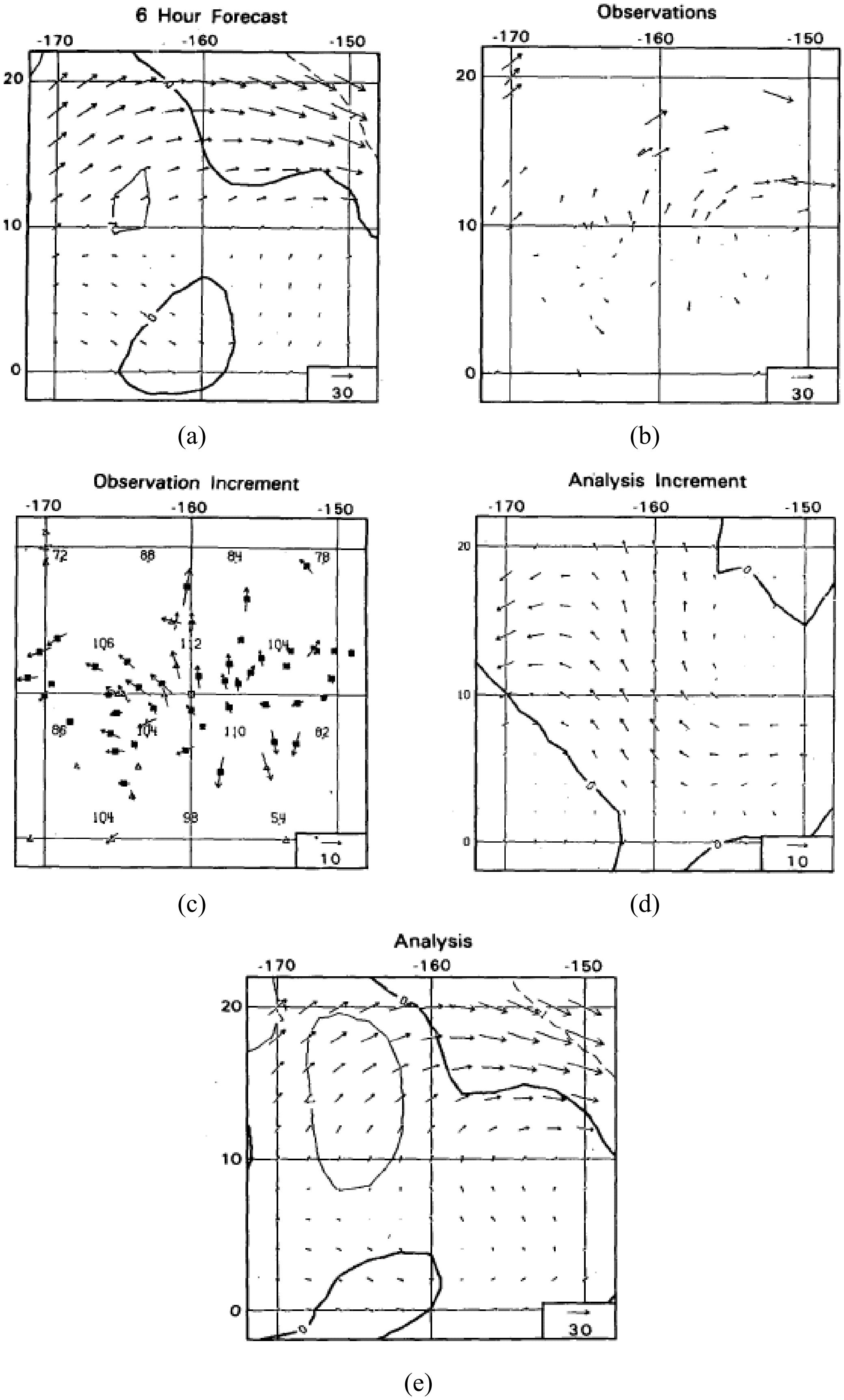

圖 3.3.2-1 200mb 風場客觀分析步驟示意圖(Daley, 1985)

第三部分為初始化，也就是對格點上的分析場做進一步的處理，以便做為數值預報的初始值之用。雖然在數值模式裡的延散(dispersion)和消散(dissipation)作用下，在一段時間內能將實際上不存在的慣性重力波之振幅削減下來，在數值模式之控制方程式間取得平衡，但這可能需要一至二天的時間才能達到平衡，因此在這段期間的預報值是不準確的，加上客觀分析中的背景場大都採用數值預報場，假如預報場不準確，則分析場的準確度也會受到影響，使得分析場和真實情況有很大的差距，所以客觀分析場在做為數值預報模式的初始場以前，必須先加以初始化。初始化可分為靜態初始化及動態初始化。靜態初始化是利用特殊方程式調整速度場及質量場使其保持平衡；動態初始化是以分析場作為初始值，並使用可使慣性動力波衰減之數值模式，然後向前向後預報數次，就可得到平衡的初始場。(曾，1997)

數值預報模式可用來準備下一個觀測時間的背景場，這種模式特別稱為同化模式(assimilating model)，圖 3.3.2-2 為資料同化的系統示意圖。它通常是根據原始方程建立的高分辨率(high-resolution)模式，具有複雜的物理過程參數化格式，這種同化模式原則上和做為數天、數週，甚至數月及長期預報的數值模式並沒有什麼不同。

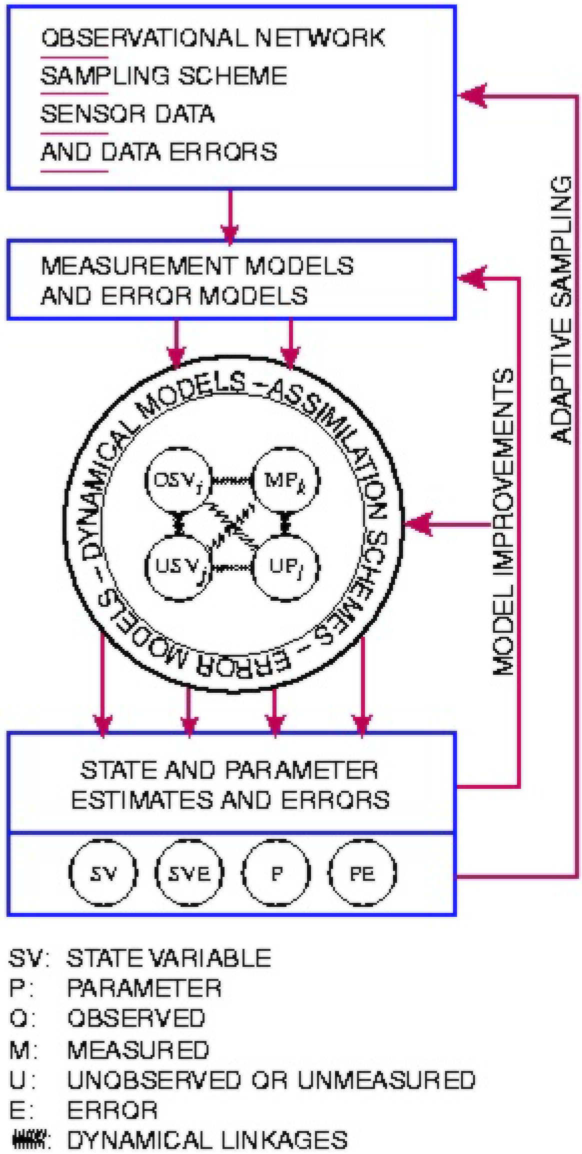

圖 3.3.2-2 資料同化系統示意圖(Allan and Pierre, 2000)

3.3.3 資料同化方法介紹

資料同化方法通常可分為二種，一為連續資料同化法(sequential method)，另一為變分資料同化法(variational method)。依時間處理過程又可分為間歇資料同化(intermittent data assimilation)與連續資料同化(continuous data assimilation)。

間歇資料同化是為考慮某一時刻，例如在 00 時，收集前後 3 小時內的資料，並做品質控制，然後將同化模式由-06 時向前預報 6 小

時得到的預報值(即 6 小時預報值)做為 00 時的背景場，接著對上述資料進行客觀分析，以得到分析場，最後做初始化工作，並進行預報。此時可以一直向前做例行的預報，或只預報 6 小時，以做為 06 時的背影場，對 06 時前後 3 小時的資料也可類似處理，圖 3.3.3-1-a 為間歇資料同化示意圖。

圖 3.3.3-1-b 表示連續資料同化的觀念，在這個情況下只要有資料進來就隨時做同化處理，至於預報可在資料同化循環期間內的任意時刻，通常是由 00 時或 12 時開始。

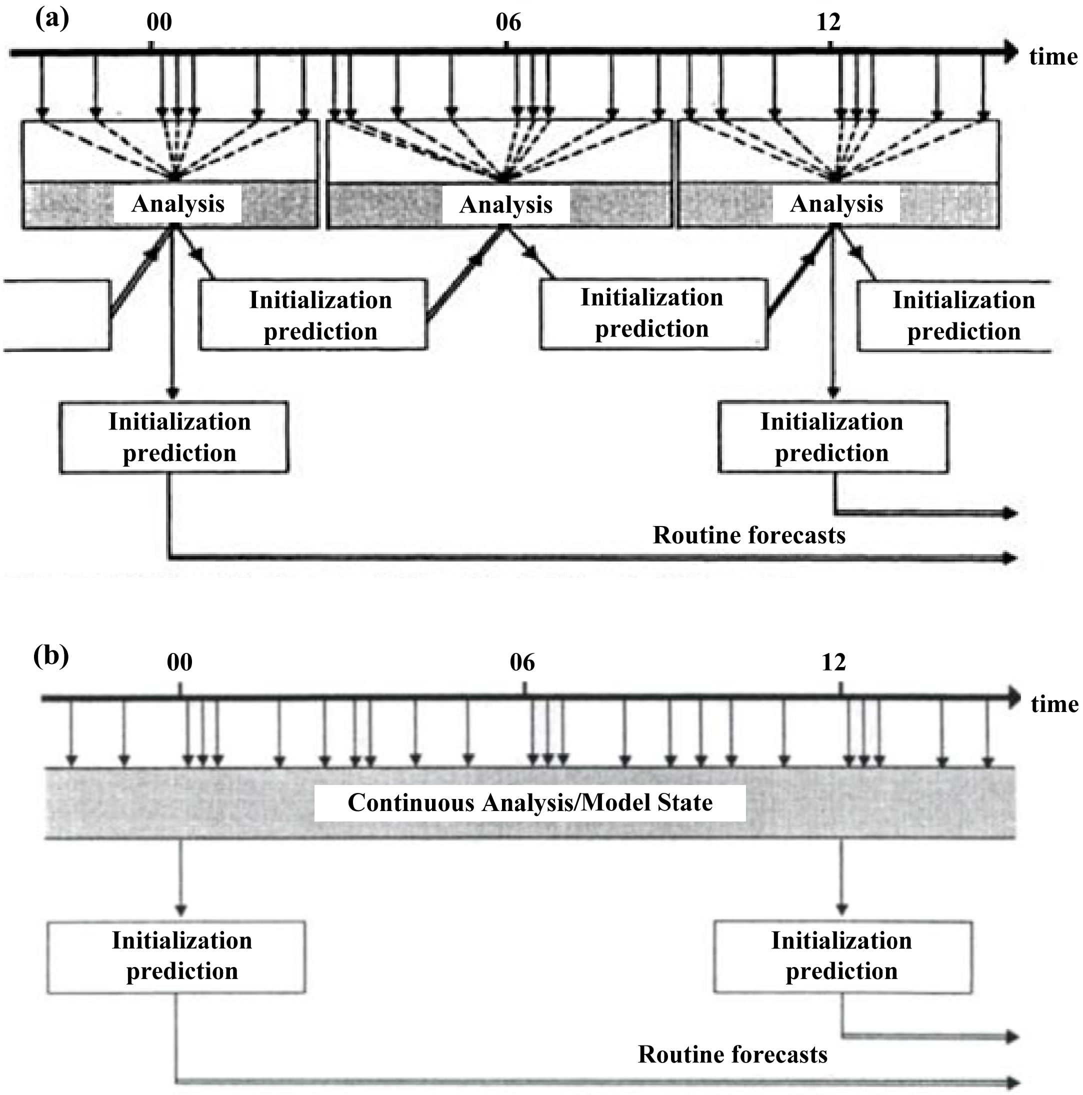

圖 3.3.3-1 間歇資料同化(a)和連續資料同化(b)示意圖(Daley, 1993)

連續資料同化乃是依據估計理論(estimation theory)，利用統計方法預測系統變數，常見的方法有卡門濾波器(KF, Kalman Filter)、最佳內插法(OI, Optimal Interpolation)、逐步訂正法(SCM, Successive Correction Method)等。而變分資料同化是根據控制理論(control theory)，針對模式預報值，從空間與時間進行全面性的調整，屬於解決平滑化的問題，常用的方法為三維變分法(3D-Var)與四維變分法(4D-Var)。

◆ 連續資料同化法(sequential method)

(1) 卡門濾波法(KF, Kalman Filter)

連續資料同化所依據的估計理論之核心即是由Kalman(1960)所導出的卡門濾波法，它可決定出一個既和動力模式相協調，又按某個準確度接近觀測值的模式變數，以做為隨後預報的初始值之用。

考慮以下的離散動力模式：

$$\mathbf{x}_n = \mathbf{\Psi}_{n-1}\,\mathbf{x}_{n-1} + \boldsymbol{\varepsilon}^q_{n-1}, \quad n=1, 2, \cdots, N \qquad (1)$$

其中 $\mathbf{x}_n$ 表示 $t = n\Delta t$ 時的狀態向量(state vector)，即模式變數組成的向量，n 為時間指標，Δt 為時間間隔。$\mathbf{\Psi}$ 稱為預報算符(prediction operator)或系統算符(system operator)，$\boldsymbol{\varepsilon}^q$ 表示模式誤差(model error)或系統噪聲(system noise)。模式誤差代表數值模式 $\mathbf{\Psi}$ 所不能描述的動力或物理過程，尤其是網格系統所不能分辨的較小尺度現象。另外，它還包括將微分方程化為差分格式時帶來的誤差。簡單地說，模式誤差包括參數化誤差和離散化誤差。(1)式中 $\mathbf{x}$ 和 $\boldsymbol{\varepsilon}^q$ 是 $M\times1$ 單列向量，而 $\mathbf{\Psi}$ 為 $M\times M$ 常數矩陣。

假設模式誤差具有下面的特性：

$$\left\langle \boldsymbol{\varepsilon}^q_n \right\rangle = 0, \qquad \left\langle \boldsymbol{\varepsilon}^q_n \boldsymbol{\varepsilon}^{q^*}_{n'} \right\rangle = \mathbf{Q}_n \delta_{nn'} \qquad (2a,b)$$

(2a)式表示模式誤差是無偏的，而(2b)式表示不同時間的模式誤差彼此不相關，但同一時間的協方差為 $\mathbf{Q}_n$。(2b)式中 $\delta_{nn'}$ 是Kronecker 符號，當 n'=n 時 $\delta_{nn'}$=1，否則等於零。

假設由 t=0 時的分析值 $\mathbf{x}_0$ 可得到初始時刻的無偏估計值 $\hat{\mathbf{x}}_0 = \langle \mathbf{x}_0 \rangle$，並且之後不使用觀測資料。在此情況下，$\mathbf{x}_n$ 的最佳估計值 $\hat{\mathbf{x}}_n = \langle \mathbf{x}_n \rangle$ 可按下面的遞推關係式(recurrence relation)計算出來：

$$\hat{\mathbf{x}}_n = \boldsymbol{\Psi}_{n-1}\,\hat{\mathbf{x}}_{n-1}, \quad \hat{\mathbf{x}}_0 = \langle \mathbf{x}_0 \rangle \tag{3a,b}$$

(3a)式是將(1)式取平均而得到的，此即為沒有充分利用非定時資料的數值預報方法。但若使用觀測資料，就必須將它們和數值預報值結合，以便改進分析。

假設觀測量是 $\mathbf{y}_n^o$，它和狀態向量 $\mathbf{x}_n$ 有下面的關係：

$$\mathbf{y}_n^o = \mathbf{H}_n\,\mathbf{x}_n + \boldsymbol{\varepsilon}_n^o \tag{4}$$

其中 $\mathbf{H}_n$ 為觀測算符，$\boldsymbol{\varepsilon}_n^o$ 為觀測誤差。此誤差亦假設無偏，且不同時間的觀測誤為不相關，但同一時間的協方差為 $\mathbf{O}_n$：

$$\langle \boldsymbol{\varepsilon}_n^o \rangle = 0, \quad \langle \boldsymbol{\varepsilon}_n^o \boldsymbol{\varepsilon}_{n'}^{o^*} \rangle = \mathbf{O}_n \delta_{nn'} \tag{5}$$

其中模式誤差和觀測誤差也可設為彼此不相關，即

$$\langle \boldsymbol{\varepsilon}_n^q \boldsymbol{\varepsilon}_{n'}^{o^*} \rangle = \mathbf{0} \tag{6}$$

利用 $\mathbf{x}_n$ 的兩個數值，一為預報值 $\mathbf{x}_n^f$，另一為觀測值 $\mathbf{y}_n^o$，可得到極小方差估計值 $\mathbf{x}_n^a$：

$$\mathbf{x}_n^a = \mathbf{x}_n^f + \mathbf{K}_n\left(\mathbf{y}_n^o - \mathbf{H}_n \mathbf{x}_n^f\right) \tag{7}$$

其中最佳增益矩陣 $\mathbf{K}_n$ 是

$$\mathbf{K}_n = \mathbf{B}_n \mathbf{H}_n^*\left(\mathbf{H}_n \mathbf{B}_n \mathbf{H}_n^* + \mathbf{O}_n\right)^{-1} = \left(\mathbf{B}_n^{-1} + \mathbf{H}_n^* \mathbf{O}_n^{-1} \mathbf{H}_n\right)^{-1} \mathbf{H}_n^* \mathbf{O}_n^{-1} \tag{8}$$

此時分析誤差 $\boldsymbol{\varepsilon}_n^a = \mathbf{x}_n^a - \mathbf{x}_n$ 的協方差矩陣為

$$\mathbf{A}_n = \left(\mathbf{I} - \mathbf{K}_n \mathbf{H}_n\right)\mathbf{B}_n = \left(\mathbf{B}_n^{-1} + \mathbf{H}_n^* \mathbf{O}_n^{-1} \mathbf{H}_n\right)^{-1} \tag{9}$$

其中 $\mathbf{B}_n$ 是預報誤差 $\boldsymbol{\varepsilon}_n^f$ 的協方差矩陣：

$$\mathbf{B}_n = \langle \boldsymbol{\varepsilon}_n^f \boldsymbol{\varepsilon}_n^{f^*} \rangle \tag{10}$$

假如已有觀測資料 $\mathbf{y}_n^o$，卻仍按(3)式進行預報，雖然可由預報值 $\hat{\mathbf{x}}_n$ 和觀測值 $\mathbf{y}_n^o$ 得到一個在極小方差下最佳的分析值 $\mathbf{x}_n^a$，但此分析值對之後的預報並無影響，即觀測值並未改進往後的預報。因此，(3)式應改為

$$\mathbf{x}_n^f = \boldsymbol{\Psi}_{n-1}\,\mathbf{x}_{n-1}^a \tag{11}$$

亦即必須使用分析值 $\mathbf{x}_{n-1}^a$ 計算下一時步的預報值。預報誤差

可依次寫為

$$\boldsymbol{\varepsilon}_n^f = \mathbf{x}_n^f - \mathbf{x}_n = \boldsymbol{\Psi}_{n-1}\,\mathbf{x}_{n-1}^a - \mathbf{x}_n = \boldsymbol{\Psi}_{n-1}\boldsymbol{\varepsilon}_{n-1}^a - \boldsymbol{\varepsilon}_{n-1}^q \tag{12}$$

將(12)式代入(10)式得到$\mathbf{B}_n$：

$$\mathbf{B}_n = \boldsymbol{\Psi}_{n-1}\mathbf{A}_{n-1}\boldsymbol{\Psi}_{n-1}^* + \mathbf{Q}_{n-1} \tag{13}$$

其中$\mathbf{A}_n$為分析誤差協方差。

(7)、(8)、(9)、(11)和(13)式稱為 Kalman 濾波器(Kalman, 1960)，其中相應的連續時間的格式則稱為 Kalman-Bucy 濾波器。Kalman 濾波器可分為 4 個部分。

◆ 給定部分：$\boldsymbol{\Psi}_n$ 、$\mathbf{H}_n$ 、$\mathbf{y}_n^o$ 等矩陣和初始條件$\mathbf{x}_0^a$和$\mathbf{A}_0$必須事先給定。

◆ 估計部分：模式誤差的協方差$\mathbf{Q}_n$和觀測誤差的協方差$\mathbf{O}_n$必須事先估計出來。這部分是 Kalman 濾波器在實際工作時問題最大的部分。

◆ 預報部分：即(11)式和(13)式。

$$\mathbf{x}_n^f = \boldsymbol{\Psi}_{n-1}\,\mathbf{x}_{n-1}^a \tag{14}$$

$$\mathbf{B}_n = \boldsymbol{\Psi}_{n-1}\mathbf{A}_{n-1}\boldsymbol{\Psi}_{n-1}^* + \mathbf{Q}_{n-1} \tag{15}$$

◆ 分析部分：即(8)、(9)和(7)式。

$$\mathbf{K}_n = \mathbf{B}_n\mathbf{H}_n^*\left(\mathbf{H}_n\mathbf{B}_n\mathbf{H}_n^* + \mathbf{O}_n\right)^{-1} = \left(\mathbf{B}_n^{-1} + \mathbf{H}_n^*\mathbf{O}_n^{-1}\mathbf{H}_n\right)^{-1}\mathbf{H}_n^*\mathbf{O}_n^{-1} \tag{16}$$

$$\mathbf{A}_n = \left(\mathbf{I} - \mathbf{K}_n\mathbf{H}_n\right)\mathbf{B}_n = \left(\mathbf{B}_n^{-1} + \mathbf{H}_n^*\mathbf{O}_n^{-1}\mathbf{H}_n\right)^{-1} \tag{17}$$

$$\mathbf{x}_n^a = \mathbf{x}_n^f + \mathbf{K}_n\left(\mathbf{y}_n^o - \mathbf{H}_n\mathbf{x}_n^f\right) \tag{18}$$

在實際執行計算時，Kalman 濾波器會發生一個很重要的問題，即計算協方差演變方程帶來的龐大計算量，(14)與(18)式代表每計算一個Δt都需要用到 $O(M)$的計算量，(15)和(16)式則是 $O(M^2)$的計算量，當 $M>10^6$時，所需之硬體設施較為先進，導致成本大幅上升，因此不適用在系統變數較多的計算上。於是許多所謂的次最佳法(SOS, SubOptimal Scheme)，均為使用以下所提的方向去克服上述的困難，簡言之，即利用系統矩陣$\boldsymbol{\Psi}_n$ 和協方差矩陣$\mathbf{A}_n$與$\mathbf{B}_n$的特性，也許能將計算量減少到 $O(M)$。

✧ 簡化或近似系統矩陣，例如採用穩態(steady)卡門增益

(Chandrasekhar type filter)；使用奇異數分離法(SVD, Singular Value Decomposition)來近似系統矩陣。

✧ 為了減少誤差傳輸，從簡化模式之機制著手，以便降低系統變數之轉置矩陣的大小，例如使用粗網格之協方差矩陣再內插至較細網格。

✧ 從近似誤差協方差矩陣著手。許多區域的海岸模式均從這種方式來解決問題，如使用平方根法來近似誤差協方差矩陣；使用平方根法及帶狀法來近似誤差協方差矩陣；使用平方根及較低秩(rank)之特徵值矩陣來近似協方差矩陣之傳輸，RRSQRT(Reduced Rank Square RooT filter)即是此方法。

在一維線性化模式上的應用可參考 Ghilet al. (1981)及 Ghil (1989)；至於二維的應用，可參考 Ghil and Malanotte - Rizzoli (1991), Cohn and Parrish (1991) 及 Dee (1991)。

對非線性情況來說，最佳濾波器方程為已知 (Jazwinsky, 1970)，但它們的解需要用到閉合假設(closure assumption)及其它的假設，例如 Lorence (1988)提到的正態分布假設。非線性濾波器最簡單近似之一就是所謂的擴張 Kalman 濾波器 (Extended Kalman filter)，即(14)與(18)式以下列的式子取代：

$$\mathbf{x}_n^f = \mathbf{F}_{n-1}\,\mathbf{x}_{n-1}^a \tag{19}$$

$$\mathbf{x}_n^a = \mathbf{x}_n^f + \mathbf{K}_n\left(\mathbf{y}_n^o - \mathbf{h}_n \mathbf{x}_n^f\right) \tag{20}$$

至於(15)、(16)和(17)式仍保留原形，但兩個矩陣的定義需改為下式：

$$\mathbf{\Psi}_n = \mathbf{F}_n^{'}\mathbf{x}_n^a \qquad \mathbf{H}_n = \mathbf{h}_n^{'}\mathbf{x}_n^f \tag{21a,b}$$

其中 $\mathbf{F}_n^{'}$ 為 $\mathbf{F}_n$ 關於 $\mathbf{x}$ 的 Jacobi 矩陣，它的第(k,l)個元素是 $\partial F_k/\partial x_l$，$\mathbf{F}_k$ 為 $M\times 1$ 單列向量 $\mathbf{F}$ 的第 k 個分量，而 $\mathbf{x}_l$ 為 $M\times 1$ 單列向量 $\mathbf{x}$ 的第 l 個分量。Bouttier (1994)使用擴張 Kalman 濾波器的一個近似來估計同化系統的預報誤差和分析誤差的協方差。

另外，系集卡門濾波法(EnKF, Ensemble Kalman Filter)則以有限個隨機樣本來估計協方差矩陣，並以蒙地卡羅法

(Monte Carlo) 求解模式相應機率密度的連續方程式稱為 Fokker-Planck 方程式或稱為 Kolmogorov 方程式。POEnKF (Partially Orthogonal Ensemble Kalman Filter)財是利用協方差矩陣之較低秩近似值來作為系集卡門濾波法之變異縮減 (variance reductor)。

(2) 最佳內插法 (OI, Optimal Interpolation)

在資料同化循環中，假如實測資料在空間分布的密度均勻，且具有高度準確性，則利用一般的內插方法就可以獲得良好的資料同化結果，若海面上的觀測資料分布不均勻，以直接內插方式進行同化分析，容易產生不真實的分析值而影響模式推算。最佳內插法是Gandin (Гандин, 1963； Gandin, 1965)為氣象資料處理而發展出來的客觀分析法，主要是建立觀測資料之統計架構，並決定最佳的權重，再將各測站上的觀測資料內插至計算格點上，以獲得最佳的分析值，作為下一時刻模式計算的初始場，又稱為統計內插法(statistical interpolation)。(陳，2004)

最佳內插法是以最小二乘法的概念，利用極小方差估計 (minimum variance estimation) 可得線性分析格式，如下：

$$\mathbf{H}_i^A = \mathbf{H}_i^P + \sum_{j=1}^{N_{obs}} \mathbf{W}_{ij}\left(\mathbf{H}_j^O - \mathbf{H}_j^P\right) \quad (22)$$

其中 N_{obs} 為實測站的數目，$\mathbf{H}^O$ 為實測波高值， $\mathbf{H}^P$ 為模式計算的起始猜測值，$\mathbf{H}^A$ 為經同化分析後的分析值，$\mathbf{W}_{ij}$ 則為各觀測站相對於計算格點的最佳權重，上標 i 表示計算格點，下標 j 表示測站指標。

由於實測波高值 $\mathbf{H}^O$ 、模式的起始猜測值 $\mathbf{H}^P$ 及分析值 $\mathbf{H}^A$ 與真值 $\mathbf{H}^T$ 之間含有誤差 ε 的存在，如下表示

$$\boldsymbol{\varepsilon}^O = \mathbf{H}^O - \mathbf{H}^T \quad (23)$$

$$\boldsymbol{\varepsilon}^P = \mathbf{H}^P - \mathbf{H}^T \quad (24)$$

$$\boldsymbol{\varepsilon}^A = \mathbf{H}^A - \mathbf{H}^T \quad (25)$$

其中 $\boldsymbol{\varepsilon}^O$ 、$\boldsymbol{\varepsilon}^P$ 及 $\boldsymbol{\varepsilon}^A$ 分別為實測波高值、模式的起始猜測值及分

析值與真值之間的偏差量，將式 (23)、(24)、(25) 代入式 (22)，可得

$$\boldsymbol{\varepsilon}_i^A = \boldsymbol{\varepsilon}_i^P + \sum_{j=1}^{N_{obs}} \mathbf{W}_{ij}\left(\boldsymbol{\varepsilon}_j^O - \boldsymbol{\varepsilon}_j^P\right) \tag{26}$$

為求得最小化的分析誤差，故以分析誤差之均方誤差 (mean square error)決定最佳化的權重 $\mathbf{W}_{ij}$，而均方誤差表示如下

$$\mathbf{E}_A^2 = \left\langle \left(\boldsymbol{\varepsilon}^A\right)^2 \right\rangle \tag{27}$$

上式尖端括號為期望算符。將式 (26) 代入式 (27)，則可表示為

$$\begin{aligned}\mathbf{E}_A^2 = &\left\langle \boldsymbol{\varepsilon}_i^P \boldsymbol{\varepsilon}_i^P \right\rangle + \sum_{j=1}^{N_{obs}} \mathbf{W}_{ik}\left\langle \boldsymbol{\varepsilon}_i^P \boldsymbol{\varepsilon}_j^O \right\rangle - \sum_{j=1}^{N_{obs}} \mathbf{W}_{ij}\left\langle \boldsymbol{\varepsilon}_i^P \boldsymbol{\varepsilon}_j^P \right\rangle + \sum_{j=1}^{N_{obs}} \mathbf{W}_{ik}\left\langle \boldsymbol{\varepsilon}_i^P \boldsymbol{\varepsilon}_k^O \right\rangle - \sum_{j=1}^{N_{obs}} \mathbf{W}_{ik}\left\langle \boldsymbol{\varepsilon}_i^P \boldsymbol{\varepsilon}_k^P \right\rangle \\ &+ \sum_{j=1}^{N_{obs}}\sum_{k=1}^{N_{obs}} \mathbf{W}_{ij}\mathbf{W}_{ik}\left(\left\langle \boldsymbol{\varepsilon}_j^O \boldsymbol{\varepsilon}_k^O \right\rangle + \left\langle \boldsymbol{\varepsilon}_j^P \boldsymbol{\varepsilon}_k^P \right\rangle\right) - 2\sum_{j=1}^{N_{obs}}\sum_{k=1}^{N_{obs}} \mathbf{W}_{ij}\mathbf{W}_{ik}\left(\left\langle \boldsymbol{\varepsilon}_j^O \boldsymbol{\varepsilon}_k^O \right\rangle + \left\langle \boldsymbol{\varepsilon}_j^P \boldsymbol{\varepsilon}_k^O \right\rangle\right)\end{aligned} \quad (28$$

假設實測值誤差 $\boldsymbol{\varepsilon}^O$ 與起始猜測值誤差 $\boldsymbol{\varepsilon}^P$ 不相關，即 $\left\langle \boldsymbol{\varepsilon}_i^P \boldsymbol{\varepsilon}_i^O \right\rangle = 0$ 、$\left\langle \boldsymbol{\varepsilon}_j^O \boldsymbol{\varepsilon}_k^P \right\rangle = 0$ ，並定義 $\mathbf{P} = \left\langle \boldsymbol{\varepsilon}^P \boldsymbol{\varepsilon}^P \right\rangle$ 、 $\mathbf{O} = \left\langle \boldsymbol{\varepsilon}^O \boldsymbol{\varepsilon}^O \right\rangle$ ，則(28)式可改寫為

$$\mathbf{E}_A^2 = \mathbf{P}_{ii} - \sum_{j=1}^{N_{obs}} \mathbf{W}_{ik}\mathbf{P}_{ij} - \sum_{j=1}^{N_{obs}} \mathbf{W}_{ij}\mathbf{P}_{ik} + \sum_{j=1}^{N_{obs}}\sum_{k=1}^{N_{obs}} \mathbf{W}_{ij}\mathbf{W}_{ik}\left(\mathbf{O}_{jk} + \mathbf{P}_{jk}\right) \tag{29}$$

其中 $\mathbf{P}$ 為起始猜測值的均方誤差矩陣，$\mathbf{O}$ 為實測值的均方誤差矩陣，將(29)對 $\mathbf{W}_{ik}$ 微分，為求最小化故令其微分結果為零，可得

$$\sum_{j=1}^{N_{obs}} W_{ij}(\mathbf{P}_{jk} + \mathbf{O}_{jk}) = \mathbf{P}_{ik}, \ k = 1,2,3,\cdots,N_{obs} \tag{30}$$

定義 $\mathbf{M}_{jk} = \mathbf{P}_{jk} + \mathbf{O}_{jk}$ ，進一步將(30)式化為聯立方程組

$$\begin{bmatrix} W_{i1} & \cdots & W_{ij} \end{bmatrix} \begin{bmatrix} \mathbf{M}_{11} & \cdots & \mathbf{M}_{1k} \\ \vdots & \ddots & \vdots \\ \mathbf{M}_{j1} & \cdots & \mathbf{M}_{jk} \end{bmatrix} = \begin{bmatrix} \mathbf{P}_{i1} & \cdots & \mathbf{P}_{ik} \end{bmatrix} \tag{31}$$

利用矩陣轉置的關係 $(W_{ij}\mathbf{M}_{jk})^T = M_{jk}^T W_{ij}^T = P_{ik}^T$，上式方程組可表示為

$$\begin{bmatrix} \mathbf{M}_{11} & \cdots & \mathbf{M}_{1j} \\ \vdots & \ddots & \vdots \\ \mathbf{M}_{k1} & \cdots & \mathbf{M}_{kj} \end{bmatrix} \begin{bmatrix} W_{1i} \\ \vdots \\ W_{ji} \end{bmatrix} = \begin{bmatrix} \mathbf{P}_{1i} \\ \vdots \\ \mathbf{P}_{ki} \end{bmatrix} \tag{32}$$

其中 $\mathbf{P}_{ki}$ 為各測站相對於計算格點起始清測值的均方誤差，$\mathbf{M}_{kj}$

為兩測站間實測值與起始猜測值的均方誤差之和。由(32)式可知，欲求取各測站分配於計算格點的最佳權重，必須求解 N_{obs} 組聯立方程組，若僅有少量的觀測站，則以高斯消去法就可以求解出最佳權重。

若已知真值的狀況下，可以順利求得實測值與起始猜測值的均方誤差，但實際上，並無法得知實際海面上的真實波高。Lionello等人(1992)曾利用指數函數表示二測站的起始猜測值均方誤差的關係，當兩測站的距離愈遠，則均方誤差影響愈小，並假設二測站的實測值誤差不相關，故實測值均方誤差為對角矩陣，其關係如下所示

$$\mathbf{P}_{kj} = \exp\left(-\frac{|\gamma_{kj}|}{L_{max}}\right) \tag{33}$$

$$\mathbf{O}_{kj} = \delta_{kj}\left(\frac{(\varepsilon_k^O)^2}{(\varepsilon_k^P)^2}\right) = \delta_{kj}\mathbf{R}_k \tag{34}$$

其中 γ_{kj} 為 k、j 二測站的距離，L_{max} 為校正長度(correlation length)，**R**為實測值與起始猜測值的均方誤差比。

(3) 逐步訂正法(SCM, Successive Correction Method)

逐步訂正法在 1950 年代被發展出來(Bergthorson and Döös, 1955； Cressman, 1959)，由於方法簡單，1970 年代被廣泛應用在客觀分析，但目前已逐漸被統計內插法取代，在 Thiébaux and Pedder (1987) 被歸類為經驗線性內插法(empirical linear interpolation)。

Cressman 方法是設計用於系統僅具有少數稀疏散之觀測資料，可用來改早期多項式弧線方法(polynomial spline methods)，使其適用於大區域中僅具低密度資料之狀態，由於國內目前海域之觀測站稀少，同時因逐步訂正法相當簡單且計算速度快，又這個方法可使用越來越準確之數值預報值當做背景場，大致上也有不錯之分析結果，因此逐步訂正法理應可用以建立具資料同化功能力作業化預測模式。

在 SCM 法中，格點上之起始估計值可設定為背景場或起始場測值，即 $X_i^0 = X_i^b$，其中 X_i^b 表背景場在第 i 個格點上之值，X_i^0 表第零次疊代之格點估計值。

在起始之估計後，將進入逐步訂正(SCM)之疊代程序，如下：

$$X_i^{n+1} = X_i^n + \frac{\sum_{k=1}^{K_i^n} w_{ik}^n (Z_k^O - X_k^n)}{\sum_{k=1}^{K_i^n} w_{ik}^n + \varepsilon^2} \tag{35}$$

其中，X_i^n 表第 n 次疊代後格點 i 之估計值；Z_k^0 表 i 格點周圍之第 k 個觀測點之觀測值；X_k^n 表 i 格點周圍之第 k 個觀測點上在第 n 次疊代後之估計值，可利用鄰近計算格點上之值以內插法求得；K_i^n 為格點 i 在影響半徑 R_n 內之觀測點數目；ε^2 為觀測誤差變異對背景場誤差變異之比值；w_{ik}^n 為權重函數(weighting function)，有不同之表示方式。Cressman (1959) 在 SCM 法中將 w_{ik}^n 定義為：

$$\begin{aligned} w_{ik}^n &= \frac{R_n^2 - r_{ik}^2}{R_n^2 + r_{ik}^2}, \quad r_k < R \\ &= 0, \quad r_k \geq R \end{aligned} \tag{36}$$

其中，r_{ik}^2 表觀測點位置 r_k 與格點位置 r_i 之距離平方；R_n 為影響半徑(radius of influence)，允許在每次疊代時變動，由(36)式可知，距格點越近，測站的資料對這個格點的影響越大，若測站 k 在影響半徑外面，則該測站對這個格點就毫無影響了。

在 Cressman 之 CSM 法中，參數 ε^2 假設為零。本法對於當觀測點與網格點重疊時且採用很小之影響半徑時，具有收斂至觀測值之能力。整體上來說，SCM 法簡單且經濟，同時可達到合理之分析效果。Bratseth (1986)研究顯示，若能適當選擇權重函數，而非採用經驗式，則 SCM 法也可以達到最佳內插法 OI 之效果。

◆ 變分資料同化法(variational method)

變分法可視為一種平滑的過程，在涵蓋整個同化的時間內，調整模式計算值至所有可用的觀測值，而許多海岸模式均使用變分法來估計模式的參數(parameter estimation)。在變分法中，定義所謂的目標函數，包含觀測值及預報值的差值與模式控制方程式及參數的約束(constraint)條件，藉由找出最佳估值使得目標函數的積分有極小值，此相應的估值稱為最大後驗機率估計值(maximum a posteriori probability estimate)。

變分學主要討論泛函(functional)求極值的問題，所謂泛函是指一個或多個函數的函數，因此變分學自然是處理連續情況的問題，而它跟極大後驗機率估值的相應連續情況有關，因此決定這個估計值的方法通常稱為變分資料同化。(曾，2006)

變分資料同化的目的是找出一組最佳的初始分析，透過疊代處理過程找出在給定同化視窗的時候，還能逼近初始猜測值與觀測資料之初始分析。此目的可透過最小化一個「目標函數」(cost function)來達成，定義為(Parrish and Derber，1992)：

$$\begin{aligned} J(\mathbf{x}) &= \frac{1}{2}(\mathbf{x}-\mathbf{x}^{b})^{T}\mathbf{B}^{-1}(\mathbf{x}-\mathbf{x}^{b}) + \frac{1}{2}[H(\mathbf{x})-\mathbf{y}^{obs}]^{T}(\mathbf{O}+\mathbf{F})^{-1}[H(\mathbf{x})-\mathbf{y}^{obs}] + J_c \\ &= J_b + J_o + J_c \end{aligned} \quad (37)$$

其中 $\mathbf{x}$ 為模式分析變數，$\mathbf{x}^{b}$ 為初始猜測值，$\mathbf{y}^{obs}$ 為實際觀測，H 是將模式格點分析轉換成觀測變數之觀測算子，為一非線性算子，B、O、F 分別為背景誤差、觀測誤差、觀測算子與代表性誤差的協方差矩陣，J_c 是為三維變分同化附加的一弱約束條件項。

藉由逐步微調初始猜測值($\mathbf{x}^{b}$)使得目標函數達到最小，此為一透過變分最小化過程而得之 x，即為所欲尋求的解。

四維變分法為三維變分法的延伸。考慮在一時間間隔內之觀測值，而不僅是某一時間的觀測值，其使用強約束條件，並尋求最佳起始值使得在同化的時間間隔內預報值最符合觀測值，通常使伴隨或稱共軛法(adjoint method)求解。若使用弱約束條件時，則形成廣義的反問題(generalized inverse)，可用 Representer 法。其它直接求解最小化目標函數，但不使用 Euler-Lagrange 方程式

的方法，包括牛頓及類牛頓法、共軛梯度法、下降法(descent method)、陡降法(steepest descent method)等。

所謂的伴隨(adjoint)理論，精神在於利用算子交換的特性。為了要方便完成算子的交換，伴隨理論在線性理論的架構下探討問題，由原線性方程有關的線性算子，經過算子交換過程後，得到作用在另一變數上的伴隨算子，其目的在迴避對原方程變數做繁瑣的直接計算而求得解答的一種方法。首先，將非線性的模式用矩陣代數符號寫為

$$\frac{\partial \mathbf{x}}{\partial t} = \mathbf{n}(\mathbf{x}) \tag{38}$$

其中 **n** 是非線性算子，**x** 為變數所組成的行向量，再將(38)式寫成數值格式

$$\mathbf{x}(t) = \mathbf{N}(\mathbf{x}(t_0)) = \int_0^t \mathbf{n}(\mathbf{x}(t'))dt' \tag{39}$$

由(39)式可知某個時間 **x**(t)可透過一算子 **N** 和初始值 $\mathbf{x}(t_0)$求得，則所求目標函數可定義成

$$\mathbf{J} = \frac{1}{2}\sum_{t=t_0}^{t_f}(x(t)-\overline{x}(t))^T \mathbf{w}(x(t)-\overline{x}(t)) \tag{40}$$

其中 $\overline{x}(t)$ 表示另一種相對狀態的變數，如觀測場、背景場，而 **J** 就是目標函數，由 x(t) 和 $\overline{x}(t)$ 在時間 t_0 和 t_f 之間的所有差值組成，是一個四維空間(三空空間+時間)所組成的函數，所以求算 **J** 的極值過程就稱為四維變分

由(39)式可知，每一個時刻的 $\overline{x}(t)$ 都可以用 $x(t_0)$ 來表示，$\overline{x}(t)$ 本身可視作已知的常數，於是(40)式可化簡成全是由 $x(t_0)$ 所組成的函數，此時問題就變成當 $x(t_0)$ 為多少時，才能得到 **J** 的極小值，將(40)式對 x(t) 微分時可得

$$\frac{\partial \mathbf{J}}{\partial \mathbf{x}(t)} = \sum_{t_0}^{t_f}\mathbf{w}(\mathbf{x}(t)-\overline{\mathbf{x}}(t)) \tag{41}$$

將(38)式作Taylor級數展開，取一階導數近似，扣除擾動高次項和非線性算子後得到

$$\frac{\partial \delta\mathbf{x}}{\partial t} = \frac{\partial \mathbf{n}}{\partial \mathbf{x}}\delta\mathbf{x} \tag{42}$$

仿照(39)式可寫成

$$\delta \mathbf{x} = \mathbf{L}(\delta \mathbf{x}(t_0)) = \int_{t_0}^{t} \mathbf{L}(\delta \mathbf{x}(t'))dt' \tag{43}$$

(43)式也可稱為正切線性模式。再將(43)式代回(42)式，得

$$\delta \mathbf{J} = \sum_{t=t_0}^{t_f} (\mathbf{x}(t) - \overline{\mathbf{x}}(t))^T \mathbf{WL}\delta \mathbf{x}(t_0) \tag{44}$$

由導數定義

$$\delta \mathbf{J} = (\nabla \mathbf{J})^T \delta \mathbf{x}(t_0) \tag{45}$$

比較(44)、(45)兩式，可知

$$\nabla \mathbf{J} = \mathbf{L}^T \sum_{t=t_0}^{t_f} \mathbf{W}(\mathbf{x}(t) - \overline{\mathbf{x}}(t)) \tag{46}$$

這裡的$\mathbf{L}^T$就是伴隨算子，由(45)式來看，可發現目標函數對初始值的梯度就是(46)式，如果定義初始伴隨變數$\delta \mathbf{x}_a(t_0)$，且$\delta \mathbf{x}(t) = \mathbf{W}(\mathbf{x}(t) - \overline{\mathbf{x}}(t))$，其滿足下列關係式

$$\delta \mathbf{x}_\mathbf{a}(t_0) \equiv \nabla \mathbf{J} = \mathbf{L}^T \sum_{t=t_0}^{t_f} \mathbf{W}(\mathbf{x}(t) - \overline{\mathbf{x}}(t)) = \mathbf{L}^T \delta \mathbf{x}(t) \tag{47}$$

則此式為伴隨模式。相較於(40)、(43)式來說伴隨模式是一個時間逆向的模式，可以想成將一組的δx向量回溯積分$\delta \mathbf{x}_a(t_0)$，同時這個向量也是目標函數對初始向量的梯度。當梯度決定後，上沿正梯度方向應用數值疊代法運算可得目標函數的極大值，沿負梯度方向可得出極小值。

3.3.4 資料同化方法可行性評估

本計畫預計使用 ROMS (Regional Ocean Modeling System)進行海象預報，針對 ROMS 資料同化的部分，將由以下的項目進行可行性評估：

1). 使用廣義穩態理論 (Generalized Stability Theory, GST)探討海洋模式中未確定的初始與邊界條件，也就是計算出切線性理論(Tangent Linear Model, TLM)的奇異向量(singular vector)而得到初始與邊界條件的誤差值，並納入海象模式中運算。

2). 將針對兩種不同的資料同化方法進行比較，四維變分法(4D-Var)和海洋逆模式(Inverse Ocean Model, IOM)。四維變分法發展可用於 ROMS 和 TOMS(Terrain-coordinate Ocean Modeling

System)，主要是對動力的部分加上一強約束，也就是假設無模式誤差值。另一方面則是採用由美國奧勒崗州立大學 (Oregon State University, OSU)最新建立的海洋逆模式，它不但把誤差值納入考量，並針對非線性解的部分使用由NSF (National Science Foundation)發展的線性估計模式做計算。

3). 為了建立最完善的海洋模式，將嘗試採用在第一項計算出的最佳結果，並參考在一些在數值天氣預報中心已實際操作的氣象預測模式。

自從 2004 年，ROMS 模式本身已完成以下與資料同化相關之項目測試：(Emanuele Di Lorenzo)

1. 過去建立 TLM 與 adjoint version 時，是無法同時針對程式碼進行測試和除錯，目前已發展測試 TL 和 adjoint version 的計算框架，因為這項重要的進展，使得往後進行資料同化前便可除去一些錯誤，而減少計算的時間長度。
2. 針對 adjoint version 的部分，已建立相關的敏感度分析平台。
3. 已完成模擬南加州灣(Southern California Bight)的物理生物耦合模式，並進行一連串的 adjoint version 敏感度試驗。
4. 對南加州灣的模式，已發展四維變分法和海洋逆模式兩方法的計算平台，並嘗試探討其解的收斂與計算效率。
5. NPZD(Nutrient Phytoplankton Zooplankton Detritus) biological ocean model裡的TLM和adjoint version已完成建立於 ROMS 內，並已針對南加州灣的硝酸鹽(N)、浮游生物(P)、浮游動物(Z)和碎屑(D)濃度等因素進行敏感度分析(圖 3.3.4-1)。(Moore et al., 2005)

另外，Lorenzo et al. (2005)曾利用南加州灣區域，測試 ROMS 配合 IOM 的計算結果(圖 3.3.4-2)，若是利用強約束試驗進行資料同化循環，比起未使用資料同化循環的結果相比，可減少 75%觀測值與預報值之間的初始誤差；若是弱約束試驗，則可減少 89%的誤差，顯示出使用資料同化的必要性。

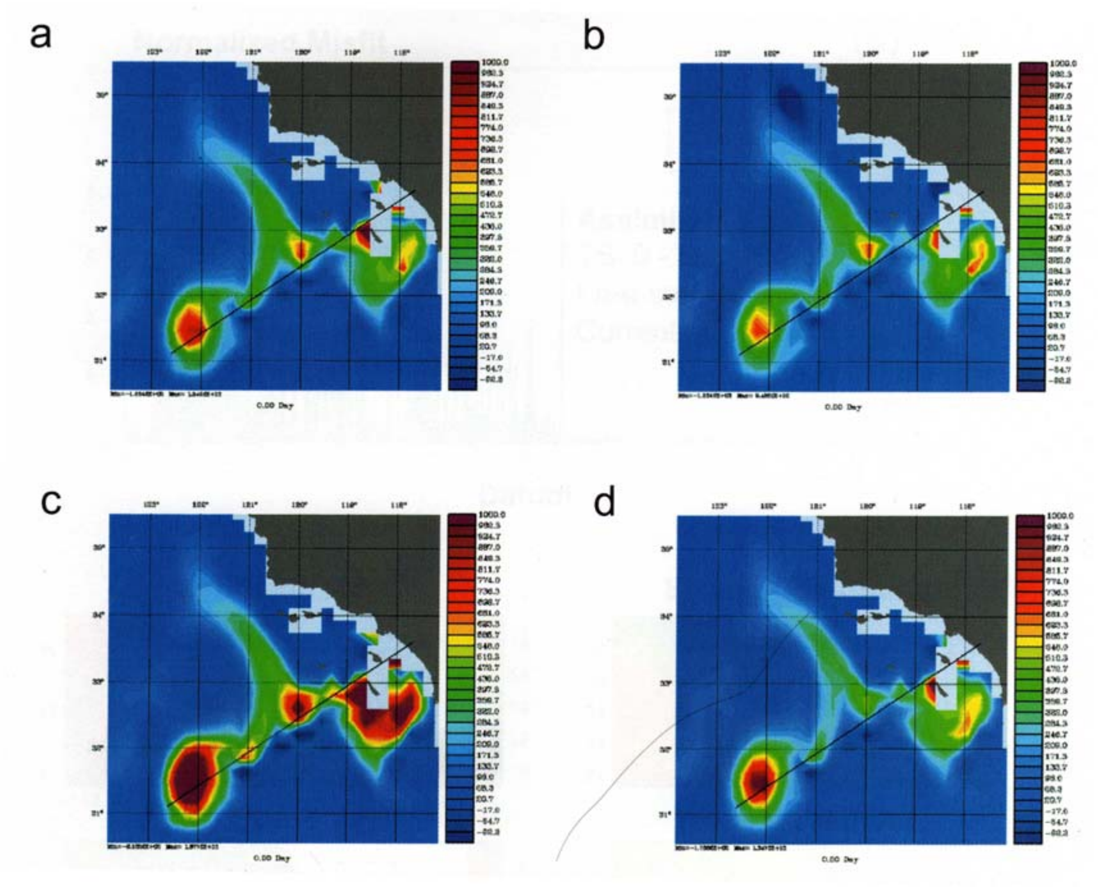

圖 3.3.4-1 (a)硝酸鹽、(b)浮游生物、(c)浮游動物和(d)碎屑濃度之敏感度分析結果(Moore et al., 2005)

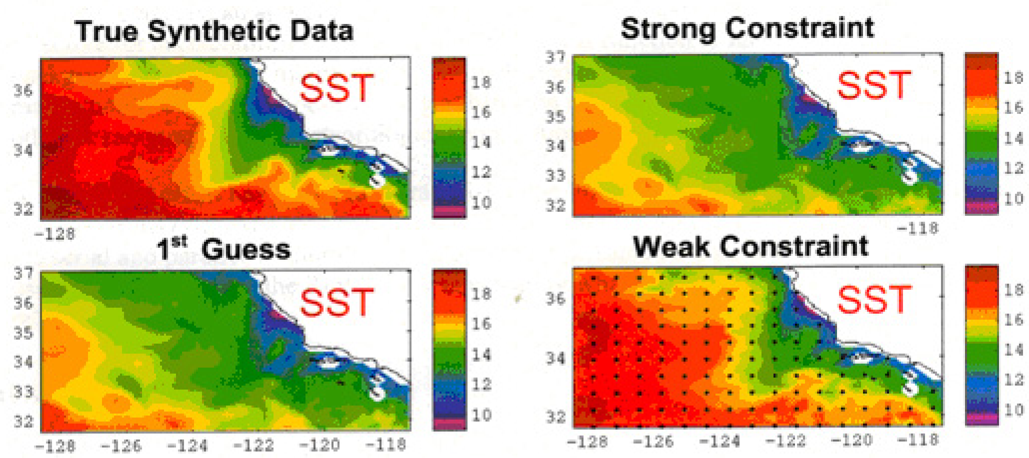

圖 3.3.4-2 SST 資料同化比較結果。左上：觀測值，左下：初次猜測場，右上：加入強約束條件，右下：加入弱約束條件(Lorenzo et al., 2005)

模式校驗及評估準則

數值模式能針對各規模尺度的現象進行分析、現報或預報，加上近年來電腦科技的進度與改善，因此使用數值模式進行研究的學者愈來愈多，但其準確度還需要由模式的預測值與實測值的比較來決定，因此美國國家海洋局(National Ocean Service)對水位及海流的模式評估定下了一些準則，以方便各海洋學家進行往後的研究。

就資料的尺度而言，不論是觀測值或是模式模擬值，最重要的就是各資料的單位必須一致。資料時間的間隔最佳為每六分鐘一筆，但若資料為水位則建議是每小時一筆，而觀測值的時間長度方面最好是每種資料都超過一年，且需針對缺漏的部分進行適當的補遺，但由於要獲得長達一年的觀測資料並不容易，因此 NOS 建議水位資料長度至少要有六個月，海流的資料則至少有要 29 天以上，如此所進行的分析才有代表性。

除了上述的準則，另外還可依據一些統計方法對模式進行評估(表 3.3-1)，依序有觀測值與模擬值的誤差(error)、平均數(SM)、均方根誤差(RMSE)、誤差的標準偏差(SD)、中心頻率(CF)、正偏移頻率(POF)、負偏移頻率(NOF)、正極端值的最大延時(MDPO)、負極端值的最大延時(MDNO)與最糟情況的極端值頻率(WOF)。針對這些項目，NOS 對 error、SM、RMSE 和 SD 並無限定，使用者可自行定義，但其它項目 NOS 則有如下標準值需遵循。(Hess et al., 2003)

$$NOF(X) \le 1\% \tag{48}$$

$$CF(X) \ge 90\% \tag{49}$$

$$POF(X) \le 1\% \tag{50}$$

$$MDPO(2X) \le L \tag{51}$$

$$MDNO(2X) \le L \tag{52}$$

$$WOF(2X) \le 0.5\% \tag{53}$$

L 為使用者自行定義之最大延時

表 3.3-1 Skill Assessment Statistics (from Hess et al., 2003)

Variable	Explanation
Error	The error is defined as the predicted value, p, minus the reference (observed or astronomical tide value, r : $e_i = p_i - r_i$.
SM	Series Mean. The mean value of a series y. Calculated as $\bar{y} = \frac{1}{N}\sum_{i=1}^{N} y_i$.
RMSE	Root Mean Square Error. Calculated as $RMSE = \sqrt{\frac{1}{N}\sum_{i=1}^{N} e_i^2}$.
SD	Standard Deviation. Calculated as $SD = \sqrt{\frac{1}{N-1}\sum_{i=1}^{N} (e_i - \bar{e})^2}$
CF(X)	Central Frequency. Fraction (percentage) of errors that lie within the limits ±X.
POF(X)	Positive Outlier Frequency. Fraction (percentage) of errors that are greater than X.
NOF(X)	Negative Outlier Frequency. Fraction (percentage) of errors that are less than -X.
MDPO(X)	Maximum Duration of Positive Outliers. A positive outlier event is two or more consecutive occurrences of an error greater than X. MDPO is the length of time (based on the number of consecutive occurrences) of the longest event.
MDNO(X)	Maximum Duration of Negative Outliers. A negative outlier event is two or more consecutive occurrences of an error less than -X. MDNO is the length of time (based on the number of consecutive occurrences) of the longest event.
WOF(X)	Worst Case Outlier Frequency. Fraction (percentage) of errors that, given an error of magnitude exceeding X, either (1) the simulated value of water level is greater than the astronomical tide and the observed value is less than the astronomical tide, or (2) the simulated value of water level is less than the astronomical tide and the observed value is greater than the astronomical tide.

在觀測資料方面，若有資料缺漏，則需進行補遺，其建議方法有線性內插法(linear interpolation)、三次樣條內插法(cubic spline interpolation)和特徵值分解法(singular value decomposition)。線性內插法只適用於缺漏資料少的情況，如果缺漏的情況嚴重，則需使用三次樣條內插法或特徵值分解法，但使用特徵值分解法時需小心其計算量大，且速度慢。另外，還建議使用傅立葉過濾器將資料裡的極值與雜訊過濾，水位資料的部分如上述所言，至少需 6 個月的資料長度，使用最小二乘調和分析法(least squares harmonic analysis)或是傅立葉調和分析法(Fourier harmonic analysis)將天文潮與非天文潮分離。

第四章 模式可行性評估

本章節將進行模式可行性的評估，由於本團隊規劃之模式系統涵蓋四個模式範圍，包含大區域的太平洋及北太平洋環流模式，以及較小範圍的西北太平洋及台灣海域海流模式。因此將選擇四個國際間以通行應用的作業化模式分為區域模式與近岸模式分別探討各個模式的特性，最後建議最適當的模式建置未來太平洋及北太平洋範圍環流系統。

4.1 區域模式

4.1.1 POLCOMS 模式

透過海洋模式的建構，可用以了解台灣附近海域時空的變化，藉由適當的邊界與參數調校，模式預測的結果最終可達到海流預報作業化的結果，POLCOMS 即為一應用於西北歐大陸棚區域、結合時、空變化的海洋生態系統作業化模式，目前應用於英國，由 POL 海洋研究中心負責發展及執行（http://cobs.pol.ac.uk/cobs/sat/）。本模式以斜壓水動力模式 POL-3DB 為主要計算核心，配合歐洲邊緣海生態模式（ERSEM）而成，其中包含了深海浮游植物、浮游動物動力、氮、磷與矽之循環等重要過程，模式架構如圖 4.1.1-1，此一水理與生態耦合模式的結果提供了物理與生物的關鍵變數之高解析空間變化，並藉由各種物理、生物過程（process）之時空變化來解釋北海春季藻華現象（spring bloom）的形成，模式中對於各種營養鹽與浮游植物的季節變化，都能模擬出與現場資料趨勢及量相符的結果；基本物理的部份則涵蓋水位、流速與溫度及鹽度等項目，配合各地潮位站與衛星資料每天進行作業化預報，並同時比對其結果，其應用可作為台灣發展相關技術之借鏡，以下針對本模式與其特點進行介紹。

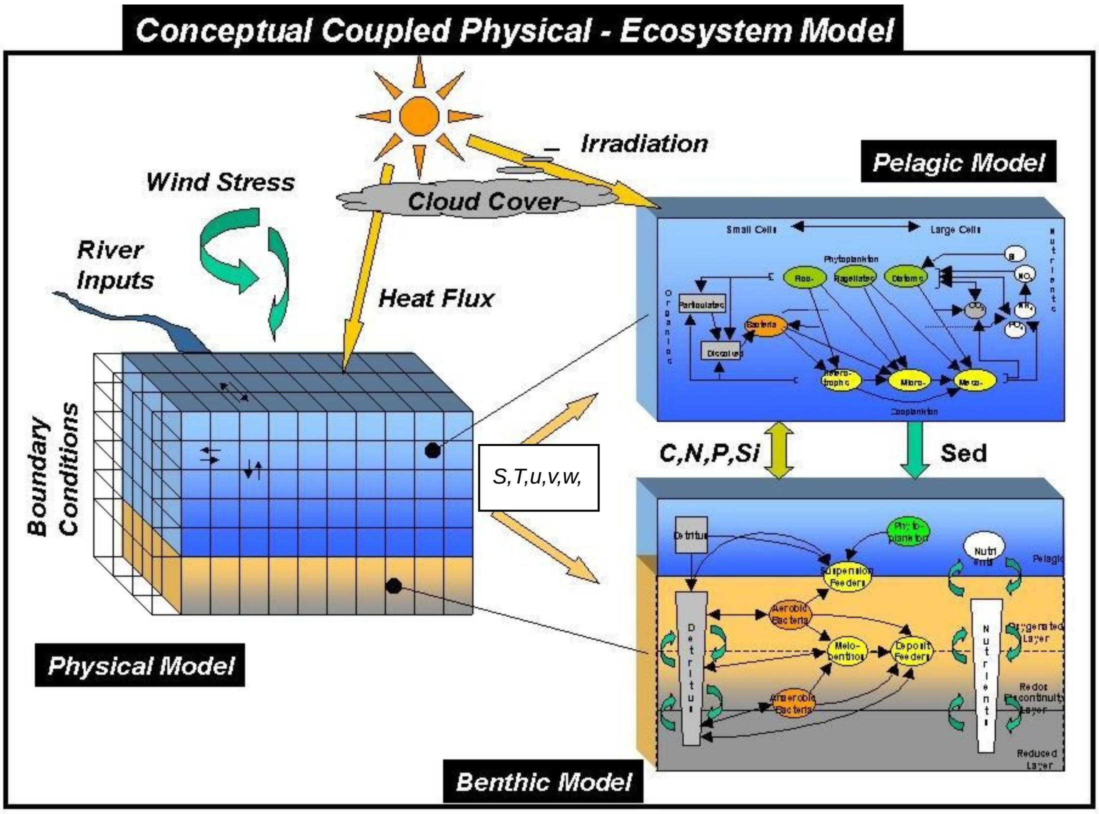

圖 4.1.1-1 POLCOMS 模式架構

4.1.1.1 水理模式

POL-3DB為有限差分之三維模式，利用基本的水動力方程式並配合Arakawa B球形座標格點（1972），溫度與鹽度皆為模擬變數，在垂直方向採用隨地形變化類似Sigma座標之s-座標系統，不同於Sigma座標的是允許Sigma間隔在水平方向上根據區域地形或動力之需求有所變化，如此可保持表層水體的格點解析度一致，特別是從大陸斜坡至大陸棚的區域，亦可獲得深海地區合理的斜溫層結果。其中，重要的數值演算法節錄如下：

- 對於物理及生態變數的水平對流利用PPM（Piecewise Parabolic Method）模組（James，1996）計算，該模組對於解析鋒面（front）的傳輸模擬可減少因演算造成的數值擴散而得以守衡。
- 動量與純量的垂直擴散藉由Mellor-Yamada-Galperin的2.5D紊流模組閉合（turbulence closure）。
- 水平壓力梯度藉由在水平面的內插演算而得，此法移除了在Sigma座標中如地形變化較大時常會產生的不正確結果。

4.1.1.2 歐洲邊緣海生態模式（ERSEM）

歐洲邊緣海生態模式（以下簡稱 ERSEM）包含了一系列物理、化學及生物的過程作用，並結合各項變數來描述整個生態系統的行為，有關生態系統的描述以功能群組（functional groups）來分類，而這些群組的行為藉由生物數量（成長、遷移與死亡）與生理過程（攝食、呼吸與排泄）來描述，整個生態系主要分為三個族群：生產者（浮游植物）、分解者（浮游與底棲細菌）與消耗者（浮游動物與底棲生物）。ERSEM基本上包含浮游生物相與底棲相，並藉由適當的過程動力機制將兩者結合，浮游生物的部分大致分類為浮游植物、浮游細菌、微浮游動物、浮游動物、營養鹽、溶氧、DOM與POM等。

生產者的碳變化可由下式計算

$$\frac{\partial C}{\partial t}=\text{攝食（吸收）碳}-\text{排泄損失的碳}-\text{呼吸損失的碳}-\text{生病損失的碳}-\text{死亡失去的碳}-\text{捕食壓力損失的碳}$$

分解者則為下式

$$\frac{\partial C}{\partial t}=\text{DOC攝食碳}+\text{碎屑降解產生的碳}-\text{呼吸損失碳}-\text{捕食壓力損失的碳}$$

消耗者的碳變化則為

$$\frac{\partial C}{\partial t}=\text{攝食（吸收）碳}-\text{呼吸損失的碳}-\text{死亡失去的碳}-\text{排泄損失的碳}-\text{捕食壓力損失的碳}$$

上述的分類將再藉由各物種所需營養鹽程度（trophic level）而細分，該程度可利用物種大小或攝食方法來區分，藉此可得到如圖4.1.1-2之食物網，碳與營養鹽在各個群組間的循環可用以描述這些物種的生理過程及族群數量，各物種在模式內無論產生多複雜的變化，該變化無法對其物種的過程預測產生實質或永久的極大差距，生態變數以最精簡但卻不遺漏任何重要影響系統能量平衡的原則來選取。氮、磷、矽與氧的化學動力變化耦合後用以描述碳在生態系統上之動力變化，食物網與營養鹽的耦合允許模式調整碳與營養鹽在空間與時

間上的變化，並使生態系統發生不一樣的行為。

浮游植物藉由三種功能群組來描述：矽藻，大小由 20 μm 至 200 μm，被浮游動物攝食；自營性鞭毛藻，大小為 2 ~ 20 μm，亦被浮游動物攝食；微浮游植物（picoplankton），大小為 0.2 ~ 2 μm，被異營性微鞭毛藻攝食。營養鹽（NO_3、NH_4與PO_4）的被攝食藉由Droop（1974）與Nyholm（1977）發現碳的同化作用過程被還原，營養鹽的攝取藉由細胞內的儲存量與外部環境量的多寡決定，微生物食物網包含細菌、異營性鞭毛藻與微浮游動物，其動力變化隨著不同之碳氮磷比而改變， Beretta-Bekker & al.（1995, 1998）描述了這個變化，細菌消耗DOC、分解碎屑物並與浮游植物競爭無機性營養鹽。異營性鞭毛藻則攝食細菌與微浮游植物，但被浮游動物攝食，微浮游動物與浮游動物亦攝食矽藻、自營與異營性鞭毛藻、微浮游植物與細菌，而微浮游動物將被浮游動物攝食，此三種主要捕食群（超微浮游動物、微浮游動物與浮游動物）亦互相競爭。

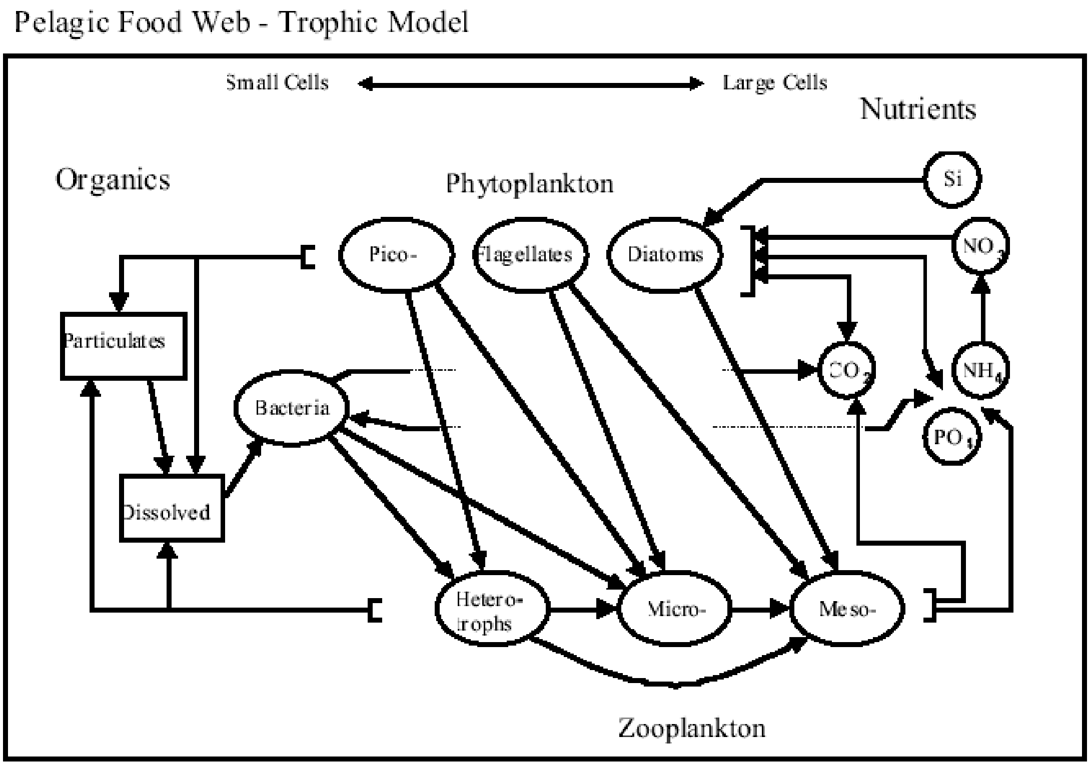

圖4.1.1-2 ERSEM食物網的基本架構

Benthic Chemistry and Food Web Model

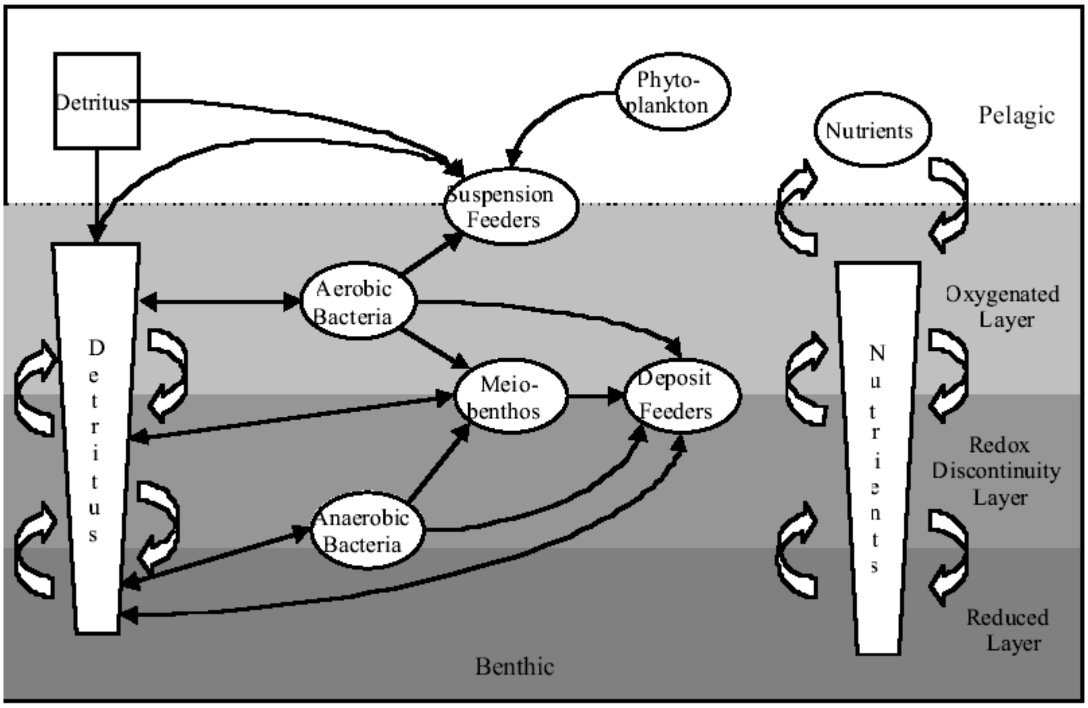

圖4.1.1-3 ERSEM底棲食物網

浮游細菌在模式中大部分由異營性細菌組成，利用已死亡之有機物質維生，有機物質包含顆粒態與溶解態，可在好氧或厭氧環境下進行相對應之分解機制。微浮游動物則包含兩種族群，微浮游動物本身與異營性鞭毛藻，大小分別為 20~200μm 與 2~20μm。浮游動物則分為肉食性與雜食姓兩種群組，碳通量的損失亦造成其他營養鹽的通量損失，因此可維持營養鹽與碳之比值。

圖4.1.1-3為ERSEM的底棲食物網架構，敘述了營養鹽與碳因好氧性與厭氧性細菌造成之循環，包含底棲生物網及因底棲生物活動造成的沉積物垂直移動變化，底棲層與浮游生物相的耦合，藉由有機碎屑沉降至底棲環境，及底棲環境因底棲生物活動而造成的營養鹽釋放來達成。

底棲食物網基本包含了底棲生物、分解者、沉積物中之有機物質、底部營養鹽與溶氧等大致分類，底棲生物包含底棲獵食性動物（epibenthic predators）、賴沉積物維生、濾食性維生、meiobenthos與infaunal predators等五個族群，每一族群藉由碳、氮與磷於底層水體的分布濃度來決定數量；分解者僅包含好氧與厭氧性細菌；沉積物中

之有機物質如前所述，可分為溶解態與顆粒態，溶解態依附在孔隙水中，可再細分為存於有氧層與無氧層之DOM；底部營養鹽則包含氨氮、硝酸氮、磷酸鹽、矽鹽與DOM。

4.1.1.3 懸浮沉積物模式

無機懸浮顆粒物質（SPM）的分佈與傳輸使用Holt與James（1999b）發展的模式來解釋其過程，為了簡化與縮短計算時間，該模式將SPM考慮為細矽土（fine silt），其沉降速度為 0.0001m s^{-1}，臨界侵蝕應力為 0.41 N m^{-2}，侵蝕常數為 0.04 gm s^{-1}，臨界沉澱應力為 0.10 N m^{-2}，這些特性在應用於東海時，應就現場實測值及狀況予以適當修改。

4.1.1.4 耦合

藉由將ERSEM程式碼在水理模式POL-3DB的時間迴圈適當地嵌入，耦合的步驟便可以達成，ERSEM利用水理模式計算得到之物理條件，包含溫度、鹽度及擴散，但並不回饋給水理模式，另外POL-3DB中的PPM對流模組提供給溫度、鹽度與SPM的對流，亦提供予生態模式中36種變數的對流變化。水理與生態模式皆由氣象資料驅動，包含太陽能流通量（solar heat flux）、風速、雲遮量等重要因子。

4.1.1.5 本模式於台灣附近海域之應用

透過適當的邊界條件引入，與模式內部參數的調整，本研究團隊利用POLCOMS模式探討黑潮在台灣鄰近海域的影響，透過建置西太平洋模式，以1/12度網格解析地形（圖4.1.1-4），模式範圍為105E~140E、15N~42N，垂直網格以20層S-coordinate描述，表底層較密，中層較寬來更為適當地描述斜溫層與斜鹽層（圖4.1.1-5）。由於河流對大陸棚海域的影響頗大，模式將東亞23條主要河川的流量及溫鹽的季節性分佈河流納入，其中又以長江與珠江流量為最大。為加速起始的速度，初始值採用HYCOM（2002）溫鹽場資料，由於兩者於垂直方向的格點定義不同，在內插過程必需檢驗其結果，為避免初始

溫鹽場造成計算過程的不穩定現象，溫鹽邊界亦採用相同的內插計算方法，並包含1度的逼近邊界層（Relaxation Zone）。氣象條件方面利用歐洲中尺度氣象預報中心（ECMWF）於2002年的預測資料，以月平均的方式驅動模式表層，其影響參數包含風場、氣壓場（圖4.1.1-6）、相對濕度、氣溫、日照度及雲遮量。

潮汐是大陸棚海域主要的動力來源，如單純以潮汐做為邊界條件長期模擬台灣週邊海域的潮流，探討潮汐在台灣附近大陸棚海域的狀況， 由圖4.1.1-7與圖4.1.1-8可觀察潮波於台灣海峽兩側推進，在海峽中段交會後反向流出，如僅以潮汐餘流來看，無論於大、小潮期間，或是年平均餘流的結果，都顯示台灣附近海域餘流極小，說明如單純以潮汐作為動力並不足以展現台灣附近海域的長期海流影響。在模式加入溫鹽與氣象條件後進行長期模擬，模式計算結果之海流分佈與文獻敘述相符(圖4.1.1-9)。

4.1.1.6 模式平行效率

由前述案例可知 POLCOMS 適用於計算模擬大尺度海流，在計算大範圍海流時，隨著模擬範圍的增加與解析度的提高，計算時間越長，在不影響計算效率下，模式本身的平行化將可提昇其計算效率，POLCOMS採用MPI函式庫作為平行化之工具，同時搭配 Recursive k-section partitioning algorithm (Berger & Bokhari 1987) 針對每顆處理器所計算之格點平均分配，達到各個處理器之計算負載平衡，同時減少各顆處理器之資料交換與溝通時間（communication time），圖4.1.1-10為前述案例設定下，不同顆處理器執行下之平行效率，隨著處理器數目的增加其平行效率越好，幾乎為一線性變化，顯示POLCOMS平行效率極佳。

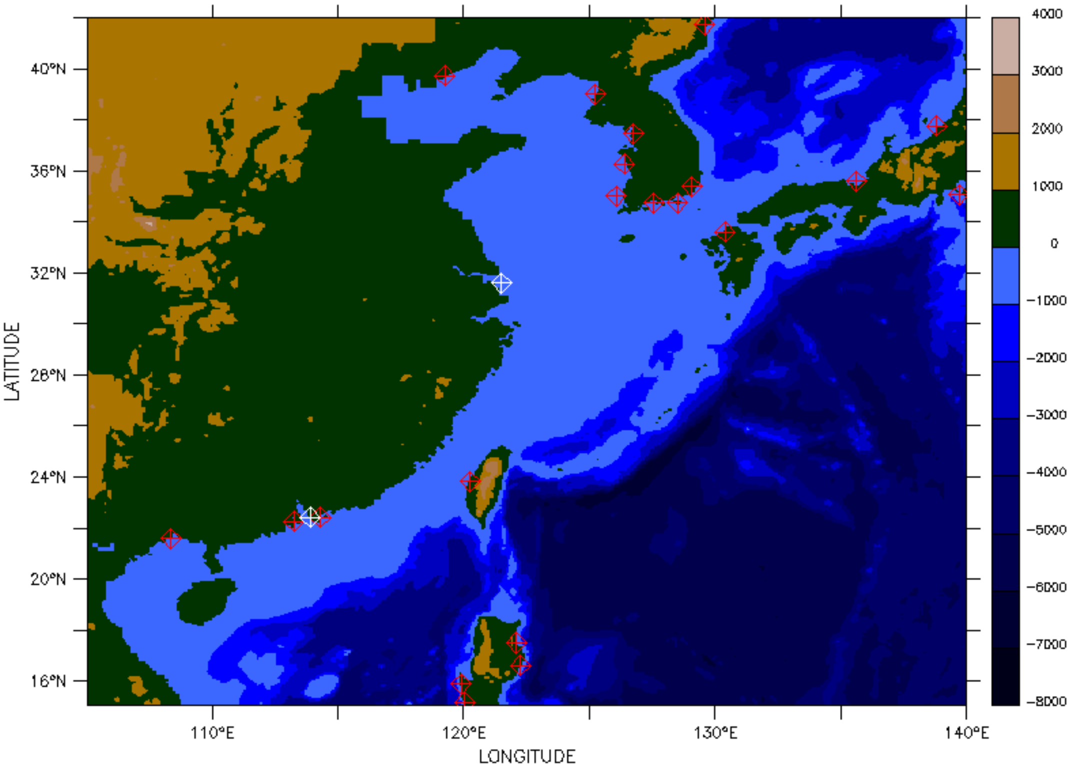

圖4.1.1-4 以POLCOMS建構西太平洋模式之地形示意圖(圖中方塊為河流邊界點)

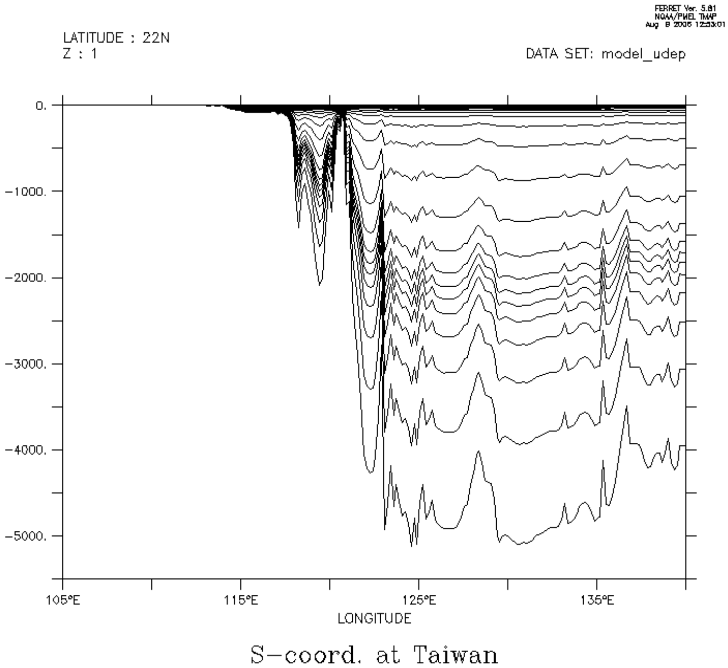

圖4.1.1-5 西太平洋模式於緯度22N之 S-coordinate 深度

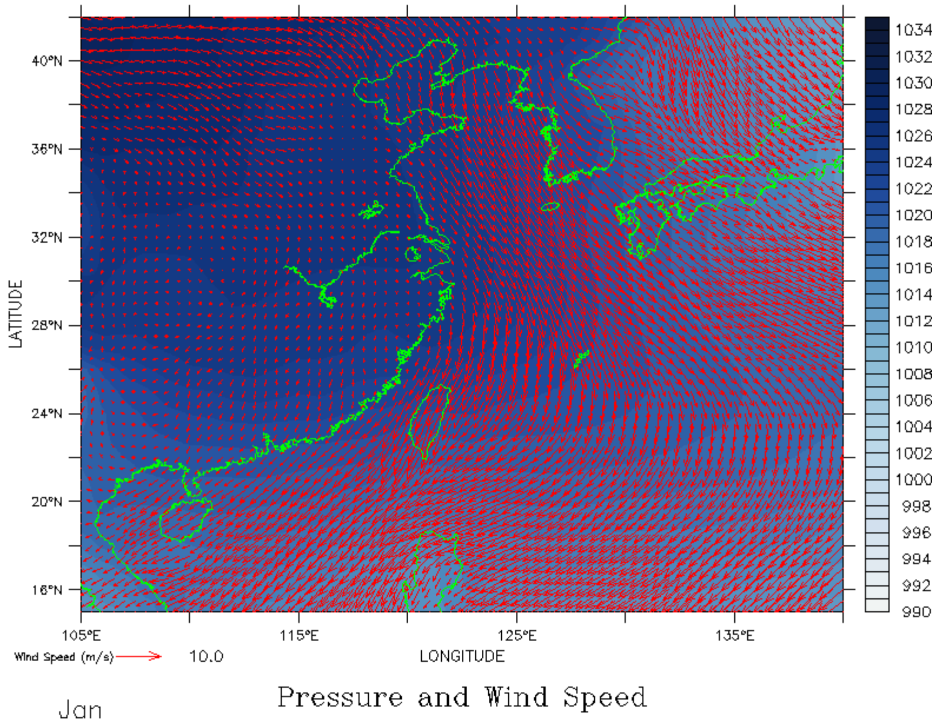

圖4.1.1-6 歐洲中尺度氣象預報中心（ECMWF）預測風場與氣壓

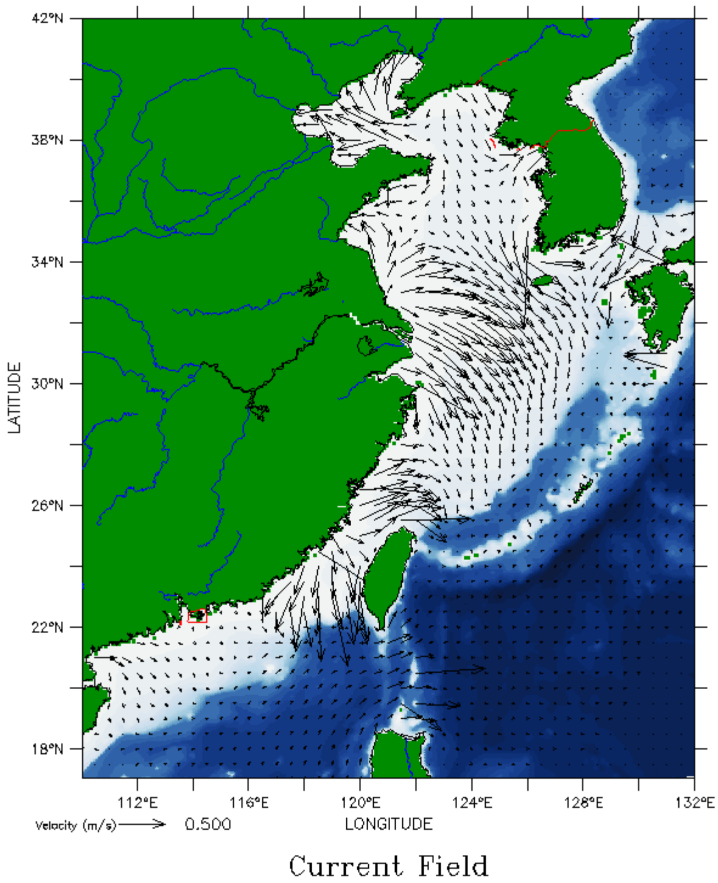

圖4.1.1-7 POLCOMS僅以潮汐作為驅動力之模式結果

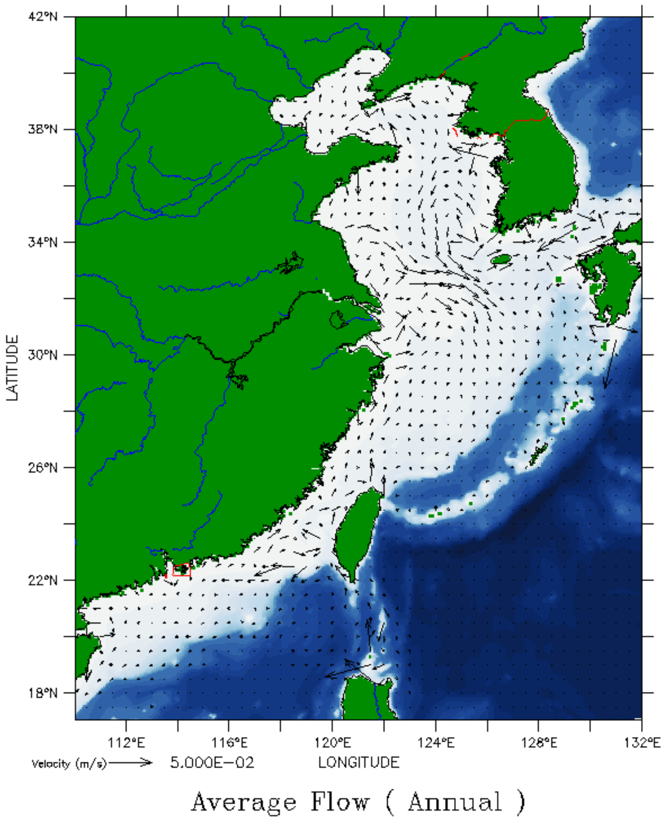

圖4.1.1-8 POLCOMS以潮汐作為驅動力之殘餘流(Residual flow)結果

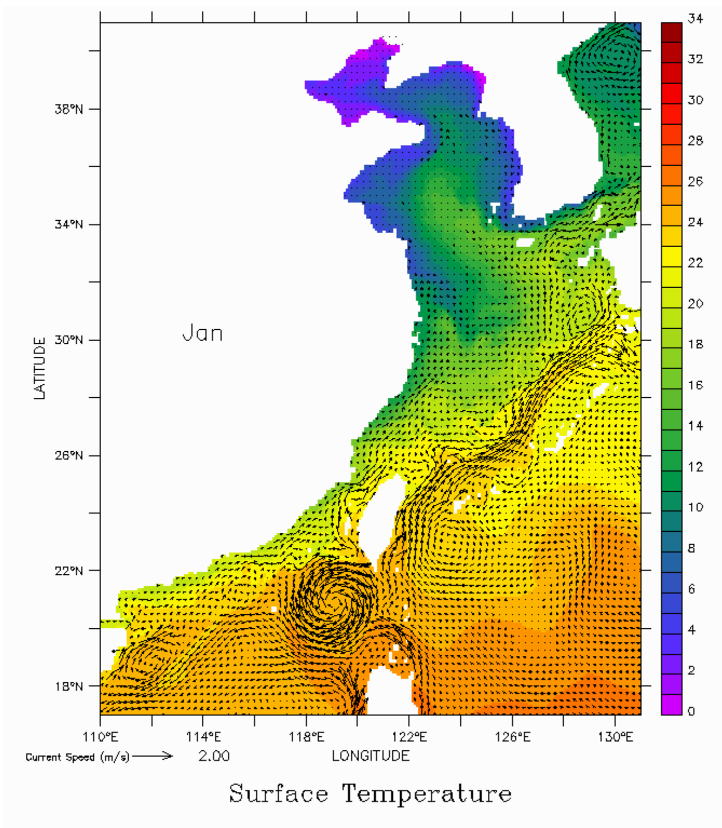

圖4.1.1-9 POLCOMS模式加入溫鹽邊界後之模擬結果

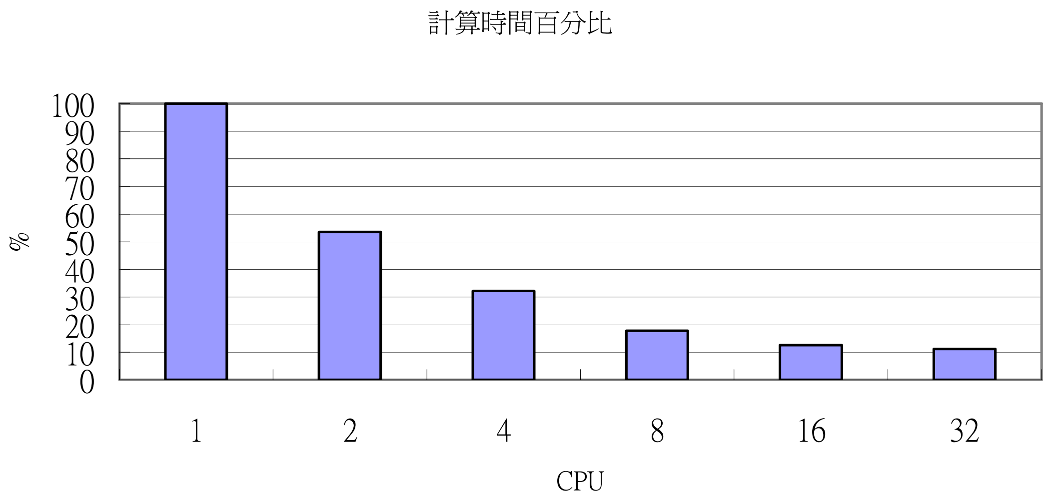

圖4.1.1-10 POLCOMS模式之平行效率

4.1.2 ROMS/TOMS模式

ROMS 由 Arango (Rutger Univesity)、Ezer (Princeton University)及 Shchepetkin (UCLA)所領導發展，經費則是由 Office of Naval Research (ONR)及 Ocean Modeling and Prediction Program 所贊助。ROMS/TOMS 發展的長期目標為可以應用在科學及作業化的領域，而且適用的區域從海岸地區到整個大洋模擬皆可。ROMS/TOMS 兩套系統本質是相同的，唯 ROMS 主要用於科學研究領域，而 TOMS 則應用在模式作業化。其為一套自由表面設定，垂直座標使用 s 座標系統，且適用範圍相當廣的模式，圖 4.1.2-1 為 ROMS 的系統架構圖，其符合 Earth System Modeling System 架構，可以很容易的與符合此架構的模式進行耦合運算。ROMS 的動態核心包含了四個模式系統，分別是 nonlinear (NLM)、tangent linear(TLM)、represented tangent linear(RPM)及 adjoint (ADM)，此四個模式系統可以藉由不同的驅動方式分開或者同時進行運算。除了上述四個模式系統，ROMS 在資料同化的也提共了兩種狀態的計算方式，分別為 Strong (S4DVAR, IS4DVAR)及 Weak (W4DAVR)，因此 ROMS 在各種狀況的使用是相當靈活的。模式主要有以下特點

- Split-explicit 計算方式
- 水平格點為正交 curvilinear 系統，垂直分層則有 s-coordinate

及 terrain-following (sigma) coordinate 可供選擇

- 程式碼使用 F90/F95 撰寫，前處理則使用 C 語言
- 完全的平行化
- 以 Bulk-parameterization (Fairall et al., 1996) 為基礎的海氣交換邊界層，可與大氣模式單向或雙向的整合
- 相當多的前處理及後處理軟體支援
- 有使用者論壇可供使用者交流及討論
- 每年皆會舉辦 workshop 會議，提供世界使用者交流的管道

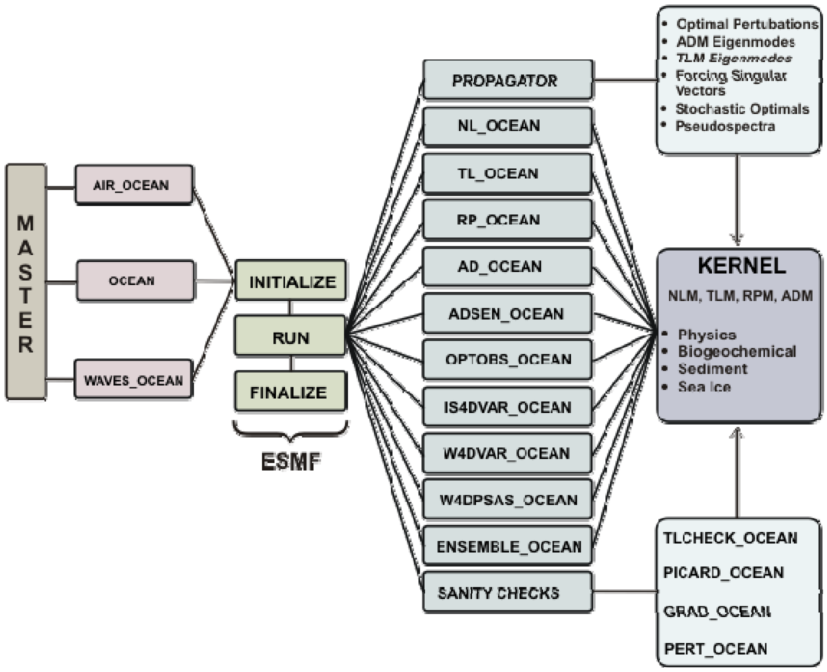

圖 4.1.2-1 ROMS 系統架構圖

4.1.2.1 基本控制方程式

以下就 ROMS 的基礎理論進行介紹，ROMS 原始的運動方程式包含了兩個假設的條件，一為 Boussinesq approximation，及水體內部的密度差異可忽略，另一為 hydrostatic approximation，及垂直壓力梯度力與浮力平衡，因此以卡氏座標表現方程式如下所述，分別為

連續方程式

$$\frac{\partial u}{\partial x}+\frac{\partial v}{\partial y}+\frac{\partial w}{\partial z}=0$$

x 及 y 方向的動量方程式

$$\frac{\partial u}{\partial t}+\vec{v}\bullet\Delta u-fv=-\frac{\partial \phi}{\partial x}+F_u+D_u$$

$$\frac{\partial v}{\partial t}+\vec{v}\bullet\Delta v-fu=-\frac{\partial \phi}{\partial y}+F_v+D_v$$

溫度及鹽度擴散方程式

$$\frac{\partial T}{\partial t}+\vec{v}\bullet\nabla T=F_T+D_T$$

$$\frac{\partial S}{\partial t}+\vec{v}\bullet\nabla S=F_S+D_S$$

靜水壓平衡方程式

$$\frac{\partial \phi}{\partial z}=\frac{-\rho g}{\rho_0}$$

狀態方程式(equation of state)

$$\rho=\rho(T,S,P)$$

其中$\vec{v}$為流速在水平(u 及 v)及垂直(w)的分量，T 為溫度，S 為鹽度，f 為科氏力係數，ϕ為動態壓力，P 為總壓力，g 為重力加速度，ρ_0為水的參考密度，ρ為水的當地密度，(D_S,D_T,D_v,D_u)為擴散項，(F_S,F_T,F_v,F_u)則為外力項。

4.1.2.2 垂直及水平邊界條件

ROMS 在垂直邊界條件的理論如下，在表層($z=\zeta(x,y,t)$)

$$K_m\frac{\partial u}{\partial z}=\tau_s^x(x,y,t)$$

$$K_m\frac{\partial v}{\partial z}=\tau_s^y(x,y,t)$$

$$K_T\frac{\partial T}{\partial z}=\frac{Q_T}{\rho_0 c_P}+\frac{1}{\rho_0 c_P}\frac{dQ_T}{dT}(T-T_{ref})$$

$$K_S\frac{\partial S}{\partial z}=(E-P)S$$

$$w=\frac{\partial \zeta}{\partial t}$$

在底層($z=-h(x,y)$)

$$K_m \frac{\partial u}{\partial z} = \tau_b^x(x,y,t)$$

$$K_m \frac{\partial v}{\partial z} = \tau_b^y(x,y,t)$$

$$\tau_b^x = (\gamma_1 + \gamma_2\sqrt{u^2+v^2})u$$

$$\tau_b^y = (\gamma_1 + \gamma_2\sqrt{u^2+v^2})v$$

$$K_T \frac{\partial T}{\partial z} = 0$$

$$K_S \frac{\partial S}{\partial z} = 0$$

$$-w + \vec{v} \bullet \nabla h = 0$$

其中 E 蒸發量，P 為降雨量，Q_T 為表層熱通量，(τ_s^x, τ_s^y) 為表層風剪力，(τ_b^x, τ_b^y) 為底床磨差力，γ_1 為線性底床摩擦係數，γ_2 為二次底床摩擦係數。

模式在進行實際狀況模擬時，同常在邊界或者是模擬範圍內皆會出現陸地點，因此水平方向的邊界條件處理便相當重要，特別是在當邊界不為一直線延伸時最需要進行處理，ROMS 會在這種條件下增加高階的邊界條件，在東西向以 u 為例表示如下

$$\frac{\partial}{\partial x}\left(\frac{hv}{mn}\frac{\partial^2 u}{\partial x^2}\right) = 0$$

在南北向則表示如下

$$\frac{\partial}{\partial y}\left(\frac{hv}{mn}\frac{\partial^2 u}{\partial x^2}\right) = 0$$

在其他變數 v、S 及 T 皆有相似的邊界條件。

4.1.2.3 網格變數配置

ROMS 水平網格變數配置採用 Arakawa C 格點位置，如圖 4.1.2-2 所示，變數水位(zeta)、密度(ρ)及動態/非動態追蹤點位於網格的中央位置，水平的流速(u 及 v)則位於網格東/西及南/北的邊緣；垂直網格配置如圖 4.1.2-3 所示，垂直分層厚度依照不同水深會有不一樣的變化，水平的動量項(流速 u、v、密度 ρ 及動態/非動態追蹤點)分配

於往格的中央，垂直流速(w)及垂直混和變數(Akt、Akv…等)則置於網格上下邊緣。

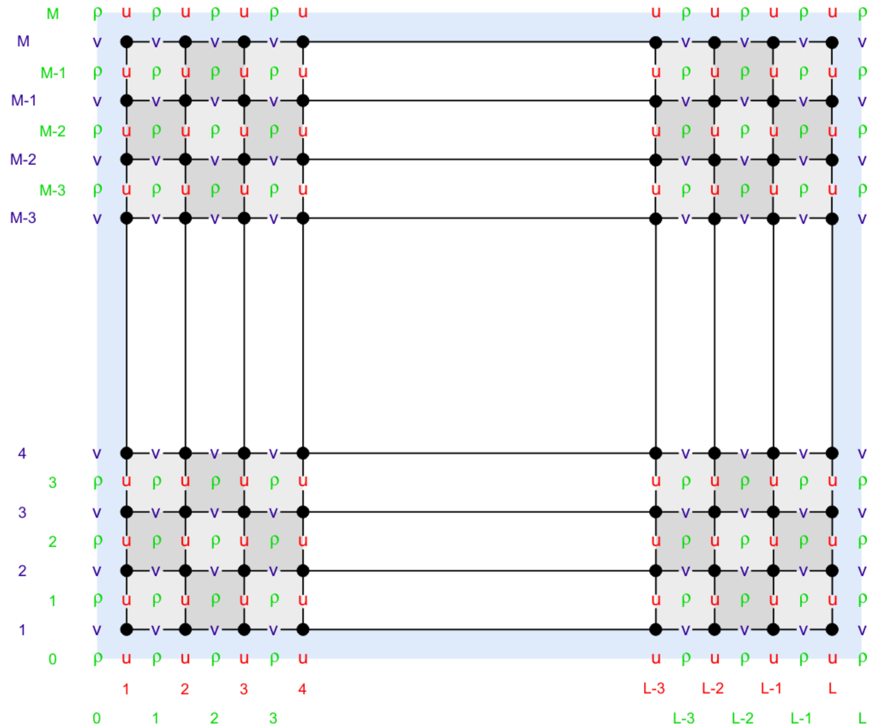

圖 4.1.2-2 ROMS 水平網格變數配置

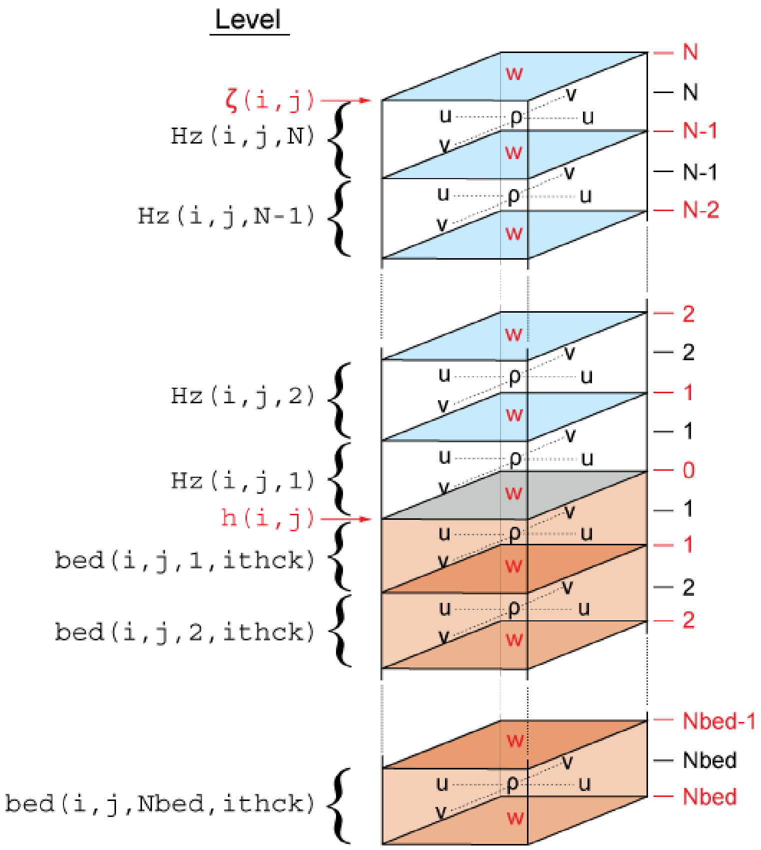

圖 4.1.2-3 ROMS 垂直網格變數配置

4.2.1.4 垂直 S 座標系統

傳統的 z 座標系統在遇到地形變化很大的地方，會產生網格不連續的現象，因此變出現了可依據地形變化等比例分配的座標系統(sigma 座標)，此座標系統最早是應用在大氣方面，其後才使用於海洋的模擬。ROMS 使用的座標系統為 S 座標，此座標系統為 Song 及 Haidvogel (1994)改進 sigma 座標系統而來，其主要的優點是可使用非等比例進行垂直分層，讓使用者可以針對有興趣的區域進行密度較高的分層，如圖 4.1.2-4。以下為 S 座標的定義：

$$\hat{x} = x$$

$$\hat{y} = y$$

$$\hat{t} = t$$

$$z = \zeta + (1+\frac{\zeta}{h})\left[h_c s + (h-h_c)C(s)\right]$$

$$C(s) = (1-b)\frac{\sinh(\theta s)}{\sinh\theta} + b\frac{\tanh\left[\theta(s+\frac{1}{2})\right] - \tanh(\frac{1}{2}\theta)}{2\tanh(\frac{1}{2}\theta)}$$

其中 s 介於 0(表層ζ)~-1(底層 h)之間，(θ,b)為 S 座標的表層及底層參數，$1<\theta\le 20$，$0\le b\le 1$，當$\theta=0$則可轉換成傳統的 sigma 座標，藉由調整 b 值則可增加或減少表層的層數。

兩種不同的座標轉換方式如下

$$(\frac{\partial}{\partial x})_z = (\frac{\partial}{\partial x})_s - (\frac{1}{H_z})(\frac{\partial z}{\partial x})_s\frac{\partial}{\partial s}$$

$$(\frac{\partial}{\partial y})_z = (\frac{\partial}{\partial y})_s - (\frac{1}{H_z})(\frac{\partial z}{\partial y})_s\frac{\partial}{\partial s}$$

$$\frac{\partial}{\partial z} = (\frac{\partial s}{\partial z})\frac{\partial}{\partial s} = \frac{1}{H_z}\frac{\partial}{\partial s}$$

其中 $H_z = \frac{\partial z}{\partial s}$ 。

經過上述的座標轉換，ROMS 的動態方程式可以轉換如下：

$$\frac{\partial u}{\partial t} - fv + \vec{v}\bullet\nabla u = -\frac{\partial\phi}{\partial x} - (\frac{g\rho}{\rho_0})\frac{\partial z}{\partial x} - g\frac{\partial\zeta}{\partial x} + F_u + D_u$$

$$\frac{\partial v}{\partial t} + fu + \vec{v}\bullet\nabla v = -\frac{\partial\phi}{\partial y} - (\frac{g\rho}{\rho_0})\frac{\partial z}{\partial y} - g\frac{\partial\zeta}{\partial y} + F_v + D_v$$

$$\frac{\partial T}{\partial t}+\vec{v}\bullet\nabla T=F_T+D_T$$

$$\frac{\partial S}{\partial t}+\vec{v}\bullet\nabla S=F_S+D_S$$

$$\rho=\rho(T,S,P)$$

$$\frac{\partial \phi}{\partial s}=(\frac{-gH_z\rho}{\rho_0})$$

$$\frac{\partial H_z}{\partial t}+\frac{\partial(H_z u)}{\partial x}+\frac{\partial(H_z v)}{\partial y}+\frac{\partial(H_z\Omega)}{\partial s}=0$$

其中

$$\vec{v}=(u,v,\Omega)$$

$$\vec{v}\bullet\nabla=u\frac{\partial}{\partial x}+v\frac{\partial}{\partial y}+\Omega\frac{\partial}{\partial s}$$

$$\Omega(x,y,s,t)=\frac{1}{H_z}\left[w-(1+s)\frac{\partial\zeta}{\partial t}-u\frac{\partial z}{\partial x}-v\frac{\partial z}{\partial y}\right]$$

$$w=\frac{\partial z}{\partial t}+u\frac{\partial z}{\partial x}+v\frac{\partial z}{\partial y}+\Omega H_z$$

垂直的邊界條件變為，表層(s=0)

$$(\frac{K_m}{H_z})\frac{\partial u}{\partial s}=\tau_s^x(x,y,t)$$

$$(\frac{K_m}{H_z})\frac{\partial v}{\partial s}=\tau_s^y(x,y,t)$$

$$(\frac{K_T}{H_z})\frac{\partial T}{\partial s}=\frac{Q_T}{\rho_0 c_P}+\frac{1}{\rho_0 c_P}\frac{dQ_T}{dT}(T-T_{ref})$$

$$(\frac{K_S}{H_z})\frac{\partial S}{\partial s}=\frac{(E-P)S}{\rho_0}$$

$$\Omega=0$$

在底層($z=-h(x,y)$)

$$(\frac{K_m}{H_z})\frac{\partial u}{\partial s}=\tau_b^x(x,y,t)$$

$$(\frac{K_m}{H_z})\frac{\partial v}{\partial s}=\tau_b^y(x,y,t)$$

$$\tau_b^x=(\gamma_1+\gamma_2\sqrt{u^2+v^2})u$$

$$\tau_b^y=(\gamma_1+\gamma_2\sqrt{u^2+v^2})v$$

$$(\frac{K_T}{H_z})\frac{\partial T}{\partial s}=0$$

$$(\frac{K_S}{H_z})\frac{\partial S}{\partial s}=0$$

$$\Omega=0$$

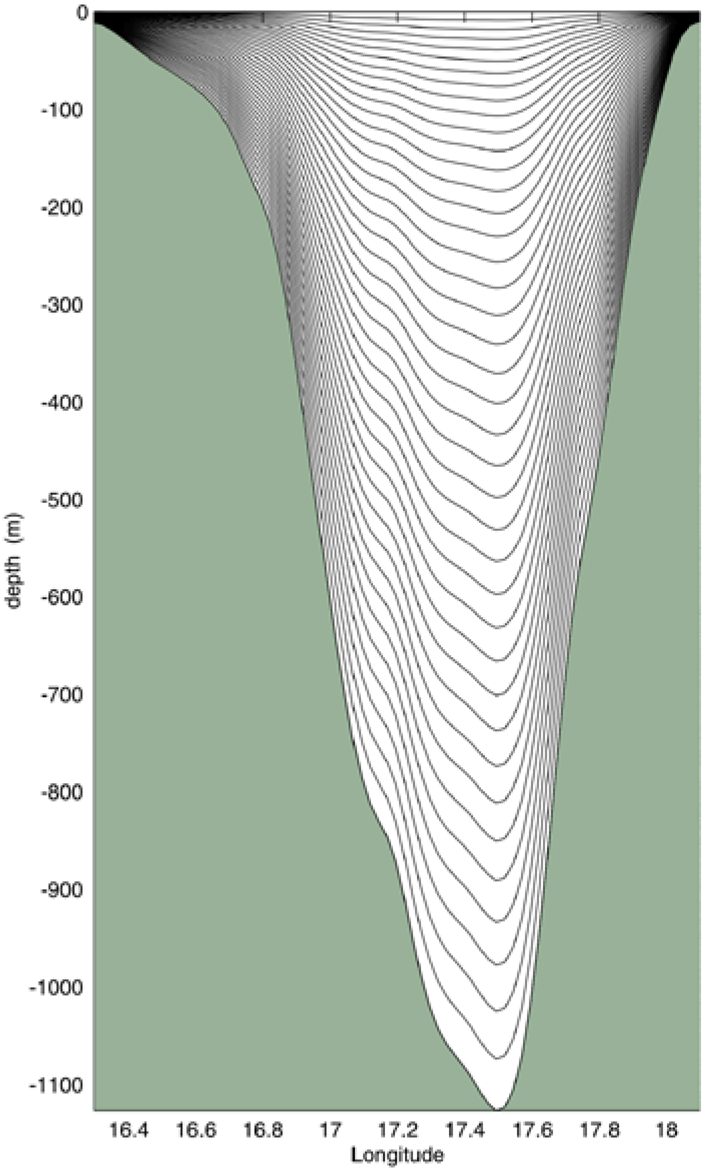

圖 4.1.2-4 ROMS 垂直 S 座標示意圖

4.2.1.5 水平 curvilinear 座標

傳統的規則網格，對於計算實際曲折的海岸線，在解析力的部份是不足的，特別是針對計算流體的運動，因此 ROMS 為了解決這個問題，在水平座標採用了可以產生不規則網格的 curvilinear 座標系統。

設定新座標軸$\xi(x,y)$及$\eta(x,y)$，則其水平弧長可以定為

$$(ds)_\xi = (\frac{1}{m})d\xi$$

$$(ds)_\eta = (\frac{1}{m})d\eta$$

其中$m(\xi,\eta)$及$n(\xi,\eta)$比例係數，其與實際的$\Delta\xi$及$\Delta\eta$是有關係的，經果座標轉換，流速項轉入新座標定義如下

$$\vec{v}\bullet\hat{\xi} = u$$

$$\vec{v}\bullet\hat{\eta} = v$$

將上式引入 ROMS 的動力機制，便可得到使用 curvilinear 及 S 座標系統的公式，轉換如下

$$\frac{\partial}{\partial t}(\frac{H_z u}{mn}) + \frac{\partial}{\partial \xi}(\frac{H_z u^2}{n}) + \frac{\partial}{\partial \eta}(\frac{H_z uv}{m}) + \frac{\partial}{\partial s}(\frac{H_z u\Omega}{mn})$$

$$-\left\{(\frac{f}{mn}) + v\frac{\partial}{\partial \xi}(\frac{1}{n}) - u\frac{\partial}{\partial \eta}(\frac{1}{m})\right\} H_z v =$$

$$-(\frac{H_z}{n})(\frac{\partial \phi}{\partial \xi} + \frac{g\rho}{\rho_0}\frac{\partial z}{\partial \xi} + g\frac{\partial \zeta}{\partial \xi}) + \frac{H_z}{mn}(F_u + D_u)$$

$$\frac{\partial}{\partial t}(\frac{H_z v}{mn}) + \frac{\partial}{\partial \xi}(\frac{H_z uv}{n}) + \frac{\partial}{\partial \eta}(\frac{H_z v^2}{m}) + \frac{\partial}{\partial s}(\frac{H_z v\Omega}{mn})$$

$$+\left\{(\frac{f}{mn}) + v\frac{\partial}{\partial \xi}(\frac{1}{n}) - u\frac{\partial}{\partial \eta}(\frac{1}{m})\right\} H_z u =$$

$$-(\frac{H_z}{m})(\frac{\partial \phi}{\partial \eta} + \frac{g\rho}{\rho_0}\frac{\partial z}{\partial \eta} + g\frac{\partial \zeta}{\partial \eta}) + \frac{H_z}{mn}(F_v + D_v)$$

$$\frac{\partial}{\partial t}(\frac{H_z T}{mn}) + \frac{\partial}{\partial \xi}(\frac{H_z uT}{n}) + \frac{\partial}{\partial \eta}(\frac{H_z vT}{m}) + \frac{\partial}{\partial s}(\frac{H_z \Omega T}{mn}) = \frac{H_z}{mn}(F_T + D_T)$$

$$\frac{\partial}{\partial t}(\frac{H_z S}{mn}) + \frac{\partial}{\partial \xi}(\frac{H_z uS}{n}) + \frac{\partial}{\partial \eta}(\frac{H_z vS}{m}) + \frac{\partial}{\partial s}(\frac{H_z \Omega S}{mn}) = \frac{H_z}{mn}(F_S + D_S)$$

$$\rho = \rho(T,S,P)$$

$$\frac{\partial \phi}{\partial s} = -(\frac{gH_z\rho}{\rho_0})\frac{\partial}{\partial t}(\frac{H_z}{mn}) + \frac{\partial}{\partial \xi}(\frac{H_z u}{n}) + \frac{\partial}{\partial \eta}(\frac{H_z v}{m}) + \frac{\partial}{\partial s}(\frac{H_z \Omega}{mn}) = 0$$

其中 z 為ζ的線性函數，因此連續方程式可以改寫為

$$\frac{\partial}{\partial t}(\frac{\zeta}{mn}) + \frac{\partial}{\partial \xi}(\frac{H_z u}{n}) + \frac{\partial}{\partial \eta}(\frac{H_z v}{m}) + \frac{\partial}{\partial s}(\frac{H_z \Omega}{mn})$$

以上即為使用 curvilinear 及 S 座標 ROMS 的基本水動力方程式。

4.2.1.6 實際案例應用

ROMS已發展相當長的時間，並且不斷地進行理論的改進及效率的增進，至今應用於實際案例及文獻數量的相當多，模擬結果與實際現象比對結果相當不錯，且未來仍會持續的發展。圖4.1.2-5為ROMS模式應用於南非CAPE TOWN的海表面溫度模擬結果與實測資料的比對結果(Penven et al., 2001)，比對結果整體趨勢相當吻合。圖4.1.2-6為ROMS模式應用於大西洋海域海表面溫度模式結果與Levitus資料比對圖，模式結果與Levits資料趨勢相當吻合。圖4.1.2-7為ROMS應用於加州模式sea surface height與TOPEX/ERS比對圖，整體趨勢相當吻合

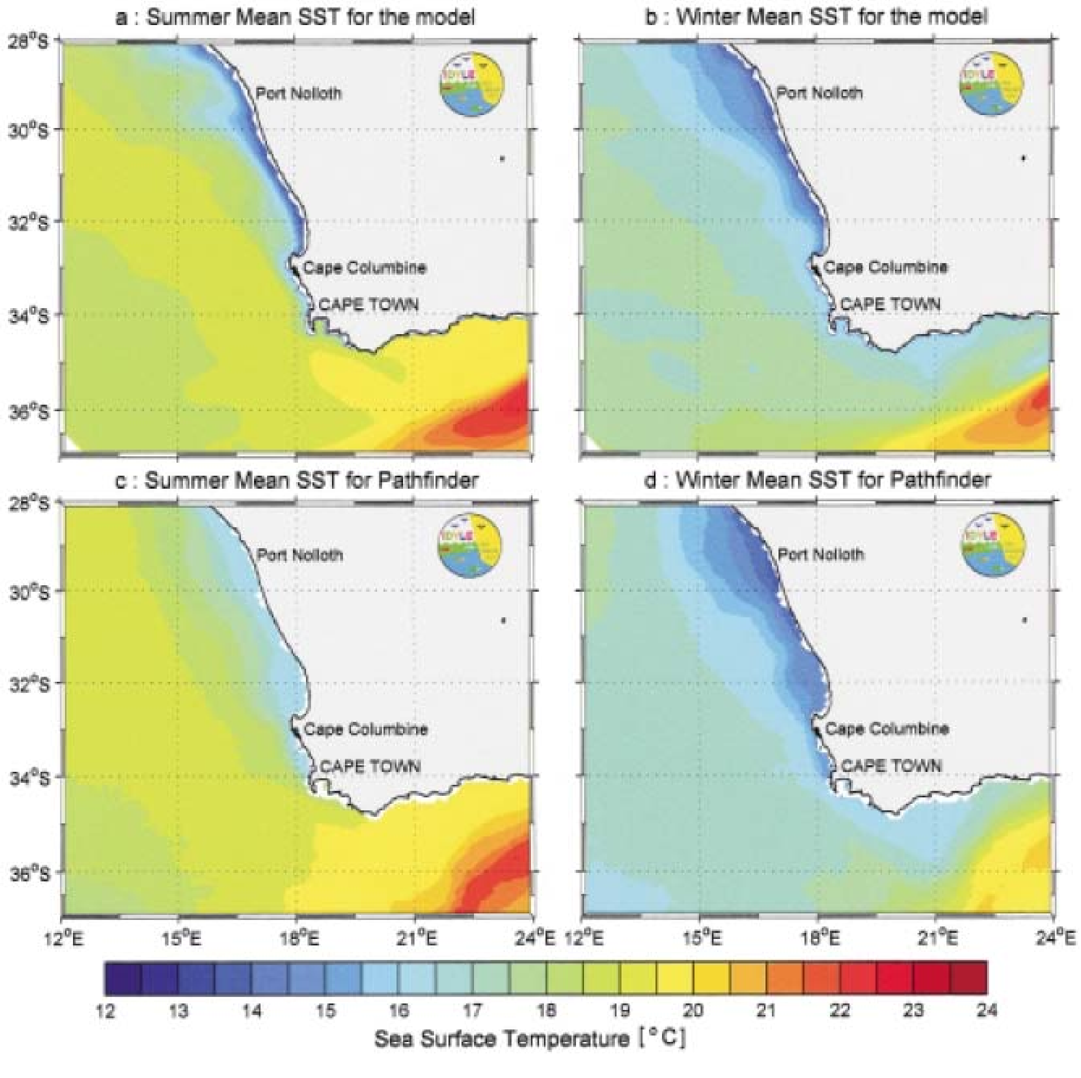

圖4.1.2-5 海表面溫度模式結果與實測資料比對圖(Penven et al., 2001)

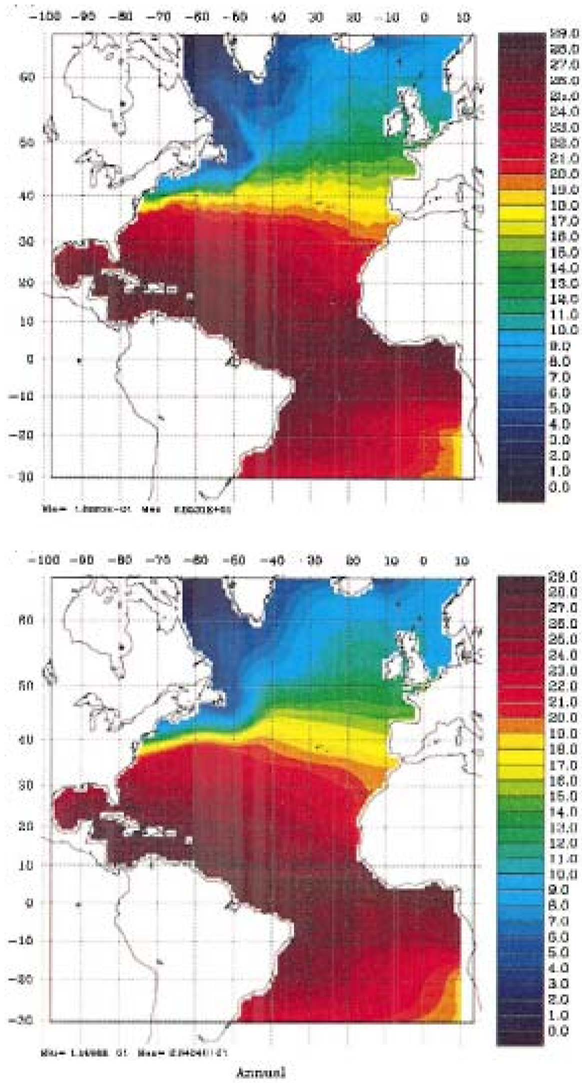

圖4.1.2-6 海表面溫度模式結果(上)與Levitus資料(下)比對圖

(Haidvogel et al., 2000)

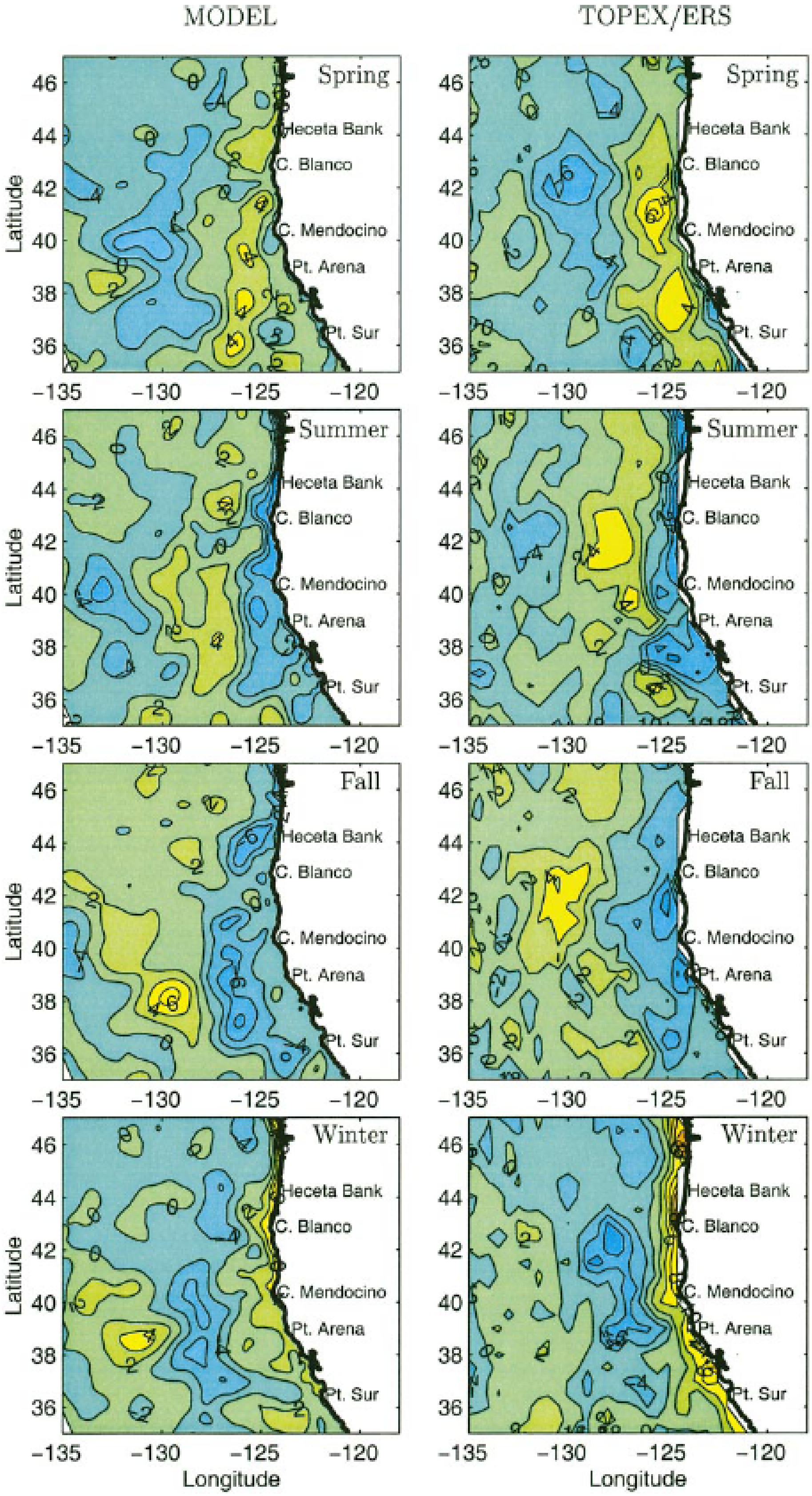

圖4.1.2-7 Sea surface Height模式結果與TOPEX/ERS比對圖

(Marchesiello et al., 2003)

4.2 近岸海域模式

4.2.1 FVCOM (Finite-Volume Coastal Ocean Model)模式簡介

4.2.1.1 模式介紹

在近海區域，近岸的陸棚與河口紅樹林由沙洲、河口、與鹽澤(salt marsh)等不規則陸地所構成，發展一數值模式來模擬這樣的不規則形狀之海陸交界系統實為挑戰，FVCOM 即為此而誕生。由數值方法來分類大部分的海洋數值模式，大抵不外乎兩種方法：有限差分(Blumberg & Mellor, 1987; Blumberg, 1994)與有限元素(Lynch & Naimie, 1993; Naimie, 1996)，有限差分法為最基礎之差分計算方法，程式容易建構與計算效率佳為其優點，卡式座標與曲線正交網格常用於水平網格之建構，然而此網格系統並無法解析極為不規則形狀之海岸地區(Blumberg, 1994)，網格需縮至較小方能解析，但時間步長將因此而受限，進而影響其計算效率。有限元素法的最大優點即為可用以解析不同海岸地區形狀，同時搭配不同的網格大小與合理的網格數目，同時保有計算的效率與預測的準確性。FVCOM 利用了有限元素的網格建構，配合將原有有限差分的控制方程積分式離散化，同時藉由計算各元素間通量方程式的變化，以有限體積計算方法來建構整個模式，有限體積的方法對於質量保守性(mass conservation)較其餘演算方法為佳，從技術層面來看，FVCOM 同時保有了有限差分容易編寫程式碼的優點與有限元素解析複雜地形的特點，本模式已成功應用於數個河口與海岸地區(Chen, C., 2000; Chen, C. & R. Beardsley. 2002)，FVCOM 的特點簡介如下：

- 不規則三角元素網格，可用以解析近岸複雜地形之區域
- 垂直方向網格可定義為 Sigma 與 S-coordinate 座標
- 乾濕點的計算(Wet/Dry)
- GOTM 紊流模式的引入
- 驅動力包含潮汐、各種氣象資料、河流等
- 不同邊界演算方法的處理
- 模組化建構，包含生物、沉積物、追蹤顆粒與極區冰模組等

- 包含資料同化模組
- 程式以 F90 編寫，並包含平行化處理
- 輸出部份採用 NetCDF 格式，方便後處理之進行

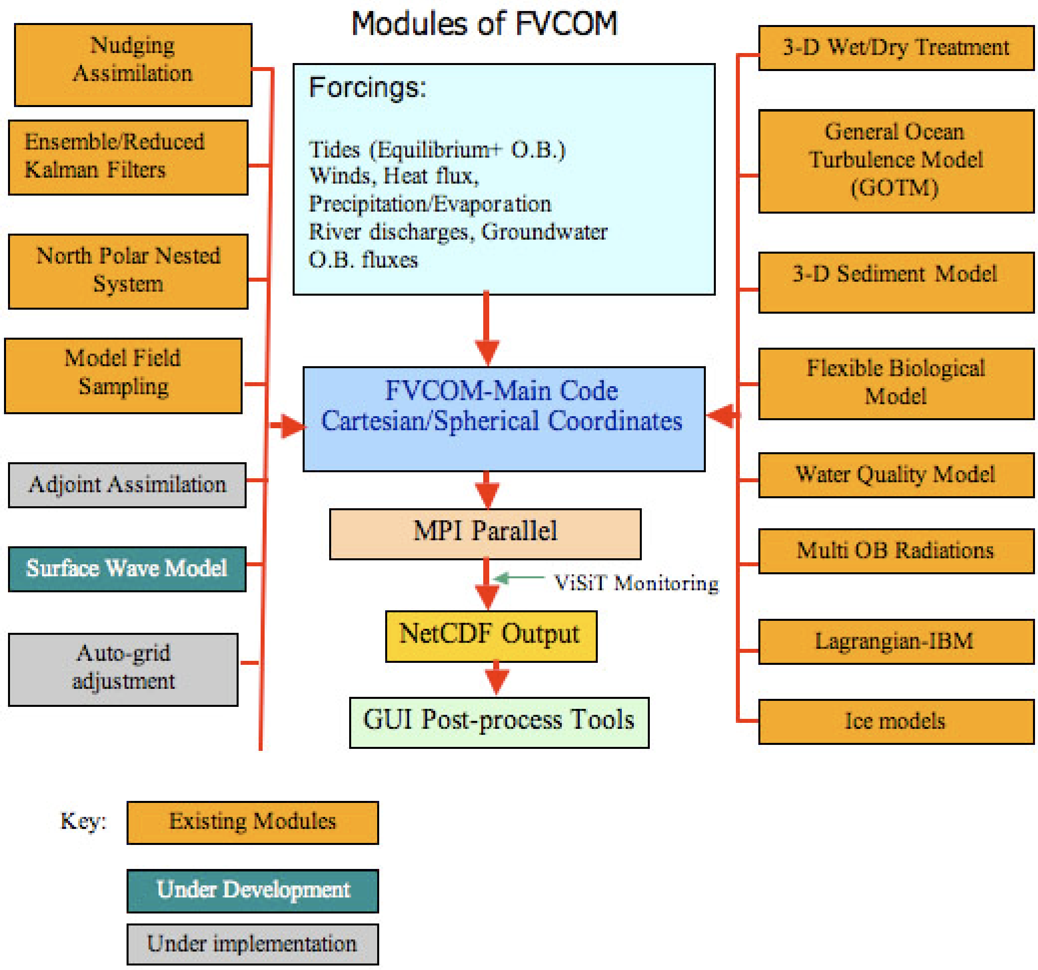

圖 4.2.1-1 FVCOM 模式架構

4.2.1.2 台灣海域之應用實例

(1)台中港

藉由有限元素法的彈性網格配置，港區複雜結構物的配置形狀洽可做為展現 FVCOM 應用於近岸區域的極佳案例，本團隊曾針對台中港區域以 FVCOM 作為研究案例，圖 4.2.1-2 為台中港網格之有限元素網格建構，在引入適當之邊界條件與風場資料後，其計算結果與實測資料的比對展示於圖 4.2.1-3、圖 4.2.1-4，其結果符合良好，顯示 FVCOM 適合應用於近岸複雜地形的解析與演算，圖 4.2.1-5 為 FVCOM 應用

於台中港之計算流矢結果。

(2) 西太平洋

FVCOM 的彈性網格配置除可應用於近岸複雜海岸線的解析外，亦可應用於大範圍區域模式，對於近岸可以較細之網格解析，深海處則以較大網格解析，可合理的降低網格數目同時保有近岸之解析度，圖 4.2.1-6 為 FVCOM 應用於西太平洋天文潮模式之網格分布，網格節點為 18595 點，網格元素為 36584 個，垂直層以 10 層 sigma 分層作為計算，其計算結果與實際資料比較相符（圖 4.2.1-7 至圖 4.2.1-9），顯示 FVCOM 亦適合模擬大範圍區域模式。

4.2.1.3 FVCOM 之平行效率

由前述案例可知 FVCOM 不僅適用於計算近岸區域，亦可模擬大尺度海流，透過彈性網格的配置可減少網格數目，然而，在計算大範圍海流時，隨著模擬範圍的增加與解析度的提高，網格數目的增加造成計算時間越長，在不影響計算效率下，模式本身的平行化將可提昇其計算效率，FVCOM 採用 MPI 函式庫作為平行化之工具，同時搭配 METIS graph partitioning libraries (Karypis and Kumar, 1998) 針對每顆處理器所計算之元素平均分配，達到各個處理器之計算負載平衡，同時減少各顆處理器之資料交換與溝通時間（communication time），圖 4.2.1-10 為西太平洋案例設定下，不同顆處理器執行下之平行效率，隨著處理器數目的增加其平行效率越好，幾乎為一線性變化，顯示 FVCOM 平行效率極佳。

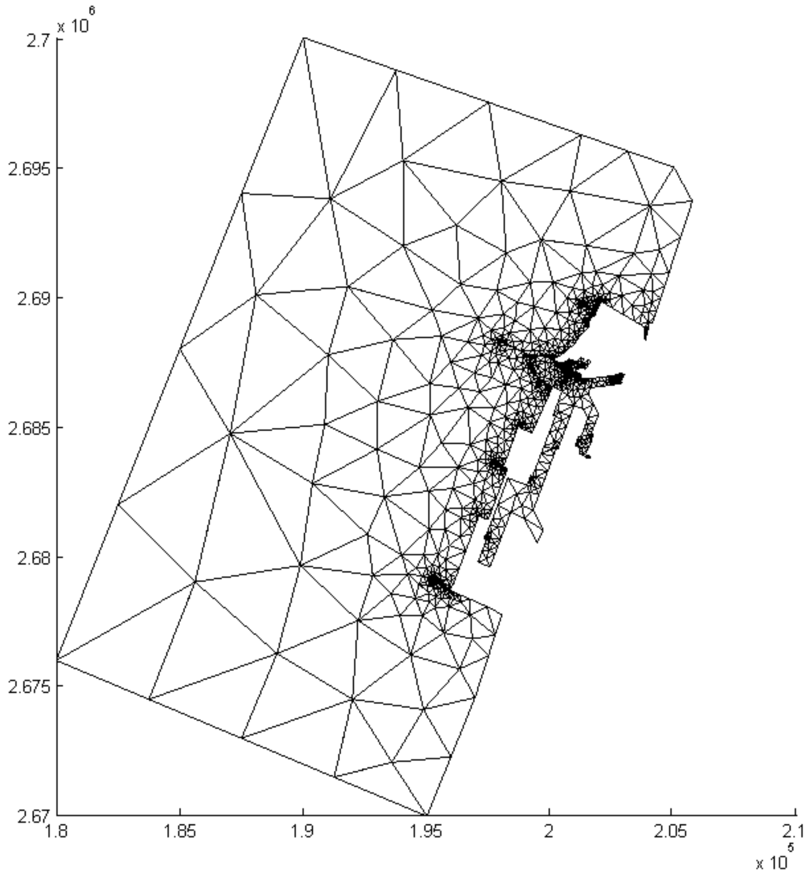

圖 4.2.1-2 台中港海域及港區模式之有限元素計算網格

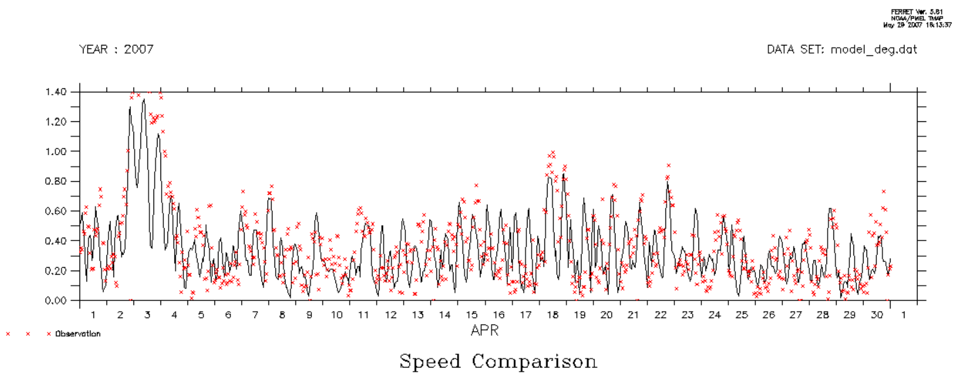

圖 4.2.1-3 FVCOM 應用於台中港區之模擬流速與實測比對

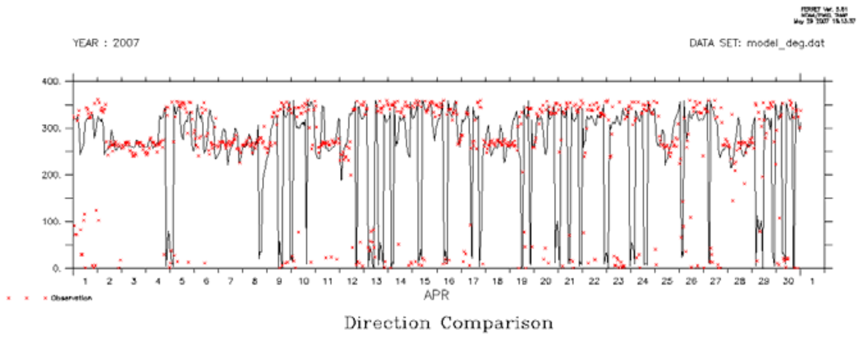

圖 4.2.1-4 FVCOM 應用於台中港區之模擬流向與實測比對

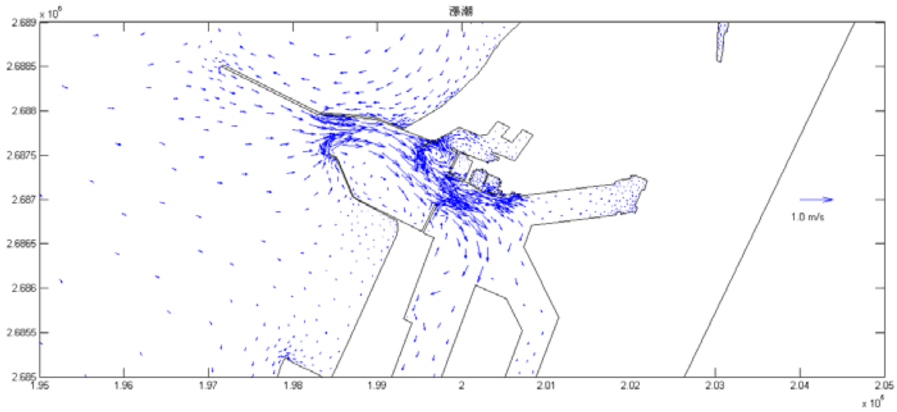

圖 4.2.1-5 FVCOM 應用於台中港區之模擬流矢圖

圖 4.2.1-6 西太平洋海域模式之 FVCOM 計算網格

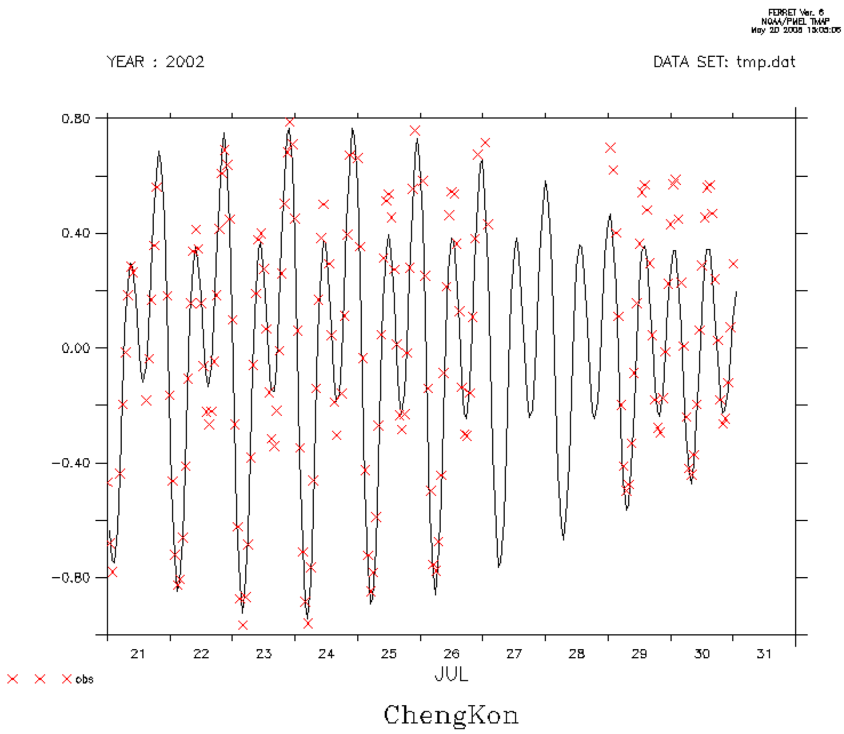

圖 4.2.1-7 以 FVCOM 計算西太平洋潮汐於成功測站之模擬結果與實測比對

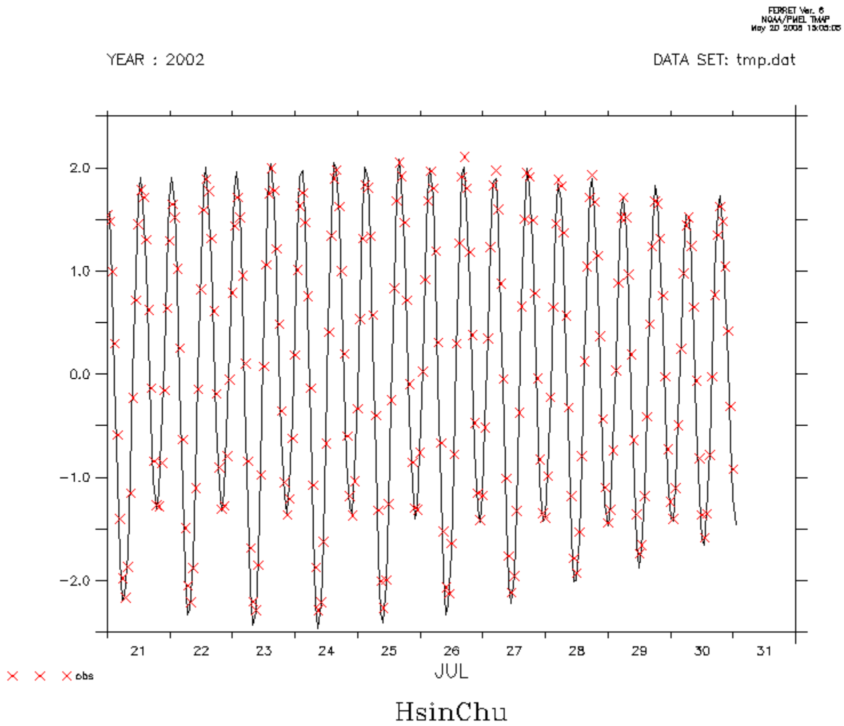

圖 4.2.1-8 以 FVCOM 計算西太平洋潮汐於新竹測站之模擬結果與實測比對

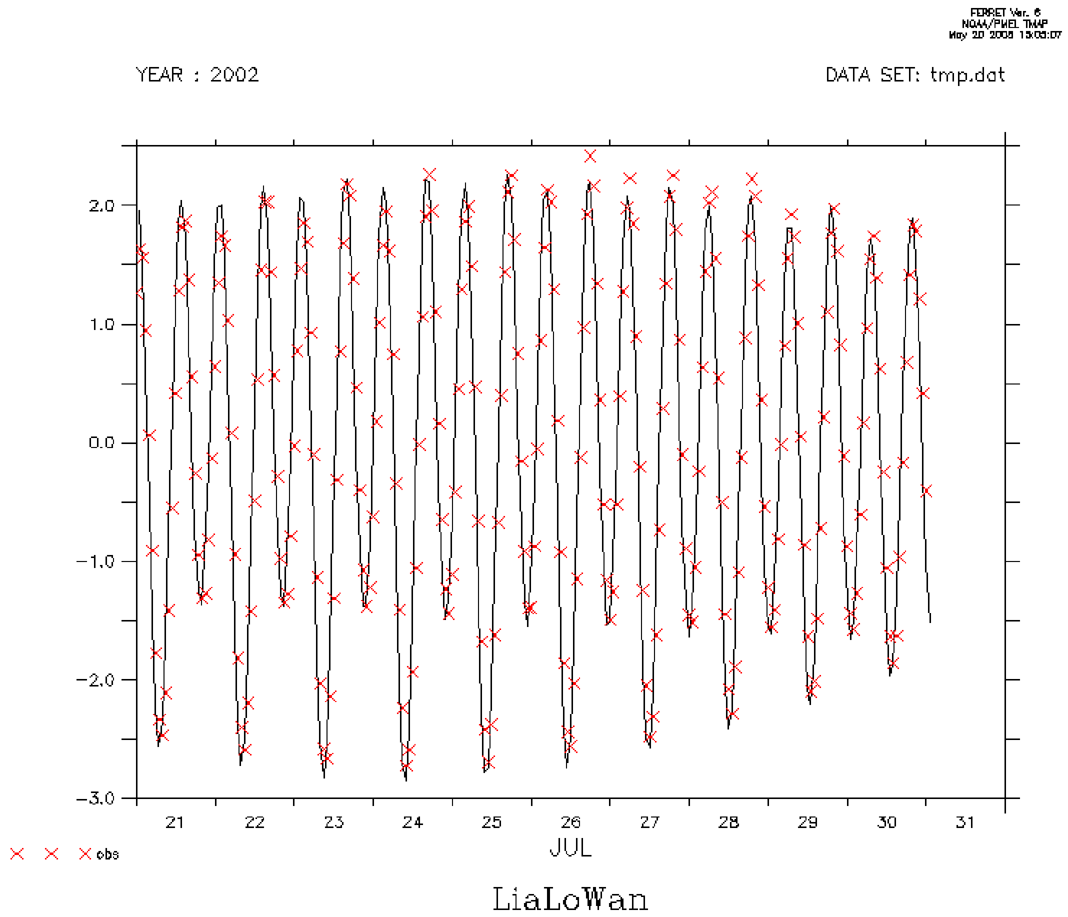

圖 4.2.1-9 以 FVCOM 計算西太平洋潮汐於金門測站之模擬結果與實測比對

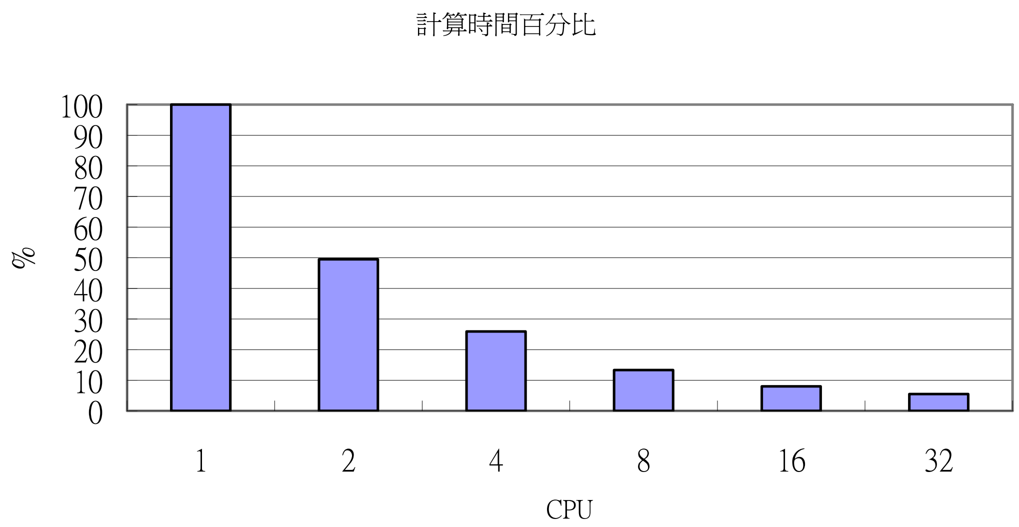

圖4.2.1-10 FVCOM模式之平行效率

4.2.2 COHERENS

此模式於 1990 至 1998 年，由歐洲聯盟贊助，結合歐洲數國的海洋學者，為了研究北海的海洋環境生態系統而聯合發展出之三維水理及生態模式，目的是藉由物理及生物數值模式來了解人類活動行為對海洋生態之影響，並做為模擬分析及預報物理與生地化的過程及監測海岸地區與大陸棚海域中污染物質傳輸的工具。

模式中關於物理、生態、沈積物之間的關係如圖 4.2.2-1 所示，其中水理模組是 COHERENS 模式動力最基本的部份，在水理模組中，除了傳輸及對流外，還包括紊流部份。當水理部份建構完整後，然後才能將水理計算所得到的結果用來進行鹽度、溫度及生態模組在水體中的計算；於真實情況下，海洋生態之間的關係與機制非常複雜的，為了加速模式的計算速度，COHERENS 生態模組部份根據 Tett(1990) 的概念，將海洋生態系簡化為三大部份，分別為浮游微生物部份、碎屑物質部份及溶解性物質部分。由於各種生地化的過程都需依賴水體，因此完整的水動力模擬是本文的基礎，以下就 COHERENS 水動力模組及生態模組的設定進行描述。

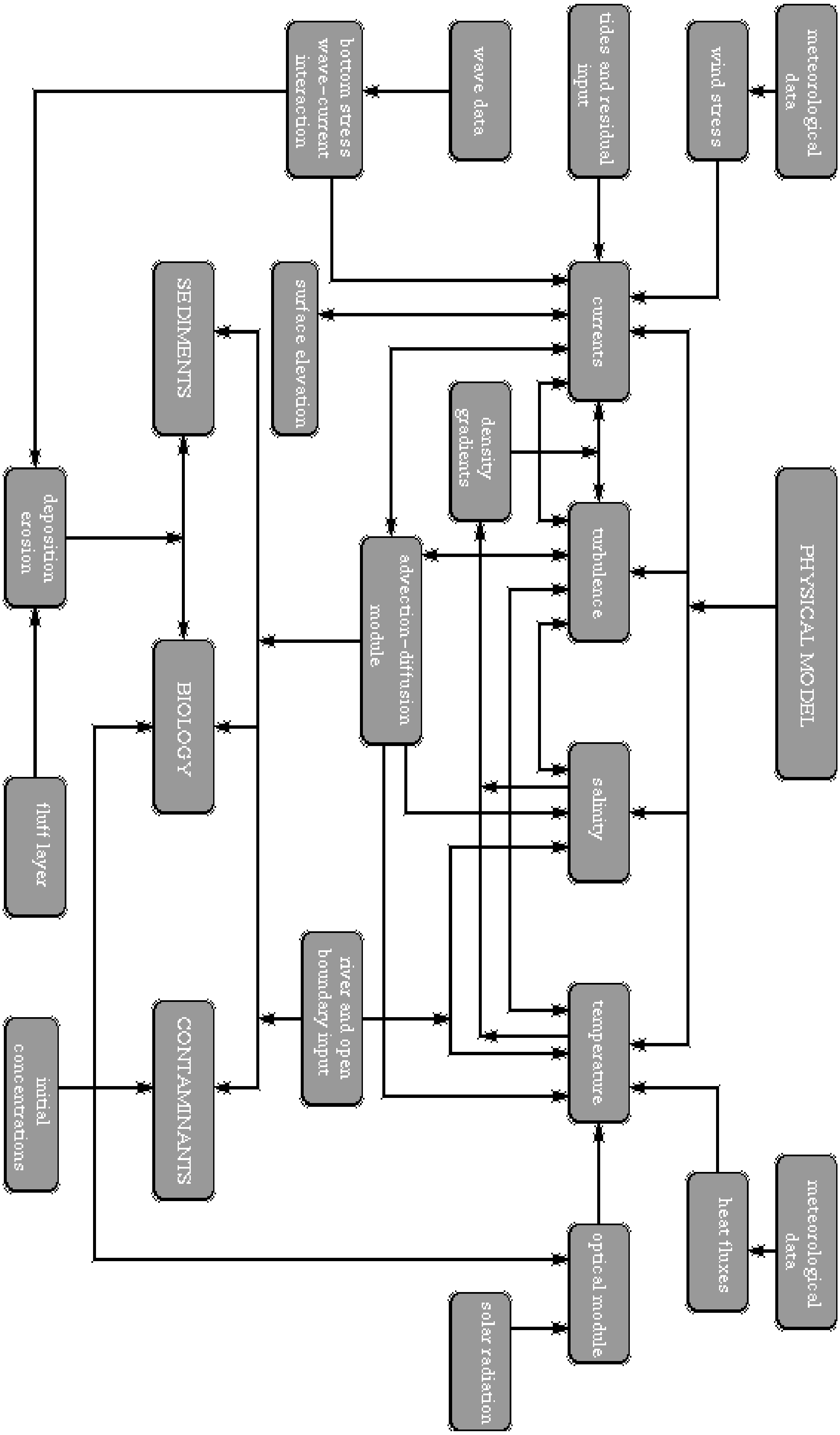

圖 4.2.2-1　COHERENS 模式物理、生態與沈積物之間相互關係圖

4.2.2.1 水動力模組

(1)模式之基本方程式及格點分佈

COHERENS 中的水動力模組以三維動量方程式、連續方程式及溫鹽的傳輸方程式描述海水的運動，動量方程式並採用 Boussinesq 及垂直方向的水靜力平衡（hydrostatic equilibrium）的假設而簡化。以有限差分的數值方法，將基本方程式以有限差分的方式表示，進而以各種不同的數值方法進行演算。基本的方程式表示如下（Luyten, 1999）：

動量方程式：

$$\frac{\partial u}{\partial t}+u\frac{\partial u}{\partial x_1}+v\frac{\partial u}{\partial x_2}+w\frac{\partial u}{\partial x_3}-fv=-\frac{1}{\rho_0}\frac{\partial p}{\partial x_1}+\frac{\partial}{\partial x_3}\left(v_T\frac{\partial u}{\partial x_3}\right)+\frac{\partial}{\partial x_1}\tau_{11}+\frac{\partial}{\partial x_2}\tau_{21}$$

$$\frac{\partial v}{\partial t}+u\frac{\partial v}{\partial x_1}+v\frac{\partial v}{\partial x_2}+w\frac{\partial v}{\partial x_3}+fu=-\frac{1}{\rho_0}\frac{\partial p}{\partial x_2}+\frac{\partial}{\partial x_3}\left(v_T\frac{\partial v}{\partial x_3}\right)+\frac{\partial}{\partial x_1}\tau_{12}+\frac{\partial}{\partial x_2}\tau_{22}$$

壓力平衡方程式：

$$\frac{\partial p}{\partial x_3}=-\rho g$$

連續方程式：

$$\frac{\partial u}{\partial x_1}+\frac{\partial v}{\partial x_2}+\frac{\partial w}{\partial x_3}=0$$

溫鹽控制方程式：

$$\frac{\partial T}{\partial t}+u\frac{\partial T}{\partial x_1}+v\frac{\partial T}{\partial x_2}+w\frac{\partial T}{\partial x_3}=-\frac{1}{\rho_0 c_p}\frac{\partial I}{\partial x_3}+\frac{\partial}{\partial x_3}\left(\lambda_T\frac{\partial T}{\partial x_3}\right)+\frac{\partial}{\partial x_1}\left(\lambda_H\frac{\partial T}{\partial x_1}\right)+\frac{\partial}{\partial x_2}\left(\lambda_H\frac{\partial T}{\partial x_2}\right)$$

$$\frac{\partial S}{\partial t}+u\frac{\partial S}{\partial x_1}+v\frac{\partial S}{\partial x_2}+w\frac{\partial S}{\partial x_3}=\frac{\partial}{\partial x_3}\left(\lambda_T\frac{\partial S}{\partial x_3}\right)+\frac{\partial}{\partial x_1}\left(\lambda_H\frac{\partial S}{\partial x_1}\right)+\frac{\partial}{\partial x_2}\left(\lambda_H\frac{\partial S}{\partial x_2}\right)$$

其中（u，v，w）：代表 X、Y、Z 方向之水流流速(ms^{-1})。

（x_1，x_2，x_3）：代表 X、Y、Z 方向。

$f=2\Omega\sin\Phi$：地球自轉所產生之科氏力。

$\Omega=2\pi/86164$（rad/s）為地球自轉頻率。

Φ 為模擬地區之緯度。

ν_T 及 λ_T 為垂直渦流（eddy）黏滯係數及擴散係數。

λ_H 為鹽度及溫度的水平擴散係數。

P：大氣壓力（Nm^{-2}）。

ρ 為水體密度($kg\ m^{-3}$)。

ρ_0 為 reference density（$kg\ m^{-3}$）。

g 為重力加速度（ms^{-2}）。

c_p 為等壓下之海水比熱

I 為日照強度（Wm^{-2}）。

水平剪力則定義如下：

$$\tau_{11} = 2\nu_H \frac{\partial u}{\partial x_1}$$

$$\tau_{21} = \tau_{12} = \nu_H \left(\frac{\partial u}{\partial x_2} + \frac{\partial v}{\partial x_1} \right)$$

$$\tau_{22} = 2\nu_H \frac{\partial v}{\partial x_2}$$

其中 ν_H 為水平擴散係數。

為了方便表示以上這些方程式，僅以卡式座標的型態表現，在實際上的應用時，COHERENS 於水平方向可選用卡式座標或球形座標。

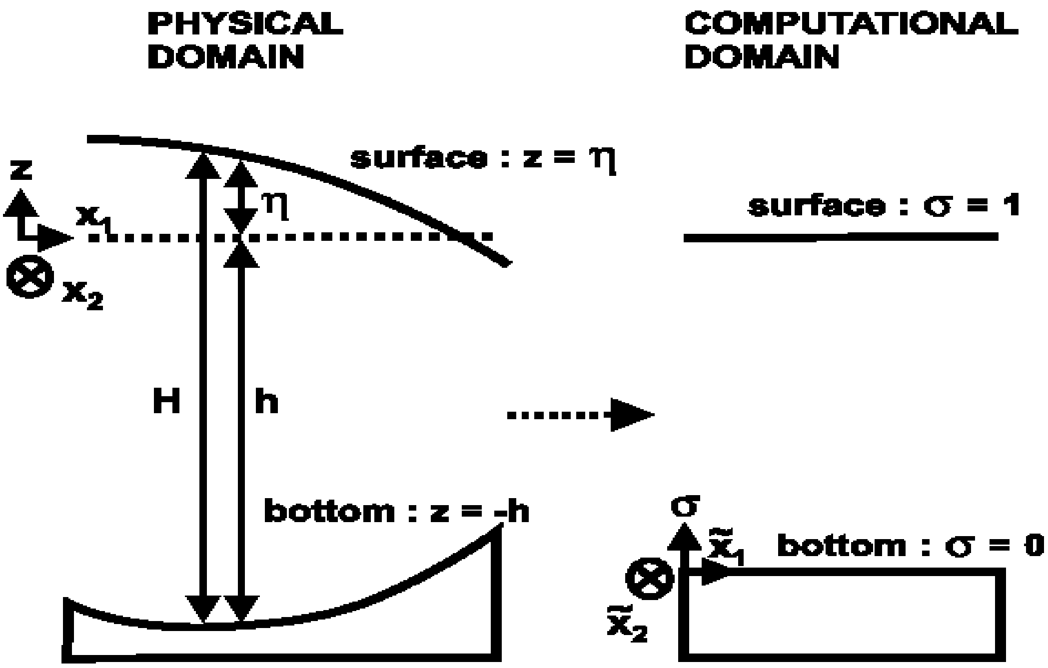

圖 4.2.2-2、垂直方向之σ座標系統(COHERENS User Documentation)

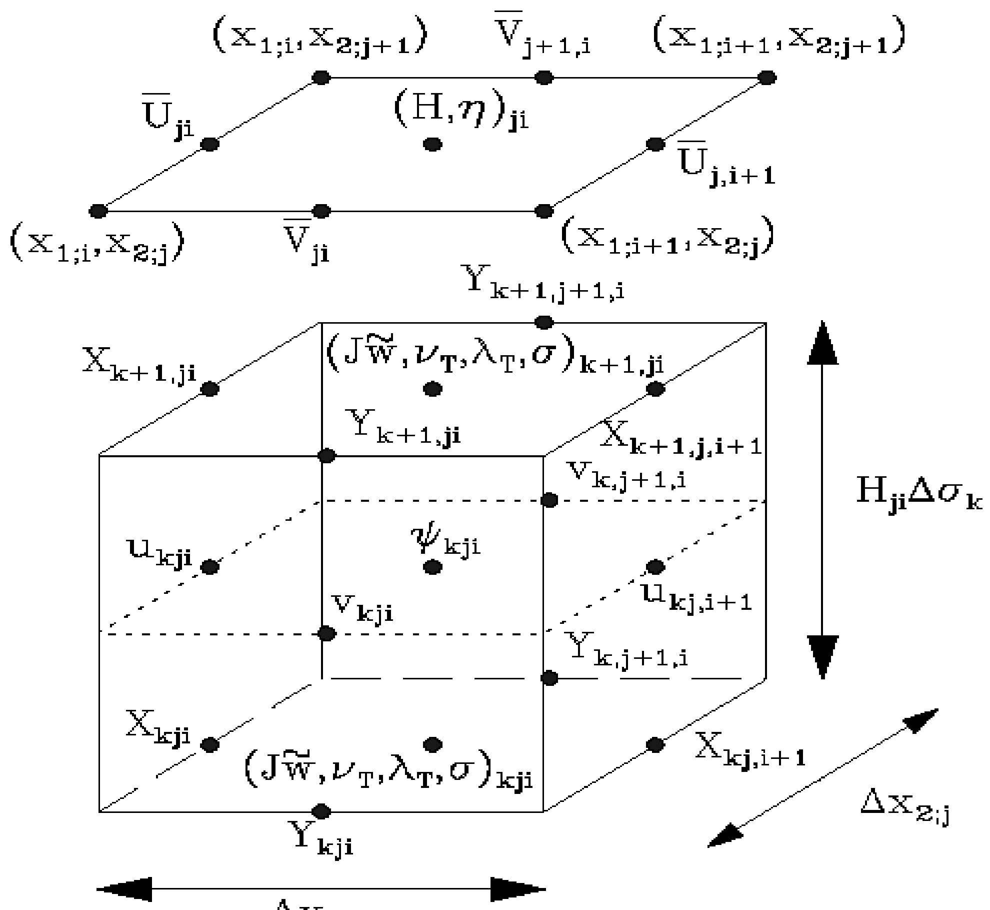

圖 4.2.2-3、二維及三維的格點分佈(COHERENS User Documentation)

因為以卡式座標系統處理底層邊界的差分計算相當繁複且不易，所以為了避免產生這樣的問題，COHERENS 使用了 Sigma 座標系統，將計算領域中垂直方向的座標，統一劃分成固定數目的層數，這樣的處理方式使得差分計算變得容易且易於了解，如圖 4.2.2-2 所示。另外，COHERENS 在水平格點方面採用了 Arakawa-C Grid 分佈，如圖 4.2.2-3 所示，此方式使得流速及壓力、水位的計算點得以交錯開來，可以容易瞭解各計算點所得到的值，同時對於開放或海岸邊界條件的劃定也變得較為容易。

(2)紊流的計算

在進行海洋的流場模擬時，最常碰到的問題是如何在垂直交換過程中輸入合理的紊流係數，這些係數不只影響了流場及溫鹽場計算的結果，相對地也影響了生物、沉積物及營養鹽的計算，所以這些係數的給定是相當重要的。為了得到在模擬中得到合理的垂直擴散係數，有許多不同的數值方法進行演算，於 COHERENS 中也包含了數種方法，其中最著名的是 2.5D Turbulence closure scheme（Mellor 和 Yamada，1982），這些數值方法涵蓋以下數個物理過程的影響：

1. 底層摩擦力而造成的紊流
2. 表層風場所造成的紊流
3. 由於波和流在底層的交互作用所加強的底部摩擦力而造成的紊流
4. 季節的循環所造成溫度的不同而產生的變化，包括斜溫層的升降
5. 因河口淡水注入海水，在水層交界處引發剪應力所造成的混合

(3)水平擴散之計算

水平擴散係數則參考一直廣泛使用中的 Smagorinsky 參數化條件（1963），與採用的格點間隔大小有關。使用方程式如下：

$\nu_H = C_{m0}\Delta x_1 \Delta x_2 D_T$ ， $\lambda_H = C_{s0}\Delta x_1 \Delta x_2 D_T$

其中

$$D_T^2 = \left(\frac{\partial u}{\partial x_1}\right)^2 + \left(\frac{\partial v}{\partial x_2}\right)^2 + \frac{1}{2}\left(\frac{\partial u}{\partial x_2} + \frac{\partial v}{\partial x_1}\right)^2$$

，Δx_1 及 Δx_2 為格點的間隔大小。

在模式中 C_{m0} 及 C_{s0} 之數值係數預設為相等的值。

(4)對流項的計算

過去在進行對流項的計算時，由於數值方法產生的誤差會造成數值擴散，有些方法甚至會讓濃度有負值的產生。COHERENS 提供了幾種數值修正的方法，包括了 Upwind scheme、Lax-Wendroff scheme、TVD superbee scheme 及 TVD monotonic scheme。 COHERENS 預設的數值方法為第三種，即 TVD superbee scheme，此種方法雖然仍有些微程度的數值擴散現象，但計算結果比其他三種的數值方法來的準確。由於計算的變數中，變數的變化可大可小，但當變化極小時，數值方法而造成的擴散將形成困擾，使得計算的結果不能呈現出應得之結果，所以對流項的計算正確與否，顯得特別重要。

(5)邊界條件

在 COHERENS 中，分成東西南北四個方向的邊界，其邊界條件可以設定為開放的海洋，河川以及陸地邊界。在邊界的輸入形式分為以下數種：

- 使用調和分析之形式輸入流速及水位
- 無水流進入
- 使用調和分析之形式輸入水位
- 使用調和分析之形式輸入流速

(6)氣象因子

氣象因子包含表面風速、大氣溫度、大氣壓力、雲量遮蓋率、相對濕度、水氣蒸發量、太陽幅射能及水體能量消失等因子，表 4.2.2-1。模式中，氣象所造成之變化影響著水溫、生化反應（例如光合作用）、空氣與水表面間交換（例如氧氣交換）等變化。其中水氣蒸發量(E_{vap})、太陽幅射能（Q_{SOL}）及水體能量散失（Q_{nsol}），由模擬時間、地點及氣候因素輸入方程式計算得知，其餘因子，由模擬地點當地資

料提供。

$$E_{vap} = Q_{la} / L_V$$

其中 Q_{la} 為潛熱（latent heat flux）散失，$L_V = 2.5008\times10^6 - 2300.T_S$ 為水氣蒸發所散失之能量（J kg^{-1}），T_S 為水表面之水溫（℃）。

$$Q_{SOL} = Q_{CS}(1-0.62 f_C + 0.0019\gamma_{\theta,\max})(1-A_S)$$

$$Q_{nsol} = Q_{la} + Q_{se} + Q_{lw}$$

Q_{CS} 為晴朗天氣下之總幅射能，f_C 為雲量遮蓋率（0~1），$\gamma_{\theta,\max}$ 為太陽在中午時之高角度，A_S 為水表面之反射率（albedo），一般海表面反射率為 0.06。

Q_{la} 為潛熱散失、Q_{se} 為水表面之熱交換、Q_{lw} 為長波幅射散失。

表 4.2.2-1 氣象因子

氣象因子	符號	單位
太陽幅射能	Q_{SOL}	Wm^{-2}
水體能量散失	Q_{nsol}	Wm^{-2}
平均風速	WIND	ms^{-1}
氣溫	SAT2	℃
大氣壓力	P2	(Pa)Nm^{-2}
水氣蒸發速率	EVAPR	Kgm^{-2}s^{-1}
降雨量	RAIN2	Kgm^{-2}s^{-1}
相對濕度	HUM2	0~1
雲遮量	CLOUD2	0~1

(7)其他計算參考

為了加快計算的進行，COHERENS 中使用了 Mode Splitting 的方法。由於密度所造成內部重力波的傳遞並不像表面重力波那麼明顯，將受重力波速度限制的水深平均正壓模組與受斜壓主導的垂直循環分開計算。如此，雖然正壓模式因時間步長必須滿足數值穩定條件的限制，但是僅需計算一層，所以可使計算速度加快；每隔一段時間後，再以正壓模組計算之水位代入斜壓模組計算其垂直流場的變化。溫度及鹽度的傳輸模式亦同時以更新的垂直流場重新計算其溫、鹽場的分佈狀況。

整體說來，COHERENS 中的水動力模組包含了以下數個特色：

1. 採用 Mode-splitting 的方法計算動量及連續方程式，加快計算的時間。
2. 溫度場及鹽度場的模擬。
3. 包含了光照的影響，表層水體因光照而產生的溫度變化可加入模式中。
4. 在動量及紊流方程式中密度的影響藉由 equation of state 來計算。
5. 紊流的影響藉由數種不同的演算方法而獲得。
6. 包括了表面風場的影響。
7. 包含波流交互作用所造成底部剪應力的加強所造成的影響。
8. 利用不同的演算法來避免計算對流項時所造成的數值擴散。

4.2.2.2 生態模組

在 COHERENS 生態模式中，嘗試以浮游微生物、碎屑有機物、溶解性營養鹽及溶氧之間的關係所建立的海洋生態系統，如圖 4.2.2-4 所示，來表達陸棚海域中海洋生態系統的變化。

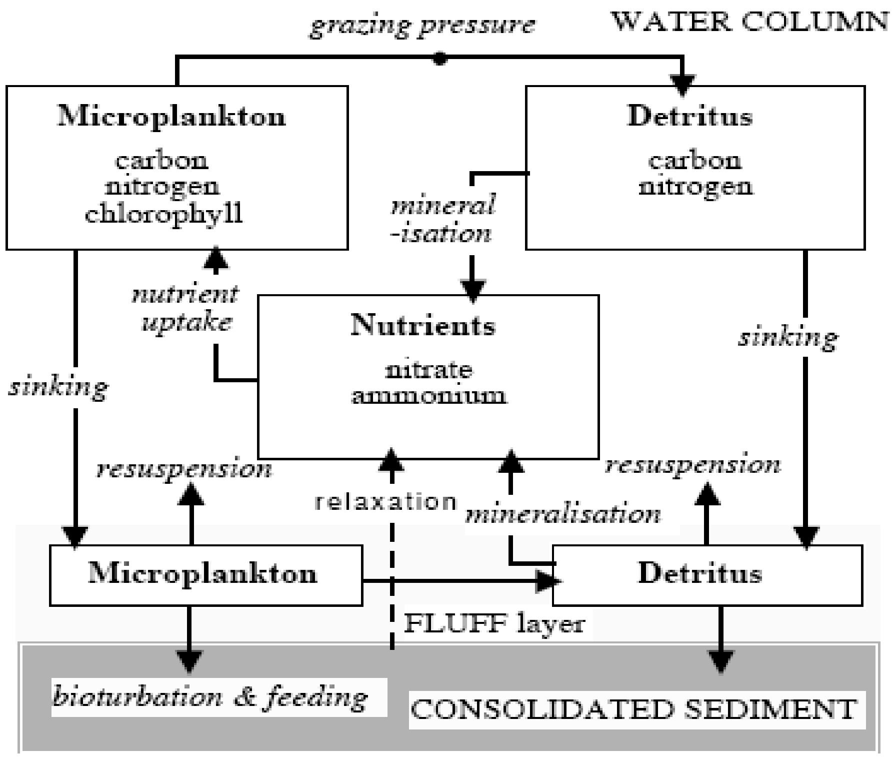

圖 4.2.2-4 COHERENS 生態模式示意圖(COHERENS User Documentation)

有關 COHERENS 生態模式的模擬變數，依照 Tett (1990a)建議，共有 8 個獨立變數，並歸類為三大部份，如表 4.2.2-2 所示。三大部份分別為浮游生物部份、溶解性物質部份及碎屑有機物質部份，以下分別進行介紹：

（一）浮游微生物(microplankton)：

小於 200 μm 之單細胞微小生物。包括屬於營異性之細菌、原生動物(zooflagellates、ciliates、heterotrophic dinoflagellates)及自營性之藍綠細菌與微細藻類(diatoms、dinoflagellates、flagellate)。以上定義是由 Tett (1987)根據 Dussart (1965)對「浮游微生物」的定義延伸而來；另外依據「微生物迴圈」理論 (Microbial Loop) 說明在浮游微生物食物鏈中，關於細菌及微小浮游植物部份，其維持生命生存之主要能量來源來自於溶解性有機物(DOM)及本身吸收光能量進行光合作用或從分解碎屑有機物中獲得。這些細菌和微小浮游植物在食物鏈中

扮演提供浮游動物或魚類主要食物來源之角色 (Azam et al, 1983；Williams 1981)。

模式中，將微藻及藍綠細菌納入浮游植物中，並且扮演浮游生物食物鏈中生產者的角色。

（二）營養鹽：

營養鹽是指浮游植物生長所需（例如氮、磷、矽或其它元素）之溶解性無機化合物。其中氮、磷元素為浮游植物生長所必需的；矽是某些浮游植物細胞壁內重要組成部份。通常在海洋環境中，氮元素為浮游植物生長過程中，控制其生長之營養鹽主要限制因子。

在 COHERENS 生態模式中，以氮作為營養鹽模擬因子，並假設其它營養鹽在陸棚海域中是充足的；此外，在浮游植物生長過程中，也需要光照來提供能量。在某些情況（例如冬天），光能量強度影響浮游植物生長更勝於營養鹽。模式中，以光能量強度及營養鹽(氮)濃度作為影響浮游植物生長速率之重要因子。

（三）碎屑有機物：

碎屑有機物包含死亡的浮游生物屍體及大型浮游動物(meso-zooplankton)捕食浮游生物過程中所遺留下的碎片（fraction）；這些碎屑有機物被水中分解者(通常為細菌)進行再礦化作用(remineralisation)分解，進而轉化為無機性營養鹽及二氧化碳，以提供給食物鏈(網)中生產者使用。

8 個獨立變數分別為浮游生物碳(microplankton carbon)和氮(microplankton nitrogen)；碎屑有機碳 (detritus carbon)和氮 (detritus nitrogen)；硝酸氮 (nitrate)、氨氮 (ammonium)、溶氧 (oxygen)以及大型浮游動物氮 (zooplankton nitrogen)。另外關於葉綠素部份，模式假設葉綠素和浮游生物體內碳呈相關函數，因此不列入獨立變數。在 COHERENS 生態模式中，主要以氮作為營養鹽模擬因子，並假設其它營養鹽在陸棚海域中是充足的，此假設與南海營養鹽利用狀況類似；此外，在浮游植物生長過程中，也需要光照來提供能量。在某些情況（例如冬天），光能量強度影響浮游植物生長更勝於營養鹽。模式中，以光能量強度及營養鹽(氮)濃度作為影響浮游植物生長速率之

重要因子。

表 4.2.2-2 COHERENS 生態及沉積物模式部份之模擬變數

模擬變數	符號	單位
浮游生物碳(microplankton carbon)	B	mmol C m^{-3}
浮游生物氮(microplankton nitrogen)	N	mmol N m^{-3}
大型浮游動物氮(zooplankton nitrogen)	ZN	mmol N m^{-3}
碎屑有機碳(detritus carbon)	C	mmol C m^{-3}
碎屑有機氮(detritus nitrogen)	M	mmol N m^{-3}
硝酸氮(nitrate)	NO_S	mmol N m^{-3}
氨氮(ammonium)	NH_S	mmol N m^{-3}
溶氧(oxygen)	O	mmol O m^{-3}
無機性沉積物(inorganic sediment)	A	g m^{-3}

4.2.2.3 實際案例

本團隊使用了 COHERENS 進行了大鵬灣及南海的模擬，圖 4.2.2-5 及圖 4.2.2-6 為大鵬灣雨季表層鹽度及溫度變化圖，圖 4.2.2-7 為 2000 年啟德颱風期間南海表層水溫分佈圖，本次模擬利用颱風模式配合 COHERNES 進行湧昇流的模擬結果，可以觀察到啟德颱風於菲律賓附近海域產生的湧昇現象。

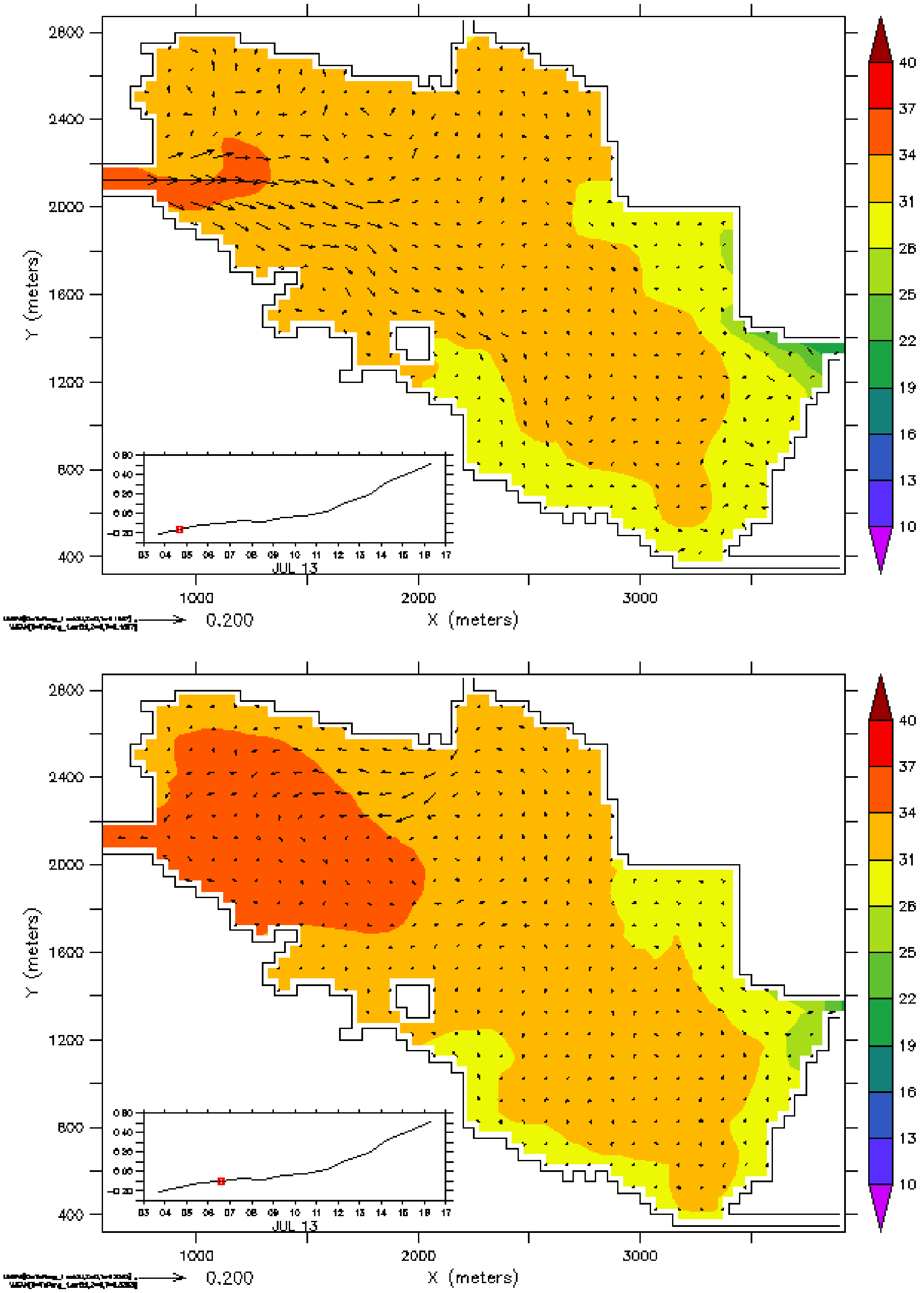

圖 4.2.2-5 大鵬灣雨季表層鹽度分佈圖

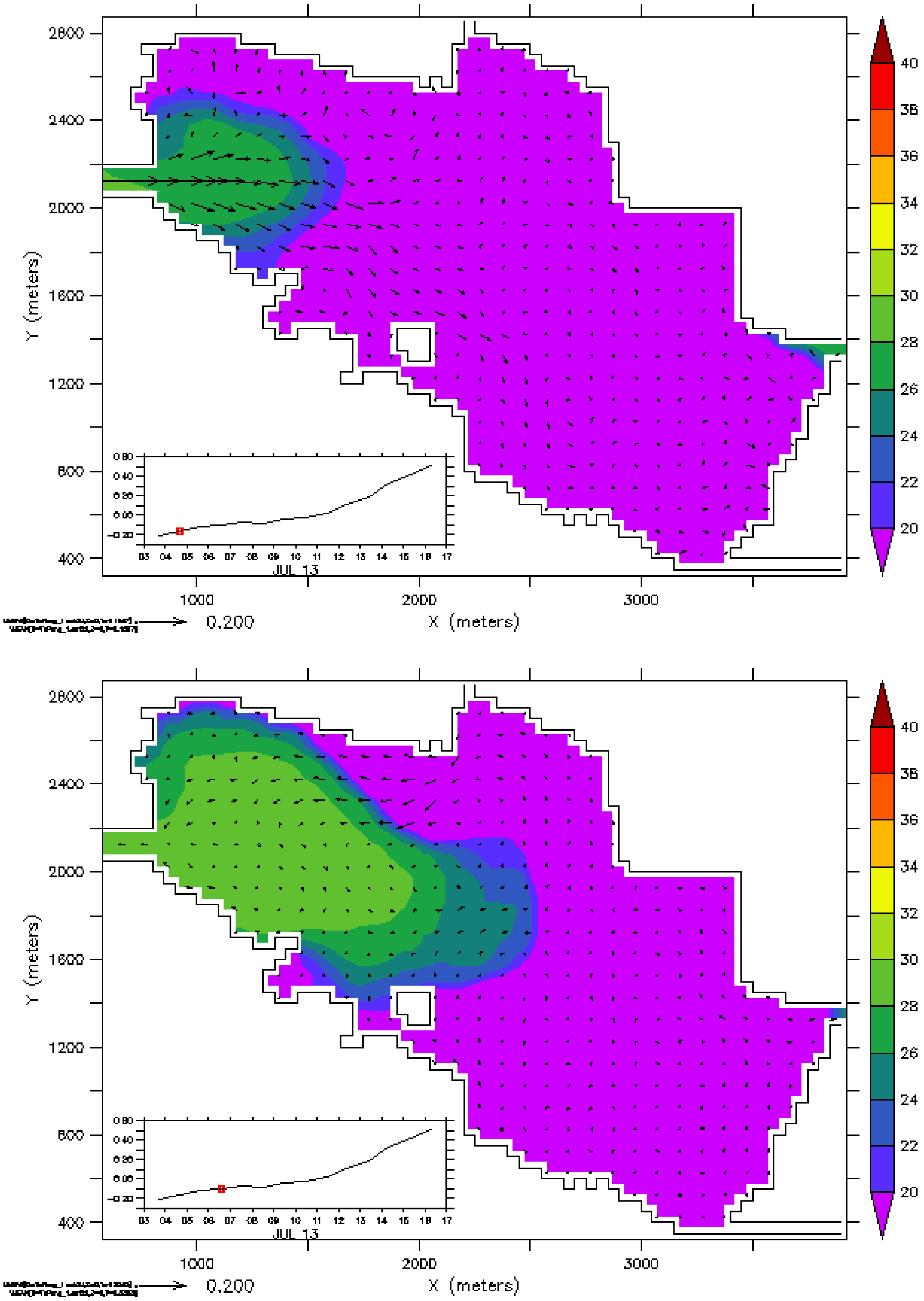

圖 4.2.2-6 大鵬灣雨季表層溫度分佈圖

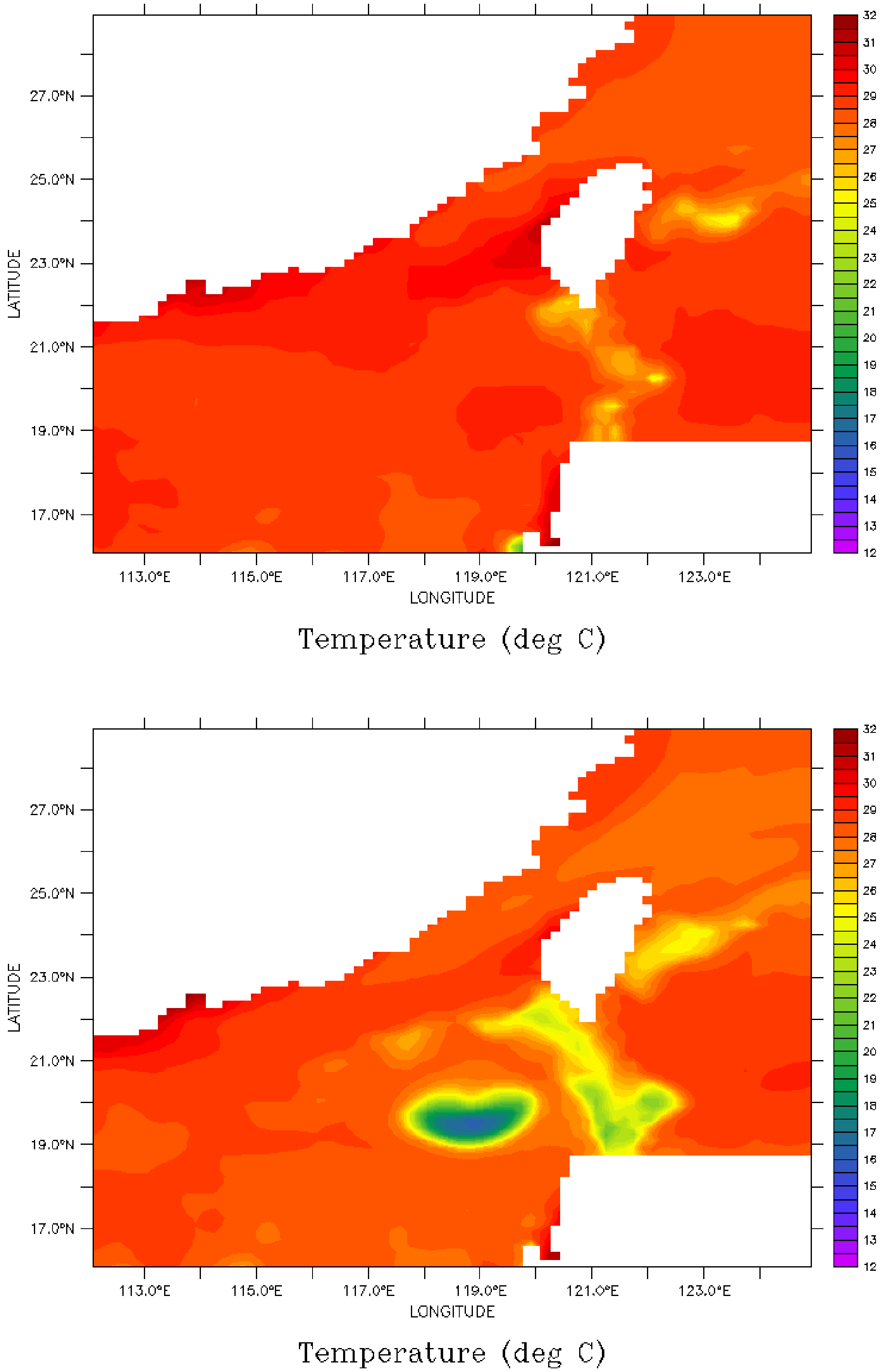

圖 4.2.2-7 啟德颱風期間南海表層水溫分佈圖

4.3 模式選擇

表 4.3-1 為上述模式特點，藉由上一節模式的特性瞭解，現階段水動力的理論皆已相當成熟，因此各個模式皆可進行海流的模擬，差別僅在模式未來是否持續發展改進、模式使用者支援是否完整、模式執行效率、模式適應性以及模式取得是否方便，綜合以上靠量的因素，本團隊建議使用 ROMS 作為未來太平洋及北太平洋環流的模擬工具，理由如下：

1. ROMS 原始碼為公開且免費使用，對於後續模式依據不同特性地點提供修改的使用彈性
2. ROMS 有完整的使用者論壇，可供使用者交流使用心得及解決使用者遇到的問題
3. ROMS 目前仍持續在發展，不斷修正細部問題及提升執行效率
4. ROMS 目前已嵌合波浪模式，未來仍會繼續嵌合大氣模式，對於未來海氣的影響更直接
5. ROMS 執行效率相當好，對於未來計算量增加仍可藉由平行計算取得合理的計算時間
6. ROMS 的網格設計對於不同的地形或海岸皆可有不錯的適應彈性

表 4.3-1 各模式特性整理表

	POLCOMS	ROMS	COHERENS	FVCOM
水平網格	正交曲面	正交曲面	正交	三角網格
垂直網格	s-coordinate	s-coordinate	Sigma coordinate	s-coordinate
平行運算	可	可	不可	可
輸出/入檔案格式	純文字	netcdf 格式	netcdf 格式	文字檔(未來改為 netcdf)
資料同化模組	有	有	無	有
是否持續發展	否	是	否	是
原始碼取得	需由特殊管道取得	網路免費取得	網路免費取得	網路免費取得
使用者論壇	無	有	無	有
交流會議	無	有	無	有

4.3.1 理想案例測試

選定使用 ROMS，為了瞭解實際的執行狀況，本團隊使用利用理想化案例來瞭解 ROMS 的模擬結果，主要測試與海流有關的項目，包括邊界條件選定、對流項方法選定。模式網格設定為 100 x 100，網格大小為 1 公里，水深為固定水深 150 公尺，ROMS 在邊界計算選擇共有四種計算方式，分別為 Chapman、Gradient、Radiation 及 Clamped 計算方法，本案例利用 M2 單一分潮進行測試，振幅為 1 公尺，三邊邊界為封閉狀態，僅東邊邊界輸入(i=100)，模式使用 2 維運算，計算時間為 10 天，模式 time step 為 25 秒，測試結果如圖 4.3.1-1 至圖 4.3.1-3。圖中 Chapman 及 Gradient 邊界設定產生的模式結果一樣，水位振幅皆接近 1 公尺，且週期為 12.42 小時，符合假設的輸入邊界條件；Radiation 邊界設定產生得的結果振幅大於輸入的邊界條件，接近 1.2 公尺，且在平潮時期會產生小幅震盪，週期則正常；Clamped 邊界設定則在振幅產生不足的現象，僅為 0.6 公尺左右，在

週期的部份也較前三者為長。總和以上結果，未來若要使用潮汐邊界輸入，邊界形式建議選擇 Chapman 或 Gradient 方式比較適合。

進行對流項的模擬，ROMS 在垂直方向提供四種對流項設定，分別為 4-th order Akima、2nd-order centered、4th-order centered 及 splines，本案例模式範圍為 100 x 100，網格解析度為 1 公里，水身為 150 公尺，模式四周為封閉邊界，垂直分層為 5 層，水體起始溫度為 30 度，模式驅動力為表面剪力，表面溫度通量為-0.001 degC m/s，模擬時間為五天。圖 4.3.1-4 為四個設定於第五天的垂直溫度分佈結果。由溫度分佈瞭解，趨勢分佈 Akuma、2nd-centered 及 splines 在結果上較接近，溫度的極值 spline 較兩者為小；而 4th-order centered 在溫度上分佈較為平滑，溫度分佈較均勻，極值也較前三者為低，未來仍需有實際案例進行模擬，才能選擇適當地垂直對流向設定。除了垂直的對流項設定，ROMS 也提供了四種水平對流項設定，分別為 Akima、2nd-order centered、4th-order centered 以及 3rd-upstream，模式的模擬環境與測試垂直對流項相同。圖 4.3.1-5 為 3rd-upstream 設定模式表中底層溫度變化。這個測試除了 3rd-upstream 水溫變化正常外，其他三組水平對流項設定皆會造成水溫激烈變化，造成模式不穩定，引此在水平對流項設定以 3rd-upstream 最佳。

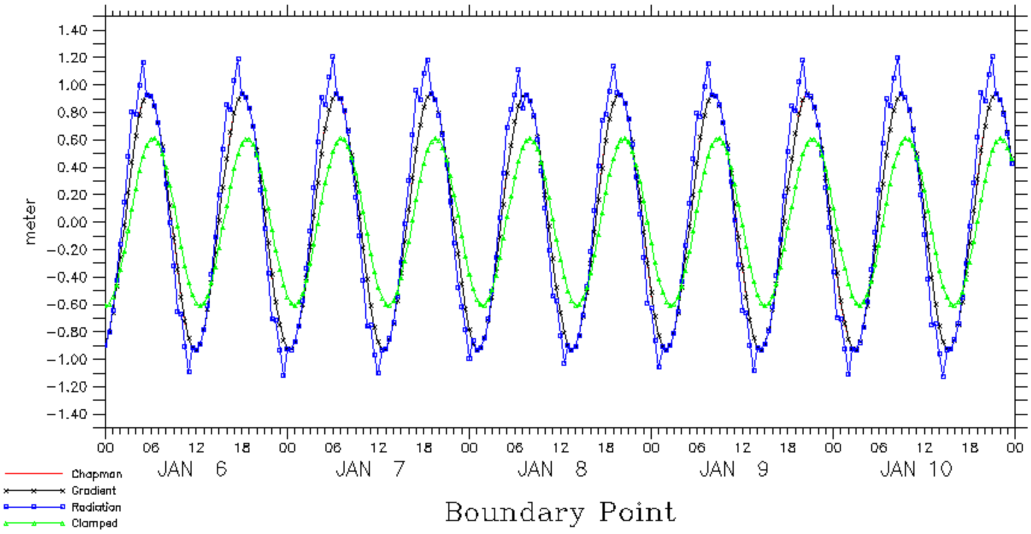

圖 4.3.1-1 開放邊界點時序圖(i=100)

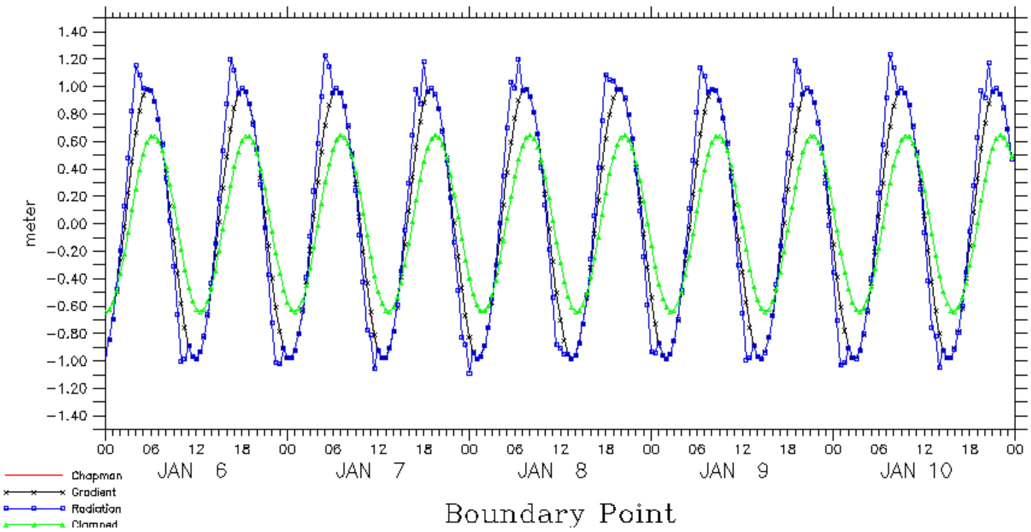

圖 4.3.1-2 中間點時序圖(i=50)

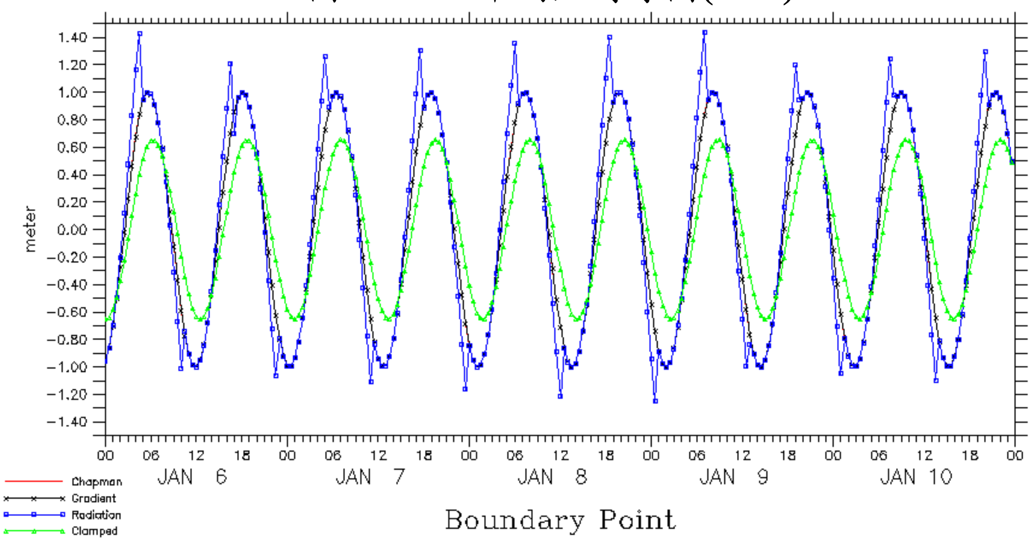

圖 4.3.1-3 封閉邊界點時序圖(i=1)

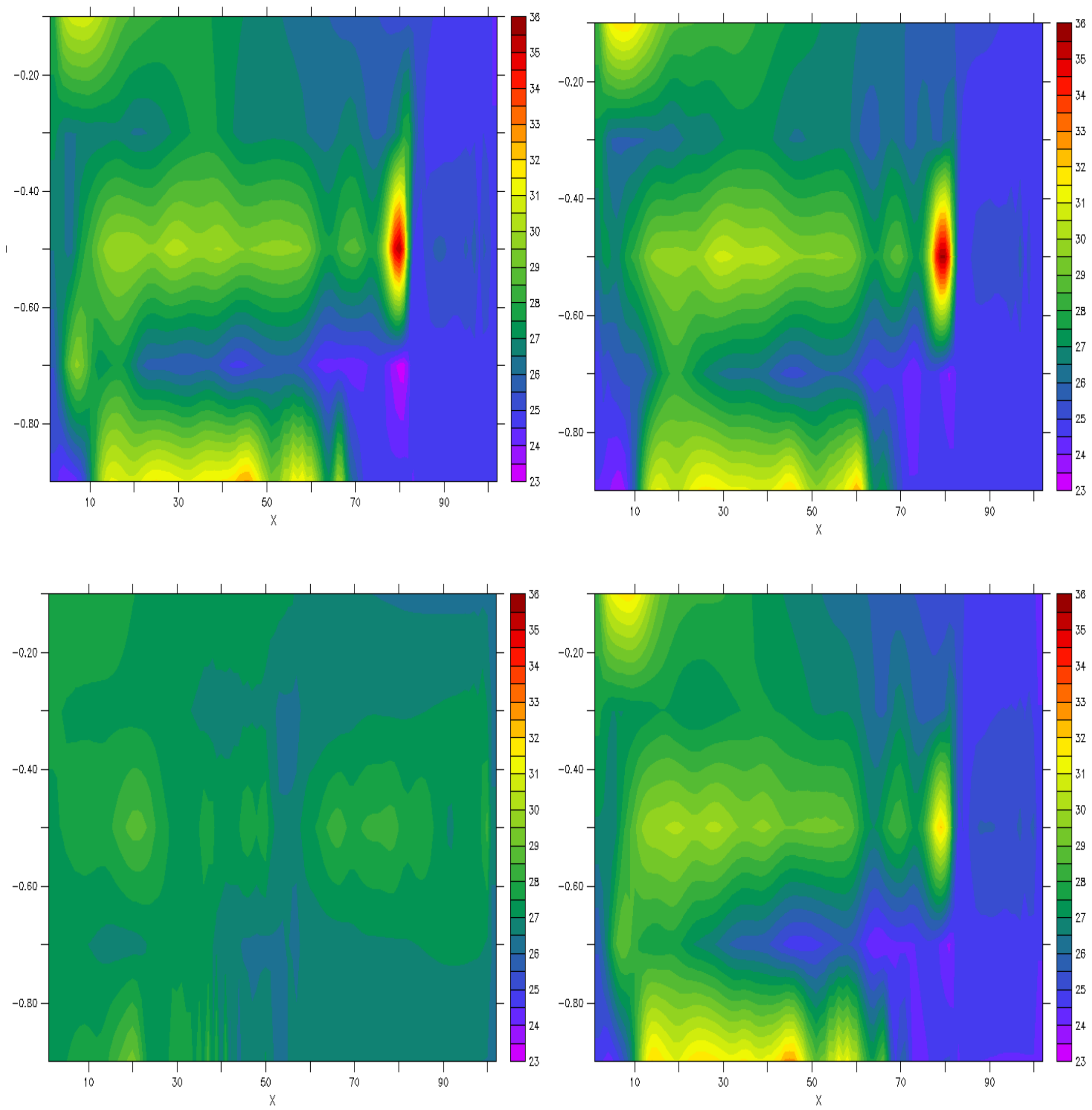

圖 4.3.1-4 垂直溫度分佈圖(j=50，縱軸為 sigma 座標，橫軸為點位)，左上：Akima，左下：4th-order centered，右上：2nd=order centered，右下：splines

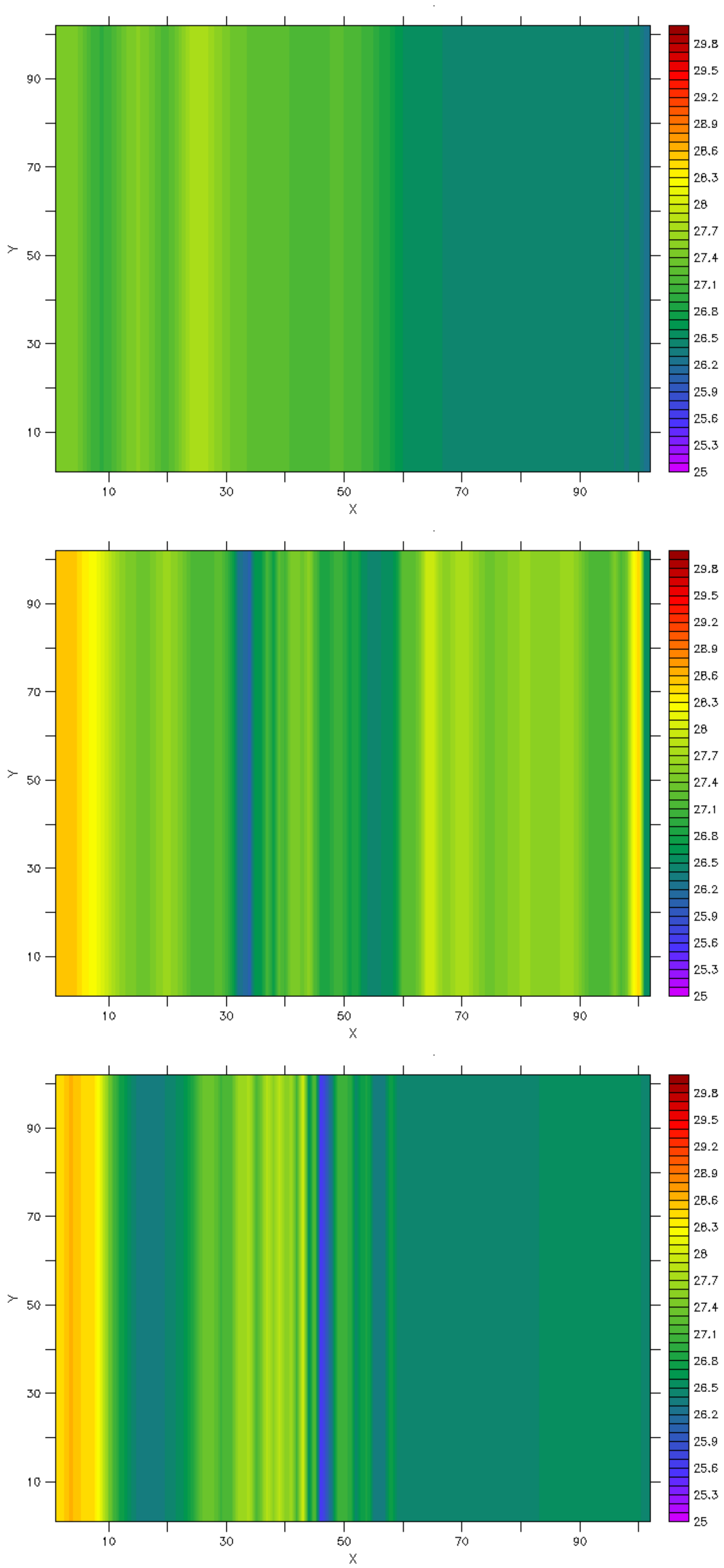

圖 4.3.1-5　3rd-upsream 設定表中底層溫度變化分佈

4.3.2 海流模式於氣象局高速計算電腦系統測試

由於未來海洋環流預報模式需移交氣象局進行運算，因此採用的模式需要於氣象局高速電腦中運算。目前氣象局的高速電腦系統。其主要由 IBM P5-575 系統所組成，此系統是使用 IBM Power5 時脈 1.5GHz 雙核心中央處理器，每一個節點連結 8 顆 power5 中央處理器，共建置了 156 個節點，共有 2496 個中央處理器可供使用，其中 138 個節點可供計算使用；主記憶體容量，有 36 個節點每個中央處理器可使用 4GB 的容量，120 個節點每個中央處理器可使用 2GB 的容量；在硬碟容量則配置了 18TB 供研究使用，14TB 供作業化使用，計算能力相當強大。在軟體的配置上，此套系統使用 IBM 自製的作業系統 AIX5L 5.3，提供 XL Fortran(95/90/77)、C 及 C++的程式編譯器，另外包含了 ESSL v4、pESSL v3、及 IMSL 等函式庫供使用者使用；平行環境則提供 Parallel Environment(PE) v4.2 供平行程式進行運算，提昇運算時效；由於此高速電腦可提供多人使用，因此各個工作的資源分配就相當重要了，目前本套系統使用 LoadLeveler(LL) v3.1 來管理工作資源的分配，以讓所有使用者可以完全充分的使用；檔案系統則使用 General Parallel File System(GPFS) v2.3，可提供快速的檔案讀寫。

ROMS 開發過程即是利用大型主機進行開發及測試，因此本團隊目前已順利將 ROMS 建置於氣象局高速電腦系統中，並且進行效率的測試。ROMS 本身提供 MPI 及 OpenMP 的平行技術，由於 OpenMP 在使用的 cpu(中央處理器)數量上會有限制，因此平行計算的部份仍使用目前通用的 MPI 架構，圖 4.3.2-1 為 ROMS 於氣象局高速電腦的平行計算效率，圖 4.3.2-2 則為實際的計算時間。ROMS 的平行效率基本上也是成線性變化，cpu 數量愈多計算計算時間愈短，約在 192 以上顆達到瓶頸，此部份因為模式網格數量不夠多，因此在 192 顆及 256 顆 cpu 的效率接近，以測試的案例來看，192 顆 cpu 是最佳的設定，未來若網格數繼續增加，在增加使用的 cpu 數量即可。

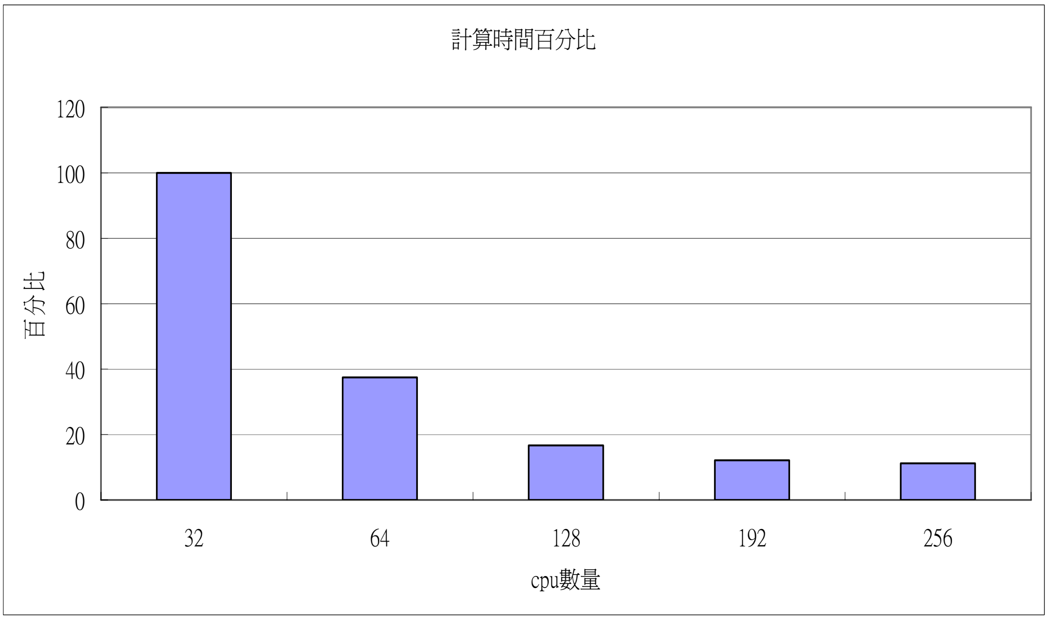

圖 4.3.3-1 氣象局高速電腦平行效率統計結果

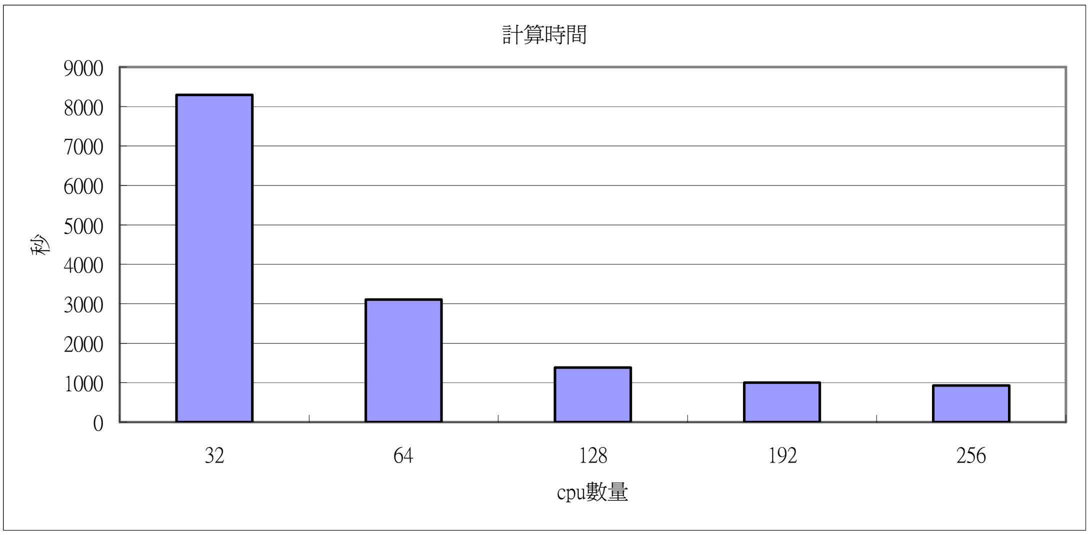

圖 4.3.3-2 氣象局高速電腦平行效率統計結果(實際時間)

第五章 國際資訊及技術交流

海流預報作業是海象預報作業中最為艱鉅的一項工作，亦是近年來歐美先進國家積極發展及改進的項目。一方面提供即時預報海流作為航運、遊憩、漁業等公私部門做為規劃管理及作業之參考，另一方面並可隨時提供救難與緊急應變之需。應用現代高速電腦之計算能力與儲存技術，配合迅速發展之資料同化技術，提升預報作業的時效與精度，提供有效即時預警資訊，研發多尺度台灣海域的海洋預報作業模式是目前海洋預報作業的重點工作。為引進國際間海洋環流模式作業化預報之經驗，特此邀請國內外專精於海洋環流預報作業化經驗之學者專家出席討論，研析國際目前先進作業模式之發展趨勢，並透過這幾位專家建立國際資訊及技術交流管道。

5.1 國際會議（海洋環流模式作業化預報研討會）

經工作會議討論決定，配合氣象局年度舉辦之天氣分析與預報研討會舉辦，今年度天氣分析與預報研討會訂於 97 年 9 月 9 日 (星期二) 至 11 日 (星期四)舉辦，本計畫籌辦之「海洋環流模式作業化預報研討會」於 97 年 9 月 10 日 (星期三)下午舉辦。邀請四位國外專家學者演講，另邀請二位國內專精於海洋環流數值模式之學者搭配演講國內相關經驗，研討會議程與國外演講者之演講內容摘要如附錄A。

5.2 資訊及技術交流

日本氣象研究所海洋研究部 (JMRI/ORD)

今年配合氣象分析研討會舉辦之國際海流預報模式研討會邀請之日本專家為蒲地政文博士（Dr. Masafumi KAMACHI），任職於日本氣象研究所海洋研究部擔任第二研究室室長。他的專長是海流模式之資料同化系統，除在研討會發表論文介紹日本海流模式及資料同化之發展與評估，亦同意接受本團隊之研究人員赴日接受資料同化處理相關之訓練與觀摩，並在反日後，隨即記達一批相關文獻提供本團隊參考，並期待與本團隊就海流作業模式相關議題進行合作交流。

美國海洋大氣總署海洋局 (NOAA/NOS)

今年（2008）海向中心聘請的國外顧問 Dr. Eugene Wei 長期在美國海洋大氣總署轄屬之國家海洋局（NOAA/NOS）服務，專長為海流模式。九月訪台期間除在本計畫所舉辦之研討會演講，報告 NOAA 近年海流作業模式之發展概況，亦參與評估本計畫，除對本計畫寄予厚望，將接受本計畫派遣研究人員赴 NOS 觀摩訓練，以期達成目標。魏博士對本計畫的評估報告參考附錄 B。

美國 SCRIPPS 海洋研究所

Dr. Luca Centurioni 任職於美國 SCRIPPS 海洋研究中心，與 NOAA GDP(Global Drifter Program)合作，負責全球漂移浮標之研發與品管及資料品質管理。台灣目前進行之黑潮計畫即由國研院海科中心與之合作進行。Dr. Centurioni 不但協助本團隊取得過去 20 年之太平洋浮標資料，亦參與指導本團隊之碩博士班學生處理浮標資料。他亦建議CWB在未來可以積極利用SVP-B海面氣壓漂移浮標校驗颱風路徑，以獲取更精確之遠洋資訊，及早修正颱風路徑預報。由於台灣並非 WMO 成員，未來在海流預報作業有許多即時資料需求，如果無法即時取得將會影響整體計畫的發展。Dr. Centurioni 經與 DBCP 討論後認為，如果 CWB 積極參與 WMO 相關觀測計畫，例如參與 SVP-B 氣壓海洋漂移浮標布放，由於可提供他國資料，本計畫亦可即時取得 GTS 資料。另外，他亦保證本計畫可以透過 US-JIMO 等管道即時取得 GTS 資料。

澳洲 IMOS eMarine Information Infrastructure, UT 及
歐洲 NEMO（Nucleus for European Modelling of the Ocean）

Dr. Roger Proctor 原任英國 Proudman Oceanographic Laboratory (POL) 海岸觀測中心主任，於今年（2008）七月起，借調澳洲配屬在 University of Tasmania (UT) 的氣象海洋研究所（IMOS），成立 eMarine

Information Infrastructure 擔任主任三年，協助澳洲整合海洋資訊研發業務。Dr. Proctor 在 POL 期間即與本團隊交流頻繁，除安排訓練博士班研究生並提供 POLCOMS 海流預報模式及全球氣象資料進行台灣海域海流循環與生地化模擬研究工作。本計畫亦在其於 2006 年由氣象局聘請擔任顧問期間評估成型，亦參加本年度舉辦之國際研討會擔任主講及顧問。未來將會是本計畫與澳洲及歐洲相關單位及計畫之重要聯絡人，目前已協助本團隊初步取得歐洲 NEMO 計畫主持人同意，未來提供全球海洋環流模式（OPA）即時預報資料，供本團隊做為太平洋模式及北太平洋模式之初始與邊界條件，對未來計畫執行有關鍵性的重要性。

第六章 結論與建議

本年度收集了各國的海洋預報系統相關資訊，包括了歐洲的NEMO及MERSEA(未來會整合進NEMO)、美國的NOAA/NRL以及日本的日本氣象廳系統(JMA/MRI.COM)，瞭解其系統的架構及運作模式，參考這些系統，於本年度提出未來建置台灣的海洋環流作業化預報模式架構的策略，並利用後三年計畫時程完成建置，下一年度預計完成最大尺度的太平洋及次大尺度的北太平洋環流模式，以提供未來中此度及小此度的邊界條件，後年度則完成西北太平洋尺度海流模式及尺度最小的台灣海域海流模式建置，最後一年則測試完成模式作業化系統介面。

本年度也利用相關文獻資料以及過去執行模式的經驗，收集了數套數值模式進行瞭解，包括區域模式POLCOMS、ROMS及近岸模式COHERENS、FVCOM，最後因為ROMS有較完整的資源及發展空間，因此建議使用ROMS作為本計畫下一年度建置海流模式的工具。

下一年度建置的太平洋海流模式，由於國內建置經驗相當少，因此對於模式所需的起始條件及驅動力國內相當缺乏，需仰賴歐美或日本地區提供，氣象局資訊中心目前有接收美國NCEP、歐洲ECMWF及日本的JMA氣象模式資料，由於資料量相當龐大，本年度僅能進行初步的資料數量統計，選出未來適合的模式預報資料，待下一年度取得實際的完整資料，便可著手進行模式的測試。

實測資料取得部份，國內海流資料大部分皆為近岸測站，缺乏大洋中的資料，因此未來比對上會出現困難，目前大洋上的實測流速密度以GDP drifter全球浮標資料可兼顧時間與空間的變化，因此未來會透過國際合作的方式繼續積極收集相關的實測資料，以作為模式比對的依據。

參考文獻

1. COHERENS 網站 http://www.mumm.ac.be/~patrick/mast/
2. HYCOM 網站 http://hycom.rsmas.miami.edu/index.shtml
3. FVCOM 網站 http://fvcom.smast.umassd.edu/FVCOM/index.html
4. JMA 網站 http://www.jma.go.jp/jma/indexe.html
5. MERSEA 網站 http://www.mersea.eu.org/
6. Naval Research Laboratory 網站 http://www7320.nrlssc.navy.mil/html/7320-home.html
7. NEMO 網站 http://www.lodyc.jussieu.fr/NEMO/
8. Ocean-modeling 網站 http://www.ocean-modeling.org/index.php
9. ROMS/TOMS 論壇 https://www.myroms.org/forum/index.php
10. ROMS 網站 http://www.myroms.org/
11. TOMS 網站 http://www.myroms.org/index.php?model=toms
12. Wiki ROMS 網站 https://www.myroms.org/wiki/index.php/Documentation_Portal
13. Гандин, Л. С. (1963) Объестивный Аналогических Полей. Гидро-метеорологическое Издательство, Ленинград (Петербург).
14. Allan R. Robinson and Pierre F.J. Lermusiaux,(2000) Overview of Data Assimilation, Harvard Reports in Physical/Interdisciplinary Ocean Science, Number 62.
15. Andrich, P., G. Madec and D. L'Hostis, (1988) Performace wvaluation for an Ocean General Circulation Model, Vectorization and Muktitasking. In Conference Proceedings of the 1988 International Conference on Supercomputing. July 4-8, St-Malo, France, AMC Press, pp 295~303
16. Andrich P., P. Delecluse, C. Lévy and G. Madec, (1988) A multitasked general circulation model of the ocean. In Science and engineering on Cray Supercomputers, Proceedings of 4th International Symposium Minneapolis, Minnesota, Cray Research, Inc. book, pp 407~428
17. Andrich P. (1986) Développement de modèle numériques océaniques pour l'étude du couplage océan-atmosphère en zone tropicale. Thèse de l'Université Pierre et Marie Curie, Paris France, 93pp
18. Arakawa, A. and V. Lamb (1977) Computational design of the basic dynamical processes of the UCLA general circulation model. *Methods in Computational Physics*, 17, 174-267.
19. Azam F., T. Fenchel, J.G. Field, J.S. Gray, L.A. Meyer-Reil and F. Thingstad, (1983) The ecological role of water-column microbes in the sea. *Marine Ecology Progress Series* 10, pp 257~263.

20. Baretta-Bekker, J.G., J.W. Baretta, A.S. Hansen and B. Riemann, (1998) An improved model of carbon and nutrient dynamics in the microbial food web in marine enclosures. *Aquatic Microbial Ecology*, Vol. 14, pp 91~108.
21. Baretta-Bekker, J.G., J.W. Baretta and E. Rasmussen, (1995) The microbial foodweb in the European Regional Seas Ecosystem Model. *Netherlands Journal of Sea Researc*h, Vol. 33, pp 363~379.
22. Berger MJ, Bokhari SH. (1987) A Partitioning Strategy for Non-uniform Problems on Multiprocessors. *IEEE Transactions on Computers* C-36, 5:570-580.
23. Bergthorson, P., and DŐŐ, B. (1955) Numerical weather map analysis, *Tellus*, Vol.36, pp. 329-340
24. Bleck, R. (1998) Ocean modeling in isopycnic coordinates. Chapter 18 in Ocean Modeling and Parameterization, E. P. Chassignet and J. Verron, Eds., NATO Science Series C: Mathematical and Physical Sciences, Vol. 516, Kluwer Academic Publishers, pp 422~448
25. Bleck, R. (2002) An oceanic general circulation model framed in hybrid isopycnic-Cartesian coordinates. *Ocean Modeling*, Vol. 4, 55-88.
26. Blumberg, A. F., (1994) A primer for Ecom-si. Technical Report of HydroQual, Inc., 66 pp
27. Blumberg, A.F. and G.L. Mellor, (1987) A description of a three-dimensional coastal ocean circulation model. In Three-dimensional Coastal Ocean Model, N.S. Heaps, Ed., *Coastal. Estuar. Sci.*, Vol. 4, pp 1~6.
28. Blumberg, A.F. and G. Mellor (1987) A three-dimensional coastal ocean model. Three dimensional models., N.S. Heaps (ed), AGU, 1-16.
29. Bouttier, F. (1994) A dynamical estimation of forecast error covariances in an assimilation system, *Mon. Wea. Rev.*, Vol. 122, pp. 2376-2390.
30. Bratseth, A. M. (1986) Statistical interpolation by means of successive corrections, *Tellus*, 38A, pp. 439-447.
31. Bryan, K. and M.D. Cox (1967) A numerical investigation of the ocean general cirdulation. Tellus, 19, 54-80.
32. Chartier, M. (1985) Un modèle numérique tridimensionnel aux équations primitives de circulation générale de l'océan. Thèse de l'Université Pierre et Marie Curie, Paris, France, 111pp
33. Chassignet, E.P., L.T. Smith, R. Bleck and F.O. Bryan, (1996) A model comparison: numerical simulation of the North and Equatorial Atlantic oceanic circulation in depth and isopycnic coordinates. *J. Phys. Oceanogr.*, Vol. 26, pp 1849~1867.
34. Chen, C**.,** (2000) A modeling study of episodic cross-frontal water transports

over the inner shelf of the South Atlantic Bight. *Journal of Physical Oceanography*, Vol. 30, pp 1722~1742.

35. Chen, C., R. C. Beardsley and P. J. S. Franks, (2001) A 3-D prognostic model study of the ecosystem over Georges Bank and adjacent coastal regions. Part I: physical model. *Deep Sea Research*, Vol. 48, pp 419~456.
36. Cohn, S. E., and D. F. Parrish (1991) The behavior of forecast error covariances for a Kalman filter in two dimensions, *Mon. Wea. Rev.*, Vol. 119, pp 1757-1785.
37. Cousins, S. and H. Xue (2001) Running the Princeton Ocean Model on a Beowulf cluster. 2001 Terrain following coordinates workshop, Boulder, august 20-22, 2001.
38. Cressman, G.. P. (1959) An operational objective analysis system, *Mon. Wea. Rev.*, Vol. 87, pp 367-374.
39. Daley, R. (1985) The analysis of synoptic scale divergence by a statistical interpolation procedure, *Mon. Wea. Rev.*, Vol. 113, pp 1066-1079.
40. Daley, R. (1993) Atmospheric Data Analysis, Cambridge University Press, ISBN 9780521458252, pp 6-24
41. Dee, D. P. (1991) Simplification of the Kalman filter for meteorological data assimilation, *Quart. J. Roy. Meteor. Soc.*, Vol. 117, pp 365-384.
42. Di Lorenzo, E., A.M. Moore, H.G. Arango, B. Chua, B.D. Cornuelle, A. J. Miller and A. Bennett (2005) The Inverse Regional Ocean Modeling System: Development and application to data assimilation of coastal mesocale eddies, *Ocean Modelling.*
43. Ezer T., H. Arango and Alexander F. Shchepetkin, (2002) Developments in terrain-following ocean models: intercomparisons of numerical aspects. *Ocean Modelling*, Vol. 4, pp249~267.
44. Fasham, M.J.R., H.W. Ducklow and S.M. McKelvie, (1990) A nitrogen based model of plankton dynamics the oceanic mixed layer. *Journal of Marine Research*, Vol. 48, pp 591~639.
45. Fischer, M., M. Latif and M. Flugel, (1997) The impact of data assimilation on ENSO simulation and predictions. *Mon. Wea. Rev.*, Vol. 125, pp 819~829.
46. Gandin, L. S. (1965) Objective Analysis of Meteorological Fields, Translated from Russian, Israel Program for Scientific Translations, Jerusalem, pp. 242
47. Gandin, L.S. (1963) Objective Analysis of Meteorological Fields, Gidrometeoizdat, Leningrd, pp.242.
48. Ghil, M. (1989) Meteorological data assimilation for oceanographers, Part I： Description and theoretical framework. *Dyn. Atmos. Oceans*, Vol. 13, p171-218.
49. Ghil, M., and P. Malanotte-Rizzoli (1991) Data assimilation in meteorology and oceanography, *Advances in Geophysics*, Vol. 33, Academic Press, San Diego,

California, North America, pp. 141-261

50. Ghil, M., S. Cohn, J. Tavantzis, K. Bube, and E. Isaacson (1981) Applications of estimation theory to numerical weather prediction, Dynamic Meteorology: Data Assimilation Methods, L. Bengtsson, M. Ghil, and E. Källén, Eds., Springer, New York, pp. 139-224.
51. Haidvogel, D. B., H. Arango, Kate Hedstrem, Aike Beckmann, Paola Malanotte-Rizzoli, and Alexander F. Shchepetkin, (2000) Model evaluation experiment in the North Atlantic Basin: simulation in nonlinear terrain-following cooridate, *Dynamic of Atmospheres and Oceans*, Vol. 32, pp239~281
52. Haidvogel, D.B., H. Arango, W.P. Budgell, B.D. Cornuelle, E. Curchitser, E.Di Lorenzo, K. Fennel, W.R. Geyer, A.J. Hermann, L. Lanerolle, J. Levin, J.C. McWilliams, A.J. Miller, A.M. Moore, T.M. Powell, A.F. Shchepetkin, C.R. Sherwood, R.P. Signell, J.C. Warner and J. Wilkin. (2008) Ocean forecasting in terrain-following coordinates: Formulation and skill assessment of the Regional Ocean Modeling System. *Journal of Computational Physics*, Vol. 227, pp3595~3624
53. Hansen, D. V. and Poulain, P. M., (1996) Processing of WOCE/TOGA drifter data, J. Atoms. Oceanic Technol., Vol. 13, pp. 900-909
54. Hansen, R.B., H.W. Ducklow and J.G. Field, (1999) The changing ocean carbon cycle, a midterm synthesis of Joint Global Ocean Flux Study. IGBP Programme Book Series, 5, Cambridge University Press.
55. Halliwell, G. (2002) HYCOM Overview.
56. Halliwell, G.R., Jr., (1997) Simulation of decadal/interdecadal variability the North Atlantic driven by the anomalous wind field. Proceeding, Seventh Conference on Climate Variations, Long Beach, CA, pp 97~102
57. Halliwell, G.R.m Jr., (1998) Simulation of North Atlantic decadal/multi-decadal winter SST anomalies driven by basin-scale atmospheric circulation anomalies. *J. Phys. Oceangr.*, Vol. 28, pp 5~21
58. Halliwell, G.R, Jr., R. Bleck and E. Chassignet, (1998) Atlantic Ocean simulations performed using a new hybrid-coordinate coean model. EOS, Fall 1998 AGU Meeting
59. Halliwell, G.R., R. Bleck, E.P. Chassignet and L.T. Smith, (2000) mixed layer model validation in Atlantic Ocean simulations using the Hybrid Coordinate Ocean Model(HYCOM). EOS, 80, OS034
60. Holt, J.T. and I.D. James, (1999b) A simulation of the southern North Sea in comparison with measurements from the North Sea Project. Part 2: Suspended Particulate Matter *Continental Shelf Research*, Vol. 19, pp 1617~1642
61. Hurlburt, H.E., M.J. Bell, G. EVENSEN, C.N. Barron, A. HINES, O.M.

SMEDSTAD and D. STORKEY,, (2002) Operational Global Ocean Prediction Systems. “En route to GODAE”, 13-15 juin/june 2002, Biarritz, France, pp 97~105

62. Hu, D., (1996) On the sensitivity of thermocline depth and meridional heat transport to vertical diffusivity on OGCMs. *J. Phys. Oceanogr.*, Vol. 26, pp 1480~1494
63. Hu, D., (1997) Global-scale water masses, meridional circulation, and heat transport simulated with a blobal isopycnic ocean model. *J. Phys. Oceanogr.*, Vol. 27, pp 96~120
64. Ishikawa, Y., T. Awaji and N. Komori (2001) Dynamical initialization for the numerical forecasting of ocean surface circulations using a variational assimilation system. *J.P.O.*, Vol. 31, pp 75~93.
65. Jazwinsky, A. H. (1970) Stochastic Processes and Filtering Theory, Academic Press, pp. 376.
66. Ji, M,. and A. Leetmaa, (1997) Impact of data assimilation on ocean initialization and El Nino prediction. *Mon. Wea. Rev.*, Vol. 125, pp 742~753.
67. Ji, M., R.W. Reynolds and D. Behringer(2000) Use of TOPEX/Poseidon sea level data for ocean analysis and ENSO prediction: Some early results. *J. Climate*, Vol. 13, pp 216~231.
68. Kalman, R. E. (1960) A new approach to linear filtering and prediction problems, Trans. ASME, Ser. D, J. Basic Eng., Vol. 82, pp 35-45.
69. Kanarska, Y., A. Shchepetkin and J.C. McWilliams. (2007) Algorithm for non-hydrostatic dynamics in the Regional Oceanic Modeling System. *Ocean Modelling*, Vol 18, pp 143~174
70. Kara, A.B., E.J. Metzger, H.E. Hurlburt and A.J. Wallcraft, (2007) An Eddy-Resolving Ocean Model for Pacific Ocean: Part 1: Deep Convection and Its Relation to SST Anomalies. *Journal of Geophysical Research*, Submitted.
71. Kara, A.B., E.J. Metzger, H.E. Hurlburt and A.J. Wallcraft, (2007) An Eddy-Resolving Ocean Model for Pacific Ocean: Part 2: Daily and Monthly SST Variability from 1990 to 2004. *Journal of Geophysical Research*, submitted.
72. Karypis, G. and Kumar, V. (1998) METIS* A Software Package for Partitioning Unstructured Graphs, partitioning Meshes, and Computing Fill -Reducing Orderings of Sparse Matrices. Version 4.0. University of Minnesota, Department of Computer Science/ Army HPC Research Center Minneapolis.
73. Large, W.G., J.C. Mc Williams and S.C. Doney, (1994) Oceanic vertical mixing: a review and a model with a nonlocal boundary layer parameterization. *Rev. Geophys.*, Vol. 32, pp 363~403
74. Large, W.G., G. Danabasoglu, S.C. Doney and J.C. Mcwilliams, (1997)

Sensitivity to surface forcing and boundary layer mixing in a global ocean model: annual-mean climatology. *J. Phys. Pceanpgr.*, Vol. 27, pp 2418~2447

75. Legendre, L. and F. Rassoulzadagan, (1995) Plankton and Nutrients dynamics in marine waters. *Ophelia*, Vol. 41, pp 153~172.
76. Lionello, P., H. Gunther and P.A.E.M. Janssen, (1992) Assimilation of Altimeter Data in a Global Third Generation Wave Model, *J. Geophys. Res.*, Vol. 97, pp. 14253-14474.
77. Lorenc, A. C. (1988) Optimal nonlinear objective analysis, *Quart. J. Roy. Meteor. Soc.*, Vol. 114, pp. 205-240.
78. Lorenzo, E.D., (2003) Seasonal dynamics of the surface circulation in the Southern California Current System. *Deep-Sea Research II*, Vol. 50, pp2371~2388
79. Lorenzo, E.D., Andrew M. Moore, Hernan G. Arango, Bruce D. Cornuelle, Arthur J. Miller, Brian Powell, Boon S. Chua and Andrew F. Bennett. (2007) Weak and strong constraint data assimilation in the inverse Regional Ocean Modeling System(ROMS): Development and application for a baroclinic coastal upwelling system. *Ocean Modelling*, Vol. 16, pp160~187
80. Luyten, P., I. Andreu-Burillo, A. Norro, S. Ponsar. and R. Proctor, (2005) A new version of the European public domain code COHERENS. 4th EuroGOOS Conference, June 6-9 2005, Brest, France
81. Lynch, D. R. and C. E. Naimie, (1993) The M2 tide and its residual on the outer banks of the Gulf of Maine, *J. Phys. Oceanogr.*, Vol. 23, pp 2222~2253.
82. Luyten P. J. (1999) COHERENS-Dissemination and exploitation of a couple hydrodynamical-ecological model for regional and shelf seas, MAS3-CT97-0088, Final Report, MUMM Internal Report, Management Unit of the Mathematical Models, 76pp.
83. Marchesiello, P., James C. McWilliams and Alexander Shcheptkin, (2003) Equilibrium Structure and Dynamics of the California Current System, *Journal of Physical Oceanography*, Vol. 33, pp753~783
84. Marsh, R., M.J. Roberts, R.A. Wood and A.L. New, (1996) An intercomparison of a Bryab-Cox-type ocean model and an isopycnic ocean model, part II: the subtropical gyre and meridional heat transport. *J. Phys. Oceangr.*, Vol. 26, pp 1528~1551
85. Marshall, J., A. Adcroft, C. Hill, L. Perelman and C. Heisey (1997) A finite volume, incompressible Navier Stokes model for studies of the ocean on parallel computers. *J.G.R.* 102, 5753-5766.
86. Marti, O. (1992) Étude de l'océan mondial: modélisation de la circulation et du transport de traceurs anthropogéniques. Thèse de l'Université de Pierre et Marie

Curie, Paris, France, 201pp
87. Moore, A.M., E. di Lorenzo, H.G. Arango, C.V. Lewis, T.M. Powell, A.J. Miller and B.D. Cornuelle (2005) An adjoint sensitivity analysis of the southern California Current circulation and ecosystem, *J. Phys. Oceanogr*.
88. Naimie, C. E. (1996) Georges Bank residual circulation during weak and strong stratification periods: prognostic numerical model results. *J. Geophys. Res.*, Vol. 101(C3), pp 6469~6486.
89. New, A. and R. Bleck, (1995) An isopycnic model of the North Atlantic, Part II: interdecadal variability of the subtropical gyre. *J. Phys. Oceangr.*, Vol. 25, pp 2700~2714
90. New, A., R. Bleck, Y. Jia, R. Marsh, M. Huddleston amd S. Barnard, (1995) An isopycnic model of the North Atlantic, Part I: model experiments. *J. Phys. Oceanogr.*, Vol. 25, pp 2667~2699
91. OPA 8.1 Ocean General Circulation Model Reference Manual
92. Parent, L., J.M. Brankart, O.M. Smedstad, A.J. Wallcraft, T.L. Townsend, P. Brasseur, H.E. Hurlburt, G.A. Jacobs and E.P. Chassignet, (2006) A data assimilative 1/12 degree North Atlantic hindcast experiment using HYCOM: towards a reduced Kalman filter approach. *Ocean Dynamics*, submitted.
93. Parrish, D.F. and J. Derber (1992) The National Meteorological Center's spectral and statistical interpolation analysis system, *Mon. Wea. Rev.*, Vol. 120, pp. 1747-1763
94. Penven, P., C. Roy, G.B. Brundrit, A. Colin de Verdière, P. Fréon, A.S. Johnson, J.R.E. Lutjeharms and F.A. Shillington, (2001) A regional hydrodynamic model of upwelling in the Southern Benguela, *South Africa Journal of Science*, Vol. 97, 4pp.
95. Price, J.F., A. Weller and R. Pinkel, (1986) Diurnal cycling: Observation and models of the upper ocean response to diurnal heating, cooling and wind mixing. *J.G.R.*, Vol. 91, pp 8411~8427
96. Roberts, M.J., R. Marsh, A.L. New and R.A. Wood, (1996) An intercomparison of a Bryan-Cox-type ocean model and an isopycnic ocean model, part I: the subpolar gyre and high-latitude processes. *J. Phys. Oceanogr.*, Vol. 26, pp 1495~1527
97. Shchepetkin, A.F. and James C. McWilliams. (2005) The regional oceanic modeling system(ROMS): a split-explicit, free-surface, topography-following-coordinate oceanic model. *Ocean Modelling*, Vol. 9, pp 347~404
98. Shriver, J.F., H.E. Hurlburt, O.M. Smedstad, A.J. Wallcraft and R.C. Rgodes, (2007) 1/32° real-time global ocean prediction and value-added over 1/16°

resolution. *Journal of Marine Systems*, Vol. 65, issues 3, pp 3~26

99. Smedstad, O.M., H.E. Hurlbut, E.J. Metzger, R.C. Rhodes, J.F. Shriver, A.J. Wallcraft and A.B. Kara, (2003) An operational Eddy resolving 1/16° global ocean nowcast/forecast system. *Journal of Marine Systems*, Vol. 40-41, pp 341~361
100. Taylor, A.H., A.J. Watson and J.E. Robertson, (1992) The influence of the spring phytoplankton bloom on carbon dioxide and oxygen concentrations in the surface waters of the northeast Atlantic during 1989. *Deep Sea Research*, Vol. 39, pp 137~152.
101. Tett P. (1990a) A three layer vertical and microbiological processes model for shelf sea., Proudman Oceanographic Laboratory, Report no. 14, 85p
102. Tett, P. (1990b) The Photic Zone. In: P.J. Herring, A.K. Campbell, M. Whitfield and L. Maddock, Light and Life in the Sea, Cambridge University Press, Cambridge, U.K., p59-87
103. Tett, P. and A.W. Walne, (1995) Observation and simulations of hydrography, nutrients and plankton in the southern North Sea. *Ophelia*, Vol. 42, pp 371~416.
104. Thacker, W.C., (2003) Data-model-error compatibility. *Ocean Modeling*, Vol. **5**, pp 233~247.
105. Thacker, W. C., and O. E. Esenkov, (2002) Assimilating XBT data into HYCOM. *Journal of Atmospheric and Oceanic Technology*, Vol. 19, pp 709-724.
106. Thiébaux, H. J., and M. A. Pedder (1987) Spatial Objective Analysis with Applications in Atmospheric Science, *Academic Press*, pp 299
107. Wallcraft, A.J., A.B. Kara, H.E. Hurlburt, and P.A. Rochford, (2003) The NRL Global Ocean Model (NLOM) with an Embedded Mixed Layer Submodel: Formulation and Tuning. *Journal of Atmospheric and Oceanic Technology*, Vol. 20, pp 1601~1615
108. Wei, Eugene and Manchun Chen, (2001) Hydrodynamic Model Development for the Port of New York/New Jersey Water Level and Current Nowcast/Forecast Model System. NOAA Technical Report NOS OCS 12.
109. Wei, Eugene and Manchun Chen, (2002) NOS EXPERIMENTAL NOWCAST/FORECAST SYSTEM FOR THE PORT OF NEW YORK?NEW JERSEY(NYEFS)：REQUIREMENTS,OVERVIEW, and SKILL ASSESSMENT. NOAA Technical Report NOS OCS 15.
110. 陳亞嵐 (2004)，近岸風浪推算資料同化之研究，國立成功大學水利及海洋工程研究所碩士論文。
111. 曾忠一 (1997)，氣象資料同化，渤海堂文化公司，ISBN 9578970471。
112. 曾忠一 (2006)，大氣科學中的反問題：反演、分析與同化(上)，鼎文書局，ISBN 9860047197。

附錄 A 國際研討會議程及論文

Central Weather Bureau 2008
Conference on Weather Analysis and Forecasting

September 9-11, 2008, Taipei, Taiwan, R.O.C.

Special Workshop on Operational Marine Forecasting

September 10, 2008

Programme

Openning

13:30 – 13:45 Opening address. Dr. Chiang-Lin Hsin (Director-General, CWB)

13:45 – 14:00 Introduction of the projects running at the Marine Meteorology and Forecasting Center, CWB. Dr. Glory Shu (Director of Marine Meteorology and Forecasting Center, CWB)

Session I (14:00 – 15:30) chairman: Dr. Eugene Wei

14:00 – 14:30 Developments in Operational Oceanography in Europe and Australia. Dr. Roger Proctor (POL, UK and UT, Australia)

14:30 – 15:00 Development of Taiwan's community ocean model. Dr. Sen Jan (NCU, Taiwan)

15:00 – 15:30 Ocean Data Assimilation and Prediction Experiments in JMA and MRI. Dr. Masafumi Kamachi (MRI, Japan)

15:30 – 16:00 Break

Session II (16:00 – 17:30) chairman: Dr. Jason C.S. Yu

16:00 – 16:30 Overview of NOAA Operational Ocean and Estuary Circulation Forecast Systems. Dr. Eugene Wei (NOAA, USA)

16:30 – 17:00 Development of multiple-grids, fully coupled numerical ocean modeling – An application of upper ocean responses to Typhoons/hurricanes. Dr. Yu-hen Tseng (NTU, Taiwan)

17:00 – 17:30 Real Time Ocean Observations from Surface Drifters. Dr. Luca Centurioni (SCRIPPS, USA)

17:30 – 18:00 General discussion and conclusions

Developments in Operational Oceanography in Europe and Australia

Roger Proctor
Proudman Oceanographic Laboratory , UK and
IMOS/eMII, University of Tasmania, Australia

Abstract

Over the next 3 years exciting developments in Operational Oceanography are planned in both Europe and Australia.

In Europe, rapid increases in human uses of marine resources and the impact of climate change are making the European shelf and coastal seas more susceptible to natural hazards, more exposed to and threatened by pollution, and potentially less valuable to national economies. Conflicts between commerce, recreation, development, environmental protection, and the management of living resources are becoming increasingly contentious and politically charged. The need for the provision of quality observational data and model hindcast/forecast products has never been greater. Co-funded by the European Commission and the Member States projects are underway or planned which will deliver this information. The MERSEA project, a 4-year pre-operational project, finishing this year, has laid the groundwork by establishing global and regional modelling systems providing a forecast once a week. The ongoing ECOOP project continues the regional theme with the aim to raise the standard of three coastal observing and forecasting systems in each of five regional seas all utilising MERSEA products, and establishing Marine Information and Decision-making Systems of Systems. The 3-year *MyOcean* project, starting this year, will establish the Marine Core Service for Europe through five data Thematic Assembly Centres and one Global and six regional Model Forecasting Centres, providing reliable, routine information for use by all the European Community. Beyond 2012 the vision is that all EU marine data will be coordinated, banked and quality assured through the establishment of EMODNET, the European Marine Observations and Data Network to enable the Marine Core Service to be sustainable indefinitely.

In Australia, the Integrated Marine Observing System (IMOS) is an ambitious 5-year project funded by the Australian national and regional governments with matching support from universities and research centres to implement and establish a multi-platform real-time observing system covering the Australian EEZ and a large part of the Indian Ocean. A complementary forecasting programme, BlueLink/BlueLink2, is developing forecasting systems to provide global, regional and coastal sea products.

Although in many respects Europe and Australia are contrasting environments the challenges facing Operational Oceanography in both regions, of data integrity and the delivery of routine, reliable model and observational products, are similar.

1.Europe

The overall strategy for delivery of marine information in European Union (EU) seas and oceans is developed under the GMES (Global Monitoring for Environment and Security, www.gmes.info), an initiative for the implementation of information services dealing with environment and security. In the marine domain the delivery of this initiative began with the MERSEA (Marine Environment and Security for the European Area, www.mersea.eu.org) project whose strategic objective was to provide an integrated service of global and regional ocean monitoring and forecasting to intermediate users and policy makers. The backbone of such monitoring and forecasting systems relies on combined use of in-situ and satellite data, numerical ocean models and data assimilation. The regional nature is critical to the delivery of the MERSEA objective and through EuroGOOS, the GOOS Regional Alliance for Europe, a number of Regional Operational Oceanographic Systems / Networks (collectively known as ROOSs) have been set up to implement best practice and achieve effective day to day collaboration. Each ROOS has a Memorandum of Understanding between participating institutes and at present there are six: Arctic GOOS, Baltic (BOOS), North West Shelf (NOOS), Biscay / Iberian (IBI-ROOS), Mediterranean collaboration (MOON) and the Black Sea GOOS.

European coastal observatories have different strengths and weaknesses arising from their geographical situations, their requirements and funding constraints. A current EU project 'European Coastal sea Operational Observing and forecasting system', (ECOOP, www.ecoop.eu), aims to build up a sustainable pan-European capacity in providing a timely, quality assured marine service (including data, information products, knowledge and scientific advice) in European coastal-shelf seas. ECOOP focuses on improving and harmonizing fifteen coastal observing and forecasting systems (Fig. 1) and integrating their data through a marine information system of systems. ECOOP is divided along the ROOS regional lines (excluding the Arctic) with 3 coastal systems taken from each region. The data integration is aimed at developing an end-to-end structure which can be more widely applied, as ECOOP develops only a subset of European coastal observatories. Europe has led the way in using instrumented ferries as platforms for measuring surface properties (http://www.ferrybox.org), whereas the application of HF radar for measuring surface currents still lags behind their use in the USA.

These past and ongoing projects pave the way for the GMES Marine Core Service (MCS) which has the objective to streamline European capacities for forecasting, monitoring and reporting on the ocean state, for both the global ocean and the regional European seas. MCS will address the requirements from national and European policies, international conventions, as well as European and international agencies, for data, information products and indicators on the environment at local to global scales. The Strategic Implementation Plan for MCS (Ryder, 2007) stresses the critical importance of the provision of global and regional products for use by downstream services and end users (Fig. 2). This vision is to be implemented over the next 3 years (2008-2011) through the project *MyOcean* which will develop a consistent and reliable MCS with a strong interactive feedback from the intermediate users who, ultimately, will be the predominant downstream service suppliers. *MyOcean* will "deliver regular and systematic reference information (processed data, elaborated products) on the state of the oceans and regional seas at the resolution required by intermediate users & downstream service providers, of known quality and accuracy, for the global and European regional seas." *MyOcean* will operate through 12 production units (building on existing real-time data processing and forecasting centres): five observation 'Thematic Assembly Centres' for sea level, sea surface temperature, sea ice and wind, ocean colour, and *in situ* measurements; which will provide information and deliver data to seven 'Monitoring and Forecasting Centres', one providing global coverage and six regional centres corresponding to the ROOSs. Each production unit will be conducting integration, operations and assessment as well as research and development. They will all be under operational commitments to deliver a service.

MCS is constructing the 'Meteorological office' for the Sea: to provide every day the best information and forecast of the physical state and lower level biogeochemical condition of the marine environment. It is the first system of this kind in the world.

Clearly this will require that Member States *in situ* monitoring networks support the quality assurance and the data collection required for a sustained MCS. This has been foreseen in the European Marine and Maritime Science, Research, Technology and Innovation Strategy where one of the essential actions is the establishment and resourcing of a European Marine Observation and Data Network (EMODNET). This would see "the establishment of permanent, sustained monitoring and observation structures and the underpinning data provision, curation, information management and dissemination needed to support good ocean governance, good science, a better understanding of ocean dynamics, improved resource utilisation and the protection of the marine environment". A case for having EMODNET was laid out in one of the background papers of the EC Maritime Green Paper Consultation Process (Anon, 2006). The paper proposed the main tasks of such a network could be:

(1) to facilitate the systematic and operational long-term collection of data necessary to understand biological, chemical and physical behaviour of seas and oceans
(2) to encourage the interoperability of data collected by different regions
(3) to ensure the quality of the data
(4) to process operationally the raw data into information that is usable by service providers and researchers
(5) to render the data easily accessible
(6) to provide a repository for data collected in EU-funded projects.

Thus, the EU has invested over €60m in these projects (with matched funding from the Member States) and over the next 3-5 years major changes in the delivery of European oceanographic products are planned to aid the implementation of downstream (i.e. local) services.

2. Australia

There are ongoing concerns about adequate marine research capability for Australia to service Australia's requirements and responsibilities, which are significant because Australia has the third largest marine jurisdiction of any nation on earth. At over 14 million km^2 Australia's Exclusive Economic Zone (EEZ) is nearly twice the surface area of the Australian continent, and its extent at high latitude and in Antarctic waters adds to the challenge.

Australia is a continent surrounded by major ocean currents on its eastern, western, northern and southern boundaries, best known of these being the East Australian Current and the Leeuwin Current (which directly affect the Australian climatic conditions and help sustain the marine ecosystems). There is evidence that these currents are changing on decadal time scales and have already impacted marine ecosystems, but the data is sparse and neither the currents nor ecosystems have been monitored in a systematic way. Research on marine climate impacts is an open book and the pages are nearly blank, because long term data has been missing.

The Integrated Marine Observing System (IMOS) is a A$92M project established with A$50M from the National Collaborative Research Infrastructure Strategy (NCRIS) and nearly equal co-investments from Universities and government agencies, including overseas partners. It is a nationally distributed set of equipment established and maintained at sea, providing streams of oceanographic data and information services that collectively will contribute to meeting the needs of marine research in both open oceans and coastal oceans around Australia. In particular, if sustained in the long term, it will permit identification and management of ***climate*** change in the marine environment, an area of research that is as yet almost a blank page. It also provides essential data to understand and model the role of the oceans in climate change, and data to initialize seasonal climate prediction models. It will provide an observational nexus to better understand and predict the fundamental connections between coastal biological processes and regional/oceanic phenomena that influence ***biodiversity***. While as an NCRIS project IMOS is intended to support research, the data streams are also useful for many societal, environmental and economic applications, such as biodiversity conservation and management of ***marine*** natural resources and their associated ecosystems, support and management of coastal and offshore industries, safety at sea, marine tourism and defence.

The IMOS strategic goal is to assemble and provide free, open and timely access to streams of data that support research on:

(1) The role of the oceans in the climate system, and

(2) The impact of major boundary currents on continental shelf environments, ecosystems and biodiversity.

The benefits of IMOS transmit to the terrestrial sectors (e.g. ***water*** management, agriculture), for example through providing a better underpinning science base from which to characterise and predict weather patterns that are connected to oceanic phenomena. The return from investing in ocean observations of the nature of IMOS was estimated through an economic analysis undertaken in 2006 by the Australian Academy of Technological Sciences and Engineering and the Western Australian Global Ocean Observing System Inc. (*Economics of Australia's sustained ocean observation system, benefits and rationale for public funding*). That study, based on only a limited set of benefiting industries concluded that the cost:benefit to the Australian economy of investing in oceans observations was better than 1:20.

The IMOS infrastructure also contributes to Australia's commitments to international programs of ocean observing and international conventions, such as the 1982 Law of the Sea Convention that established the Australian EEZ, the United Nations Framework Convention on Climate Change, the Global Ocean Observing System (http://www.ioc-goos.org/) and the intergovernmental coordinating activity Global Earth Observation System of Systems (http://www.earthobservations.org/).

IMOS is made up (Fig. 3) of nine national facilities that collect data, using different components of infrastructure and instruments, and two facilities that manage and provide access to data and enhanced data products, one for in situ data and a second for remotely sensed satellite data. The observing facilities include three for ***bluewater and climate observations*** (Argo Australia, Enhanced Measurements from Ships of Opportunity and Southern Ocean Time Series), three facilities for ***coastal currents and water properties*** (Moorings, Ocean Gliders and HF Radar) and three for ***coastal ecosystems*** (Acoustic Tagging and Tracking, Autonomous Underwater Vehicle and a biophysical sensor network on the Great Barrier Reef). The principal operators of the facilities are the major players in marine research in Australia. The value from this infrastructure investment lies in the coordinated deployment of a wide range of equipment aimed at deriving critical data sets that serve multiple applications (Fig. 4). Additional information on IMOS is available at http://www.imos.org.au.

Implementation of IMOS facilities began in the period July to October 2007. IMOS has attracted strong support from the States, including Queensland for the Great Barrier Reef and South Australia for the Great Australian Bight. It is too early to assess the accomplishments relative to the IMOS goals, but progress has been good. Setting up an observing system in the ocean is challenging because of the harsh environmental conditions, and the need to develop Australian capability in using some of the equipment. Never-the-less, the IMOS facilities are on track to achieve their planned goals, and some have already demonstrated a leading role in the international development of the Global Ocean Observing System.

3. Summary

There is a need to ***sustain the capability being implemented*** through these current investments, to maintain long-term monitoring and forecasting capability required to support marine research and applications. IMOS in its present form is directed toward a proof of concept and building capability whereas the European systems are more advanced. The focus on research attracts co-investment from research agencies; however, they usually are not in a position to make a commitment to long-term sustained observing. There is a mistaken belief that research agencies should develop techniques and, once proven, they can be implemented by so called operational agencies. But operational agencies cannot accept a new mission without new, sustained support and this has been recognized in Europe through funding of the *MyOcean* project and in Australia through the BlueLink/BlueLink II projects.

The process for development of marine and environmental infrastructure needs to address the need for sustained observing *from the outset*. Experience over the past 25 years has demonstrated that sustained environmental observations serve the purposes of both research and operational agencies. It is recognized that both types of agency can be the home for sustained observing infrastructure, and there need to be appropriate incentives to encourage this to happen. A long-term commitment to ocean observing can be made on the basis of a staged development, where completion of one stage and proof of concept springs the release of already committed resources for the next stage.

There is a need to develop and prove applications of IMOS data in ***societal and industrial applications*** as well as research. This has been recognized in Europe through a series of data management initiatives, the latest of which is SeaDataNet (www.seadatanet.org) and which paves the way for EMODNET. Although in Australia there has been some engagement, with the tourism sector for example, a marine observing system has not existed in the past, and most industries do not have experience in using sustained marine data products. There needs to be more incentive to attract investment and sharing of resources from industries.

The data-streams produced by IMOS have a wide range of applications in research and in societal, environmental and economic activity. No single application or small set of applications however will be so profitable that they could cover the cost of the whole system. Monitoring the marine environment has to be a public-good function, much like the weather service, a fundamental operational objective of *MyOcean*.

In Australia national coordination, and in Europe continent-wide coordination, is required to produce innovative products and services that will justify public expenditure by contributing to the sustainability of both regions EEZs. The European Union has established Global Monitoring for Environment and Security (GMES) for this purpose. A similar initiative in Australia—call it Australian Monitoring for Environment and Security (AMES)—could use the data from a number of ongoing related environmental observing activities, including the weather service, IMOS, hydrological monitoring, Tsunami warning system and other environmental monitoring to produce innovative products and services. The purpose of a body to coordinate Australian monitoring for environment and security would be to ensure the maximum national benefit from public investment by coordinating inter-dependent institutions to produce innovative services using satellites, new sensor technologies and in situ sensor networks.

So, as can be seen, despite the different geographical contexts and status of development, many of the problems which Europe and Australia face to establish and implement sustained oceanographic products are essentially the same.

4. References

Anon, (2006), European Marine Observation and Data Network (EMODN) Background Paper 4a of the Maritime Green Paper Consultation Process. SEC (2006) 689.

Ryder, P., (2007), Sustainable Marine Environmental Information Services to meet collective European needs. EuroGOOS publication 26, December 2007

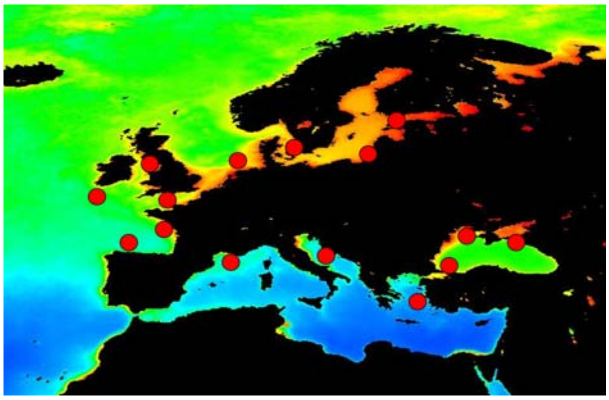

Fig.1 Locations of ECOOP coastal observing and forecasting systems

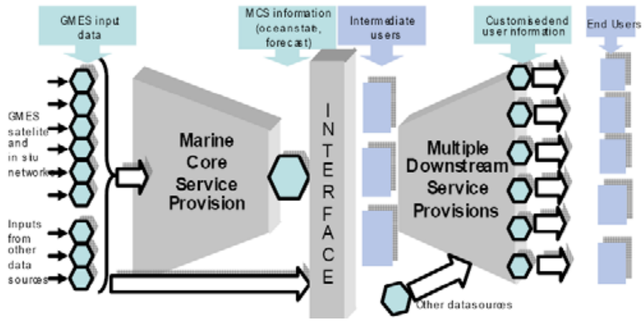

Fig. 2 The position of the MCS in the overall chain of service delivery (from Ryder 2007)

Fig. 3 The IMOS data facilities and their regional node implementation

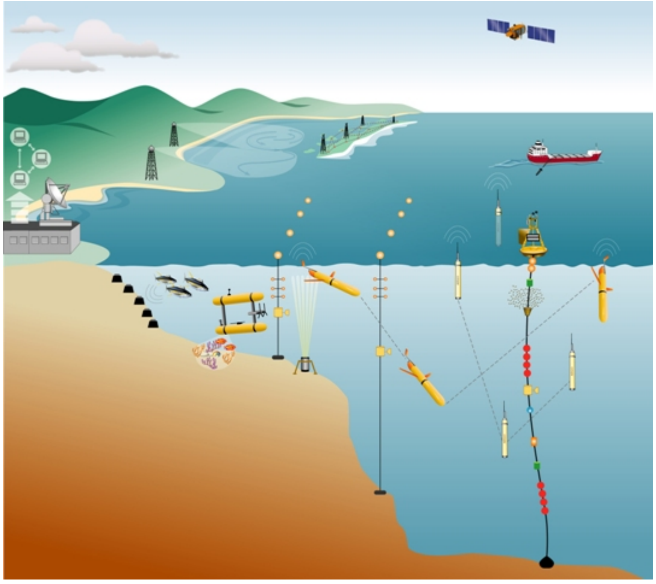

Fig. 4 Schematic of the range of equipment deployed in IMOS

Development of Taiwan's community ocean model

Sen Jan[1], Yu-Heng Tseng[2], Chih-Kai Hu[1], Chao-Tsung Chiu[1] and Shao-Hua Chen[1]
[1]Institute of Hydrological and Oceanic Sciences, National Central University
[2]Department of Atmospheric Science, National Taiwan University

Abstract

The purpose of this project is to develop a three-dimensional, multi-scale, community ocean model. The scope of the development ranges from tide (wave) models to basin-scale circulation models. The model domains will cover the entire North Pacific Ocean with 1/4° horizontal grid resolution and down to the surrounding seas in the vicinity of Taiwan with 1/128° horizontal resolution. A three-year plan is proposed. The major tasks for the first year are listed in the following. (1) Establishing computing facilities, manpower and observational database; (2) developing the prototypes of 3-D, 1/12°, 51 -layer tide and 1/4°, 26 z-level North Pacific circulation models independently; and (3) conducting the required observations including tidal sea level measurement and drifter observation for the model validations. In the second and following years, the main tasks are (1) performing further model development to improve the accuracy and resolution, and (2) offering the model products online and improving the model dynamic along with the development. The associated drifting trajectory and contaminant dispersion models will be incorporated to the system. It is expected that associated investigators could gain substantial modeling experience through the project. The ultimate goal aims to build a public-released oceanic model for general oceanographic community and enhance Taiwan's ocean nowcasting/forecasting ability.

1. Introduction

Taiwan is located along the southeast Coast of the Asian continent, across the Taiwan Strait from the mainland China. It acts as the pivot on the west edge of the Pacific Ocean. The surrounding seas in the vicinity of Taiwan are strategically important and knowledge of the temperature, salinity and velocity fields is crucial for understanding the physical oceanography. An observation system around Taiwan will be established under the support from the National Applied Research Laboratories (NARL) in the near future. The physical observations system, together with a comprehensive modeling system play an important role in understanding and predicting marine environmental conditions, particularly those during episodic and extreme events.

This project will develop a three-dimensional, multi-scale, community ocean model system. The scope of the system development ranges from tide (wave) models to basin-scale circulation models. The model domains will cover the entire North Pacific Ocean with 1/4° horizontal grid resolution and down to the surrounding seas in the vicinity of Taiwan with 1/128° horizontal resolution. At the current stage, each component of the integrated model system is developed independently. Here we report on the development of a high-resolution tidal model in the vicinity of Taiwan and a coarse-resolution primitive equation North Pacific Ocean circulation model in order to simulate multi-scale dynamics accurately. The tidal model includes very detailed small-scale tidal impacts while the large scale circulation model is used to the general and providing adequate boundary conditions for the tidal model. The current model development will be integrated into an ocean modeling system and can be used in many future applications, e.g. ocean ecosystem, typhoon-included circulation and climate change studies. Eventually, the circulation and tide models will be merged into a single model. The two models are described individually below.

2. Model description

At current stage, the community model development is divided into two parts: the circulation model and the tide model. The basic settings of the two models are described as follows.

2.1 Circulation model

The circulation model is a fourth-order accurate, collocated Arakawa-A grid similar to DieCAST (Dietrich/Center for Air Sea Technology) model described in Dietrich (1997), Dietrich et al (2004a) and Tseng et al. (2005). The control volume equations include fluxes of the conservation properties (momentum, heat and salt) across control volume faces. The model domain covers the entire North Pacific Ocean ranging from 30°S to 60°N and from 100°E to 80°W (Fig. 1) with horizontal resolution 1°/4.

Model bathymetry is established using unfiltered ETOPO2 depth data[1] supplemented with 1-min depth archive in the Asian seas from Taiwan's Ocean Data Bank. The vertical resolution is linear-exponentially stretched by 26 levels. The layer thickness varies from 13.28 m in the top layer to 891.02 in the bottom layer. The vertical mid-points of the layers are at depths 6.46, 20.51, 36.34, 54.35, 75.02, 98.94, 126.82, 159.55, 198.20, 244.07, 298.77, 364.26, 442.91, 537.65, 652.04, 790.43, 958.13, 1161.62, 1408.85, 1709.48, 2075.34, 2520.88, 3063.73, 3725.44, and 4532.33 m. Within each horizontal grid, longitudinal resolution is uniform and latitudinal resolution is specified such that each control

[1]http://www.ngdc.noaa.gov/mgg/global/relief/ETOPO2/ETOPO2v2-2006/ETOPO2v2c/

volume is approximately square (Mercator grid); thus, the model control volumes decrease with increasing latitude as do the typical ocean eddy sizes.

The surface wind forcing is obtained from the interpolated monthly Hellerman and Rosentstein's wind stresses (Hellerman and Rosenstein, 1983). The Levitus'94 climatology (Levitus and Boyer, 1994) is used to initialize the model and determine its surface sources of heat and fresh water (evaporation minus precipitation) using the non-damping approach described in Dietrich et al. (2004b). The northern boundary is closed. The southern boundary condition (30°S) is slowly nudging toward climatology in a sponge layer. The bottom is insulated, with no-slip conditions parameterized by a nonlinear bottom drag. Sub-grid scale vertical mixing is parameterized by eddy diffusivity and viscosity using a modified Richardson number dependent formula (Staneva et al., 2001; Tseng et al., 2005) based on Pacanowski and Philander (1981). Background lateral viscosity (or diffusivity) is 200 m^2/s.

2.2 Tide model

The three-dimensional baroclinic tide model is modified from the Princeton Ocean Model described in Blumberg and Mellor (1987). The nonlinear primitive equation model with Boussinesq and hydrostatic approximations is driven by the barotropic tidal forcing. The vertical axis is transformed to the σ–coordinate by $\sigma=(z-\eta)/(H+\eta)$, where z is positive upward with the origin placed at the mean sea level, η is the sea level fluctuation and H is the mean water depth. The governing equations and essential model settings were delineated in Jan et al. (2007). The model is bounded within 99.25°–135.25°E and 2.25°–43.25°N with 1°/12 horizontal resolution (Fig. 2). There are 51 uneven σ layers in the vertical with $\sigma_k=-($0.002, 0.004, 0.006, 0.008, 0.01, 0.012, 0.014, 0.018, 0.022, 0.026, 0.03, 0.034, 0.037, 0.045, 0.053, 0.061, 0.069, 0.077, 0.085, 0.1, 0.116, 0.132, 0.148, 0.179, 0.211, 0.243, 0.274, 0.306, 0.337, 0.369, 0.4, 0.432, 0.464, 0.495, 0.527, 0.558, 0.59, 0.621, 0.653, 0.684, 0.716, 0.748, 0.779, 0.811, 0.842, 0.874, 0.905, 0.937, 0.968, 1), from k=1 (surface) to 51 (bottom). The bottom topography was established using the revised ETOPO2.

The motionless ocean is subsequently driven by the tidal potential and prescribed tidal sea levels on all open-ocean boundaries through a forced radiation condition similar to that used by Blumberg and Kantha (1985). The tidal sea levels on the open boundaries are computed using harmonic constants compiled in a database (hereafter NAO.99) described in Matsumoto et al. (2000). The depth-averaged tidal current velocity normal to the open boundaries is determined by

$$\mathbf{u}_{nB}=\mathbf{u}_{2D}+C\ (\eta_B-\eta_{pre})\ /H \qquad (1)$$

where u2D is calculated from a fine-tuned, two-dimensional tide model of Jan et al. [2004], C ($=\sqrt{gH}$) is the phase speed of a shallow water gravity wave, η_B is sea level calculated by the three-dimensional tidal model, and η_{pre} is prescribed tidal sea level on open boundaries. A flow relaxation scheme described by Engedahl (1995) is applied to the internal mode velocity and temperature in a 1° wide strip adjacent to open boundaries to eliminate artificial reflections.

3. Preliminary results

Fig. 3 shows the circulation model simulated instantaneous North Pacific Ocean current speeds at the first day of year 54. Early results show realistic: Kuroshio intrusion and retreat through Luzon Strait and over southern East China Sea; formation of a warm core eddy in northern South China Sea in winter; seasonal variation of circulation in Taiwan Strait; and big Kuroshio meander over Izu Ridge southeast of Japan. Of special interest are: Kuroshio intrusions into Luzon Strait and possible instability; Kuroshio response to typhoons and meso-scale eddies; and variability of circulation in the South and East China Seas and Taiwan surrounding seas. These are also contemporary interests not only in Taiwan but also in the world's oceanographic communities.

The harmonic constant derived from model results are validating with observations and NAO.99. Fig. 4 shows the model-simulated co-tidal charts for the O1, K1, M2 and S2 constituents in the Luzon Strait (LS) as an example. The averaged sea level root-mean-square discrepancies, which considers both amplitude and phase differences, are 2.2, 2.9, 2.5 and 1.0 cm respectively for O1, K1, M2 and S2 as compared with the sea level calculated from NAO.99 at depths greater than 200 m in 115̃127°E and 18̃23°N. The associated goodness of fit relative to the sea level calculated from NAO.99 is 95.4, 93.7, 98.7 and 98.8% for O1, K1, M2, and S2, respectively, suggesting that barotropic tides are reasonably reproduced in the model. Fig. 5 shows the model-simulated depth-averaged tidal current ellipses of the O1, K1, M2 and S2 constituents in the LS. Briefly, the current amplitudes are of similar magnitude ~0.2 m/s for the O1, K1 and M2 and relatively small, 0.1 m/s, for the S2 in the LS. The barotropic tidal currents are much weaker, <0.1 m/s, in the deep Pacific Ocean and the deep northern South China Sea (SCS). The intensification of the barotropic tidal currents in the LS is mainly due to the narrowing and shoaling topographic effects when tidal waves propagate westward from the deep western Pacific into the SCS through the two submarine ridges in the LS. The characteristic of diurnal tides, which are quasi-resonant, partial-standing waves in the SCS with a meridional nodal band roughly across the LS, also contributes to the barotropic tidal current strengthening.

4. Summary

The development of the Taiwan Community Modeling System is now underway. The ultimate goal aims to build a public-released oceanic model for general oceanographic community and enhance Taiwan's ocean nowcasting/forecasting ability. The tidal model has been used in some operational rescue plan. The circulation model has been used in some studies of the ocean responses to typhoons. The integrated modeling system will be accomplished in the near future.

5. References

Blumberg, A. F. and L. H. Kantha, (1985), Open boundary condition for circulation models. J. of Hydra. Eng., 111, 2, 237-255.

Blumberg, A. F. and G. F. Mellor, (1987), A description of a three dimensional coastal ocean circulation model. In: Three-Dimensional Coastal Ocean Models, Coastal and Estuarine Stud., vol. 4, edited by N. Heaps, pp. 1-16, AGU, Washington D.C.

Engedahl, H., (1995), Use of the flow relaxation scheme in a three-dimensional baroclinic ocean model with realistic topography, Tellus, Ser. A, 47, 365-382.

Dietrich, D. E., (1997), Application of a modified Arakawa 'a' grid ocean model having reduced numerical dispersion to the gulf of Mexico Circulation. Dyn. Atmos. and Oceans, 27, 201-217.

Dietrich, D. E., A. Mehra, R. L. Haney, M. J. Bowman, and Y.-H. Tseng, (2004a), Dissipation effects in North Atlantic Ocean modeling. Geophys. Res. Lett., 31, L05302, doi:10.1029/2003GL019015.

Dietrich, D. E., R. L. Haney, V. Fernandez, S. A. Josey, and J. Tintore, (2004b), Air-sea fluxes based on observed annual cycle surface climatology and ocean model internal dynamics: A precise, non-damping zero-phase-lag approach applied to the Mediterranean Sea. J. Mar. Sys., 52, 145-165.

Hellerman, S. and M. Rosenstein, (1983), Normal monthly wind stress over the world ocean with error estimates, J. Phys. Oceanogr., 13, 1093-1104.

Jan, S, C.-S. Chern, J. Wang, and S.-Y. Chao, (2007), Generation of diurnal K1 internal tide in the Luzon Strait and its influence on surface tide in the South China Sea. J. Geophys. Res., 112, C06019, doi:10.1029/2006JC004003

Levitus, S. and T. P. Boyer, (1994), World Ocean Atlas 1994. Vol. 4: Temperatures, NOAA Atlas NESDIS. U.S. Department of Commerce, Washington, D.C.

Matsumoto, K., T. Takanezawa, and M. Ooe, (2000), Ocean tide models developed by assimilating Topex/poseidon altimeter data into hydrodynamical model: a global model and a regional model around Japan. J. Oceanogr., 56, 567-581.

Pacanowski, R. C. and S. G. H. Philander, (1981), Parameterization of vertical mixing in numerical models of tropical oceans, J. Phys. Oceanogr., 11, 1443-1551.

Staneva, J. V., D. E. Dietrich, E. V. Stanev, and M. J. Bowman, (2001), Rim current and coastal eddy mechanisms in an eddy-resolving Black Sea general circulation model. J. Mar. Syst., 31, 137-157.

Tseng, Y.-H., D. E. Dietrich, and J. H. Ferziger, (2005), Regional circulation of the Monterey Bay region-hydrostatic versus non-hydrostatic modeling, J. Geophys. Res. 110, C09015, doi:10.1029/2003JC002153.

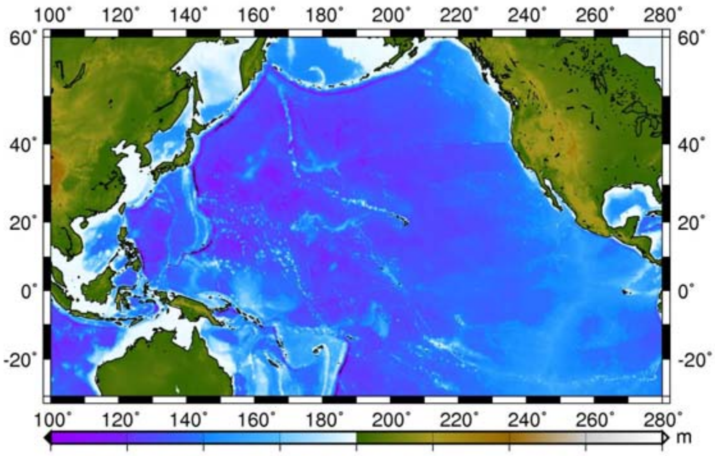

Fig. 1 Model topography for the 1°/4 North Pacific Ocean circulation model.

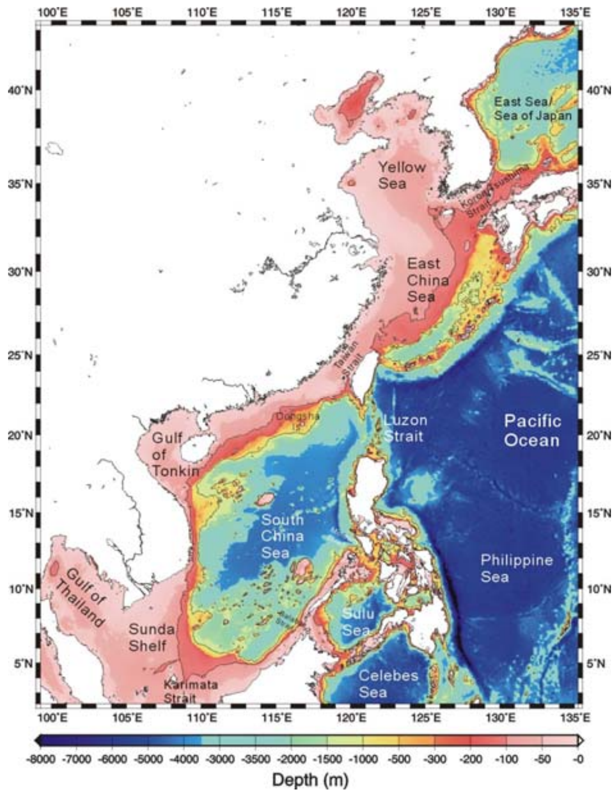

Fig. 2 Bathymetry of the three-dimensional model domain, including the East Asian seas and northwest Pacific Ocean.

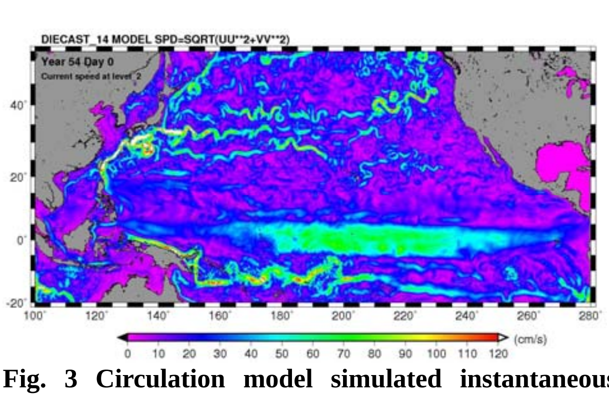

Fig. 3 Circulation model simulated instantaneous North Pacific Ocean current speeds at the first day of year 54.

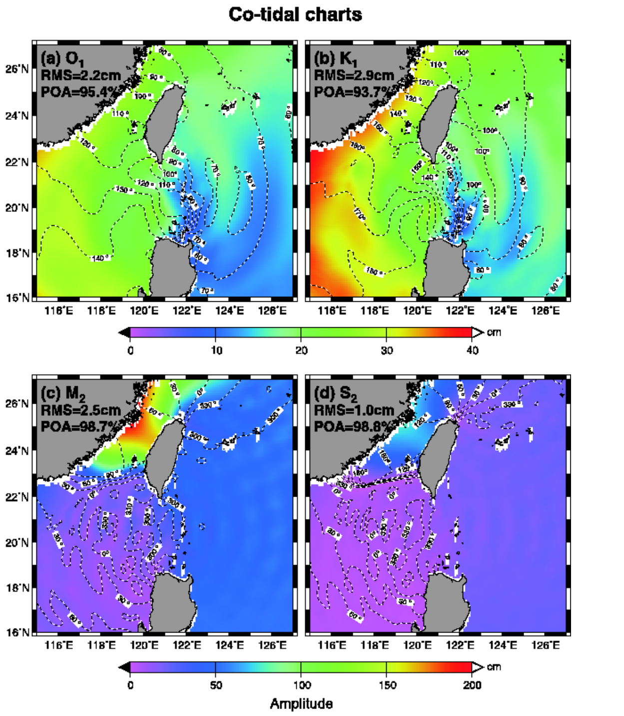

Fig. 4 Co-tidal charts for simulated (a) O1, (b) K1, (c) M2 and (d) S2 constituents.

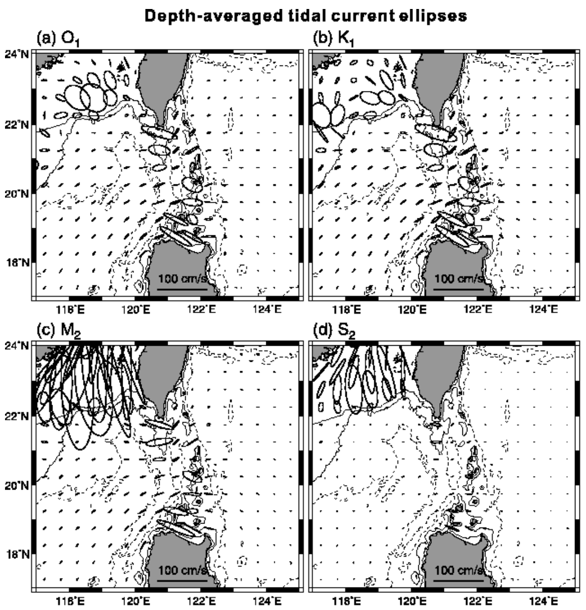

Fig. 5 Depth-averaged tidal current ellipses for simulated (a) O1, (b) K1, (c) M2 and (d) S2 constituents.

Ocean Data Assimilation and Prediction Experiments in JMA and MRI

Masafumi Kamachi, Norihisa Usui, Hiroyuki Tsujino,
Yosuke Fujii, Satoshi Matsumoto and Shiroh Ishizaki
Meteorological Research Institute,
Japan Meteorological Agency

Abstract

We discuss the current status of operational ocean data assimilation and prediction in a category “Ocean Weather” (mesoscale to coastal ocean states) in the international project “Global Ocean Data Assimilation Experiment (GODAE)”. It is shown how ocean observing systems act as an important role for understanding ocean phenomena through data assimilation; water mass and its pathway are analyzed through data assimilation; recent operational predictions of ocean state are performed; long range variability is analyzed with ocean analysis/reanalysis. These issues are discussed with examples mainly adopted from the projects of Meteorological Research Institute (MRI) ocean data assimilation system MOVE/MRI.COM and its operation in Japan Meteorological Agency (JMA). Possible future developments are also addressed.

.

Key word: Ocean prediction, data assimilation, operational system. Western North Pacific

1. Introduction

Recent developments of observing system, modeling and data assimilation method enable us to estimate and predict ocean state operationally. As a result, seasonal to interannual forecasting, fisheries, marine safety, offshore industry, management of shelf/coastal areas, security applications, and improved information for related fields (marine biogeochemical process and numerical weather prediction) are among the expected beneficiaries of ocean data assimilation and prediction.

The Meteorological Research Institute multivariate ocean variational estimation (MOVE/MRI.COM) System has been developed as the operational ocean data assimilation system in Japan Meteorological Agency. A multivariate three-dimensional variational (3DVAR) analysis scheme with vertical coupled temperature–salinity empirical orthogonal function modes is adopted.

The MOVE/MRI.COM system has two varieties, the global (MOVE/MRI.COM-G) and North Pacific (MOVE/MRI.COM-NP) systems (Usui et al., 2005). The aims of MOVE/MRI.COM-G are initialization of MRI coupled GCM for seasonal-interannual forecasting and reanalysis. The period of the reanalysis product is 1948 to 2007. The aims of MOVE/MRI.COM-NP are initialization of ocean forecasting in the North pacific (esp. around Japan) and reanalysis, which period is 1993-2007.

Information about the systems and recent publications are given in the MRI homepage http://www.mri-jma.go.jp/Dep/oc/oc.html.

2. GODAE

The Global Ocean Data Assimilation Experiment (GODAE) started from 1997, and was conducting its main demonstration phase from 2003 to 2005. Operational and research institutions from Australia, Canada, China, France, Japan, Norway, United Kingdom, United States are performing global oceanic data assimilation and ocean forecasting in order to provide regular and comprehensive descriptions of ocean fields such as temperature, salinity and currents at high temporal and spatial resolution.

This demonstration phase will be followed by a consolidation and transition phase from 2005 to 2008 where synthesis and transition to operational systems will take place. Climate and seasonal forecasting, navy applications, marine safety, fisheries, the offshore industry and management of shelf/coastal areas are among the expected beneficiaries of GODAE. The integrated description of the ocean that GODAE will provide will also be highly beneficial to the research community.

The rationale and scope of GODAE, its strategy and guiding principles have been presented in the GODAE Strategic Plan. It also identified the required inputs, outputs and main functional components of GODAE and defined a GODAE "Common" of materials that need to be shared during the Project. It gives a detailed description of the main components of GODAE, from the measurement networks through to the end users, as they currently exist, and identifies a number of issues and areas that need to be addressed. Figure 1 describes the main functional components of GODAE and the ways in which they are interacted. The components include:

Measurement networks
Data assembly centres
Data servers
Modelling/assimilation centres
Product servers
Application centres or service providers
End-users

The aim of the GODAE common is to instil modern scientific practice into the building of operational oceanography. It is based on the concepts of open access to data and products and open scientific investigation.

Its scope is broad and includes (see GODAE Strategic Plan):

(a) Assimilation products from existing national, pre-operational and operational, activities;
(b) Data products developed specifically for GODAE through existing facilities (e.g. from the GODAE High Resolution Sea Surface Temperature (GHRSST) pilot project);
(c) Infrastructure, such as data and product servers, assembled specifically for GODAE;
(d) The knowledge base accumulated through joint development, intercomparison experiments, and other GODAE collaborations.

The IGST (International GODAE Science steering Team) has played the leading role in building the GODAE common (Fig. 2). The vision of GODAE has always been to build on existing resources and programs, and to extract the greatest value from them by improved collaboration.

The other issue is links to various intergovernmental initiatives (e.g. the Global Ocean Observing System (GOOS), the Joint WMO/IOC Technical Commission for Oceanography and Marine Meteorology (JCOMM) and the World Climate Research Program (WCRP)), international bodies like the Committee for Earth Observing Satellites (CEOS) and the Partnership for Observations of the Global Ocean (POGO), and related research Programs such as CLIVAR and IMBER.

In summary the GODAE provides encouragements, promotion and framework for the development of operational oceanography (the GODAE partners). A clear appreciation and commitment to the rationale for the GODAE common has been needed to fuel the energy and enthusiasm that will be needed to build it. The comprehensive 12 years results of GODAE project will be reported in the Final GODAE Symposium (http://www.godae.org/Final-GODAE-symposium.html).

3. MOVE/MRI.COM

MOVE/MRI.COM systems are composed of OGCMs and a variational analysis scheme which synthesizes the observed information (i.e., temperature, salinity and SSH) together with the OGCMs.

3.1 Model

The numerical code for the OGCMs used in the MOVE/MRI.COM system is the MRI community ocean model (MRI.COM). MRI.COM has been developed in JMA/MRI and is independent of any other popular OGCM code (Ishikawa et al. (2005)). It is a multilevel model code that solves the primitive equations under the hydrostatic and Boussinesq approximations. The vertical coordinate is a terrain following-depth ($\sigma - z$) hybrid, i.e., the levels near the surface follow the surface topography. It enables us to adopt a fine vertical resolution near the surface because it prevents the uppermost layer from vanishing during integration when the free surface variation is explicitly solved. For momentum advection, MRI.COM uses the generalized enstrophy-preserving scheme (Arakawa, 1966) along with the Takano–Oonishi scheme, which contains the concept of diagonally upward/downward mass momentum fluxes along a sloping bottom (Takano, 1978, Oonishi, 1978 and Ishizaki and Motoi, 1999). The no-slip condition is adopted for lateral boundaries. Bottom friction is parameterized according to Weatherly (1972).

The OGCM used in MOVE/MRI.COM-G is a model with a global domain (model G). On the other hand, MOVE/MRI.COM-NP employs two models, namely the North Pacific and western North Pacific models (models NP and WNP). Model WNP is nested into model NP, i.e., the boundary conditions for the western, eastern, and southern boundaries in model WNP are passed from model NP (one-way nesting). Daily outputs from model NP are linearly interpolated both in time and space to replace boundary data of model WNP at every time step.

The model domain of model G extends from 75°S to 75°N globally. The grid spacing in the zonal direction is 1° and that in the meridional direction is 0.3° within 5°S–5°N, and 1° poleward of 15°S and 15°N. There are 50 levels in vertical. The bottom topography is based on ETOPO5 (NOAA, 1992). The northern boundary is closed, i.e., an artificial wall is set. The isopycnal diffusion (Redi, 1982) and the isopycnal thickness diffusion (Gent and McWilliams, 1990) (GM), the background coefficients for vertical diffusion by Tsujino et al. (2000) (Tsujino00), the harmonic viscosity with the parameterization of Smagorinsky (1963) (SMA63), and the level-2.5 turbulent closure scheme of Mellor and Yamada (1982) (MY2.5) are all used in model G.

The model is driven by daily wind stress, heat flux, and fresh water flux fields calculated from NCEP–NCAR reanalysis (NCEP R-1; Kalnay et al., 1996). Latent and sensible heat flux fields are calculated with the bulk formula of Kara et al. (2000) (Kara00). The solar heat flux penetrates surface layers according to Paulson and Simpson (1977). The fresh water flux of NCEP R-1 is adjusted by adding time-independent (space-dependent) flux correction terms (Vialard et al. (2002)).

The domain of model WNP extends from 15°N to 65°N, and 117 °E to 160°W, with a grid spacing of 1/10° × 1/10° around Japan. This model is nested into model NP, whose model region is from 15°S to 65°N, and 100°E to 75°W with a grid spacing of 1/2° × 1/2°. All lateral boundaries of model NP are closed although they are planned to be nested in model G. Models NP and WNP have the same vertical grid spacing (54 levels). Bottom topographies in models NP and WNP are based on Smith and Sandwell (1997) (Smith–Sandwell). The configurations of models NP and WNP are the same as model G, except for a few differences. The biharmonic viscosity with a parameterization based on SMA63 (Griffies and Hallberg, 2000), instead of harmonic viscosity, and the turbulent closure scheme of Noh and Kim (1999) (Noh–Kim), instead of MY2.5, are used in models NP and WNP. Biharmonic diffusion, instead of isopycnal diffusion and GM, is used in model WNP. The models are driven by the daily wind stress and flux fields calculated from the NCEP–DOE AMIP-II reanalysis (NCEP R-2; Kanamitsu et al., 2002). Models NP and WNP adopted the bulk formula of Kondo (1975) (Kondo75), instead of Kara00, for latent and sensible heat fluxes. The water flux is corrected by restoring SSS to the climatology with a restoring time of 1 day (the time-independent correction term is not applied). A sea ice model with the elastic-viscous-plastic dynamics of Hunke and Dukowicz (1997) and the thermodynamics of Mellor and Kantha (1989) (EVP sea ice model) is also applied in models NP and WNP.

3.2 Assimilation system

The analysis fields for models G, NP, and WNP are calculated separately. The analysis scheme adopted in the MOVE/MRI.COM system is a multivariate 3DVAR analysis scheme with vertical coupled T–S EOF modal decomposition of a background error covariance matrix. The scheme is based on Fujii and Kamachi, 2003c and Fujii et al., 2005. The amplitudes of the coupled EOF modes are employed as control variables and the analyzed temperature and salinity fields are represented by the linear combination of the EOF modes in the scheme.

The preconditioned optimizing utility for large-dimension analysis (POpULar; Fujii and Kamachi, 2003b and Fujii, 2005) is applied for minimizing the nonlinear cost function. This scheme can minimize a cost function including a constraint of the background without inversion of a background error covariance matrix, even if the function is nonlinear. It is useful for handling the correlation among background errors.

The regions of the models G, NP, and WNP are divided into 22, 7, and 10 subregions, respectively. EOF modes are calculated in each subregion for each model from world ocean database 2001 (WOD2001; Conkright et al., 2002), as well as the representativeness error covariance matrix, according to Fujii and Kamachi (2003b). We retained 12 dominant modes in each subregion. In fact, more than 85% of the total variance can be explained by the dominant 12 modes although this estimate will differ from one in a different subregion. The Gaussian function is adopted as the horizontal correlation model applied in the background covariance matrix B. The e-folding scales along latitude and longitude lines are also different in different subregions and are decided from Kuragano and Kamachi (2000).

The model temperature and salinity fields are corrected by the analysis result through the incremental analysis updates (IAU) technique (Bloom et al., 1996). The assimilation period is 1/3 month.

Temperature, salinity and along-track SSH observations are employed in the analysis. The temperature and salinity observations were collected from WOD2001 and the global temperature–salinity profile program (GTSPP) database (Hamilton, 1994). We also adopted the along track SSH anomaly data of TOPEX/Poseidon (T/P), Jason, ERS, ENVISAT (Kuragano and Shibata, 1997) after adding it to the mean SDH calculated from a preliminary analysis using temperature and salinity observations alone.

3.3 experimental conditions

The assimilation experiment (analysis/reanalysis) was conducted from January 1948 to December 2007 for global and North Pacific systems, and from January 1985 to September 2007 for western North Pacific system.

Hereafter we introduce the western North Pacific version (MOVE/MRI.COM-WNP). The assimilation period is 1/3 month: the first and second assimilation periods in a month are 10 days and the third one varies from 8 to 11 days. Temperature and salinity profiles above 1500 m, and SSHA data are assimilated. Temperature and salinity data are collected from WOD2001 and Global Temperature-Salinity Profile Program (GTSPP) database. The SSHA data is the along track data from the TOPEX/Poseidon, Jason-1, ERS-1/2 and ENVISAT altimeters, which are extracted from the SSALTO/DUACS delayed time multimission altimeter products (CLS 2004). The model is driven by wind-stress and heat fluxes from the National Centers for Environmental Prediction (NCEP) - Department of Energy (DOE) Atmospheric Intercomparisons project (AMIP-II) reanalysis (Kanamitsu et al. 2002; hereafter NCEP2). Latent and sensible heat fluxes are re-calculated in the model using model sea surface temperature (SST) and the bulk formula of Kondo (1975). The fresh water flux is corrected by restoring sea surface salinity toward the monthly mean climatology with a restoring time of 1 day to prevent a model drift.

138 cases of prediction experiments for the Kuroshio path variability south of Japan were conducted from February 1993 to July 2004. Predictions start at the first day of every month and are integrated for 90 days. The wind-stress and heat fluxes used in the prediction experiments are NCEP2, the same as in the assimilation experiment. We should treat an external forcing as an unknown factor in the prediction. However, we treat it here as a known factor because our objective is to assess the predictive skill of the assimilation scheme and the dynamical model when a perfect external forcing is given. The predictive skill obtained from this protocol could be affected by the use of predictive forcing.

4. Analysis/Reanalysis and Prediction Results and Perspective

We conducted analysis/reanalysis experiments. Here we introduce some results of the western North pacific version.

Figure 3 shows comparison of the velocity field by the assimilation result and independent ADCP observation. Velocity field is recovered well. The correlation coefficients of the zonal (meridional) velocity between the two datasets is 0.84 (0.47). Figure 4 shows temperature and salinity distributions along two JMA's observation lines. The assimilation scheme (multivariate 3DVAR) works for representing temperature and salinity fields of the subtropical (Kuroshio) and subpolar (Oyashio) waters. The water mass property (temperature and salinity) along JMA's hydrographic observation lines around Japan are plotted in the Fig. 5. The mean water mass property, though some lines (PH line in the subtropical-subpolar boundary region, bottom layer in the Japan Sea along PM line) shows biases of the property. Using the analysis/reanalysis dataset prediction experiments are conducted. A result of the predictability is shown in Fig.6. It compares model prediction with persistency and climatological variability. It shows 40-60 days predictability (Usui et al. 2006, 2008).

GODAE will enter a new era under JCOMM with the continuation of its activity, and in addition, with coastal and biogeochemical applications. JMA's operational and MRI's research groups will also have the plans of the same direction as GODAE under JCOMM.

5. Reference

Arakawa A., (1966), J. Compt Phys., 119-143.

Bloom S C, Takacs L L, Da Silva A M, Ledvina D, (1996), Mon. Wea. Rev., 124, 1256-1271.

Collecte, Localisation, Satellites (CLS), (2004),: CLS-DOS-NT-04.103, Toulouse, France, 42pp.

Fujii Y. ,(2005), J. Oceanogr., 61, 167-181.

Fujii Y, Kamachi M., (2003a), J. Geophys Res., 108(C9), 3297, doi:10.1029/2002JC001745.

Fujii Y, Kamachi M., (2003b), J. Oceanogr., 59, 173-186.

Fujii Y, Kamachi M., (2003c), Tellus, 55A, 450-454.

Fujii Y, Ishizaki S, Kamachi M., (2005), J. Oceanogr., 61, 655-662.

Griffies SM, Hallberg RW., (2000), Mon. Wea Rev., 128, 2935-2946.

Hamilton D., (1994), Earth System Monitor.

Holland WR, Chow JC, Bryan FO, (1998), J. Climate, 11, 1487-1493.

Hunke EC, Ducowicz JK, (2002), Mon. Wea Rev., 130, 1848-1865.

Ishikawa I, Tsujino H, Hirabara M, Nakano H, Yasuda T, Ishizaki H., (2005), Technical Reports of the Meteorological Research Institute, No.47 (in Japanese)}

Ishizaki H, Motoi T., (1999), J. Atmos Oceanic Technol., 16, 1994-2010.

Kamachi M, Kuragano T, Sugimoto S, Yoshita K, Sakurai T, Nakano T, Usui N, Uboldi F., (2004), J. Oceanogr., 60, 269-282.

Kanamitsu M, Ebisuzaki W, Woollen J, Yang S-K, Hnilo JJ, Fiorino M, Potter GL, (2002), Bull. Amer Meteor Soc., 83, 1631-1643.

Killworth PD, Stainforth D, Webb DJ, Paterson SM, (1991), J. Phys Oceanogr., 21, 1333-1348.

Kondo J., (1975), Bound.-Layer Meteorol., 9, 91-112.

Kuragano T, Kamachi M., (2000), J. Geophys. Res., 105, 955-974.

Kuragano T, Kamachi M, (2003), J. Oceanogr., 59, 765-781.

Mellor GL, Ezer T, (1991), J. Geophys Res., 96, 8779-8795.

Mellor GL, Kantha L, (1989), J. Geophys. Res., 94, 10937-10954.

Noh Y, Kim H-J, (1999), J. Geophys. Res., 104, 15621-15634.

Ocean Climate Laboratory, (1999), National Oceanographic Data Center.

Smith WHF, Sandwell DT, (1997), Science, 277, 1956-1962.

Spall MA, Holland WR, (1991), J. Phys Oceanogr., 21, 205-220.

Toth Z, Kalnay E., (1997), Mon. Wea. Rev., 125, 3297-3319.

Tsujino H, Usui N, Nakano H, (2006), J. Geophys Res., *Geophys. Res.*, 111 , C11001, doi:10.1029/ 2005JC003118

Usui, N., H. Tsujino, Y. Fujii, M. Kamachi, (2006), Ocean Dynamics, vol.56, 607-623, DOI 10.1007/ s10236-006-0084-z

Usui, N., H. Tsujino, H. Nakano, and Y. Fujii, (2008), J. Geophys. Res. (in press)

Weatherly GL, (1972), J. Phys Oceanogr., 2, 54-72.

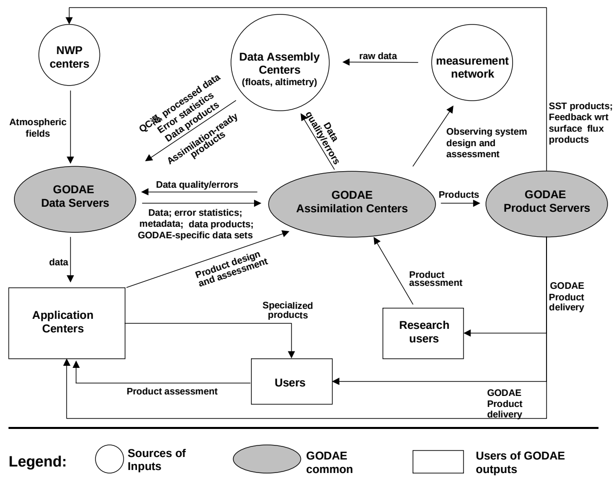

Fig.1 GODAE backbone: A schematic diagram that is illustrating the relationship between the functional components of GODAE and the transmission of data and information between them (GODAE Startegic Plan).

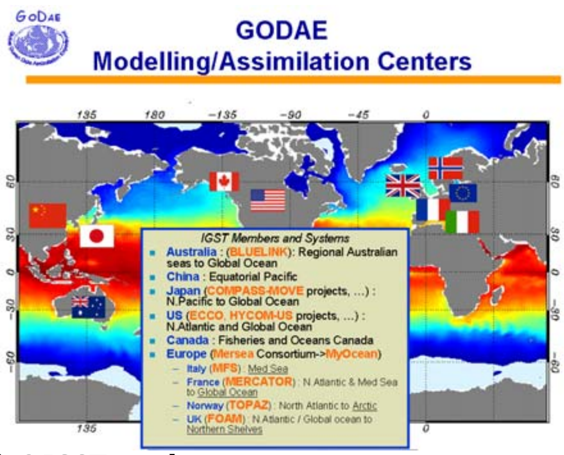

Fig.2 IGST member systems.

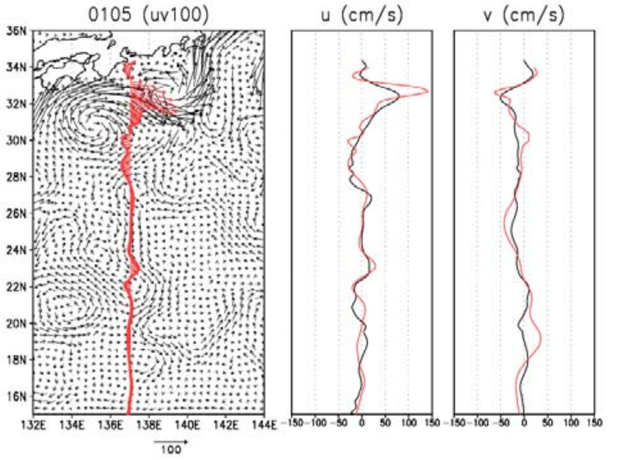

Fig. 3 Compariso of velocity fields. Black: assimilation, Red: ADCP observation.

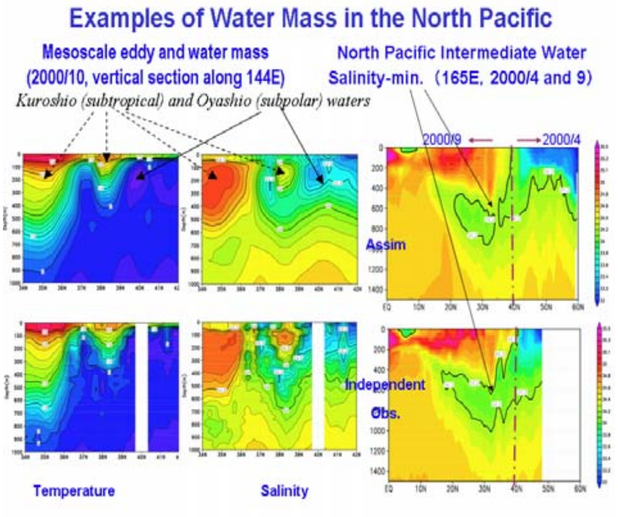

Fig.4 Comparison of temperature and salinity distribution along 144e and 165E.

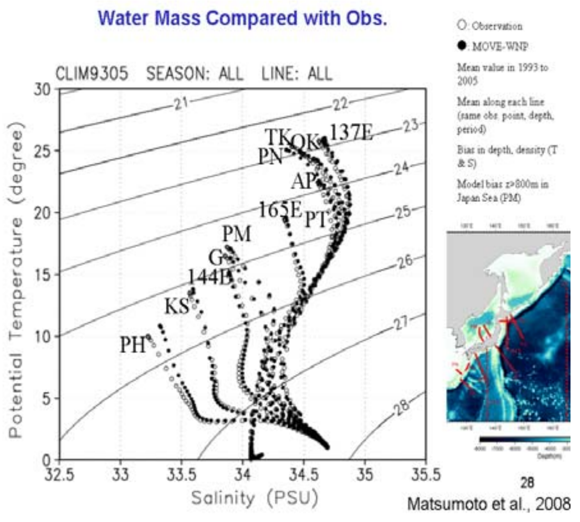

Fig.5 Comparison of water property (T-S diagram) along JMA's hydrographicsections (see right figure for the positions).

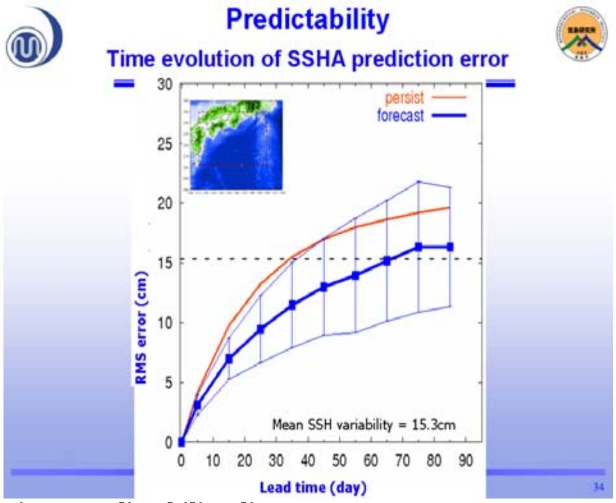

Fig. 6 Predictability diagram.

Operational Circulation Forecast Systems in NOAA

Eugene Wei
NOAA/National Ocean Service
Silver Spring, Maryland, USA

Abstract

Several ocean and estuary/bay/lake circulation forecast systems are running operationally at NOAA's National Weather Service (NWS) and National Ocean Service (NOS) computing facilities to provide real-time ocean conditions and forecast guidance to users in the commercial industry, educational institution, and other government agencies for navigational safety, emergency response, and research development and applications. Base on numerical ocean models, these forecast systems focus on short term and real time operational forecasts up to weekly time scales with domains ranging from basin, region, to estuarine and lake. The numerical model resolution is designed to be capable of resolving mesoscale eddies or small scale coastal features.

The basin-scale ocean forecast system, Real Time Operational Forecast System (RTOFS - Atlantic), based on the HYbrid Coordinate Ocean Model (HYCOM) has been running operationally at NWS since 2006. This eddy resolving model system replaces the previous Princeton Ocean Model (POM) based Coastal Ocean Forecast System (COFS). RTOFS emphasizes on the coastal ocean, the loop current and the Gulf Stream regions and provides nowcasts and forecasts of sea level, current, temperature, and salinity for the entire North Atlantic Ocean.

There are nine operational forecast systems, based on POM and others, running operationally at NOS since 2002. During the system development, the core models are evaluated by NOS standard skill assessment procedures to ensure the model performance quality. The Coastal Ocean Model Framework (COMF) has been implemented to standardize all model operations including data ingestion and product dissemination. Under the NOS's Physical Oceanographic Real-Time System (PORTS) and monitored by the Continuous Operational real-Time Monitoring System (CORMS), these operational forecast systems provide nowcast and forecast guidance of water level, current velocity, temperature and salinity for mariners navigating in the Chesapeake Bay, New York Harbor, Galveston Bay and Channels, St. Johns River, and all five Great Lakes (Erie, Ontario, Huron, Michigan, and Superior). Currently, three estuarine forecast systems are under development using Regional Ocean Model System (ROMS) for Delaware Bay, Chesapeake Bay (2nd generation), and Tampa Bay. Future development will be focused on a regional scale with sufficient detail in the estuary.

1. Introduction

One of NOAA's missions is the protection of life and property and to support environmental management and economic development in the coastal domain. The objective for developing and implementing ocean and estuarine circulation forecast model systems is to fulfill this critical mission within NOAA. These forecast systems, consists of a general circulation model and forced with surface and lateral boundary conditions, provide near real-time ocean conditions and short term (with time-scale 2 to 3 days) forecast guidance to the users. The information provided by circulation forecast systems includes sea surface height (water elevation) and three-dimensional current velocity, temperature and salinity. A control framework processes the input/output datasets required by the forecast system and controls operational sequences.

This paper presents an overview of the development procedure for operational circulation forecast systems (OFS) within NOAA. These systems include the basin-scale Real-Time Operational Forecast System (RTOFS) at NWS and nine estuarine/bay/lake operational forecast systems at NOS. Modeling framework designed to standardize model system development and operations under operational environment are discussed. The evaluation of the forecast system core model performance is based on their hindcast and semi-operational skill assessment.

2. Basin Scale Forecast System RTOFS

RTOFS (Atlantic) (Spindler, et. al., 2006) is a basin-scale ocean forecast system based on the dynamical model HYDCOM, jointly developed by the University of Miami, the Naval Research Laboratory (NRL), and the Los Alamos National laboratory (LANL). The system has been running operationally at NWS's National Centers for Environmental Prediction (NCEP) for the Atlantic Ocean (Fig. 1) covering from about 30^0 S to 70^0 N. The bathymetry is shown in Fig. 2.

The goals of RTOFS are: (1) to establish operational high resolution (eddy resolving) ocean forecast system for short-term forecasts (about 7 days) of the Atlantic Ocean with US deep and coastal waters well resolved, (2) to provide nowcasts and forecasts of sea levels, currents, temperatures, and salinity, emphasizing on the coastal ocean, the Loop Current and the Gulf Stream regions, (3) to provide seamless boundary and initial conditions to regional ocean physical and biogeochemical models, (4) to enable the coupling of circulation-wave ocean models with one-way and two-way interactions, and (5) to couple with atmospheric-ocean hurricane forecast.

The surface forcing on the model includes atmospheric fluxes from 3-hour NCEP Global Forecast System (GFS). Open boundaries are relaxed to temperature and salinity climatology. River discharges from US Geological Survey (USGS) are specified as inflows. Body and boundary tides are included. Eight tidal constituents (M2, S2, N2, K1, P1, O1, K2, and Q1) are used. Data ingested during the nowcast data assimilation cycle includes: SST from GOES AVHRR and in-situ data; SSH from JASON GFO; and S and T from ARGOS, XBT, and CTD.

The model system is run once a day starting with a 24 hours data assimilation to update the ocean condition. The model then makes a 120 hours forecast. Examples of RTOFS forecast SST, SSH, surface salinity, and surface current velocity are shown as Fig. 4.

NCEP will establish a RTOFS global model system to provide boundary conditions to other basin or regional models such as RTOFS-Atlantic and future RTOFS-Northeast Pacific and RTOFS-Hawaii. This global forecast system will server as a backbone for all other NCEP requirement such as Hurricane Weather Research and Forecasting (HWRF) and ecological modeling requirement.

3. Estuaries/Bay/Lakes Forecast Systems

There are nine estuarine/coastal/lake operational forecast systems (Fig. 3) currently running at Centers for Operational and Oceanographic Product and Services (CO-OPS) within NOAA's NOS. They are: Chesapeake Bay, New York Harbor, Galveston Bay and Channels, St. Johns River, and all five Great Lakes (Erie, Ontario, Huron, Michigan, and Superior). Three others are under development and scheduled to become operational in 2009: Delaware Bay and Tampa Bay forecast systems and retrofitting Chesapeake Bay forecast system.

Except at the Great Lakes where the primary circulation driven force from wind and fresh river flow, the NOS estuarine forecast systems take observed water level as open boundary conditions for the nowcast. Tidal predictions added to the wind driven water level forecast from NWS's operational Extra Tropical Storm Surge (ETSS) model are specified at the estuary/bay entrance for the model to produce 30 hours forecast guidance of water level, current velocity, and salinity and temperature. Surface elevation forecasts from other basin scale models are also under consideration for open boundary condition including NWS's RTOFS and Navy Coastal Ocean Model (NCOM). The nowcast and forecast guidance from these estuaries/lakes forecast systems are then disseminated on the Internet as station time series, vector plots, and contours.

The first operational forecast system, Chesapeake Bay Operational Forecast System (CBOFS, Fig. 4) was implemented in 2002 (Gross, 2000). This forecast system, based on Model for Environmental Circulation and Assessment (MECCA, Hess, 2000) model runs four times a day and provides water levels over the entire Chesapeake Bay for promoting navigation safety. Water surface elevations from tidal predictions and subtidal water level at Chesapeake Bay Bridge Tunnel are specified as the lateral boundary conditions. Observed (met pack at NOS water level stations) and model forecasted winds (North American Mesoscale, NAM) are used for surface forcing.

The New York Operational Forecast System (NYOFS), based on Princeton Ocean Model (POM, Blumberg and Mellor, 1987), was implemented in 2003. A higher resolution fine grid, covering inland navigational channels, is nested within a coarser grid which covers the entire New York Harbor nearby estuary (Fig. 5(a)) (Wei and Chen, 2002). The fine grid model receives boundary conditions from the coarse grid is capable of providing detail current velocity on navigational channels shown in Fig. 5(b). These current velocity fields are critical for Coast Guard to determine the "right-of-way" for vessel navigating in a narrow waterway. In addition to the observed and forecasted surface elevations specified at Sandy Hook, NY and Kings Point, NY, winds and the river inflows are also input to the model.

The Galveston Bay Operational Forecast System (GBOFS) was developed with POM model (Schmalz, 2000) for Galveston Bay and Houston Channel, Texas. A fine grid covers the navigation channel through the Galveston Bay is nested in the coarse grid as shown in Fig. 6(a). The surface current velocity forecast is shown in Fig. 6(b).

The St. John's River (SJROFS) Operational Forecast Systems developed with Environmental Fluid Dynamic Code (EFDC) model (Zhang, et al., 2006) was implemented in 2005. Fig. 7(a) shows the model grid. Fresh river inflow from upstream reservoir and run off from hydrological watershed to the St. John's River, Florida meet the sea water intrusion at the coast is clearly indicated in a snapshot of salinity forecast contour shown in Fig. 7(b).

The five Great Lake Operational Forecast Systems (GLOFS, including Lakes Erie, Ontario, Huron, Michigan, and Superior) were original developed by NOAA's Great Lake Environment Research Laboratory (GLERL) and Ohio State University (Schwab and Bedford, 1994). The systems were running at GLERL since 1997. They were transferred to NOS and became operational in 2006 (Kelley, et. al., 2007).

GLOFS is designed to provide improved predictions of water levels, water currents and water temperatures in the Great Lakes for commercial recreation and emergency response. There is no tide and salinity in the Great Lakes, the hydrodynamic circulation in the lakes is driven by wind set-up and the temperature gradient induced by river inflow, the wind and heat flux exchange with atmospheric at the surface.

Nowcast and forecast guidance produced from each of five Great Lakes OFS are graphically disseminated on the Internet. Fig. 8 shows the surface temperature of Lake Erie and the surface current velocities of Lake Huron produced by the GLOFS.

4. Modeling Framework

The operation and maintenance of all NOS forecast systems require a comprehensive and integrated management system to ensure the integrity and the production quality of forecast system operation procedure. The Coastal Ocean Model Framework (COMF) (Gross, et. al., 2006) at NOS has been developed for this purpose. COMFS is a set of standards and tools for developing and maintaining NOS's OFS. The goal of COMF is to provide a comprehensive software infrastructure to increase ease of use, performance, portability, interoperability, and reuse in forecast models of estuaries, coastal ocean and Great Lakes. COMFS also provides a software framework for individual scientists, model production, and the critical operational environment.

The COMF consists of several logically and simply defined modules. Each module is composed of Unix scripts, FORTRAN programs, Perl scripts, and graphic routines to perform various tasks. A main shell script in each OFS provides the primary interface and controls the timing, acquisition of data, running of the models, generation of site specific output, generation of graphics and dissemination of results via a web interface.

Module functionality and sequential execution of COMF are: (1) set environment variables for directories, (2) test computer system, (3) create the start and end times of each designed simulation run, (4) acquire input data, (5) reform and quality control input data, (6) perform hydrodynamic simulation, (7) archive simulation input and output data, (8) generate graphics, (9) create run flags, and (10) purge old files.

These modules provide standardization to the operational forecast systems and simplify their creation. Among all modules, the unified data access and quality control modules are the most significant and complicated. A complete collection of data access tools are provided to grab data of water level, wind, river discharge, salinity and temperature from several data sources including NOS' National Water Level Observation Network (NWLON) or Physical Oceanographic Real-Time System (PORTS) stations, US Geological Survey (USGS) rivers, and National Data Buoy Center (NDBC) Coastal Marine Automated Network (C-MAN). NOAA forecast model guidance from North American Mesoscale atmospheric model (NAM) and Extra Tropical Storm Surges (ETSS) model are also accessed with the same routines.

Model forecast run flags produced from Module 8 contain information for NOS's 24x7 Continuous Operational Real-Time Monitoring System (CORMS) to display on Internet web page (Fig. 9). This color display shows the forecast system operational status of input data acquisition, model runs, graphic generation, and archive process. The information provides CORMS operators who monitor the real-time data and forecast system operational status.

All forecast systems developed and transferred to NOS operational status will be standardized within COMF. The time and cost efficiency for forecast system development and production will be increased under COMF. Effort to improve the accuracy and efficiency of OFS process will be a continuous development task by infusing new methods.

5. Operational Forecast System Evaluation

In developing and implementing forecast models to support navigational and environmental applications in coastal waters, the policies and procedures for the evaluation of NOS nowcast/forecast models are required in order to ensure that these models have been developed and implemented in a scientifically sound and operationally robust way (Hess, et al., 2003). The complete forecast system evaluation includes: (1) standardization of model output and products, documentation, and skill assessment and operation procedures, (2) periodic review, (3) skill assessment, and (4) product quality control, and (5) documentation. Since the primary user of the products is the navigational community, and their concerns are under-keel clearance and maneuvering in port areas, the primary variables to be evaluated are water levels, currents, and water density. The skill assessment of model system performance becomes the focus point for the evaluation. The components of skill assessments include: (1) the quantities relevant to navigation, (2) the time series of observed and predicted variables, (3) data processing techniques, (4) the model run scenarios, (5) the comparison statistics or quantities, (6) the target values, (7) comparison of forecast method, and (8) acceptance criteria.

The skill assessment statistics that can quantify model performance are easily calculated quantities that provide relevant information on the important categories of model behavior. The standard suite of statistics gives a global assessment of errors, and includes: (1) series mean (SM), (2) root mean square error (RMSE), (3) standard deviation (SD) of error, (4) central frequency (CF), i.e., the frequency the errors lie within specified limits, (5) positive outlier frequency (POF), i.e., the frequency of model outliers higher than the observed, (6) negative outlier frequency (NOF), i.e., the frequency of model outliers lower than the observed, (7) maximum duration of positive outliers (MDPO), and (8) maximum duration of negative outliers (NDPO).

The primary variables for the standard suite statistics in terms of importance for navigation in U.S. coastal waters and ports are: (1) for under-keel clearance - the magnitude of water levels, the times and amplitudes of high and low water; (2) for vessel maneuvering - the speed and direction of the currents, the time, amplitudes, and direction of the maximum flood and ebb currents, and the starting times and end times of slack water; and (3) for density - salinity and temperature.

The target criteria for those statistic parameters are set based on user requirements. For example, for most of the vessels navigating in coastal waterways and channels, the target criteria for water level prediction error threshold is 15 cm and the central frequency is 90%. This means that 90% of the time the water level forecast errors, when compared with observations, should be less than 15 cm for the system to meet NOS implementation standard.

The skill assessment will apply to model data, at locations where observations are available, from five model simulation scenarios during the model development. They are: (1) astronomical tide only simulations, (2) hindcast, (3) semi-operational nowcast, (4) semi-operational forecast, and (5) persistence forecast. These simulation scenarios are designed not only to ensure the accuracy of model calibration and verification process ((1) and (2)) but also to measure the model system nowcast/forecast performance capability under the operational environment ((3) to (5)).

A software package (Zhang, et. al., 2006) has been developed at NOS to compute the standard suite statistics automatically using data files containing observed, nowcast, and forecast variables. Based on the requirement of the forecast system model application, this skill assessment software acquires the observations and/or NOS standard tide predictions from available NOS database. Observations are quality controlled with gap filled to match with model data time series. The model data from each model simulation scenario are read in and compared with observations to calculate skill assessment statistics in tables which can be incorporated into model evaluation reports. The skill assessment results provide the System Design and Implementation Team (SDIT) the information to determination of the system status from development to implementation.

6. Summary

Operational circulation forecast systems in NOAA provide valuable ocean condition information of water levels, currents, salinity and temperature to the marine community for navigation safety, commercial cargo efficiency, emergency response, and ecological and environmental studies. The development and implementation of those forecast systems require standardized framework to manage a unified process for efficient operation and maintenance. The performance of the core model within the forecast system needs to be evaluated by a standard skill assessment procedure to ensure the quality of the forecast system products.

7. References

Blumberg, A.F. and G.F. Mellor, (1987), A Description of a Three-dimensional Coastal Ocean Circulation Model, In: Three-dimensional Coastal Ocean Models, Coast and Estuarine Science, Vol. 4 (Heaps, N.S. ed.), American Geophysical Union, Washington, D.C., 1-16.

Gross, T, K. Bosley, and K. Hess, (2000), The Chesapeake Bay Operational Forecast System (CBOFS): Technical Documentation, NOS Technical Report OCS/CO-OPS 1. 69 pp.

Gross, T, H. Lin, Z. Bronder, and M. Vincent, (2006), Coastal Ocean Modeling Framework: COMF, NOAA Technical Report, NOS CS 22. 145 pp.

Kelley, J., P. Chu, A. Zhang, G. Lang, and D. Schwab, (2006), Skill Assessment of NOS Lake Michigan Operational Forecast System (LMOFS), NOAA Technical Memorandum NOS CS 10. 65 pp.

Hess, K., T. Gross, R. Schmalz. J. Kelley, F. Aikman, and E. Wei, and M. Vincent, (2003), NOS Standards For Evaluating Operational Nowcast and Forecast Hydrodynamic Model Systems, NOAA Technical Report NOS CS 17. 47 pp.

Hess, T, (2000), MECCA 2 Program Documentation, US Department of Commerce NOAA, NOAA Technical Report NOS CS 5. 49 pp.

NOS, (1999), NOS Procedure for Developing and Implementing Operational Nowcast and Forecast Systems for PORTS. NOAA Technical Report NOS CO-OPS 020. 33 pp.

Schmalz, R., (2000), Three-dimensional Hydrodynamic Model Developments for a Galveston Bay Nowcast/Forecast System, NOAA Technical Report NOS CS 9. 167 pp.

Schwab, D. and K. Bedfort, (1994), Initial Implementation of the Great Lakes Forecasting System: A real-time for Predicting Lake Circulation and Thermal Structure, Water Pollution Res. J. of Canada, 29, 203-220.

Spindler, T., I. Rivin, L. Burroughs and C. Lozano, (2006), NOAA Real-Time Ocean Forecasting System RTOFS – (Atlantic), Technical Procedure Bulletin, MMAB 2006-02, No 250. 8 pp.

Wei, E. and M. Chen, (2002), NOS Experimental Nowcast/Forecast system for the Prot of New York/New Jersey (NYEFS): Requirements, Overview, and Skill Assessment, NOAA Tech. Report, CS15, Silver Spring, Maryland. 53pp.

Zhang, A., K. Hess, E. Wei, and E. Myers, (2006), "Implementation of Model Skill Assessment Software for Water Level and Current in Tidal Regions. NOAA Technical Report NOS CS 24. 61 pp.

Zhang, A., E. Myers, and F. Aikman, (2006), The St. Johns River Operational Forecast System (SJROFS) and Its Skill Assessment, NOAA Technical Report, NOS CS 23. 58 pp.

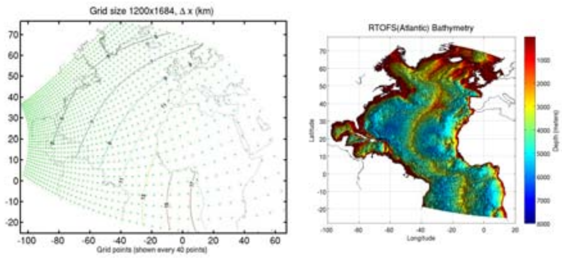

(a) (b)

Fig. 1 RTOFS HYCOM (a) model grid, (b) model bathymetry.

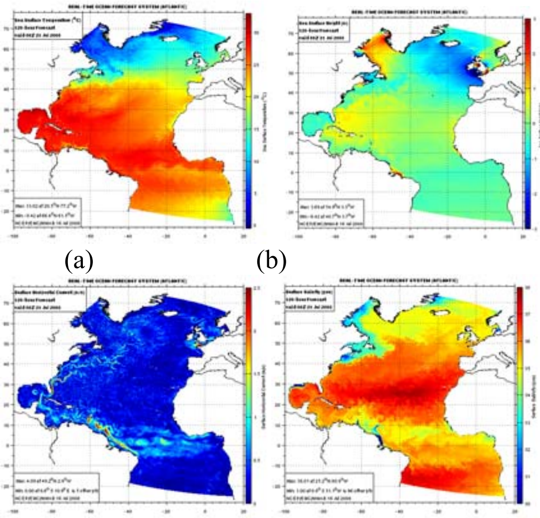

(a) (b)

(c) (d)

Fig. 2 RTOFS forecasts of (a) SST, (b) SSH, (c) surface current velocity, and (d) surface salinity.

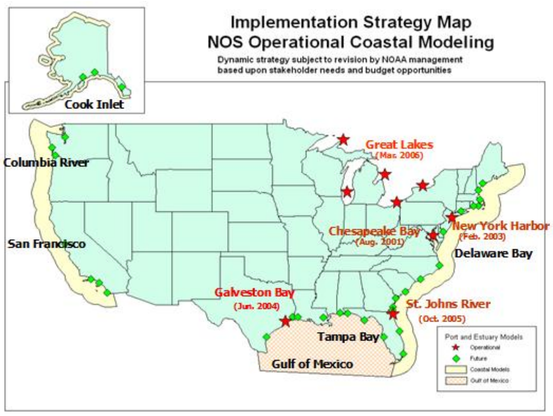

Fig. 3 NOS operational forecast systems.

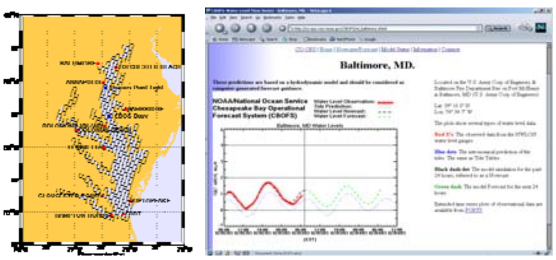

(a) (b)

Fig. 4 CBOFS: (a) model grid, and (b) water level nowcast and forecast at Baltimore Harbor.

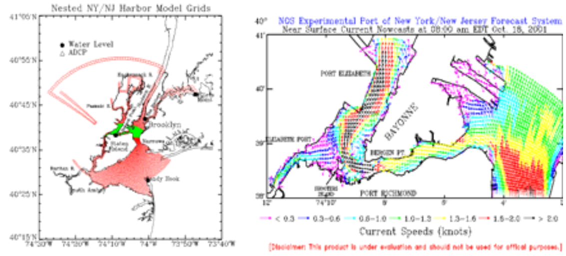

Fig. 5 NYOFS: (a) nested model grids, (b) surface current velocity within the nested fine grid.

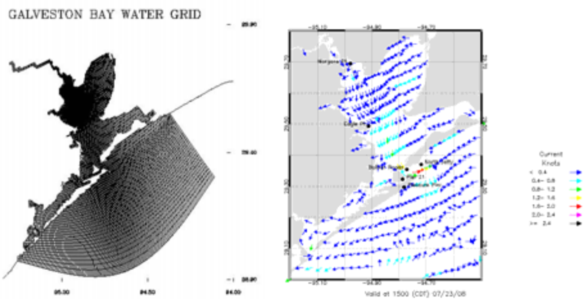

(a) (b)

Fig. 6 Galveston forecast system (a) model grid, and (b) current velocity forecast.

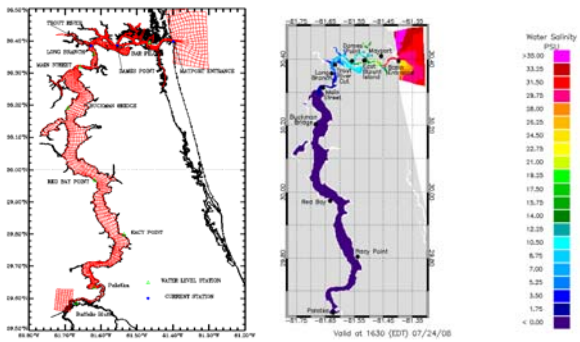

(a) (b)

Fig. 7 St. John's River forecast system (a) model grid and (b) surface salinity forecast.

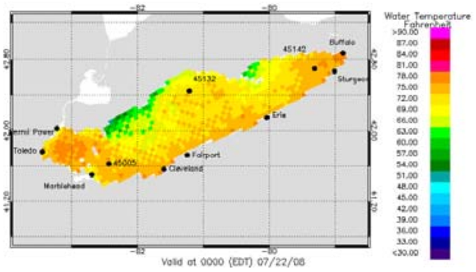

(a)

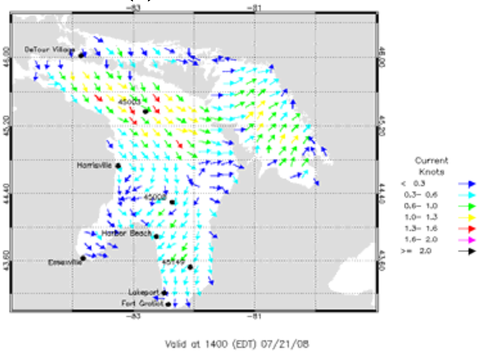

(b)

Fig. 8 (a) Surface temperature forecast at Lake Erie and (b) Surface current forecast at Lake Huron.

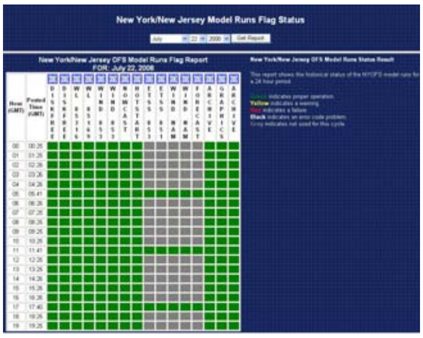

Fig. 9 CORMS model status display for Lake Huron OFS.

Development of Multiple-grids, Fully Coupled Numerical Ocean Modeling-An Application of Upper Ocean Responses to Typhoons

Yu-Heng Tseng[1], Sen Jan[2], I-I Lin[1], Ya-ting Chang[3], T. Y. Tang[3]
[1]Department of Atmospheric Sciences, National Taiwan University
Institute of Oceanography, Nation
[2]Institute of Hydrological and Oceanic Sciences, National Central University
[3]Institute of Oceanography, National Taiwan University

Abstract

The ocean response to typhoon Kai-tak is simulated using a 4th-order-accurate basin-scale ocean model. The model is based on a multiple-grids, fully coupled model framework which uses 1/8° horizontal resolution for the western domain and 1/4° resolution for the eastern domain, respectively. The surface winds in the typhoon Kai-tak are obtained directly from the QuikSCAT satellite images blended with the ECMWF wind fields. An intense nonlinear mesoscale eddy is generated with Rossby number O(1) and 50-100km horizontal scale south of Taiwan. Nearly inertial oscillation is clearly observed in the model. More than 8°K sea surface temperature (SST) drop is found in both observation and simulation. We attribute this significant SST drop to the influence of slow moving typhoon, initial stratification and bathymetrically-induced upwelling in South China Sea.

Key word: typhoons, ocean response

1. Introduction

It is well-known that typhoons (called hurricanes in Atlantic Ocean) draw their energy from the warm ocean. The energy input from the ocean to typhoons and associated intensification depends largely on the upper ocean heat content (Lin et al., 2005). Pre-existing ocean mesoscale features have far more important in the heat and moisture fluxes feeding the storm than just SST as noted in previous studies. Shay et al. (2000) noted an abrupt change in the intensity of hurricane Opal (9/28-10/5, 1995) when it passed over a large Warm Core Eddy (WCE). Hurricane Katrina in August 2005 also experienced very similar intensification while passing over Loop Current and WCE regions. These examples show the role of warm oceanic features in providing a positive feedback to the overlying storm by intensifying the storms.

Typhoons also cause significant SST cooling which provides negative feedback to the overlying storm by weakening the intensity of the storm. For example, satellite images show that SST dropped more than 9°C and 11°C in response to the passage of typhoons Kai-tak (Lin et al., 2003) and Ling-ling (Shang et al., 2008), respectively.

In general, the primary mechanisms accounting for typhoon-forced sea surface cooling are mixed layer depth (vertical mixing/entrainment) and thermocline depth (upwelling driven by the wind stress curl of the typhoons), exchange of air-sea heat fluxes and the storm's intensity and translation speed (Price, 1981). Intense, slowly moving typhoons usually cause larger SST response (Price, 1981). Since evaporation due to high winds over warm water sustains the thermodynamic cycle of a tropical cyclone (TC) (Emanuel, 2003). SST cooling is though to inhibit cyclone intensification, preventing the typhoons from attaining its potential intensity. When a typhoon encounters the WCE, the SST cooling may be greatly suppressed primarily due to deep mixed-layer and thermocline depths of the WCE.

Early studies of upper-ocean response to typhoons include field observations (e.g. Shay et al., 1989; Jacob et al., 2000) and three-dimensional numerical ocean models (Price, 1981). Recent studies emphasize more on the understanding of the dynamical processes/ interactions with atmosphere, ocean heat contents and ocean currents (e.g. Wu et al., 2008; Tsai et al., 2008; Oey et al., 2007; Sheng et al., 2007). Typically, the ocean's response to typhoons can be divided into two stages; forced and relaxation stages. During the forced stage, the hurricane winds drive the mixed-layer currents, SST cooling by vertical mixing (entrainment) and air-sea heat exchanges (mainly due to loss of latent heat flux). The barotropic response consists of a geostrophic current modifying the sea surface height. The relaxation stage response following a hurricane's passage is primarily due to inertial-gravity oscillations excited by the typhoon. The mixed-layer velocity oscillates with a near-inertial period and hence so does the divergence and the associated upwelling and downwelling (Tsai et al., 2008).

However, no detailed study has been emphasized on the cause and mechanism of the significant temperature drop for certain typhoons. The oceanic responses to typhoons differ from one to the other in several respects making the study of the processes difficult. It is further complicated by preexisting oceanic features that modulate the upper ocean heat, mass and momentum balance due to horizontal advection. A model that resolves these mesoscale features must be used to study the oceanic response to typhoons. Larger cooling of SST in typhoon Kai-tak is found mainly because of strong Ekman upwelling associated with the local topography in SCS and a relatively shallow and warm mixed layer. Similar mechanism may be used to describe the unique 11°C temperature drop after the passage of typhoon Ling-ling. The typical coastal upwelling significantly enhanced the sea surface cooling.

The main objectives of this paper are (1) to study the effect of a slowly moving typhoon (typhoon Kai-tak) in the South China Sea, (2) to quantify the physical processes controlling the upper-ocean thermal structure and surface cooling during typhoon passage and (3) to assess the model's ability to reproduce the observed behavior of the oceanic responses to a typhoon without data assimilation. This paper is organized as follows: section 2 describes the passage of the typhoon Kai-tak and relevant observation. Section 3 details the model configuration and results. The mechanism causing the significant SST drop is also investigated. Summary is given in section 4.

2. Typhoon Kai-tak and observation

Typhoon Kai-Tak was a category 2 typhoon in the Saffir-Simpson hurricane scale. It lingered at a quasi-stationary slow speed (0-1.4 m/s) on the northern SCS from 5 to 8 July, 2000 before it proceeded speedily (>6.1 m/s) northwards thereafter (Central Weather Bureau, Taiwan), see Fig. 1 for the best track. Before Kai-Tak's arrival, the SCS is characterized by warm SST predominantly above 30°C. The wind speed was between 5 to 10 m/s. During 5-8, July, Kai-tak's strong wind (20-40 m/s) dominated the wind field. Immediately after Kai-Tak's departure, on 9 July, a cold SST (21.5-24°C) pool (118-120°E, 19-20.5°N) of size comparable to Kai-Tak's 150 km Radius of Maximum Wind (RMW) co-located with the typhoon's track was observed. The minimum SST of 21.5°C was found at the center (118.9°E, 19.9°N) of the cold pool. In comparison with the pre-typhoon condition (30.7°C), the SST dropped as much as 9°C.

Remote-sensed data provided unique opportunity to investigate the surface temperature drop. Two remote-sensed datasets are used in the earlier study (Lin et al., 2003), QuikSCAT, and Tropical Rainfall Measuring Mission (TRMM) Microwave Imager (TMI), respectively. They measure ocean surface wind vector (QuikSCAT) and sea surface temperature (TMI) day and night under both clear and cloudy conditions. The cloud penetrating capability of TMI allows the entire area of entrainment (location of the bloom patch) to be sensed. Here, we also use QuikSCAT to provide the wind forcing in the simulation.

3. Model simulations

3.1 Model description

The Dual-grids, Paicific Ocean Model (DUPOM) used herein is based on the fourth-order accurate, collocated Arakawa-A grid DieCAST (Dietrich/Center for Air Sea Technology) model (Dietrich et al., 2008; Tseng et al., 2005). The control volume equations include fluxes of the conservation properties (momentum, heat and salt) across control volume. The model domain covers the entire North Pacific Ocean ranging from 30°S to 60°N and from 100°E to 80°W (Fig. 2). To reduce the computational time, a duo-grid approach is adopted based on a multiple-grid framework, which uses higher resolution to resolve eddies more realistically (Dietrich et al., 2008). A 1°/8 resolution is used west of 150°E where it is needed to resolve the detailed Kuroshio and regional circulations, while a 1°/4 resolution is used east of 150°E (Fig. 2). The grids are fully two-way-coupled each coarser time step (time steps are different for both grids) with a single coarse grid overlapping (i.e. 2×2 in fine grid cells). The meander and eddy exchanges are seamless at the interface without applying intergrid sponge layers or special treatments. Further details about the multiple-grid approach can be found in Dietrich et al. (2008). Model bathymetry is interpolated from unfiltered ETOPO2 depth data supplemented with the Taiwan's National Center for Ocean Research 1-minute depth archive in the Asian seas. The vertical resolution is linear-exponentially stretched by 26 layers, with a 6 m thick top layer. Both grids share the same vertical grid. Within each grid, longitudinal resolution is uniform and latitudinal resolution is generated such that varying latitude and longitude grid increments are equal everywhere (Mercator grid).

The surface wind forcing in the based model is obtained from the interpolated monthly Hellerman and Rosentstein winds (Hellerman and Rosenstein, 1983). The Levitus'94 climatology is used to initialize the model and to determine its surface sources of heat and fresh water (e-p) using the non-damping approach described in Dietrich et al. (2004). The northern boundary is closed and the southern boundary condition (30°S) is slowly nudging toward climatology in a sponge layer. The bottom is insulated, with non-slip conditions parameterized by a nonlinear bottom drag. Sub-grid scale vertical mixing is parameterized by eddy diffusivity (for temperature and salinity) and viscosity (for momentum) using a modified Price (1981) schemes described in Sheng et al. (2006). Background lateral viscosity (or diffusivity) is 100 m^2/s and 200 m^2/s, respectively.

3.2 Initial and boundary conditions for typhoon Kai-tak simulation

We take the model year 23, July 1st as the initial conditions for the Typhoon Kai-tak's simulation. Initial temperature and salinity are based on the South East Asia Time-series (SEAT) station (116°E, 18°N) observation before typhoon Kai-tak's passage in July, 2000. All model integrations are started on July 3, 2000.

The model is then driven by fields of 10 m wind stress extracted from six-hourly 2.5° ERA40. It is well-known that the ERA40 product does not adequately resolve the tropical cyclones. In this study, we further blend the ERA-40 winds with the QuikSCAT analyzed winds. Since ERA40 is updated every six hours while the QuikSCAT wind (twice per day) provides more realistic wind field and may not be consistent with ERA40, a special smoothing procedure is performed. We take the difference between the QuikSCAT and ERA-40 winds at each of the discrete observations and times. This difference is merged into an "extended winds window" (EWW) grid which is larger than the localized QuikSCAT wind field. The difference is then set to zero at the boundary of EWW and a Poisson spreader is applied to spread the difference between the QUikSCAT wind and the EWW grid boundaries. In order to minimize the nudging at EWW grid boundaries, the EWW should extend laterally at least an eddy size beyond the QuikSCAT wind fields. The blended wind fields are then interpolated back to the DUPOM domain.

Following Oey et al. (2006), the wind stress is calculated from the wind fields using a bulk formula:

$C_d = 0.0012$, $|u_a| \le 11$m/s
$= 0.00049 + 0.000065\,|u_a|$, $11 < |u_a| \le 19$ m/s
$= 0.00136 + 2.34\times10^{-5}|u_a| - 2.32\times10^{-7}|u_a|^2$, $19 < |u_a| < 100$m/s

where $|u_a|$ is the wind speed. The maximum wind speed is ~40 m/s from the QuikSCAT. The formula incorporates the limited drag coefficient in high wind speeds (Powell et al. 2003). All wind stresses are assumed to be in dynes/cm-cm and to have magnitude less than 100dynes/cm^2.

3.3 Model results

Fig. 3 shows the sea surface height superimposed by the surface velocity vector after 90 hour (i.e. July 6, 2000). The eye-wall winds drive a strongly-out-of balance cyclonic flow, as indicated by the vectors that reveal a big outward flow component of the cyclonic spinning water. The very intense nonlinear mesoscale vortex has scale 50-100 km.

During the passage of typhoons, sudden change of the surface wind stress could generate inertial motions in the upper ocean (Gill, 1982). In the north SCS, the averaged inertial period is about 35 hr (20°N). We further compare the model velocities with those measured at the ADCP mooring station KA1 (under Kuroshio Upstream Dynamics Experiment, KUDEX). To separate rapidly fluctuating inertial motions from otherwise relatively low frequency inertial currents, we applied a 6 hour low-pass filter to the observed currents. Fig. 4 shows the comparison between the modeled and observed currents. Both model and observation show clear inertial oscillations ~32 hr.

Two extremely surface cooling events after the passage of typhoons occurs (>9°C) in SCS (Lin et al., 2003; Sheng et al., 2008), including typhoon Kai-tak. How did such a drastic response happen? Entrainment mixing is in general the primary mechanism accounting for the SST response (Price, 1981). However, for a slow-moving cyclone (translation speed <4 m/s), such as, Kai-Tak, strong upwelling occurs with entrainment and the response is significantly enhanced (Price, 1981). The maximum cooling (and upwelling) is in a ring around the core of the typhoon which appears to start in the northeast corner of the typhoon where wind forced upslope flow may be involved (Fig. 5). This appears to have been forced by the inertial dynamics of a fast current by the winds up the shelfslope in the northeastern SCS. The return flow downslope can also create strong eddies by release of potential energy, thus giving some significant mixing.

Fig. 6 shows 90 hour vertical subsidence calculated at 45 m depth. It is clear to see strong vertical upwelling when the typhoon hovered in the northeastern SCS. The maximum vertical velocity can reach 30m/day (negative subsidence is upward) near the center of typhoon. Further, the continuous Ekman pumping is also enhanced by the topographical upwelling which can be seen in Fig. Fig. 7 further shows the bottom currents along the topography. Very strong alongshore currents are associated with strong upward motion near the Philippine coastal shelf. The isobaths are also shown in Fig. 7.

4. Summary

We illustrate an application of a multiple domains modeling development work using the simulation of the ocean response to typhoon Kai-tak. An intense nonlinear mesoscale eddy is generated with O(50-100km) horizontal scale in the northeastern SCS. Inertial oscillation is clearly observed. More than 8°K sea surface temperature (SST) drop is found in both observation and simulation. This significant SST drop results from the influence of slow moving typhoon, initial stratification and bathymetrically-induced upwelling in the region where the typhoon hovered.

5. References

Dietrich, D.E., R.L. Haney, V. Fernandez, S.A. Josey, and J. Tintore, (2004), Air-sea fluxes based on observed annual cycle surface climatology and ocean model internal dynamics: A precise, non-damping zero-phase-lag approach applied to the Mediterranean Sea, J. Mar. Syst. 52, 145-165.

Dietrich, D. E., Y.-H. Tseng, R. Medina, S. A. Piacsek, M. Liste, M. Olabarrieta, M. J. Bowman, and A. Mehra, (2008), Mediterranean Overflow Water (MOW) simulation using a coupled multiple-grid Mediterranean Sea/North Atlantic ocean model, J. Geophys. Res., 113, doi:10.1029/2006JC003914..

Emanuel, K., (2003), Tropical cyclones. Annual Rev. Earth Planet. Sci., 31, 75-104.

Hellerman, S., and M. Rosenstein (1983), Normal monthly wind stress over the world ocean with error estimates, J. Phys. Oceanogr, 13, 1093-1104.

Lin, I-I, C.-C. Wu, K. A. Emanuel, I-H. Lee, C. Wu, and F. Pan, (2005), The interaction of supertyphoon Maemi (2003) with a warm ocean eddy, Mon. Wea. Rev., 133, 2635-2649.

Lin, I-I, W.T. Liu, C.C. Wu, G.T.F. Wong,C. Hu, Z. Chen, W.D. Liang, Y. Yang, and K.K. Liu, (2003), New evidence for enhanced ocean primary production triggered by tropical cyclone, Geophys. Res. Lett., 30, 1718, doi:10.1029/2003GL017141.

Oey, L.-Y., T. Ezer, D.-P. Wang, S.-J. Fan, and X.-Q. Yin, (2006), Loop Current warming by Hurricane Wilma, Geophys. Res. Lett., 33, L08613, doi:10.1029/2006GL025873.

Oey, L.-Y., T. Ezer, D.-P. Wang, X.-Q. Yin, and S.-J.

Fan., (2007), Hurricane-induced motions and interaction with ocean currents. Cont. Shelf Res. 27:1249-1263.

Powell, M.D., P.J. Vickery, and T.A. Reinhold, (2003), "Reduced drag coefficient for high wind. speeds in tropical cyclones" Nature, 422, March 20 pp.279-283

Price, J. F., (1981), Upper ocean response to a hurricane. J. Phys. Oceanogr., 11, 153–175.

Shang, S., L. Li, F. Sun, J. Wu, C. Hu, D. Chen, X. Ning, Y. Qiu, C. Zhang, and S. Shang, (2008), Changes of temperature and bio-optical properties in the South China Sea in response to Typhoon Lingling, 2001, Geophys. Res. Lett., 35, L10602, doi:10.1029/2008GL033502.

Jinyu Sheng, Xiaoming Zhai, Richard J. Greatbatch, (2006), Numerical study of the storm-induced circulation on the Scotian shelf during hurricane Juan using a nested-grid ocean model, Prog. Oceanogr., 70, 233-254.

Sheng, J., L. Wang, S. Andréfouët, C. Hu, B. G. Hatcher, F. E. Muller-Karger, B. Kjerfve, W. D. Heyman, and B. Yang, (2007), Upper ocean response of the Mesoamerican Barrier Reef System to Hurricane Mitch and coastal freshwater inputs: A study using Sea-viewing Wide Field-of-view Sensor (SeaWiFS) ocean color data and a nested-grid ocean circulation model, J. Geophys. Res., 112, C07016, doi:10.1029/2006JC003900.

Tsai, Y. L., C.S. Chern and J. Wang, (2008), The upper ocean response to a moving typhoon, J. Oceanogr., 64, 115-130.

Tseng, Y.-H., D.E. Dietrich, J.H. Ferziger, (2005), Regional circulation of the Monterey Bay region-hydrostatic versus non-hydrostatic modeling, J. Geophy. Res., 110, C09015, doi:10.1029/2003JC002153.

Wu, C.-R., Y.-L. Chang, L.-Y. Oey, C.-W. J. Chang, and Y.-C. Hsin, (2008), Air-sea interaction between tropical cyclone Nari and Kuroshio, Geophys. Res. Lett., 35, L12605, doi:10.1029/2008GL033942.

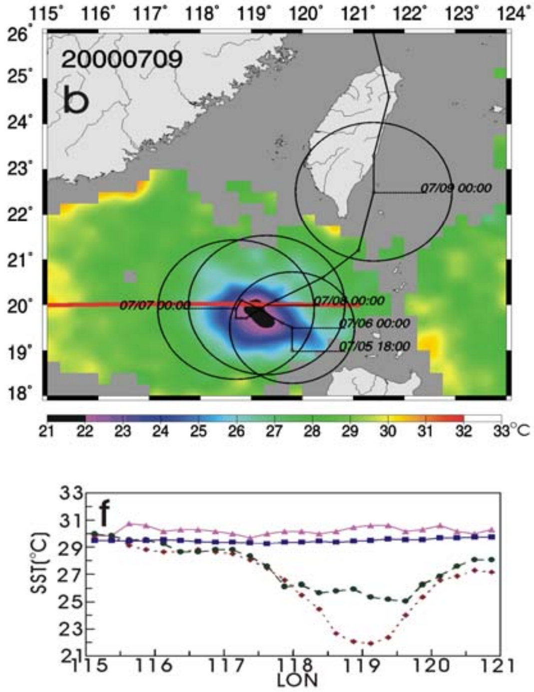

Fig. 1 (top) TRMM TMI/SST image on 9 July, 2000; (bottom) Comparisons along 20°N, pink: 7/1-7/3, 2000, Brown: 7/9, 2000, Green: 7/12-14, 2000, Blue 3-year (1998, 1999, 2001) climatological average of SST for July (Lin et al., 2003).

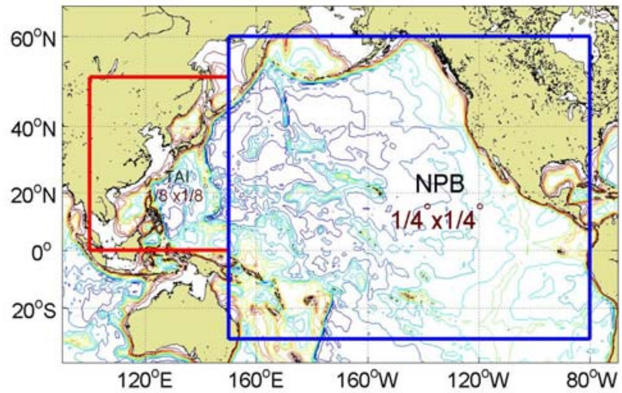

Fig. 2 Model domain and resolution.

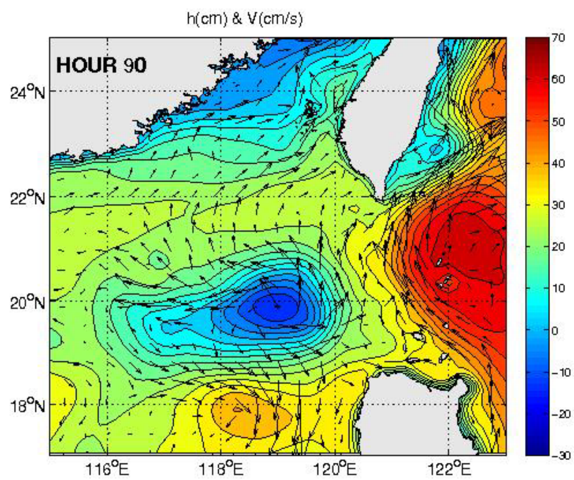

Fig. 3 Sea surface height superimposed by surface velocity vector.

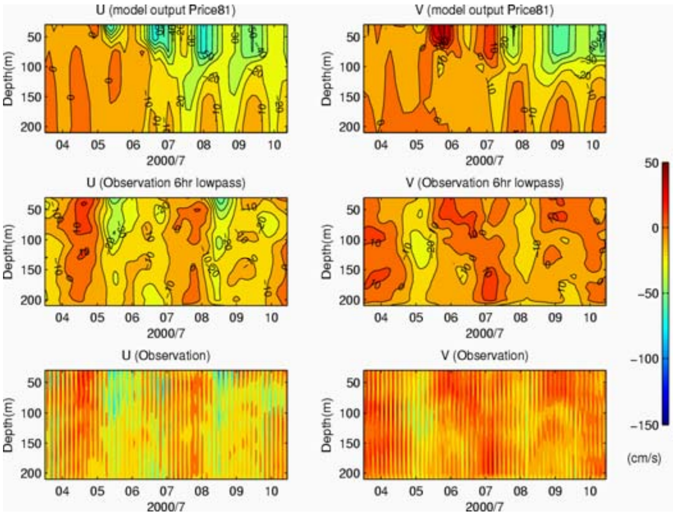

Fig. 4 Comparison between the modeled and observed velocity components.

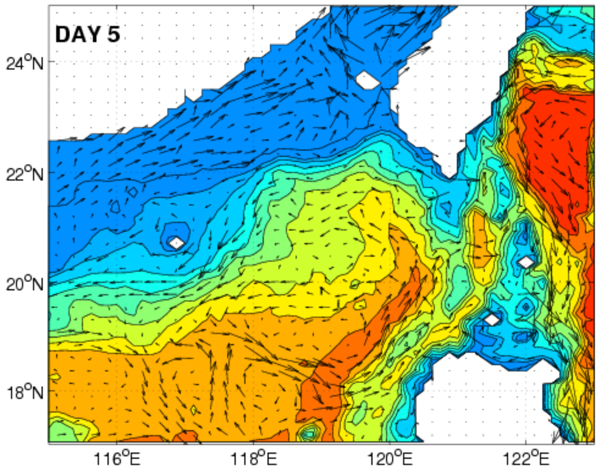

Fig. 7 bottom current vectors above the bathymetry. Isobaths are shown in color.

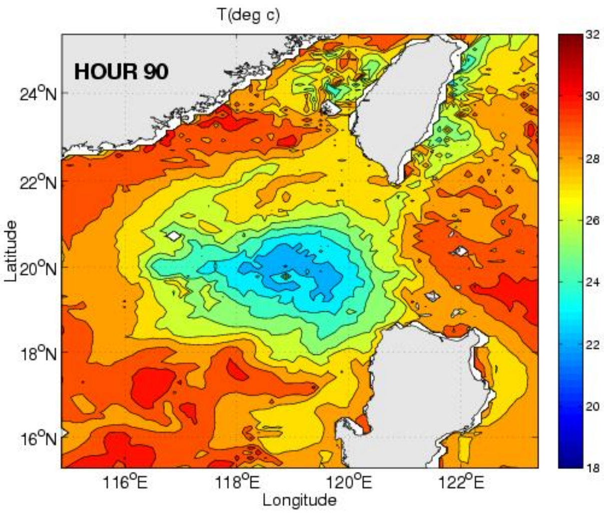

Fig. 5 Modeled sea surface temperature on hour 90.

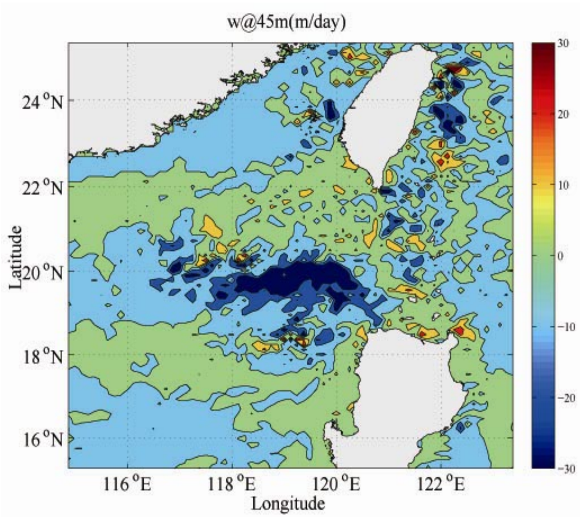

Fig. 6 Daily averaged vertical subsidence on day 4 at 45 m.

Real Time Ocean Observations from Surface Drifters

L.R Centurioni and P.P. Niiler
The Scripps Institution of Oceanography

Abstract

This note provides an overview of the methods used to make real-time observations of the physical properties of the upper ocean and of the atmospheric boundary layer from instruments drifting at the ocean surface. We begin with a description of the Global Drifter Program, which provides global coverage of 15 m depth currents and sea surface temperature observations. Atmospheric sea level pressure is also measured over a large portion of the aqueous globe. Several meteorological offices use the atmospheric sea level pressure data, which are available on the Global Telecommunication System, to improve their forecast. The Global Drifter Program data are freely accessible and are used by scientists around the world for scientific research. Recently, more specialized drifters have been developed to measure sea surface salinity, wind velocity and vertical profiles of temperature and currents and are used for specific, space-time confined, observational programs. The methods described are cost-effective since they involve minimal sea-going operations, mostly from ships of opportunity, and do not require specifically trained personnel.

1 Introduction

The purpose of this note is to provide an overview of established and emerging methodologies to make real-time observations of the upper ocean and in the atmospheric boundary layer from instruments drifting at the ocean surface. A global array of Lagrangian (water following) drifters has now been operational for several years, and yet more sophisticated drifting instruments are being developed as new technologies and faster telecommunication options become available. These instruments are long lived and rugged and, for example, they have been successfully deployed in front of hurricanes. Measurements of vertical profiles of three dimensional velocity are becoming a new powerful tool to study the physical processes of the open ocean and in coastal seas and estuaries. Examples of technical developments and applications will be given.

2 The Global Drifter Program (GDP)

The Global Drifter Program (GDP) is an important component of the Global Ocean Observing System of NOAA and a scientific activity of the Data Buoy Cooperation Panel (DBCP), a joint body of the World Meteorological Organization (WMO) and of the Intergovernmental Oceanographic Commission (IOC). It is the first oceanographic operational global array to have reached its full implementation on September 18, 2005. The GDP maintains an array 1250 Surface Velocity Program (SVP) drifters (Fig. 1) and involves international co-operation of more than 15 countries.

The goal of the GDP program is to provide accurate measurements of the 15 m depth horizontal ocean currents, Sea Surface Temperature (SST), atmospheric pressure, surface salinity and wind velocity and to facilitate the use of the data for operational and scientific purposes. The AOML (NOAA) maintains a public data archive.

All the SVP drifter data are transmitted through the Argos satellite system and posted free of charge on the Global Telecommunications System (GTS) to help the weather centers to produce improved forecast.

The SVP drifter is designed with a drag area ratio larger than 40. The drifters therefore behave like true water followers (Niiler et al. 1995) with a very contained slip due to the wind (Pazan; Niiler 2001). The SVP drifter development and several examples of scientific applications of drifter data are discussed by Niiler (2001). Fig. 2 shows the most recent status of the global drifter array. The distribution of the SST and velocity sensing drifters is rather uniform (red and blue dots), but that is not the case for Sea Level atmospheric Pressure (SLP) sensing devices (blue dots), since the barometer array is largely maintained by individual countries participating in the program.

Enhancing the SLP array in the tropical and Pacific and Atlantic Oceans would result in more accurate regional weather forecast products. The Global Drifter Program has a long-standing history of co-operation with national agencies to achieve global coverage.

The handling of drifter's data is relatively straightforward. The following is an example of how atmospheric pressure data are treated: 160 SLP samples (taking approximately 160s) are collected each hour and the following de-spiking algorithm is used to filter SLP data (Barometer Drifter Design Reference, available online at http:// www.jcommops.org/doc/DBCP/svpb_ design_manual. pdf):

- take the median of the lowest 10 points of 160;
- calculate the median of the points within the entire set of 160 points that are within 1 hPa of the 10 point median;
- store as 12 bit count: 0 => 800.0 hPa and 4095 =>

1209.5 hPa, with 0.1 hPa resolution;

• if 15 or more of the 160 samples include communication errors, the sampled set is deemed corrupt, and the transmitter count is set to zero.

Previously measured pressure data are stored in the drifter controller for 12 hours for redundancy in data transmission.

The GDP is one of the most successful oceanographic operational programs, and, to date, there are more than 300 scientific publications based on drifter data. Recent examples include a computation of the global Sea level (Niiler et al. 2003), a research paper on the Kuroshio intrusion in the South China Sea through the Luzon Strait during the winter monsoon (Centurioni et al. 2004) and an investigation of the dynamics of the California Current System (Centurioni et al. 2008).

3 The Autonomous Drifting Ocean Station (ADOS)

The ADOS is composed of a 0.46 m diameter surface buoy with a tether to which a drogue can be attached to make it a Lagrangian device. It can carry several sensors such as a radiometer, an hydrophone for measuring ambient noise, a SST sensor and a barometer. The version with the hydrophone, from which the wind speed can be inferred, wind vane and SLP sensor is also known as the Minimet (Fig. 3).

The ADOS can also be conFig.d without the drogue but with a 150 m long tether to which several low-cost, inductively coupled thermistors and pressure sensors are attached. In this case the ADOS is not a water following device. Both the Minimet the and the ADOS with thermistor chain have been successfully deployed from air (Fig. 4 and Fig. 5) to observe the thermal structure of the upper ocean (Fig. 6) and the wind field associated within hurricanes (Fig. 7).

The ADOS data are commonly transmitted through the Argos satellite system.

The most recent Minimet development is the upgrade of the wind speed sensor with an acoustic anemometer.

4 Open-ocean 3-D velocity observations from drifters: the ADOS-V

In recent years we have begun exploring the methodology to measure three-dimensional velocity profiles from drifting platforms. The ADOS fitted with the thermistor chain has been modified to accommodate a longer tether (200 m) and two or three Acoustic Current Profilers by Nortek. We refer to this instrument as to the ADOS-V (Fig. 8).

A GPS receiver has been added to compute absolute horizontal velocity profiles (i.e. referenced to Earth's co-ordinates). Twenty inductively coupled pressure and temperature sensors are attached to the 200 m long cable, with a spacing of approximately 9 m. Communications through the Iridium satellite system is being implemented for the transmission of all the data (position, temperature pressure and three-dimensional velocity). As of now, the ACP is the most expensive components of the system, and they limit the expendability of the ADOS-V. We anticipate that this will change once a market large enough to justify a significant ACP cost reduction will be established.

Arrays of ADOS-V can be quickly deployed from aircrafts and voluntary observing ships and should be used, for example, whenever spatial and temporal coherent oceanic processes need to be observed from closely spaced arrays.

As an example of applications of the ADOS-V technology, a study on the properties of Large amplitude Internal Waves (LIW) in the northern South China Sea (nSCS) was performed in April and May 2007 with an array of eight ADOS-V. Wave groups with two or three solitary-like waves are known to propagate throughout the deep waters of the nSCS during spring tides and are thought to be generated within the Luzon Strait by interaction of the tidal flow with the topography.

Accurate vertical profiles of temperature and velocity (Fig. 9) can be used for example to locate points of equal phase as the LIW groups propagate through the ADOS-V array and to compute the local phase speed of the waves, which, in this case, is of 2.8 m/s. Other properties of the waves, such as their nonlinearity and their spatial homogeneity and stability as they propagate through the array can be investigated with this methodology.

5 The restrained ADOS-V: a lightweight, self deploying coastal mooring.

The ADOS-V has recently been reconFig.d into a light weight coastal mooring. The layout of the sensors is similar to the one discussed in the previous section, the only differences being that a larger weight at the bottom and a larger surface floatation element are used, and an acoustic release is also included if the instruments needs to be recovered (Fig. 10).

The schematic shown here pertains to a 135 m long device that can be deployed in approximately 120 m of water. Alike the ADOS-V, the restrained version can be packed inside a deployment box and can be parachuted from aircrafts or can be deployed from ships of opportunity. We are in the process of implementing real-time data transmission of pressure, temperature and 3-D velocity profiles through the Iridium satellite system. Two units will be deployed for the first time in a pilot experiment in the southern East China Sea.

6 Shallow water observations from drifters: the River Drifter

Understanding the kinematics and the hydrodynamics of near-shore flows in very shallow water is essential to study and predict morphological changes of the coastline, sediments transport and their dispersal. A new instrument called the River Drifter (RD), was designed to bridge the gap between 2-D and 3-D data acquisition in shallow waters, such as lagoons, river estuaries and tidal flats, essentially by using a Lagrangian platform as a vehicle from which three-dimensional vertical profiles of velocity and local bottom depth measurements are made. The RD (Fig. 11) is based on the CODE design (Davis 1985) and measures GPS location, three-dimensional water velocity with a 1 or 2 MHz ACP (with a nominal range of 12-25 and 5-12 m, respectively), depth of the bottom, bottom characteristics and sea surface temperature.

The RD is lightweight (just over 4 Kg) and the data telemetry is through Iridium. Full functionality tests of the first unit (Fig. 12) have been successfully conducted and the instrument is ready for scientific research operations.

The RD can be packed compactly using water soluble paper tape and fits inside a deployment cardboard tube (Fig. 13).

7 Concluding remarks

The methodologies and the technical developments presented here are answering the need of modern oceanography for autonomous, low cost, self-deploying instruments which can both be used for operational purposes and yet provide data of enough good quality to support new scientific discoveries, The GDP being perhaps the best example. New venues to improve this technology are constantly explored and new sensors are being added. The addition of thermistor chains and profiling current meters is opening far reaching research and operational opportunities, ranging from the study of how the ocean and the atmosphere interacts to observations of surface gravity waves in the world oceans.

8. Concluding remarks

Centurioni, L. R., P. P. Niiler, and D. K. Lee, (2004), Observations of inflow of Philippine Sea surface water into the South China Sea through the Luzon Strait. J Phys Oceanogr, 34, 113-121.

Centurioni, L. R., J. C. Ohlmann, and P. P. Niiler, (2008), Permanent Meanders in the California Current System. J Phys Oceanogr, 38, 1690–1710.

Davis, R. E., (1985), Drifter Observations of Coastal Surface Currents during Code - the Method and Descriptive View. J Geophys Res-Oceans, 90, 4741-4755.

Niiler, P. P., (2001), The world ocean surface circulation. Ocean Circulation and Climate, G. Siedler, J. Church, and J. Gould, Eds., Academic Press, 193-204.

Niiler, P. P., N. A. Maximenko, and J. C. McWilliams, (2003), Dynamically balanced absolute sea level of the global ocean derived from near-surface velocity observations. Geophysical Research Letters, 30.

Niiler, P. P., A. Sybrandy, K. Bi, P. M. Poulain, and D. Bitterman, (1995), Measurements of the water-following capability of holey-sock and TRISTAR drifters. Deep-Sea Research 1, 42, 1951-1964.

Pazan, S. E., and P. P. Niiler, (2001), Recovery of near-surface velocity from undrogued drifters. J Atmos Ocean Tech, 18, 476-489.

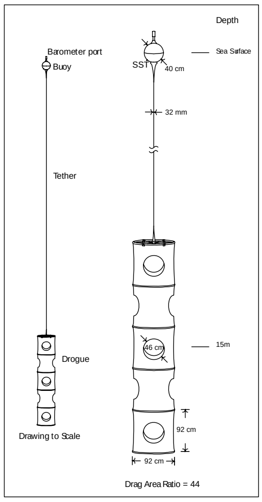

Fig. 1 Schematic of a SVP drifter with a barometer. The water depth at the center of the drogue is 15 m.

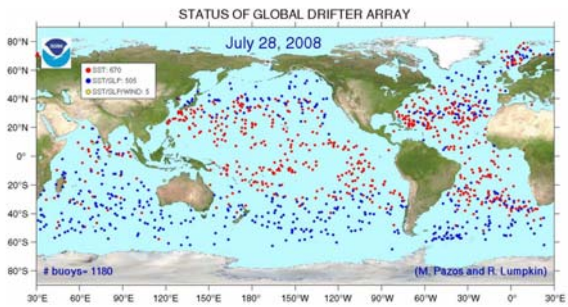

Fig. 2 Status of the Global Drifter Array as of July 28, 2008 (courtesy of M. Pazos and R. Lumpkin, available online at http:/www.aoml.noaa.gov/phod/ graphics/dacdata/ globpop.gif).

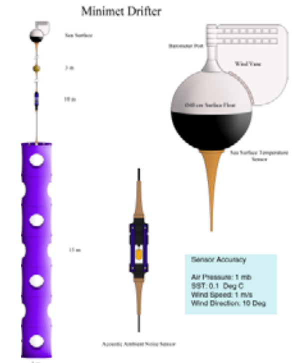

Fig. 3 Schematic of the Minimet drifter.

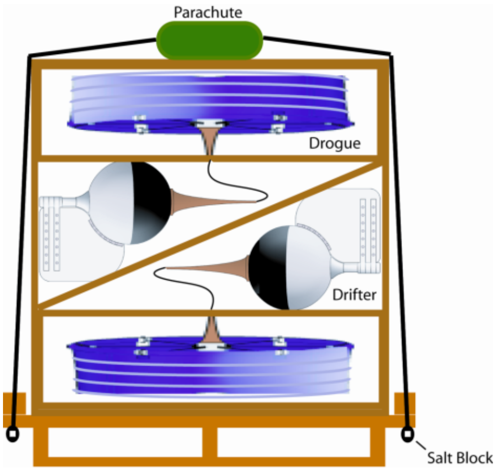

Fig. 4 Two Minimets are contained in the air deployment box, which is held together with straps and salt blocks. The package dissolves when is in the water thus freeing the instruments.

Fig. 5 The box with the Minimets is being deployed from a C-130.

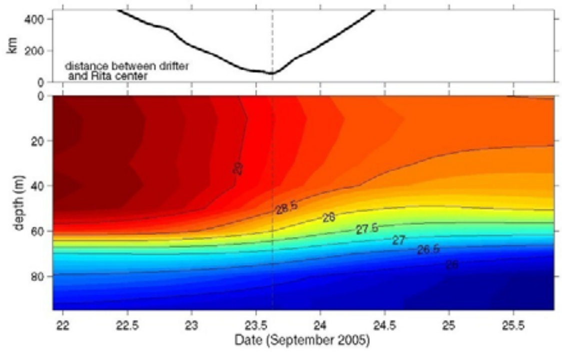

Fig. 6 Changes in the temperature field during the passage of hurricane Rita.

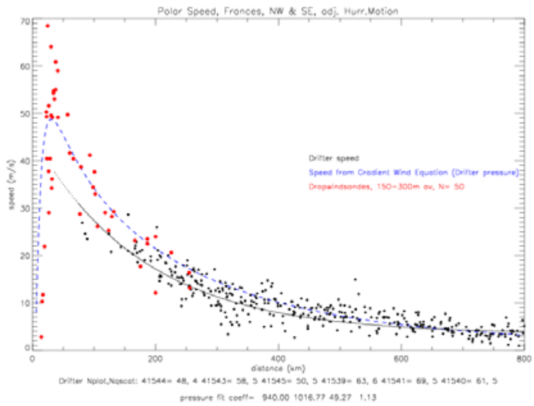

Fig. 7 Comparison of azimuthal wind speed measurements from the Minimet's hydrophone (black), SLP data (blue) and dropwindsondes (red). Hurricane Frances. The large speeds from dropwindsondes are due to localized swirls in front of the hurricane.

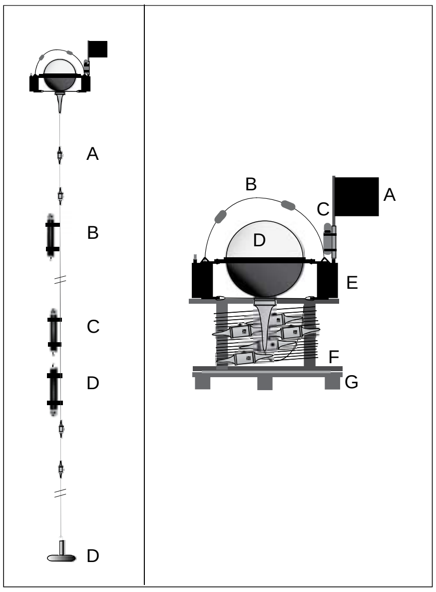

Fig. 8 ADOS-V schematic. Left: the surface element is connected to a tether on which the temperature and pressure sensors (A), one 1MHz Aquadopp at 25 m depth (B), two 400 KHz Aquadopps (C and D) at 110 m depth and a 20 Kg weight (D) are attached. The spacing between the temperature and pressure sensors is approximately 9 m. Right: the ADOS-V tether is wrapped around a wooden reel (F) which is mounted on a pallet through a spinning wheel. The spherical buoy (D) is mounted on a rectangular cross-section toroidal anodized aluminum buoy (E). A flag (A) and a strobe light (C) are attached to the aluminum buoy together with a bridle used for recovering the ADOS-V.

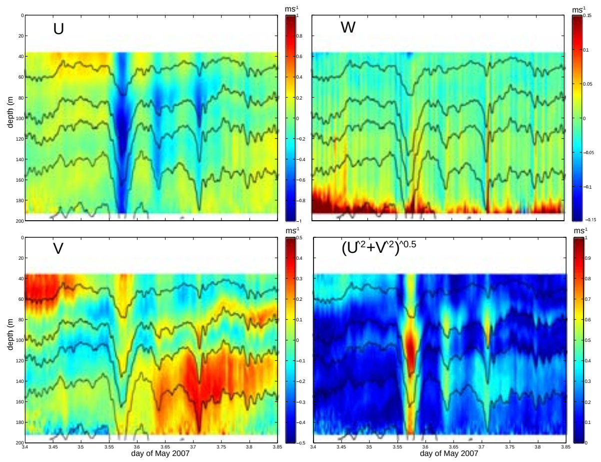

Fig. 9 Three-dimensional absolute velocity profiles and horizontal flow speed measured from the ADOS-V. The following isotherms are also shown: 25°C, 22.5° C, 20° C, 17.5° C and 15° C. U, V and W are the eastward, northward and vertical upward velocity respectively.

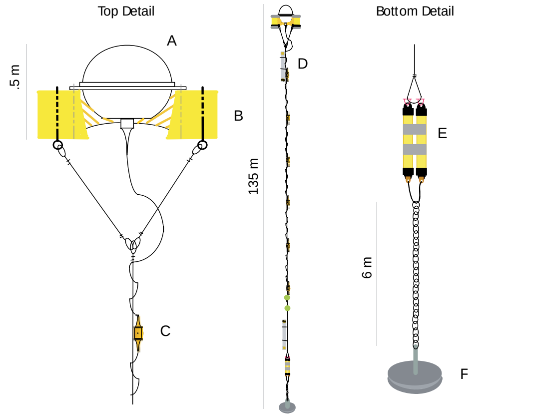

Fig. 10 Schematic of the restrained ADOS-V. A: ABS sphere with electronics and batteries. B: foam buoy. C: Inductive temperature and pressure sensor. D: acoustic current profiler. E: acoustic releases. F: weight.

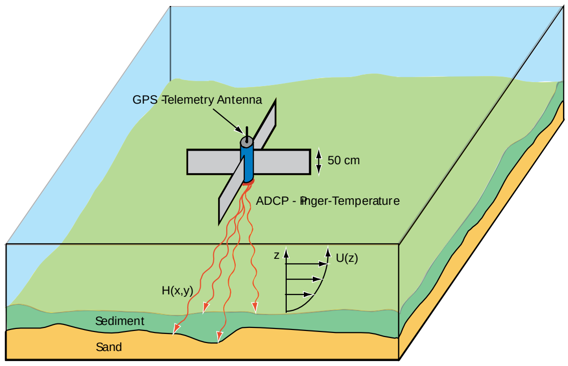

Fig. 11 Schematic of the river drifter (not to scale).

Fig. 12 River Drifter and detail of the acoustic head with the profiling current meter and the bottom pinger.

Fig. 13 Left: river drifter wrapped with water soluble paper tape. Right: river drifter inside the deployment cardboard tube.

附錄 B Dr. Eugene Wei 對本計畫的評估報告

<u>Marine Meteorology Center Visiting Summary</u>

Eugene Wei
NOAA/National Ocean Service
October 8, 2008

This brief report summarizes my visiting to the Marine Meteorology Center (MMC) of the Central Weather Bureau (CWB) during the week of September 8 – 12, 2008. This report describes my personal opinions regarding the ongoing MMC project: Developing Real-time Ocean Current Forecasting System for the Seas around Taiwan, by Professor Jason Yu of National Sun-Yet-San University.

During this visiting, I have attended CWB's Annual Forecast and Analysis Conference and MMC's Special Workshop on Marine Forecast System. In addition to presenting a technical paper titled: "Operational Circulation Forecast Systems in NOAA" (included in the Conference Symposium) at MMC Special Workshop, I also delivered another presentation to MMC staffs titled: NOS Operational Forecast Systems Skill Assessment and Modeling Framework. I was also briefed by MMC Director Hsu and her staffs with MMC missions, particularly the wave and circulation forecast operations.

Overall, I am impressed with MMC operations and performance under limited staffs and resources. With additional tasks and upcoming operational real-time ocean current forecast systems and the associated projects, it is suggested that MMC to add full time staffs in order to effectively carry out the workload.

1. Operational Ocean Current Forecasting System Development

1.1. Development Plan

The project development plan proposed by Prof Yu is well written and technically sound. The task milestone of this 4-year plan is well defined. The most challenge tasks of the entire project will be the data assimilation and the model nesting.

1.1.1. Data Assimilation in ROMS

As Dr. Roger Proctor pointed out that if the Pacific and Northwest models are required to show the correct circulation and Kuroshio location, the data assimilation (e.g., satellite SST and surface current – I believe) is definitely a must. To the best of my knowledge, so far we, at NOAA and NOS, do not have ROMS data assimilation experience. ROMS provides simple data assimilation such as OI and nudging to more sophisticated adjoint method. Prof Yu may start the task with simple SST nudging. For more advanced adjoint method, Prof Yu may need to seek assistance from ROMS experts (John Wilkin of Rutgers University, Kate Hedstrom of University of Alaska, and Emanuele (Manu) Di Lorenzo of Georgia Institute of Technology). (Note: Not sure what type of assistance they may offer, free or with a charge).

1.1.2. Model Nesting

The proposed approach to the final forecast systems for the seas around Taiwan includes 2 to 3 layers of model nesting. ROMS provides the options of running nested models as one model. This requires further study of any successful application, especially for a real time forecast system. Therefore, it is suggested that the nesting be done as external boundary forcing approach. Verification studies of nesting approach are also recommended to investigate the tecchnique feasibility to ensure the product quality.

1.1.3. Model System Skill Assessment

As demonstrated in my presentations at MMC Special Workshop and to MMC staffs, the model system skill assessment is a very important component of the forecast system development at NOAA's NOS. For an ocean current forecast system model, some type of skill assessment should be developed in order to demonstrate the model capability and product quality. NOS's skill assessment matrix can be a good reference.

1.2. Prof Yu Laboratory Resources

While visiting National Sun-Yet-San University in Kaohsiung, I was briefed by Prof Yu of his laboratory facility and resources. It seems that the computer resources of Prof Yu's laboratory is capable of conducting the proposed modeling work, at least during the development and the preliminary operational stages. The qualification of major project staffs (one post-doc equivalent Ph.D. candidate and one Ph.D. student) meet the project requirement but may need advanced ROMS modeling in-depth guidance from Prof Yu or other experts (from other institutions) in order to ensure the project completion schedule.

2. MMC Responsibility and Resource for Development, Implement, and Operation of Real-time Ocean Current Forecasting System

2.1. MMC Capability

It seems to me that at present MMC lacks of staff resources in handling the task. MMC needs to add qualified personnel with strong numerical modeling and oceanographic background and training in order to carry out this multi-year task. Although there is a similarity in implementing and operating a wave forecast system and a circulation forecast system, there still exists significant differences in technique and data requirement including the boundary and surface forcing and forecast guidance characteristics.

Therefore, it is my suggestion that the staff designated to be responsible for operating circulation forecast system, i.e., Ms. Chen, to work closely with the project Principle Investigator Prof. Yu's staffs during all the development phases. MMC should provide and encourage tranning opportunity for Ms. Chen regarding ROMS modeling and the circulation forecast system real-time operation.

2.2. Operational Plan

2.2.1. Data Bank

Implementing and operating the proposed real-time ocean current forecast system at CWB involves different aspects such as the computational resource capability and the associated data base. It seems that CWB computational resource is adequate for handling this task in addition to existing atmospheric and oceanographic forecasting operations. However, the data for driving the real-time ocean current forecast system can be significantly different from data for other existing systems such as atmospheric and wave forecasting systems; for example, the real-time surface drifter data and near real-time SST for data assimilation. The set-up of data tank within CWB computer system for the ocean current forecast system is critical to the success of the project. A plan of establishing the data bank (or addition to the existing one for atmospheric) should be drafted before the ROMS model starts testing on CWB computer system.

2.3. Long Term Goal and Applications

It would not be too early to plan ahead the applications before the ocean current forecast system been operational at CWB. The immediate applications for an operational ocean current forecast system fall into two categories: hazard material trajectory modeling and the search and rescue mission. Collaborating with other government agency such as EPA and Coast Guard becomes critical to demonstration the application of an operational ocean current forecast system. MMC should carefully draft the detailed plan considering the technique function capability of these two agencies in utilizing the information that MMC's operational ocean current forecast system can offer. To what extend that MMC would like and can involve in these applications sometimes not depending on scientific technique but rather, in reality, the political circumstances.

The long term goal of the operational ocean current forecast system should tie to MMC mission. For example, MMC should develop several individual, detailed small scale forecast system for each of local area of Taiwan coast nested in a larger domain ? or an unstructured grid includes the entire Taiwan coast with detailed features covering local small area ?

3. Conclusions

I am grateful of MMC Director Hsu and Prof Yu for this visiting opportunity at MMC and NSYSU and the involvement of this project. This visiting surely helps me exchanging experiences with scientists in Taiwan. I will be glad to continue my contribution, if requested by MMC or NSYSU, to provide my service to the project, and MMC or NSYSU, and for the people of our homeland, Taiwan.

附錄 C 海流模式於氣象局高速電腦計算測試報告

由於未來海洋環流預報模式需移交氣象局進行運算，因此採用的模式需要於氣象局高速電腦中運算。目前氣象局的高速電腦系統。其主要由 IBM P5-575 系統所組成，此系統是使用 IBM Power5 時脈 1.5GHz 雙核心中央處理器，每一個節點連結 8 顆 power5 中央處理器，共建置了 156 個節點，共有 2496 個中央處理器可供使用，其中 138 個節點可供計算使用；主記憶體容量，有 36 個節點每個中央處理器可使用 4GB 的容量，120 個節點每個中央處理器可使用 2GB 的容量；在硬碟容量則配置了 18TB 供研究使用，14TB 供作業化使用，計算能力相當強大。在軟體的配置上，此套系統使用 IBM 自製的作業系統 AIX5L 5.3，提供 XL Fortran(95/90/77)、C 及 C++的程式編譯器，另外包含了 ESSL v4、pESSL v3、及 IMSL 等函式庫供使用者使用；平行環境則提供 Parallel Environment(PE) v4.2 供平行程式進行運算，提昇運算時效；由於此高速電腦可提供多人使用，因此各個工作的資源分配就相當重要了，目前本套系統使用 LoadLeveler(LL) v3.1 來管理工作資源的分配，以讓所有使用者可以完全充分的使用；檔案系統則使用 General Parallel File System(GPFS) v2.3，可提供快速的檔案讀寫。

ROMS 開發過程即是利用大型主機進行開發及測試，且提供多種平台供使用者設定，本團隊目前使用的測試系統為 PC cluster(AMD 及 INTEL 系統)，使用的作業環境為 Linux，程式編譯器為 PGI fortran(f90)，平行運算編譯器為 mpif90，此部份與氣象局的高速電腦(IBM 系統)設定不同，IBM 程式編譯器為 XL fortran(xlf90)，平行運算編譯器則為 mpxlf90，因此需要進行模式運算環境設定的修正。另外由於氣象局高速電腦使用者相當的多，在執行程序上也與一般個人電腦不同，需透過專屬的排程工具進行運算程式的分配。因此本團隊與駐氣象局 IBM 電腦工程師李長華先生不斷討論及測試，目前已順利將 ROMS 建置於氣象局高速電腦系統中，並且進行程式執行效率的測試。ROMS 本身提供 MPI 及 OpenMP 的平行技術，氣象局高速電腦也同步安裝了 MPI 及 OpenMP 環境，因此選擇效率較好得平行環境進行計算。以下為兩者在氣象局高速電腦運算的環境設定檔。

使用 MPI 平台進行運算

```
#!/bin/ksh
#
#@ jobname    =ROMStest
#@ output     = $(jobname).$(jobid)
#@ error      = $(output)
#@ node = 16
#@ total_tasks=256
#@ resources = ConsumableCpus(1)
#@ job_type = parallel
#@ node_usage = not_shared
#@ network.MPI = sn_all,shared,US
#@ class = research
#@ queue

export TASKS_PER_NODE=16
export CPUS_PER_NODE=32
export nproc=2

#     $MPIPATH/bin/mpirun -np $nproc OceanM
echo "mpi 256"
time poe oceanM -procs $nproc    ocean_upwelling_mpi.in > log_mpi
```

使用 OpenMP 平台進行運算

```
#!/bin/ksh
#
#@ jobname    =ROMStest
#@ output     = $(jobname).$(jobid)
#@ error      = $(output)
#@ node = 1
```

```
#@ tasks_per_node = 32
#@ resources = ConsumableCpus(2)
#@ job_type = parallel
#@ node_usage = not_shared
#@ network.MPI = sn_all,shared,US
#@ class = research
#@ queue

export TASKS_PER_NODE=16
export CPUS_PER_NODE=32

export OMP_NUM_THREADS=2
export XLSMPOPTS="stack=512000000"

#    Run OpenMP oceanO
echo "OpenMP 32"
time oceanO < ocean_upwelling_omp.in > log_omp
```

由於 OpenMP 在使用的 cpu(中央處理器)數量上會有限制，氣象局高速電腦上限為一個節點共 16 顆 cpu(32 顆核心)，因此平行計算的部份仍使用目前通用的 MPI 架構，圖 C-1 為 ROMS 於氣象局高速電腦的平行計算效率。本次測試的網格數量為 656 x 1280 x 16 共 13,434,880 個網格點，模式計算天數為 5 天。ROMS 的平行效率基本上也是成線性變化，cpu 數量愈多計算計算時間愈短，約在 192 以上顆達到瓶頸，此部份因為模式網格數量不夠多，因此在 192 顆及 256 顆 cpu 的效率接近，以測試的案例來看，192 顆 cpu 是最佳的設定，繼續增加 cpu 數量並沒辦法再提高計算效率，未來若網格數繼續增加，再增加使用的 cpu 數量即可。

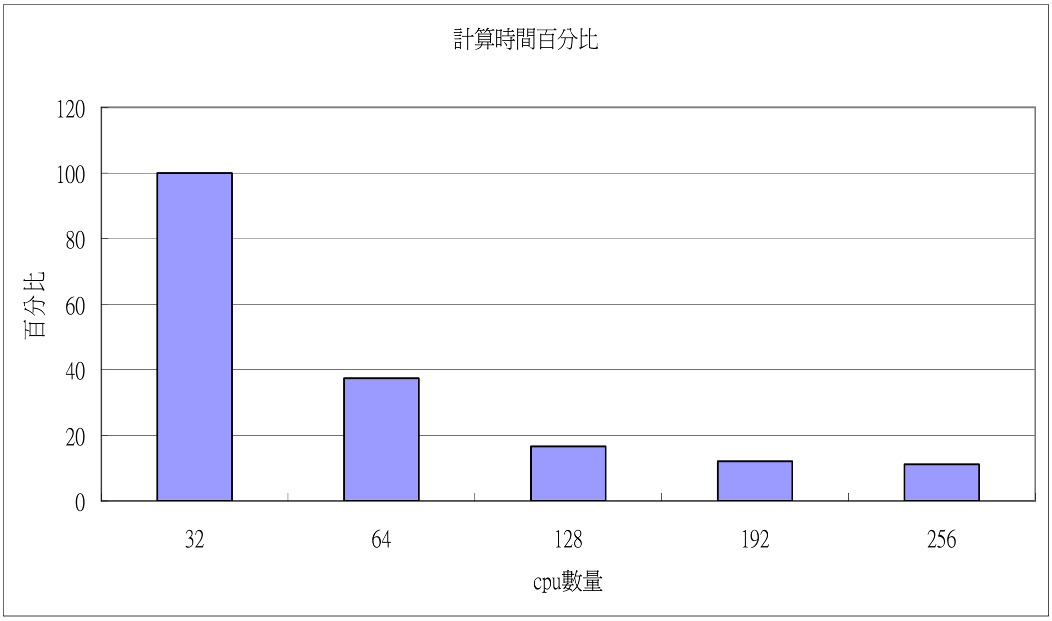

圖 C-1 氣象局高速電腦平行效率統計結果

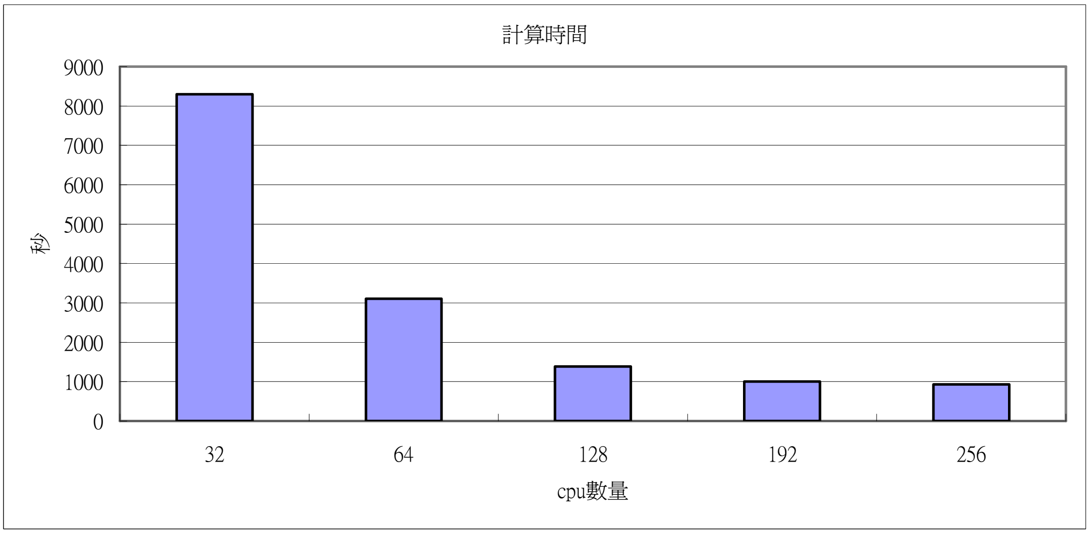

圖 C-2 氣象局高速電腦平行效率統計結果(實際時間)

附錄 D 工作進度會議

「三維海流預報作業模式建置及校驗分析研究」計畫案

【 期初討論會 】

時　　間：97 年 2 月 25 日(星期一)下午 3:00
地　　點：本局 616A 室
出席人員：徐月娟主任、于嘉順老師、朱啟豪課長
記　　錄：陳琬婷

壹、討論事項：

1. 計畫執行期間，每 2 個月舉行一次工作會議(97 年 3、5、7、9、11 月)。
    - 3 月工作會議預定於 3 月 3 日下午 2 時 30 分舉行。
    - 4 月 23 日至 25 日出席在台大舉行的 ”Numerical Ocean Modeling and Prediction” 國際研討會，收集相關資料及討論。
    - 5 月工作會議需邀請海軍及國內相關學者與會。
    - 7 月工作會議討論重點為模式上機測試內容及範圍。
    - 9 月工作會議需邀請國內相關學者與會。
    - 11 月工作會議可與國際研討會同日辦理。
2. 預定於 6 月 16 至 20 日當週期間擇一日召開期中審查會議(初步擇定 6 月 16 日或 17 日)。期中報告於 6 月 9 日前繳交。
3. 期中、期末審查委員應符合「交通部暨所屬機關委託研究作業規定」邀請局外專家學者 5 人再加上主任等局內委員共 9 人，需先簽奉局長核准及請局長指派審查會議主席。
4. 請于教授提出海流模式所需的海氣象資料目錄，海象中心可協助查詢本中心及本局資訊中心、預報中心、衛星中心、科技中心之國內外氣象資料蒐集或產出項目。
5. 邀請資訊中心及 IBM 駐局人員李長華先生出席 3 月分工作會議，使工作團隊瞭解 IBM 之軟硬體環境。

貳、散會

本會議於 16：00 結束。

「三維海流預報作業模式建置及校驗分析研究」計畫案

【 97 年 3 月工作會議 】

時　　間：97 年 3 月 3 日(星期一)下午 2:40
地　　點：本局 616B 室
出席人員：徐月娟主任、于嘉順老師、朱啟豪課長、江朕榮
紀　　錄：陳琬婷

壹、上次會議決議事項進度報告：

項次	項目	目前進度
1	查詢本中心及本局資訊中心、預報中心、衛星中心、科技中心之國內外氣象資料蒐集或產出項目。	• 資訊中心：朱課長已寫簽稿會核單給資訊中心。資訊中心表示需要一些時間做統整，約 3 月 20 日前可完成。 • 預報中心：該中心資料皆已放上中央氣象局網頁。(已整理成清單，如附件一。) • 科技中心：自行至 NCEP/GDAS 網站下載。 • 海象中心產品清單，如附件二。 • 已聯繫過衛星中心，但主管出差，無法得到確切答覆，會繼續聯絡。 • 再持續聯絡盧孟明博士。
2	邀請資訊中心及 IBM 駐局人員李長華先生出席 3 月分工作會議，使工作團隊瞭解 IBM 之軟硬體環境。	資訊中心回覆：資訊中心人員不面對外界廠商，若有問題透過電話詢問即可。

貳、討論事項

1. 請海象中心協助查詢局內關於 ECMWF 及 NCEP 資料下載情形，以及是否有 QuickSCAT 以外的衛星風場資料。

2. 關於期中期末審查委員事宜，請朱課長確認交通部的專家學者名單。

3. 模式需要的資料大概有雲遮量、降雨、日照時間、相對溼度、溫度、sea surface height 等項目。關於局內模式之詳細資料，待資訊中心之資料清單公布後(約 3 月 20 日前)，再進行討論。

4. 請海象中心協助統計海溫觀測站的施測時間，作為評估模式及校驗時參考。

5. 今年度 5 月前會將關於模式的相關文獻整理完成，預計 6 月~9 月間擇一較合適的模式安裝至海象中心安管內主機實際測試。模式範圍初步選定為西太平洋區域。

6. 交通部對於計劃報告書，有文件格式之規定，請計畫執行單位遵照此規定撰寫報告書。

7. 計畫完成後須填報 GRB 網站，請計畫主持人於填寫前就填寫內容與本中心討論，以便於計畫績效之統計。

參、散會

本會議於 16：00 結束。

「三維海流預報作業模式建置及校驗分析研究」計畫案

【 97 年 5 月工作會議 】

時　　間：97 年 5 月 13 日(星期二)下午 2:30
地　　點：本局 616B 室
出席人員：徐月娟主任、于嘉順老師
紀　　錄：陳琬婷

壹、討論事項：

1. 請提供中央氣象局 97 年天氣分析與預報研討會的徵稿格式規定。
2. 目前海洋模式議程時間預訂於 9 月 10 日下午，已經邀請到的演講者計有 dr.魏….。會再與曾于恆教授聯絡，聯繫 4 月 23 日到台大的專家學者，有意願參加者，可由此計畫下支付在台的膳食費。
3. 期中報告預計於 6 月 15 日左右完成，預計於 6 月 24 或 27 日進行期中簡報。期中報告審查通過後，預計開始著手模式的測試準備工作。

貳、散會

本會議於 14：50 結束。

「三維海流預報作業模式建置及校驗分析研究」計畫案

【97 年 9 月工作會議 暨 國外顧問討論會】

時　　間：97 年 9 月 12 日(星期五)上午 10:30
地　　點：本局 616B 室
出席人員：徐月娟主任、于嘉順教授、魏靖松博士(NOAA)、
Dr. Roger Proctor (IMOS)、尤皓正博士、朱啟豪課長、黃華興技正、
林芳如技士、陳琬婷研究助理
紀　　錄：尤皓正

壹、討論事項：

1. Model and operation

(1) For the Pacific & northern Pacific model, using ROMS is appropriate decision for setting the operational models.
(2) If the operational global ocean simulation results could be obtained for setting the open boundary conditions from either Australian met office or US Navy, running northern Pacific model will be sufficient and the domain can be extended westward to 90E (or 95E) for including the exchanges between SCS and Indonesia islands, resolution of the model can be finer too.
(3) ROMS is suitable for model the NW Pacific regional seas, curvilinear coordinate for the horizontal description and S-coordinate for vertical layers will be used.
(4) Unstructured grid model, eg FVM or FEM may also be the candidate for running the coastal model, can even included in the regional forecast operations by mesh refinement.
(5) For coastal area model, ROMS & FVCOM can both be the candidate for operation, but the resolution need to increase till 1/60 degree to resolve coastline and maintain certain Kuroshio features, but no need to be very accurate on this.
(6) CWB meteo forecast data can be provided on 00:00 and 12:00 everyday. Operation need to be finished and release to public at 16:00 everyday.
(7) Horizontal resolution and the number of vertical layers of the models must be finer than the resolution of the external models,.
(6) The model results are open to public, ie CGA, etc. CGA can use the forecast information on disaster decision support, ie oil spill prediction and missions on search and rescue. Surface temperature and current information (upwelling zone) can be used by fisheries.

2. Data requirements

(1) Riverine data can be obtained from the Water Resources Agency or world river database. However, real-time data may not be easy to get and a hydrological model may required.
(2) CWB met forecast will be used by the models, in principle. Longer meteo-forecast may obtained through NCEP or ECMWF for the Pacific model, at least one month forecast is required.
(3) Satellite data such as SSH and SST may be used for data assimilations. Drifters can offer surface currents. Drogue data for ocean profiles may obtained from GTS.

3. Computing resources

(1) Require at least 256 cores (or CPUs) on CWB cluster for the operation.
(2) Require PGI compiler (including C and MPI for no limit or 256 CPUs version)
(3) Software installation permission like MPI or GNU make! (Achieved by "pseudo" user?)
(4) Firewall limit! CWB may need to open certain outside IP address (from NSYSU) to link CWB machine, and release permission (including files transfer and certain ports) for remote control to test the operation model.

貳、散會

本會議於 14:00 散會。

「三維海流預報作業模式建置及校驗分析研究」計畫案

【 97 年 11 月工作會議 】

時　　間：97 年 11 月 17 日(星期一)下午 2:00
地　　點：本局 616B 室
出席人員：徐月娟主任、于嘉順老師、陳炫杉博士、朱啟豪課長、林芳如技士、江朕榮
紀　　錄：陳琬婷

壹、討論事項：

1. 已向資訊中心資料管制課提出資料申請：
   - NCEP AVN(NA 05 & NA09)
   - JMA GPV_GSM(JG06)
   - UK(UK01)
   - NFS
   - ECMWF(EC01)

   承辦人回覆若需申請 2007 全年資料需時 2 至 3 個月，故決議先申請較近年月的資料以供模式測試用。
2. NEMO(Nucleus for European Modelling of the Ocean)目前已回覆答應提供預報資料，未來取得後可供測試使用。
3. 建議模式北太平洋範圍南邊界應延伸至南緯 20 度。惟明年度計劃所發展之模式範圍或精度若有變動，請於服務建議書及審查會議中提出並說明。
4. 本計畫需要增加本局平行運算電腦設備，需另爭取預算購置 1 個機櫃及儲存設備。
5. 請廠商特別注意驗收標準表中所應完成之工作事項，以利期末審查會議進行及驗收工作。
6. 期末審查會議預計於 12 月 15 日上午 10:00 進行，一併進行下年度計畫審查會議。

貳、散會

本會議於 15：00 結束。

註：七月份的工作會議及九月份的工作會議依照規定由期中審查及國際研討會及專家會議取代

附錄E 交通部中央氣象局97年度委託研究計畫期末簡報內容重點表

交通部中央氣象局97年度委託研究計畫期末簡報內容重點表

計畫名稱：三維海流預報作業模式建置及校驗分析研究(1/4)

(一)年度計畫預定與實際工作內容比較

預期成果工作項目		
預定工作內容	實際工作內容	差異說明
1. 收集世界各國海洋環流預報模式發展現況 2. 舉辦國際研討會 3. 建立國際與國內合作技術與資料交流管道 4. 於氣象局高速電腦測試公開的海流模式 5. 評估及建議台灣海域作業化海洋環流預報模式系統 6. 訂定模式發展策略	1. 於期末報告中介紹 2. 已於九月份舉辦 3. 藉由研討會的舉辦，已可與國外學者聯繫 4. 完成測試，參考期末報告 5. 詳述於期末報告 6. 詳述於期末報告	

註：1. 請依年度計畫書內「預期成果」項逐一說明其研究情形及達成度，屬「查核點」應特別表示達成情況。
2. 若有分項計畫，請依分項計畫逐項填寫。
3. 工作內容請儘量依條列舉、數量化方式具體說明。
4. 差異說明涵蓋研究工作之突破及研究進度之落後，所遭遇之困難等。

（二）資源運用探討

1. 經費運用
2. 人力運用
3. 重要設備採購、裝設及使用情形

（三）計畫之執行困難及其建議

附錄F 政府科技計畫成果效益報告

政府科技計畫成果效益報告

壹、 基本資料：

計畫名稱：三維海流預報作業模式建置及校驗分析研究(1/4)
主 持 人：于嘉順
審議編號：
計畫期間(全程)： 97 年 2 月 18 日至 100 年 12 月 31 日
年度經費：3,600 千元　全程經費規劃：16,900 千元
執行單位：國立中山大學

貳、 計畫目的、計畫架構與主要內容

一、計畫目的：

台灣海域為東亞航運必經之地，近年來的經濟快速開發，台灣對外的航運更趨頻繁，尤其是石化工業的興起，油品及化學品的進出口更增加了海域遭受船難與污染的危機，阿馬斯號的油污染以及韓籍化學輪三湖兄弟號在新竹外海沈沒所造成的長期影響更是深遠。由於台灣附近海流經過所形成的生態系統豐富，亦是漁產豐盛的海域，近年興起的海面箱網養殖漁業與政府為保護漁業資源在台灣海域投擲大量的人工魚礁，更是易遭受污染的傷害。即時的海流預報作業，不但可以提供航運業者與航管單位即時的海流預報資訊，更可以提供做為早期預警與管理的工具，一旦船難發生時，亦可有立即的海流預報資訊，提供緊急應變單位預測油污染或化學品污染的漂移方向及擴散區域。此外，緊急的海難救助之搜尋工作，亦亟需詳盡的全域三維海流資訊，以提供救難單位即時預測評估搜救對象的可能地點，減低搜尋資源投入的成本，確保搜尋作業時效，因此即時海流預報作業確為緊急應變不可或缺的重要資訊。

近年來世界各地的氣象及海洋學者積極研究全球氣候變遷的問題，尤其是海流及海水溫度對海象及氣象的影響，海流的預報與長期模擬分析更是廣泛的被討論著。台灣附近海域的海流極為複雜，北太平洋環流-「黑潮」流經台灣東部海域，除了強盛的海流亦帶來高溫與高鹽度的海水環境，進入琉球海溝時亦有部分進入台灣北部海域，與來自台灣海峽的海流結合進入東海，每年東北季風期又會阻擾部分的表層洋流而促成黑潮的支流經過台灣南部海域進入南海北部及台灣海峽的南部。除了黑潮洋流的影響，秋

冬的東北季風及夏季的西南季風均對台灣附近的海流有相當的影響。在台灣海峽及東海等大陸棚海域，潮汐又是一個主導海流的動力，季節變動所造成的溫度與河水排放的淡水亦會影響海流的分布，颱風所造成的擾動期間雖然不長，但是可以造成非常劇烈的局部影響，因此一套涵蓋大範圍、多尺度、能夠達成預報時效的海流即時預報模式是海象預報作業極為重要的工作。

海流預報作業一直是海象(洋)預報作業中最為艱鉅的一項工作，亦是近年歐美先進國家中一項積極發展及改進的項目。一方面提供即時預報海流作為航運、遊憩、漁業等公私部門做為規劃管理及作業之參考，另一方面並可隨時提供救難與緊急應便之需。應用現代高速電腦之計算與儲存技術之提高，運用在預報作業的時效與精度，提供有效的即時預警。研發多尺度台灣海域的海洋預報作業模式是急需完成的重點工作。

二、計畫架構(含樹狀圖)：

參考國際上海流預報系統，規劃了台灣海域海流預報作業化模式系統，整體海洋環流預報作業化模式系統架構如圖 2-1 所示，主要分為兩個部份，一為模式系統，包括太平洋環流模式、北太平洋模式、西北太平洋模式及台灣海域模式，另一部份則為觀測資料系統，包括衛星資料、測站資料、浮標資料及船測資料，用以讓模式進行資料比對，並且可與模式進行資料同化，得到更精確的模式結果。

影響海流的因素相當多，而且各因素的尺度也不同，有全球尺度的大氣因子、洋流及潮流，中尺度的渦流系統，也有受到海岸線及區域地形影響的小尺度因子。為了要將大尺度的影響因素包含進來，模式的模擬範圍需要擴大，而為了解析區域因素，模式網格的精度需要增加，如此條件下，計算的網格數會以數十倍甚至數百倍增加，以目前現有的電腦計算架構，並無法達成此一目標，利用單一網格來模擬海流的狀況是不可能的，因此最好的方式就是利要巢式網格系統，所以在模式系統的部份，本團隊設定了四個階層的網格系統。

第一層太平洋環流模式，利用全球大氣模式作為驅動條件，進行太平洋洋流(北太平洋環流及南太平洋環流系統) 系統的模擬，結果可作為下一層模式的邊界條件。北太平洋模式則進行更細部的北太平洋環流模擬，由於使用太平洋環流模式的結果當成邊界條件，因此可將影響包含進北太平

洋模式內。西北太平洋模式則在將範圍縮小，精度提高，並使用北太平洋模式的模擬結果作為邊帖條件輸入，模擬此區的流場狀況，如此可將洋流的影響帶入，並且可以模擬中尺度的渦流系統。最後一層則是解析度及範圍最小的台灣海域模式，利用西北太平洋模式的結果當成邊界輸入，將洋流及渦流的影響帶進此系統，而解析度小可以解析更細部的海岸線及海底地形，透過此巢狀網格的機制，可以得到更精確的台灣海域海流狀況。

模式系統建置完成，需要實測資料進行模式效驗及比對，因此海洋環流預報作業化模式系統架構包含了觀測資料系統。由於模式系統涵蓋的範圍從全球範圍到區域範圍，因此所需要的資料量相當龐大，包括衛星資料(大範圍)、測站資料 (區域)、浮標資料 (區域)及船測資料 (區域)。取得的資料除了進行模式的比對之外，同時也會建立一套資料同化的方式，以增加模式作業化預報的精確度。

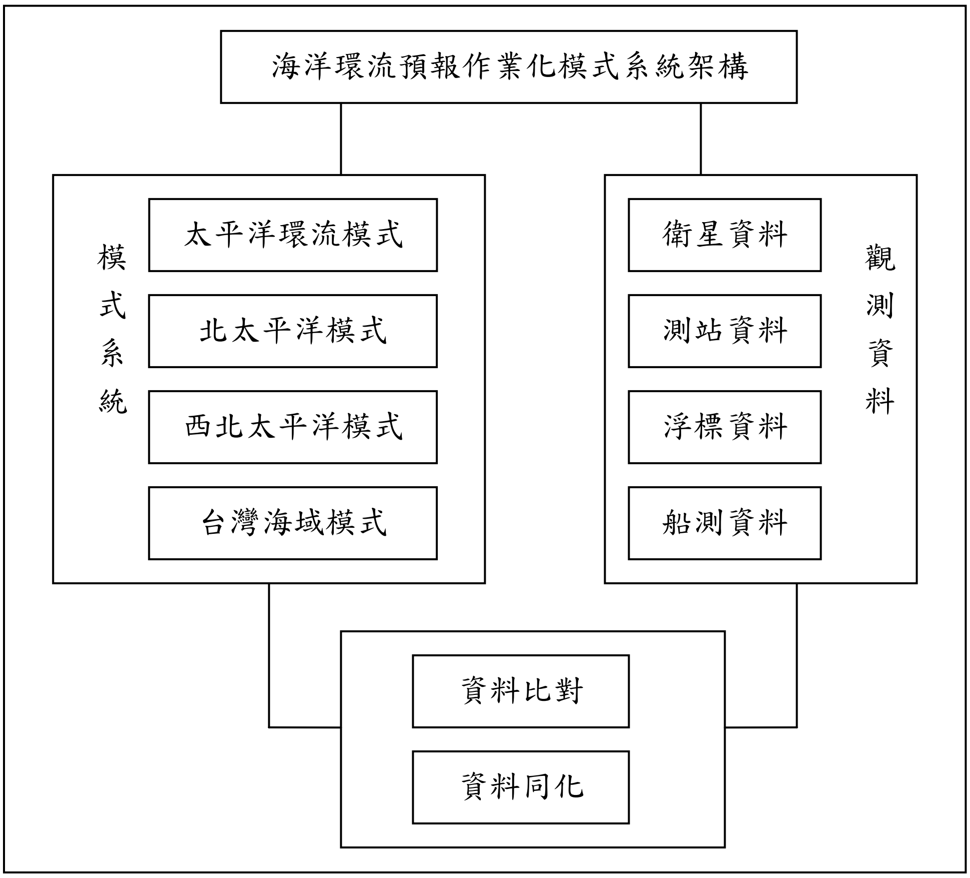

圖 2-1 台灣海流模式預報系統架構圖

三、計畫主要內容：

本計畫擬分四年進行，此為第一年，工作項目如下：

第一年 97 年(2008)：台灣海域海洋環流及潮流作業預報系統建置可行性評估，模式架構的評估，訂定未來分年必須達成的工作目標及成果。並收集分析相關文獻與資料。

(1) 蒐集分析目前世界各國作業海洋環流預報模式的發展現況，含數值方法、模式發展、作業策略、資料需求、預報能力及軟硬體相關技術指標等項目。
(2) 評估及建議中央氣象局台灣海域作業化海洋環流預報模式系統。
(3) 舉辦與本計畫相關之國際研討會一次，邀請實際負責作業化海流預報之國際專家學者與會，至少需涵蓋歐洲、美國及亞洲太平洋地區等地專家學者各一位，各主持一場演講及討論，所有經費均由本計畫支付。
(4) 建立國際與國內合作技術與資料交流管道。
(5) 於中央氣象局高速計算電腦系統測試網路上可公開使用之海流模式，並附完整測試報告。
(6) 訂定模式發展策略，含各模式範圍、解析度及模式系統的嵌合數量、方式等，提供後續年度目標的詳細資訊。例如：模式動力過程、模式所需資料（氣象及海象）、模式組合或嵌合之解析度及預報的範圍。

參、 計畫經費與人力執行情形

一、計畫經費執行情形：

項目 會計科目	預算數(執行數)				備註
	主管機關預算 (委託、補助)	自籌款	合計		
			金額(元)	占總經費%	
一、經常支出					
1.人事費			2,000,000(100)		
2.業務費			1,040,000(100)		
3.差旅費			600,000(100)		
4.管理費			360,000(100)		
5.營業稅					
小計					
二、資本支出					

小計						
合計	金額					
	占總經費%					

請將預算數及執行數並列，以括弧表示執行數

<u>與原計畫規劃差異說明</u>：

二、計畫人力執行情形：

(一)計畫人力：

計畫名稱	執行情形	總人力(人年)	研究員級	副研究員級	助理研究員級	助理
	原訂					
	實際					
	差異					
	原訂					
	實際					
	差異					

說明：

<u>研究員級</u>：研究員、教授、主治醫師、簡任技正、若非以上職稱則相當於博士滿三年、或碩士滿六年、或學士滿九年之研究經驗者。

<u>副研究員級</u>：副研究員、副教授、助研究員、助教授、總醫師、薦任技正、若非以上職稱則相當於博士、碩士滿三年、學士滿六年以上之研究經驗者。

<u>助理研究員級</u>：助理研究員、講師、住院醫師、技士、若非以上職稱則相當於碩士、或學士滿三年以上之研究經驗者。

<u>助理</u>：研究助理、助教、實習醫師、若非以上職稱則相當於學士、或專科滿三年以上之研究經驗者。

(二)主要人力投入情形(副研究員級以上)：

姓名	計畫職稱	投入主要工作及人月數	學、經歷及專長	
			學　歷	
			經　歷	

姓名	計畫職稱	投入主要工作及人月數	學、經歷及專長	
			專 長	
			學 歷	
			經 歷	
			專 長	

<u>與原計畫規劃差異說明</u>：

肆、 計畫已獲得之主要成就與量化成果(output)

(請就主要成就依學術成就(科技基礎研究)、技術創新成就(科技整合創新)、經濟效益(經濟產業促進)、社會影響(社會福祉提升、環保安全)、其它效益(政策管理及其它)方面，擇主要之成就填報。)(如學術成就代表性重要論文、技術轉移經費/項數、技術創新項數、技術服務項數、重大專利及項數、著作權項數等項目，含量化與質化部分，請將本計畫之實際產出重要之績效先勾選表一，再依序填寫已勾選之各項績效成果，填寫說明詳如表二，本作業可至政府研究資訊系統《網址：http://www.grb.gov.tw》填報績效表格，選取列印後將產出表貼入)

本表必填!!!!!!

表一　科技計畫之績效指標(請依計畫性質勾選項目，色塊區為必填)

計畫類別 / 績效指標	1	2	3	4	5	6	7	8	9	99
	學術研究	創新前瞻	技術發展(開發)	系統發展(開發)	政策、法規、制度、規範、系統之規劃(制訂)	研發環境建構(改善)	人才培育(訓練)	研究計劃管理	研究調查	其他
A 論文										
B 研究團隊養成	V									
C 博碩士培育	V									
D 研究報告	V									
E 辦理學術活動										
F 形成教材										
G 專利										

計畫類別 / 績效指標	1 學術研究	2 創新前瞻	3 技術發展(開發)	4 系統發展(開發)	5 政策、法規、制度、規範、系統之規劃(制訂)	6 研發環境建構(改善)	7 人才培育(訓練)	8 研究計劃管理	9 研究調查	99 其他
H 技術報告										
I 技術活動										
J 技術移轉										
S 技術服務										
K 規範/標準制訂										
L 促成廠商或產業團體投資										
M 創新產業或模式建立										
N 協助提升我國產業全球地位或產業競爭力										
O 共通/檢測技術服務										
T 促成與學界或產業團體合作研究										
U 促成智財權資金融通										
V 提高能源利用率										
W 提升公共服務										
X 提高人民或業者收入										
P 創業育成										
Q 資訊服務										
R 增加就業							∨			
Y 資料庫										
Z 調查成果										
AA 決策依據										

表二　請依上表勾選合適計畫評估之項目填寫初級產出、效益及重大突破(填寫說明如表格內容)

本表必填!!!!!!

	績效指標	初級產出量化值	效益說明	重大突破
學術成就(科技基礎研究)	A 論文	0	論文發表在國際上重要研討會或期刊(篇數)、被引用次數及影響係數、論文獲獎(次數)	
	B 研究團隊養成	系內、校內跨領域、跨校或跨組織合作團隊數目	形成研究中心或實驗室數目:1	
	C 博碩士培育	參與計畫執行之碩士研究生(3)及博士研究生(4)	研究生畢業後從事之相關行業人數	產值(薪資)
	D 研究報告	2	引用	
	E 辦理學術活動	1	1	

伍、 評估主要成就及成果之價值與貢獻度(outcome)

(請以學術成就(科技基礎研究)、技術創新成就(科技整合創新)、經濟效益(經濟產業促進)、社會影響(社會福祉提升、環保安全)、其它效益(政策管理及其它)等項目詳述)

一、 學術成就(科技基礎研究) (權重 100 %)

二、 技術創新(科技整合創新) (權重 0 %)

三、 經濟效益(經濟產業促進) (權重 0 %)

四、 社會影響(社會福祉提升、環保安全) (權重 0 %)

五、 其它效益(政策管理及其它) (權重 0 %)

陸、 與相關計畫之配合

若無，可不填。

柒、 後續工作構想之重點

後三年工作重點如下：

第二年 98 年(2009)：參考第一年計畫之評估建議，建立太平洋海域環流模式及北太平洋模式與校驗。

(1) 建立及校驗太平洋模式，模式範圍需涵蓋整個太平洋，水平網格不可大於 1/3 度，模式垂直分層以變化地形相對座標或是等密度分層至少 20 層。

(2) 建立及校驗北太平洋模式，模式的範圍需涵蓋 10°N 到 70°N，西起亞洲大陸東至美洲大陸，水平的解析度為 1/6 度，模式垂直分層以變化地形相對座標 20 層。

(3) 蒐集建置水深地形資料，以提供模式使用。

(4) 氣象資料輸入以中央氣象局每日氣象預報資料為主，並取得國際氣象單位提供之氣象資料以資比對。

(5) 訂定校正年份與驗證年份，並收集相關資料以資校驗。

(6) 預報時效測試與高速計算平行處理測試。

(7) 提供初步模式系統的預報案例。

(8) 製作模式操作手冊。

第三年 99 年(2010)：建立西北太平洋區域模式及台灣海域細格點模式與校驗

(1) 建立及校驗西北太平洋區域模式，模式的範圍需涵蓋 10°N 到 50°N，100°E 到 150°E。其水平網格不得小於 1/12 度，模式垂直分層以變化地形相對座標 25 層。

(2) 建立及校驗台灣海域細格點模式，模式的範圍需涵蓋 21°N 到 27°N，117°E 到 123°E，其水平網格必須解析台灣沿海複雜之海岸地形，定網格系統不得大於 1/60 度或以非正交網格系統（FEM 或 FDM），模式垂直分層以變化地形相對座標 15 層。

(3) 蒐集建置水深地形資料，以提供模式使用。

(4) 氣象資料輸入以中央氣象局每日氣象預報資料為主，並取得國際氣象單位提供之氣象資料以資比對。

(5) 訂定校正年份與驗證年份，並收集相關資料以資校驗。

(6) 預報時效測試與高速計算平行處理測試。

(7) 提供初步模式系統的預報案例。

（8） 製作模式操作手冊。

第四年 100 年(2011)：建立各層次模式作業化接合介面、模式系統測試與評估、長期模擬測試及分析、作業化模式上線測試，參與每日預報作業與觀測結果比較。

（1） 測試及校驗各級模式並建立各模式接合介面。

（2） 測試與評估模式耦合之敏感度至少一年。

（3） 因應中央氣象局電腦設備之軟硬體，完成模式程式最佳化的設定。

（4） 模式系統的測試結果與實測或文獻資料比對分析。

（5） 完成中央氣象局海洋環流作業系統建置及評估報告。

捌、 檢討與展望

四年期計畫完成後，預期得到以下成果：

1. 多尺度台灣海域即時海流預報作業模式將有能力提供高解析度且較準確的海域海流即時資訊予各級政府或民間單位，以規劃各種相關的國防、建設、觀光、資源開發、緊急應變、救援任務與污染防治等政策。
2. 長期海流模擬分析將可提供海洋開發、航運安全、漁業資源及遊憩活動之設計及管理決策之依據。
3. 海流模式在未來可以和大範圍波浪數值預報模式結合做更具有整體性的波浪預報。
4. 海流模式亦可在未來和氣象數值預報模式結合做大氣海洋整體性結合預報。

填表人：于嘉順 聯絡電話： 07-5252000#5173 傳真電話： 07-5255173
E-mail： jasonyu.nsysu@gmail.com

主管簽名：＿＿＿＿＿＿＿＿＿＿

附錄 G 期中審查會議紀錄及廠商回覆

交通部中央氣象局 97 年度委託研究計畫

「三維海流預報作業模式建置及校驗分析研究（1/4）」

期中報告審查會議

會 議 紀 錄

壹、時　　間：民國 97 年 7 月 18 日（星期五）下午 14 時 00 分

貳、地　　點：本局 205 會議室

叁、主　　席：紀副局長水上（徐月娟主任代）　　　　紀錄：陳琬婷

肆、出席委員：國立臺灣大學林銘崇教授、國立臺灣大學曾于恆助理教授、國立成功大學高家俊教授、氣象檢校中心劉文俊主任、海象測報中心徐月娟主任

伍、列席人員：海象測報中心相關人員

陸、執行單位：國立中山大學于嘉順

柒、主席報告：略

捌、執行單位簡報：略

玖、97 年度委託研究計畫期中報告審查委員意見及建議事項：

一、林銘崇教授

（一）台灣海域海流預報作業化系統之可行性評估，依據原則為何？

（二）針對選用 ROMS 之具體優劣點，可做適度說明。

（三）本計劃係引進現有模式，測試項目宜有不同之環境重點考量。

回覆：

謝謝委員建議，本團隊會在期末報告中仔細描述。

二、高家俊教授

（一）本計劃收集多種海洋模式進行評估，內容頗有參考價值。

（二）本計劃擬採用 ROMS 為作業化模式主體，請加強說明採用 ROMS 的理由，以確定其選擇之正確性。

（三）未來海流模式是否實用，端賴實測資料做為驗證，氣象局需立刻著

附錄 H 期末審查會議紀錄及廠商回覆

交通部中央氣象局 97 年度委託研究計畫

「三維海流預報作業模式建置及校驗分析研究（1/4）」

期末報告審查會議

會 議 紀 錄

壹、時　　間：民國 97 年 12 月 15 日（星期一）上午 10 時 00 分

貳、地　　點：本局 205 會議室

叁、主　　席：紀副局長水上　　　　　　　　紀錄：林芳如

肆、出席委員：國立臺灣大學林銘崇教授、國立臺灣大學曾于恆教授、
國立成功大學高家俊教授、交通部運輸研究所港灣技術研究中心蔡立宏研究員、氣象局第一組葉天降組長、
氣象儀器檢校中心劉文俊主任、海象測報中心徐月娟主任、
氣象科技研究中心主任鄭明典

伍、列席人員：海象測報中心相關人員

陸、執行單位：國立中山大學

柒、主席報告：略

捌、執行單位簡報：略

玖、97 年度委託研究計畫期末報告審查委員意見及建議事項：

一、林銘崇教授

（一）工作團隊對於海流模式特性之了解相當深入，整體規劃完備。

（二）最終台灣海域模式提供資訊之應用範圍（針對使用者）或界線可稍作說明。

（三）SWAN 模式基本上屬近岸模式範疇，研究報告指出 ROMS 可將 SWAN
納入，屬於近岸之 FVCOMS 是否亦可納入 SWAN 模式？

二、高家俊教授

（一）年度計畫符合合約內容。

（二）台灣海域模式向東、向北應擴大，最好能擴充 5 度，至少應有 3 度，以利實際用途。

（三）台灣海域模式的產品下游用戶的需求為何？請定義清楚。

（四）台灣海域模式所需的實測資料為何？請於第二年結束前提出來，氣象局應配合擬訂觀測計畫，如此可確保四年計畫完成時，模式產品具有更高公信力。

三、曾于恆助理教授

（一）分析評估不夠完整，缺乏比較(side by side comparison)，優缺點？需詳列，用 tables 等等。

（二）為什麼選擇 ROMS？(p4-p45)無說服力，需加強 why？

（三）Ans 澳洲模式(Roger Proctor pointout) why not？

（四）資料同化用何種方法？此章節可略(或另列計畫)

（五）BGC 是否需要考慮(At this stage)？ if not, why include such a big amount of discussion.

（六）AGRIF(adaptatine, mesh refinement) requires careful evaluation

（七）MERCATR + U.S. system (NOT compatable) This is not working.

（八）觀測系統並未整合在本計畫，這將增加驗證與實際 operational 的可行性(至少網路上的公開資料可供使用)。

（九）整個進入系統的運行時間須審慎評估(computational time)，資料進入等等，整合系統上介面須建立。

（十）日本模式為何不嘗試使用，已有 1/10 度 resolution global model 比 France 好。

（十一）平行效率，計算時間最佳化比較需加入，可做成 tables，須提出最佳的 CPU 數、時間估計等等提供給 CWB。

（十二）FVCOM 與 ROMS 整合需要評估完整。

（十三）觀測資料進入系統的界面須加入模式發展中。

四、蔡立宏研究員

（一）本研究收集各國海洋洋流預報模式，對於理論基礎、數值方法、資料需求、適用範圍、執行方法、步驟均有詳盡的說明及分析。並做評估最後選擇 ROMS 模式，作為未來太平洋及北太平洋環流模擬計

算之工具。研究成果充實，提供本研究及其他研究應用之參考，並進行人員訓練以及與國際交流，研究工作值得肯定。

（二）建議在期中審查會中，受委託單位對於委員意見的回覆或執行情形，應列表說明。

（三）P3-8 中提到在進行資料同化過程，誤差分為自然誤差及重大誤差，重大誤差可以透過檢驗或捨棄處理，文中提到自然誤差可以妥善處理，請補充說明。

（四）3.3.3 資料同化方法包括：1.連續資料同化法 2.變分資料同化法。P3-22 中連續資料同化法中包括：a 卡門濾波法 b 最佳內插法 c 逐步訂正法 d 變分資料同化法相矛盾，標號應修正。

（五）P4-46 提到 ROMS 提供 4 種水平對流項設定（Akima, 2^{nd}-order centered, 4^{th}-order centered, 3^{rd}-upstream 模式）只有附 3^{rd}-upstream 模式的分析圖 p4-49，其他設定項將造成模式不穩定，是否可提供其他設定項之結果分析圖。

（六）P4-47 之圖 4.3.1-3 封閉邊界點時序圖中，少了紅色的 Chapman 曲線。P4-48 及 P4-49 座標軸請標明並標示單位。

五、葉天降組長

（一）對海流模式做相當深入蒐集與討論，同時也對各項工作依時程完成，驗收合格。

（二）對報告書建議：

1.按統一格式，提供摘要，並對應完成項目之執行情形摘要性陳述。

2.在模式比較到選擇部分，能在提供一比較表，清楚顯示主要項目（精確度、計算效率、支援度與參與、資料同化、格點組合、所需經費等）各模式之優劣。

3.部分文字錯誤需修正（特別是結論、建議章）。

（三）cwb 目前即時收集天氣預報模式國外資料，若有海流/海象資料需蒐集也可建議 cwb 進行蒐集。另，總計算需求概估，也可提供給氣象局參考，以進行相關系統建置之參考。

六、劉文俊主任

（一）對各國模式有充分的瞭解。

（二）完成環流模式作業化的研討會。

（三）國際資訊交流管道暢通。

（四）從簡報上看，台灣海峽的海流資料相對不足，台灣本身可提供的海流資料比較近岸，輸入模式的可能性不大，如何補齊不足，是否可能加入大陸觀測之資料？

七、徐月娟主任

無。

八、鄭明典主任

此報告對於海流模式的發展現況與趨勢說明相當清楚，很有參考價值。對於未來發展策略的論述合理，作業化發展的規劃實用明確，後續應可按部就班推動。建議本計畫應與氣象局全球海氣偶合模式發展計畫多合作。

拾、審查結果：

請受委託單位依審查委員意見修改期末報告後通過。

拾壹、散會：中午 12 時 10 分

期末審查意見辦理情形

台灣大學林銘崇教授	
審查意見	意見回覆
1. 工作團隊對於海流模式特性之了解相當深入，整體規劃完備。	謝謝委員肯定。
2. 最終台灣海域模式提供資訊之應用範圍（針對使用者）或界線可稍作說明。	目前僅以建置模式為前提，未來計畫的成果使用，原則上可應用範圍廣泛，需與氣象局協調。
3.SWAN 模式基本上屬近岸模式範疇，研究報告指出 ROMS 可將 SWAN 納入，屬於近岸之 FVCOMS 是否亦可納入 SWAN 模式？	目前的版本尚未加入波浪的影響，然其發展架構有將波浪涵蓋，因此未來的版本或有機會納入 swan，未來也可自行發展。

成功大學高家俊教授	
審查意見	意見回覆
1. 年度計畫符合合約內容。	謝謝委員肯定
2. 台灣海域模式向東、向北應擴大，最好能擴充 5 度，至少應有 3 度，以利實際用途。	謝謝委員建議，由於台灣海域為第三年才建置，因此可在進行調整，本團隊會將委員意見納入修正，以目前計算效率應可達成。
3. 台灣海域模式的產品下游用戶的需求為何？請定義清楚。	台灣海域模式的產品(水位、三維流場、溫度及鹽度)主要可提供政府機關救災參考、研究人員使用、一般民眾查詢等，然最終的使用權仍需由氣象局訂定。
4. 台灣海域模式所需的實測資料為何？請於第二年結束前提出來，氣象局應配合擬訂觀測計畫，如此可確保四年計畫完成時,模式產品具有更高公信力。	謝謝委員建議。台灣海域模式所需要的比對觀測資料主要為實測水位、流速、溫度及鹽度，目前在海峽方面較為缺乏，因此未來會進行更詳細的實測資料蒐集，瞭解缺乏的項目，可提供氣象局未來觀測計畫的參考，亦提出 SVP-B 2010 年的預算建議。

台灣大學曾于恆助理教授	
審查意見	意見回覆
1. 分析評估不夠完整，缺乏比較(side by side comparison)，優缺點？需詳列，用	謝謝委員建議。完稿補列各模式比較的表格。

tables 等等。	
2. 為什麼選擇 ROMS？(p4-p45)無說服力，需加強 why？	由於計畫執行時間僅一年，要進行模式一對一的比對難度太高，不同的案例會有不同的結果，目前水動力理論發展相當成熟，各模式的理論基礎也相當類似，對於海流模擬皆無問題，因此本團隊主要針對模式未來持續發展、網格的適應性、計算效率、是否容易取得、使用者支援以及使用者人數等方向進行考量。
3. Ans 澳洲模式(Roger Proctor pointout) why not？	謝謝委員建議。目前澳洲的系統仍然在進行整合發展，亦在評估是否以 POLCOMS 或是 ROMS 取代，與國際同發展，且本團隊未能取得相關資訊，因此未放入考量中。
4. 資料同化用何種方法？此章節可略(或另列計畫)	謝謝委員建議。目前資料同化僅為初步構想，原始計畫需求並未明列，未來是否能夠完成，本團隊並無法保證，目前僅是納入考量，希望未來可以建立一些介面及方式。
5. BGC 是否需要考慮(At this stage)？ if not, why include such a big amount of discussion.	目前並無考慮 BGC，僅就模式特性進行介紹，瞭解模式的整體架構。
6. AGRIF(adaptatine, mesh refinement) requires careful evaluation	謝謝委員提醒，未來使用 AGRIF 時將會仔細測試驗證。
7. MERCATR + U.S. system (NOT compatable) This is not working.	謝謝委員建議。目前本團隊是以取得其最後的計算結果引入模式中計算，並非進行 MERCATR + U.S. system 的系統整合。
8. 觀測系統並未整合在本計畫，這將增加驗證與實際 operational 的可行性(至少網路上的公開資料可供使用)。	謝謝委員建議。本團隊會積極收集相關的觀測資料，並增對不足的部份提供氣象局，作為未來觀測系統設置的參考。
9. 整個進入系統的運行時間須審慎評估(computational time)，資料進入等等，整合系統上介面須建立。	謝謝委員建議，本團隊於模式建制的同時，會同步進行輸入資料介面的建立，以利未來資料進入。
10. 日本模式為何不嘗試使用，已有 1/10 度 resolution global model 比 France 好。	謝謝委員建議，若本團隊也能取得日本模式的結果，會評估加以應用。
11. 平行效率，計算時間最佳化比較需	謝謝委員建議。由於目前僅使用假設的

加入，可做成 tables，須提出最佳的 CPU 數、時間估計等等提供給 CWB。	案例初步的評估計算效能，未來使用實際案例建置完成後，會提供氣象局實際的計算時間及計算效率。
12. FVCOM 與 ROMS 整合需要評估完整。	謝謝委員建議。目前近岸的部份暫定使用 FVCOM，未來仍有變化的空間，因此本團隊會仔細評估未來模式接合的部份。
13. 觀測資料進入系統的界面須加入模式發展中。	謝謝委員建議。觀測資料進入模式是未來模式比對及進行資料同化的重要介面，本團隊會於建置模式的過程中同步建立觀測資料進入模式的介面。

港灣技術研究中心蔡立宏研究員	
審查意見	意見回覆
1. 本研究收集各國海洋洋流預報模式，對於理論基礎、數值方法、資料需求、適用範圍、執行方法、步驟均有詳盡的說明及分析。並做評估最後選擇 ROMS 模式，作為未來太平洋及北太平洋環流模擬計算之工具。研究成果充實，提供本研究及其他研究應用之參考，並進行人員訓練以及與國際交流，研究工作值得肯定。	謝謝委員肯定。
2. 建議在期中審查會中，受委託單位對於委員意見的回覆或執行情形，應列表說明。	此部份已於期末定稿修正。
3. P3-8 中提到在進行資料同化過程，誤差分為自然誤差及重大誤差，重大誤差可以透過檢驗或捨棄處理，文中提到自然誤差可以妥善處理，請補充說明。	自然誤差主要為儀器誤差(instrument error)產生，因此可透過資料品管過程及校正儀器解決。
4. 3.3.3 資料同化方法包括：1.連續資料同化法 2.變分資料同化法。P3-22 中連續資料同化法中包括：a 卡門濾波法 b 最佳內插法 c 逐步訂正法 d 變分資料同化法相矛盾，標號應修正。	此部份已於期末定稿修正。
5. P4-46 提到 ROMS 提供 4 種水平對流項設定（Akima, 2nd-order centered, 4th-order centered, 3rd-upstream 模式）只	由於模式不穩定造成數值爆掉，其他三個設定未能產生結果，因此未能將圖放上。

有附 3rd-upstream 模式的分析圖 p4-49，其他設定項將造成模式不穩定，是否可提供其他設定項之結果分析圖。	
6. P4-47 之圖 4.3.1-3 封閉邊界點時序圖中，少了紅色的 Chapman 曲線。P4-48 及 P4-49 座標軸請標明並標示單位。	1.Chapman 曲線與綠色線重合，倒至圖上看不到。 2.平面圖座標軸為格點數，因此沒有單位。

中央氣象局葉天降組長	
審查意見	意見回覆
1. 對海流模式做相當深入蒐集與討論，同時也對各項工作依時程完成，驗收合格。	謝謝委員肯定。
2. 對報告書建議： (1).按統一格式，提供摘要，並對應完成項目之執行情形摘要性陳述。 (2).在模式比較到選擇部分，能在提供一比較表，清楚顯示主要項目（精確度、計算效率、支援度與參與、資料同化、格點組合、所需經費等）各模式之優劣。 (3).部分文字錯誤需修正（特別是結論、建議章）。	謝謝委員建議，此部份會於期末定稿報告一併修正。
3. cwb 目前即時收集天氣預報模式國外資料，若有海流/海象資料需蒐集也可建議 cwb 進行蒐集。另，總計算需求概估，也可提供給氣象局參考，以進行相關系統建置之參考。	1.謝謝委員建議 2.謝謝委員建議。由於目前仍未有實際的案例進行評估，以今年度設定的案例來說，氣象局高速電腦的計算量皆可負荷，因此未來實際系統建置完成後，會繼續進行實際運算量的評估，提供氣象局參考。

劉文俊主任	
審查意見	意見回覆
1. 對各國模式有充分的瞭解。	謝謝委員肯定。
2. 完成環流模式作業化的研討會。	謝謝委員肯定。
3. 國際資訊交流管道暢通。	謝謝委員肯定。
4. 從簡報上看，台灣海峽的海流資料相對不足，台灣本身可提供的海流資料比較近岸，輸入模式的可能性不大，如何	1. 資料不足確實為模式發展的問題，台灣海流模式的邊界輸入仍需使用大範圍模式產生的結果，實測資料主要仍然以

補齊不足，是否可能加入大陸觀測之資料？	比對為主,未來可考慮參與 GDP 計畫(以建議氣象局於 2010 年起加入)，於台灣海峽內放置浮標取得資料。 2.大陸的觀測資料，目前暫時未能有管道取得，此部份仍需努力，若未來有機會能取得相關資料，本團隊也會積極納入。

中央氣象局徐月娟主任	
審查意見	意見回覆
無	

中央氣象局鄭明典主任	
審查意見	意見回覆
1. 此報告對於海流模式的發展現況與趨勢說明相當清楚，很有參考價值。對於未來發展策略的論述合理，作業化發展的規劃實用明確，後續應可按部就班推動。建議本計畫應與氣象局全球海氣偶合模式發展計畫多合作。	謝謝委員肯定。本團隊也希望能與氣象局相關計畫進行合作，如此可節省未來發展的時間以及避免資源重複的浪費。

手規劃海流觀測，方能獲得〝有意義〞相關數據確認數值模式成果之可信度。

回覆：

謝謝委員建議，本團隊會持續努力，並仔細評估。

三、曾于恆助理教授

（一)邊界條件須格外注意,特別是下邊界近赤道系統 radiative type cannot work well。

（二）資料同化所需資料來源項須增加，現有 Argo、drifters 於台灣週遭海域資料仍不夠完整。

（三）IBM P5-575 資料傳遞在平行化版本選擇效率的增加須小心考慮，如何發展現有模式的平行化，特別是 openMP 的效能無法提高。

（四）須注意 Nesting 的 Coupling。

（五）目的須清楚評估具體計畫。

回覆：

謝謝委員建議，本團隊會持續修正及仔細評估。

四、劉文俊主任

（一）期中報告能依時程完成，內容完整。

（二）本局應及早因應海科資料庫資料 Release 之問題。

回覆：

謝謝委員肯定。

五、徐月娟主任

無。

拾、審查結果：期中審查通過。

拾壹、散會：下午 15 時 15 分